Neuroprotective Effects of FGF20 on Dopamine Neurones

Boshoff, Eugene

Awarding institution:
King's College London

Title: Neuroprotective Effects of FGF20 on Dopamine Neurones

Author: Eugene Boshoff

Neuroprotective Effects of FGF20 on Dopamine Neurones

Eugene Louis Boshoff

PhD in Integrative Biomedicine

King’s College London
Wolfson Centre for Age Related Diseases

Abstract

Recent findings have demonstrated fibroblast growth factor-20 (FGF20) to have neuroprotective effects on dopamine neurones *in vitro*. In this thesis, FGF20's neuroprotective effects on dopamine neurones were further investigated. A ventral mesencephalic (VM) embryonic dopamine neurone culture system and a partially lesioned 6-hydroxydopamine (6OHDA) rat model of Parkinson's disease (PD) were established in which FGF20 was evaluated for its neuroprotective effects both *in vitro* and *in vivo*. Using immunohistochemistry, FGF20 and at least three of its receptors (fibroblast growth factor receptor (FGFR) 1, 3, and 4) were demonstrated to be localised to dopamine neurones and glial cells in the rat nigrostriatal tract and in VM embryonic dopamine neurone cultures. *In vitro*, FGF20 protected VM embryonic dopamine neurones against 6OHDA toxicity, and, *in vivo*, chronic supra-nigral delivery of FGF20 protected nigrostriatal dopamine neurones against a partial 6OHDA lesion. Importantly, FGF20 also preserved motor function in the 6OHDA lesioned rats. In a separate *in vivo* study, experiments were carried out to investigate whether pharmacological inhibition of FGFR activation is able to potentiate 6OHDA-induced nigrostriatal degeneration in the rat, and results from this study suggest that the endogenous FGF system might play a protective role in the nigrostriatal tract. Additionally, in PC12 cells, FGF20's neuroprotective effects against 6OHDA toxicity were demonstrated to be mediated by the FGFRs at the receptor level, and by the ERK1/2 MAPK pathway at the intracellular level. Others have shown the heparin sulphate proteoglycan, agrin to potentiate *FGF2* stimulated ERK1/2 activation and neurite outgrowth in PC12 cells. It was demonstrated here that agrin potentiates FGF20 stimulated ERK1/2 activation, but it fails to potentiate FGF20's neuroprotective effects in PC12 cells. Taken together, these findings provide further support for FGF20's neuroprotective potential in PD.

Acknowledgements

First and foremost, I would like to thank my supervisor, Susan Duty for all the help and support that she provided me with, and for being an exceptionally resourceful and supportive mentor throughout my PhD. I am also extremely grateful to our histology manager, Carl Hobbs, for the enormous contribution he made to all the immunohistochemistry experiments carried out during my PhD, not only through all his advise and mentoring, but also through the generous quantities of antibodies that he provided me with. A big thank you to everyone in the lab for being great colleagues and for all the help they gave me, but also for being great friends, and for making the last 4 years such an enjoyable and stimulating time. A special thank you also to my wife, Ana for all her love, support and encouragement, and for all the happiness and fun that she brings to my life outside of work. To my family, and in particular my mother and father I would also like to say a big thank you for all their support. Last but not least, I would like to express my gratitude to my funding source, the Capacity Building Award in Integrative Mammalian Biology funded by the BBSRC, BPS, HEFCE, KTN, MRC, and SFC.

List of Abbreviations

ABC: Avidin-biotin complex

aCSF: Artificial cerebrospinal fluid

ATP: Adenosine triphosphate

BBB: Blood brain barrier

BDNF: Brain-derived neurotrophic factor

BSA: Bovine serum albumin

CNS: Central nervous system

COMT: Catechol-O-methyl transferase

DAB: Diaminobenzidine

DAG: Diacylglycerol

DIV: Days in vitro

DMEM: Dulbecco's modified eagles medium

D-PBS: Dulbecco's phosphate buffered saline

DPX: Dibutyl phthalate in xylene

ECM: Extracellular matrix

VEGFR2: Vascular epithelial growth factor receptor 2

ERK1/2: Extracellular regulated kinase-1/2

ESCs: Embryonic stem cells

FBS: Foetal bovine serum

FGF: Fibroblast growth factor

FGFR: Fibroblast growth factor receptor

5-HT: 5-Hydroxytryptamine

FRS2: FGFR substrate 2

Gab1: GRB2-associated-binding protein 1

GAD67: Glutamate decarboxylase-67

GAPDH : Glyceraldehyde-3-phosphate dehydrogenase

GDNF: Glial-derived neurotrophic factor

GFAP: Glial fibrillary acidic protein

GSH: Glutathione

GWAS: Genome wide association studies

hESCs: Human embryonic stem cells

HRP: Horseradish peroxidase

HSPGs: Heparin sulphate proteoglycans

HuCD: Human neuronal protein

Iba1: Ionised calcium binding adapter molecule 1

Icv: Intracerebroventricular

IFNγ: Interferon-γ

Ig: Immunoglobulin

IL-1β : Interleukin-1β

IL-6: Interleukin-6

IMS: Industrial methylated spirits

iNOS : Inducible nitric oxide synthetase

IP_3: Inositol-(3,4,5)-trisphosphate

iPSCs: Induced pluripotent stem cells

JNK: Jun N-terminal kinase

LBs: Lewy bodies

L-DOPA: L-3,4-Dihydroxyphenylalanine

LRRK-2: Leucine rich repeat kinase 2

MAO-B: Monoamine oxidase-B

MAPK: Mitogen activated protein kinase

MHB: Medial habenula

MPP^+: 1-methyl-4-phenylpyridium

MPTP: 1-Methyl-4-phenyl-1,2,3,6-tetrahydropyridine

MRI: Magnetic resonance imaging

NeuN: Neuronal nuclei

NGF: Nerve growth factor

NHPs: Non-human primates

NMDA: N-Methyl-D-aspartate

NSCs: Neural stem cells

PD: Parkinson's disease

PDK: Phosphoinositide dependent protein kinase

PFA: Para-formaldehyde

PH: Pleckstrin homology

Phosho-ERK1/2: Phosphorylated extracellular regulated kinase-1/2

PI-3K: Phosphatidylinositol 3-kinase

PINK-1: PTEN-induced putative kinase 1

PIP: Phosphatidylinositol phosphate

PIP_2: Phosphatidylinositol-(4,5)-bisphosphate

PKB/Akt : Protein kinase B/RAC-alpha serine/threonine protein kinase

PKC: Protein kinase C

PLA_2: Phospholipase A_2

PLC-γ: Phospholipase C-γ

PLD: Phospholipase D

PMS: Phenazine methosulfate

RIPA: RadioImmunoPrecipitation Assay

ROS: Reactive oxygen species

RTKs: Receptor tyrosine kinases

Shb: SH2 domain-containing adapter protein B

Shc: Src homology 2 domain containing

Shp2/PTPN11: Tyrosine phosphatase non receptor type II

6OHDA: 6-Hydroxydopamine

SN: Substantia nigra

SNc: substantia nigra pars compacta

SNCA: α-Synuclein

SNPs: Single nucleotide polymorphisms

SNr: Substantia nigra pars reticulata

Sos: Son of sevenless

TBS: Tris buffered saline

TH: Tyrosine hydroxylase

TNFα : Tumour necrosis factor-α

Ub: Ubiquitin

UCH-L1: Ubiquitin C-terminal hydrolase L1

UPS: Ubiquitin proteasome system

VM: Ventral mesencephalic

Table of Contents

List of Figures

Chapter 2

Chapter 3

Chapter 4

Chapter 5

Chapter 1. General Introduction

1.1. Parkinson's Disease

Parkinson's disease (PD) is a progressive neurodegenerative movement disorder that affects 1-2% of people over 60, and 3-5% of people over 85 (Alves *et al.*, 2008). In PD, the extensive loss of nigrostriatal dopamine neurones leads to the development of a range of motor deficits, including tremor, rigidity, akinesia, and bradykinesia (Samii *et al.*, 2004). Around 90% of PD cases are sporadic or idiopathic, and the aetiological factors that cause these sporadic forms of PD are still poorly understood. Familial forms of PD, on the other hand, only account for <5% of PD cases, and they are caused by a number of well characterised single gene mutations. In the majority of cases of PD (>90%), the onset of motor symptoms usually occurs between the ages of 60-70 (Samii *et al.*, 2004). In a small number of cases of early onset PD (~5-10%), motor symptoms, however, appear at a much earlier point in life, usually before the age of 41 (Muthane *et al.*, 1994).

A key pathological hallmark of PD is the presence of eosinophilic cytoplasmic protein inclusions in the dopamine neurones of the substantia nigra pars compacta (SNc), as well as other areas of the brain (Schulz & Falkenburger, 2004). These inclusions are called Lewy bodies (LBs), and they consist mainly of lipids, neurofilament, and a number of other proteins, including, α-synuclein (SNCA), synphylin-1, ubiquitin (Ub), and enzymes of the ubiquitin proteasome system (UPS) (Chung *et al.*, 2001). In PD, LB pathology and neuronal degeneration is by far the most pronounced in the nigrostriatal dopaminergic pathway, but it is not limited exclusively to this specific region of the brain. Less extensive LB pathology and neuronal degeneration, relative to the nigrostriatal tract, is also observed in several other regions of the brain, including the raphe nucleus, the locus coeruleus, the nucleus basalis of Meynert, the amygdala, the dorsal motor nucleus of the vagus, and the basal reticular nuclei of the brainstem (Agid *et al.*, 1989; Ziemssen & Reichmann, 2007; Ferrer, 2011). Moreover, in addition to the cardinal motor symptoms that characterise the disease, PD patients often also suffer from a range of non-motor symptoms, and it is thought that these symptoms are caused by pathology in these other affected areas of the brain. Examples of such non-motor symptoms include, depression, dementia, olfactory deficits, constipation, urinary incontinence, and sleep disturbances. For instance, the dorsal raphe nucleus is important in the regulation of mood, and it is believed that

degeneration of this nucleus gives rise to depression in PD patients (Tan *et al.*, 2011), while dementia is attributed to degeneration of the nucleus basalis of Meynert, an area of the brain that plays an important role in cognition (Bohnen & Albin, 2011). The locus coeruleus and other nuclei of the brainstem play an important role in regulating alertness and circadian rhythms, and it is, thus, thought that degeneration in these nuclei is partly responsible for the sleep disturbance symptoms in PD (Simuni & Sethi, 2008). The symptoms of constipation and urinary incontinence, on the other hand, are classical symptoms of autonomic dysfunction, and they are, thus, believed to be caused by pathology in the dorsal motor nucleus of the vagus, a nucleus which plays an important role in regulating output from the autonomic nervous system (Simuni & Sethi, 2008).

1.2. Aetiology of PD

The aetiology leading to dopamine neurone degeneration in PD remains incompletely understood. Research has, however, provided evidence for the likely involvement of numerous factors in the aetiology of PD; and it is likely that neuronal cell death ultimately results from multiple detrimental insults synergistically damaging dopamine neurones to a fatal degree (Sulzer, 2007). The non-genetic contributory factors most widely studied, include oxidative stress, mitochondrial dysfunction, ubiquitin proteasome system (UPS) dysfunction, exposure to environmental toxins, and neuroinflammation. A brief overview of the evidence implicating each of these factors in the aetiology of PD is described in the sections below.

Monozygotic twin studies have ruled out a major involvement of genetic factors in the development of sporadic PD (Tanner *et al.*, 1999). Mutations in a number of different genes have, on the other hand, been shown to cause familial forms of PD, including the *α-synuclein* (*SNCA*), *PTEN-induced putative kinase 1* (*PINK-1*), *DJ-1*, *leucine rich repeat kinase 2* (*LRRK-2*), *parkin*, and *ubiquitin C-terminal hydrolase L1* (*UCH-L1*) genes (Cordato & Chan, 2004). The *SNCA* gene encodes the SNCA protein, a protein that is widely expressed by both neurones and glial cells throughout the CNS (Bennett, 2005). In neurones, SNCA is most abundantly present in pre-synaptic nerve terminals, but the function of the protein, however, remains poorly understood. Three missense substitution mutations (A30P, E53T, and E46K), and a number of duplication and triplication mutations in the *SNCA* gene have been demonstrated to cause autosomal dominant familial forms of PD that are characterised by an early onset and rapid progression of motor symptoms (Tan & Skipper, 2007; Bekris *et al.*, 2010). The *PINK-1*

gene encodes the PINK-1 protein, a ubiquitously expressed mitochondrial serine/threonine protein kinase enzyme, while the *DJ-1* gene encodes the DJ-1 protein, a highly conserved protein that is widely expressed in neurones and glial cells, but whose function is still unknown (Dodson & Guo, 2007). Mutations in both the *PINK-1* and *DJ-1* genes have been found to cause rare autosomal recessive early onset familial forms of PD (Tan & Skipper, 2007; Bekris *et al.*, 2010). The *LRRK-2* gene codes for the LRRK-2 protein, a protein kinase whose exact function is also still unknown (Biskup & West, 2009). Six mutations in the *LRRK-2* gene have been found to cause autosomal dominant forms of familial PD, and unlike most of the other forms of familial PD which are mostly characterised by early onset of disease, *LRRK-2* familial PD cases are associated with late onset of motor symptoms that are typical of sporadic PD (Tan & Skipper, 2007; Bekris *et al.*, 2010). This has lead to a number of *LRRK-2* familial cases of PD being misdiagnosed as sporadic cases (Tan & Skipper, 2007). The *parkin* and *UCH-L1* genes are functionally related as they both code for proteins that form part of the UPS. The *parkin* gene codes for an ubiquitin E3 ligase enzyme (Mizuno *et al.*, 2001), while *UCH-L1* codes for an abundant de-ubiquitinating enzyme that is specifically localised to neurones (Setsuie & Wada, 2007). Mutations in the *parkin* gene cause autosomal recessive juvenile onset forms of parkinsonism, which accounts for ~50% of all cases of familial PD (Tan & Skipper, 2007; Bekris *et al.*, 2010). Notably, *parkin* associated familial forms of PD are characterised by having atypical pathological features as inclusions are absent in most cases (Tan & Skipper, 2007; Bekris *et al.*, 2010). A single substitution (I193M) mutation in the *UCH-L1* gene has been documented to cause an extremely rare early onset autosomal recessive form of PD, which has, thus far, only been detected in two siblings (Tan & Skipper, 2007; Bekris *et al.*, 2010). Moreover, recent results from genome wide association studies (GWAS) have demonstrated that genetic factors also appear to play a contributory role in the aetiology of sporadic PD, as specific single nucleotide polymorphisms (SNPs) in a number of different genes increases the risk of developing PD (Bekris *et al.*, 2010; Nalls *et al.*, 2011). Interestingly, SNPs in both the *SNCA* and *LRRK-2* genes have been found to increase the incidence of sporadic PD (Mizuta *et al.*, 2006; Nalls *et al.*, 2011; Saad *et al.*, 2011). The mechanisms through which all of the above mentioned mutations cause PD pathology or increase the risk of developing PD, however, remain poorly understood, and substantial research efforts are currently dedicated to uncovering these mechanisms.

1.2.1. Oxidative Stress

A range of free radical species, including, for example, the superoxide and the hydroxyl radicals, are generated as by-products of many metabolic reactions taking place in cells. Cells have got a range of detoxifying mechanisms, which normally inactivates these highly reactive entities, and maintains them at non-toxic levels (Halliwell, 2006). The superoxide dismutase enzyme, for example, catalyses the conversion of superoxide into the non-radicals, H_2O_2 and O_2. The tripeptide glutathione (GSH) also plays an important anti-oxidant role in cells by inactivating free radicals through reduction reactions. However, if free radical levels builds up to toxic levels in a cell, they can cause cellular dysfunction by their ability to react with proteins and nucleic acids, leading to a distortion of their structure and function (Halliwell, 2006). Additionally, free radicals can react with plasma membrane lipids to set off a cascade of lipid peroxidation (Halliwell, 2006). This process ultimately also leads to cellular dysfunction by increasing plasma membrane permeability, and by inactivating receptors, enzymes, and ion channels (Halliwell, 2006). Oxidative damage can occur either when detoxifying mechanisms are overwhelmed by the generation of abnormally high levels of free radicals and/or when the functioning of free radical scavenging mechanisms are for some reason impaired.

It has been reported that several markers of oxidative stress are increased in the substantia nigra (SN) of PD patients. Levels of 4-hydroxy-2,3-nonenal, a marker of lipid peroxidation, and 8-hydroxyguanosine, a marker of nucleoside oxidation, are found at ~6 and ~16 fold higher levels, respectively, in the SN of PD patients when compared to age matched controls (Yoritaka *et al.*, 1996; Zhang *et al.*, 1999). Decreased levels of reduced GSH have also been shown to be present in the remaining nigral neurones of PD patients compared to age matched controls (Sofic *et al.*, 1992; Pearce *et al.*, 1997). Interestingly, in healthy brains, there is already a greater level of oxidative stress in the SN compared to other brain regions (Floor & Wetzel, 1998). It has been proposed that this increased oxidative stress load could make dopamine neurones more vulnerable to cell death, and this might account for why dopamine neurones are preferentially lost in PD. The increased level of oxidative stress has been attributed to the dopamine catabolic pathway producing high levels of free radicals (Hald & Lotharius, 2005). Dopamine can be broken down by either an enzymatic pathway or through auto-oxidation. The latter pathway produces the highly reactive free radical species, dopamine-quinone as a by-product. Additionally, both pathways also produce H_2O_2 as by-products. Although H_2O_2

itself isn't a free radical, it can be converted into the hydroxyl radical in the presence of ferrous iron through the so called Fenton reaction (Hald & Lotharius, 2005). The presence of significantly higher levels of iron in the SN of PD brains compared to control brains have provided further evidence in support of this theory (Dexter *et al.*, 1989).

1.2.2. Mitochondrial Dysfunction

Mitochondria play an essential role in the normal functioning of cells. Through the respiratory chain, mitochondria produce adenosine triphosphate (ATP) molecules that act as an energy source that facilitates many of the biochemical reactions within cells. Substantial evidence has implicated mitochondrial deficits in the aetiology of PD. There is a 35% reduction in complex 1 mitochondrial activity in the SN of PD patients compared to aged match controls (Schapira *et al.*, 1989). A reduced amount of mitochondrial complex 1 protein in the SN of PD patients has also been reported (Mizuno *et al.*, 1989). Furthermore, two mitochondrial complex I inhibitors, 1-methyl-4-phenyl-1,2,3,6-tetrahydropyridine (MPTP) and rotenone, are both dopamine neurone toxins that are capable of inducing dopamine neurone degeneration and parkinsonian-like symptoms when administered to animals (Betarbet *et al.*, 2000; Richardson *et al.*, 2007). More recently, PD pathology (progressive nigrostriatal dopamine neurone degeneration) and progressive motor deficits were also reproduced in a transgenic mouse strain in which the important mitochondrial transcription factor, Tfam was knocked out (Ekstrand *et al.*, 2007).

It is proposed that complex 1 deficiency can lead to neuronal cell death through two mechanisms (Sherer *et al.*, 2002). Complex 1 deficiency can lead to a shortage of ATP within a neurone. This in turn will cause the partial depolarisation of a neurone's plasma membrane, as Na+/K+ ATPase pumps don't have sufficient energy available to them to maintain the resting membrane potential. This partial depolarisation removes the Mg^{2+} block in N-methyl-D-aspartate (NMDA) receptors, which allows the receptors to be activated by excitatory inputs of much lower magnitudes than that which is normally required. Additionally, in PD, pathological changes in the basal ganglia circuitry lead to the subthalamic nucleus becoming hyperactive. As glutamatergic afferents from the subthalamic nucleus have been shown to project onto the SNc (Blandini *et al.*, 2000), it is likely that abnormally high levels of glutamate are being released in the SNc in PD. This reduced activation threshold of the NMDA receptors

combined with increased glutamate release in the SNc subsequently leads to the excessive activation of NMDA receptors which, ultimately, stimulates excitotoxic cell death by allowing the entry and accumulation of toxic levels of intracellular Ca^{2+} (Keane *et al.*, 2011). Another consequence of complex 1 dysfunction is the augmented production of free radicals at the level of the electron transport chain (Keane *et al.*, 2011). It is, therefore, thought that the toxic effects mediated by complex 1 dysfunction can also be caused by these free radicals causing oxidative damage to cellular proteins, lipids, and nucleic acids.

1.2.3. Ubiquitin Protein System Dysfunction

The ubiquitin proteasome system (UPS) constitutes the main catabolic pathway through which damaged or unwanted cellular proteins are broken down (Hegde & Upadhya, 2007). The UPS system consists of two main components. One component comprises of a series of enzymes (ubiquitin (Ub) activating, conjugating and ligating enzymes) that act to attach polyUb chains to target proteins, which marks proteins for later degradation. The 26S proteasome comprises the second component, and this multi-subunit tubular protein engulfs polyUb labelled proteins and digests them into small polypeptides. As mentioned earlier, both Ub and UPS enzymes are found within the LBs that are present in PD, and these findings provided the first evidence that UPS dysfunction might contribute to the aetiology of PD. Moreover, the presence of the inclusion bodies themselves points to a possible dysfunctioning of the UPS in PD, as inhibition of the UPS leads to the formation of inclusion bodies (McNaught *et al.*, 2004). Several other findings have also provided substantial support for a role of UPS dysfunction. Both the *parkin* and *UCH-L1* genes code for proteins of the UPS, and mutations in either of these genes cause familial forms of PD (Cordato & Chan, 2004). Proteasome activity in the SN of PD patients has been shown to be significantly lower compared to controls (McNaught *et al.*, 2003). Furthermore, proteasome inhibitors such as epoxomicin and lactacystin have been shown to induce dopamine neurone degeneration and LB inclusion formation both *in vitro* and *in vivo* (***detailed in section 3.1.1.2***). The nature of the UPS dysfunction that occurs in PD and the mechanism through which such dysfunction contributes to PD is still poorly understood, and it is currently under investigation (Olanow & McNaught, 2006).

1.2.4. Toxic Environmental Factors

Experimental, clinical and epidemiological findings have suggested that exposure to a number of environmental pesticides and metals might contribute to the aetiology of PD. It has to be noted, though, that no environmental factor has, thus far, been conclusively shown to contribute to the development of PD.

In the early sixties, MPTP was found to induce a parkinsonian syndrome nearly indistinguishable from PD, after a group of drug addicts accidentally injected themselves with this toxic heroin analogue. The toxin was later shown to also produce a PD-like syndrome in mice and primates that is associated with the selective degeneration of nigrostriatal dopamine neurones (Schober, 2004). The widespread presence of several MPTP analogues in the environment opened the possibility that environmental toxins might contribute to dopamine neurone degeneration in PD (Collins & Neafsey, 2002). Epidemiological research also identified pesticide exposure to be a risk factor for PD (Ascherio *et al.*, 2006). Furthermore, several studies have also found that a number of factors that are associated with increased exposure to industrial toxins and pesticides, including rural living, farming, and well water drinking also increase the risk of developing PD (Monte, 2001). These findings have to be interpreted with caution, however, as a nearly equal number of studies have found no association between the above mentioned factors and PD (Lai *et al.*, 2002). A number of pesticides with an analogous structure to MPTP, including o-PCB, tinuvin123, paraquat, and the B-carbolines have subsequently been reported to be toxic to dopamine neurones (Monte, 2001). Furthermore, in one study, the B-carbolines, norharman and harman and their methylation enzymes were found to be elevated in the cerebrospinal fluid of 12 out of 22 PD (Matsubara *et al.*, 1995). A few cases of sporadic PD have also been reported after exposure to paraquat (Sanchez-Ramos *et al.*, 1987), and this toxin also induces mild dopamine neurone degeneration with SNCA aggregation in mice (McCormack *et al.*, 2002). Several other pesticides unrelated to MPTP have also been implicated in PD aetiology, including rotenone, and the organochlorines (Monte, 2001). Interestingly, it has been revealed that a synergistic toxic effect on dopamine neurones is brought about when some toxins are co-administered (Monte, 2001). The two widely used pesticides, maneb and paraquat, for example, act synergistically to cause dopamine neurone degeneration when co-administered in mice (Thiruchelvam *et al.*, 2000).

A smaller body of evidence has also suggested that metal exposure might contribute to the aetiology of PD. Epidemiological research has found a range of

transition metals, including manganese, copper, iron, and mercury to increase the risk of PD after chronic occupational exposure (Gorell *et al.*, 1999). Studies with post-mortem brain tissue from normal and PD patients have provided further support for an involvement of iron. In normal brains, substantially higher concentrations of iron has been shown to be present in the SN compared to most other brain regions (Zecca *et al.*, 1994). Iron concentrations have also been shown to be increased in the SN of a group of PD patients when compared to aged matched controls (Dexter *et al.*, 1989). Through the Fenton reaction, iron has the ability to greatly enhance the conversion of H_20_2 into the hydroxyl free radical. And because H_2O_2 is produced as a by-product of dopamine metabolism, it has been suggested that increased levels of iron might contribute to dopamine neurone degeneration by augmenting oxidative stress levels in these neurones (Dexter *et al.*, 1989).

1.2.5. Neuro-Inflammation

Recent findings have indicated that neuro-inflammatory processes might also play a contributory role in causing the nigrostriatal degeneration in PD. Evidence supporting this notion comes mainly from immunohistochemical studies carried out in post-mortem brain tissue which have shown a number of inflammatory markers to be present at raised levels in the SN of PD patients. Several pro-inflammatory cytokines, including interleukin-1β (IL-1β), interleukin-6 (IL-6), tumour necrosis factor-α (TNFα), and interferon-γ (IFNγ), and also pro-inflammatory mediators, including prostaglandin-E_2 (PGE_2) are present at raised levels in glial cells within the SN of PD brains (Wu *et al.*, 2002; Teismann & Schulz, 2004; Hirsch & Hunot, 2009; Long-Smith *et al.*, 2009). Additionally, raised levels of IL-1B, IL-6, TNFα, and IFNγ have also been detected in the cerebrospinal fluid and serum of PD patients (Wu *et al.*, 2002; Hirsch & Hunot, 2009; Long-Smith *et al.*, 2009). IFNγ, TNFα, and IL-1B all stimulate increased nitrite production through a CD23-dependent mechanism in astrocytoma cultures (Hunot *et al.*, 1999; Teismann & Schulz, 2004). It has, thus, been suggested that raised levels of these cytokines in the SN might contribute to dopamine neurone cell death by increasing nitric oxide production to toxic levels by stimulating inducible nitric oxide synthetase (iNOS) activity (Hunot *et al.*, 1999). Increased production of nitric oxide has the potential to cause cytotoxic effects due to the tendency of nitric oxide to react with superoxide radicals to produce highly reactive peroxynitrite radicals, which damage

cellular proteins and DNA by forming adducts with them (Hald & Lotharius, 2005). Support for this possibility is provided by immunohistochemistry results showing increased levels of iNOS and nitrotyrosine to be present in glial and dopamine neurones in the SN of the PD brain, respectively (Hunot *et al.*, 1999). Furthermore, CD23 has been shown to be present in nigrostriatal dopamine neurones in PD but not control brains (Hunot *et al.*, 1999).

Moreover, it has been suggested that microglia, the resident immune cells of the brain might play an active role in causing this postulated neuroinflammatory-induced nigrostriatal dopamine neurone degeneration. There is a consistent and substantial increase in the number of activated microglia present in the SN of post-mortem PD brains when compared to control (Mirza *et al.*, 2000; Wu *et al.*, 2002), and using an MRI technique, increased numbers of activated microglia have also been demonstrated to be present in the midbrain in a group of early-stage PD patients (Ouchi *et al.*, 2005). This contention is, however, highly speculative as it is only based on indirect evidence showing microglia to have the capability to produce a number of molecules with cytotoxic potential when they become activated, including reactive oxygen species (ROS), reactive nitrogen species, pro-inflammatory cytokines, prostaglandins, and proteases (Banati *et al.*, 1993; Kreutzberg, 1996; Wu *et al.*, 2002; Long-Smith *et al.*, 2009). It is, however, feasible that both the activated microglia and the inflammatory markers detected in the SN of PD brains do not actually play any active role in causing the nigrostriatal neurodegeneration in PD, as no convincing direct evidence have implicated neuroinflammation to cause degeneration of nigrostriatal dopamine neurones thus far. Instead it is possible that the activated microglia and inflammatory mediators play a non-pathological passive role in regulating the phagocytosis of degenerating dopamine neurones, and that their presence in the SN of PD brains is wholly secondary to the degeneration of the dopamine neurones.

1.3. Current Pharmacological Treatments for the Motor Symptoms in PD

All of the pharmacological treatments that are currently used clinically to treat the motor symptoms of PD bring about their therapeutic effects by enhancing dopaminergic neurotransmission in the brain. The dopamine precursor, L-3,4-dihydroxyphenylalanine (L-DOPA) has been used to provide symptomatic relief for PD since the 1960s, and it still remains the gold standard pharmacological treatment for PD today (Mercuri & Bernardi, 2005). L-DOPA is usually administered orally, and as L-DOPA's central

bioavailability is significantly reduced due to extensive peripheral metabolism, it is normally co-administered with the peripheral DOPA decarboxylase inhibitor, carbidopa, which acts to greatly enhance L-DOPA's central bio-availability (Rezak, 2007). In the PD brain, L-DOPA is taken up into the remaining functional nigrostriatal dopaminergic neurones, where it enters into the dopamine synthesis pathway, and becomes converted into dopamine. L-DOPA, thus, acts to increase dopamine neurotransmission in the dopamine deficient striatum by increasing dopamine synthesis. This leads to an increase in extracellular striatal dopamine levels, which in turn acts to increase striatal dopamine receptor activation to more normal levels.

In more recent times, two additional classes of dopamine neurotransmission augmenting drugs have also come to be used routinely to treat the motor symptoms of PD, monoamine oxidase-B (MAO-B) inhibitors, and dopamine receptor agonists (Rezak, 2007). MAO-B enzymes are localised throughout the striatum, where they catalyse the breakdown of dopamine, and the MAO-B inhibitors, thus, acts to boost dopaminergic neurotransmission in the striatum by preventing the breakdown of endogenous pools of dopamine. Two MAO-B inhibitors are currently approved for the treatment of PD, selegiline and rasagiline. Selegiline only produces very mild therapeutic effects and it is for this reason rarely used clinically (Thobois *et al.*, 2005). Rasagiline, on the other hand, is a much more potent inhibitor of MAO-B, and it is more commonly used clinically, as it has been shown to provide much more effective symptomatic relief compared to selegiline (Rezak, 2007). A number of different dopamine receptors agonists are currently approved for treating PD, including ropinirole, pramipexole, and bromocriptine. This class of drugs bring about their therapeutic effect by directly activating hypostimulated dopamine receptors on the medium spiny striatal GABAergic neurones. Both rasalgiline and all of the dopamine receptor agonists, however, have inferior therapeutic efficacy when compared to L-DOPA, and as a monotherapy they only provide effective symptomatic relief in early PD (Schapira, 2009). Both the dopamine receptor agonists and the MAO-B inhibitors have nevertheless been shown to provide therapeutic benefits in advanced disease when used as adjuvant therapy in combination with L-DOPA (Singh *et al.*, 2007).

In most cases, L-DOPA treatment provides effective symptomatic relief for the motor symptoms in PD for around 3-5 years after treatment is initiated. L-DOPA, however, fails to provide satisfactory long term symptomatic relief due to the development of serious and debilitating motor complications with prolonged L-DOPA

use (Singh *et al.*, 2007). These motor complications include dyskinesias, and also so called 'on-off' and 'wearing off' phenomena. L-DOPA-induced dyskinesias or LID are involuntary movements that take either a choreic or dystonic form, and they most often coincide with peak L-DOPA plasma levels. The 'on-off' phenomenon refers to the unpredictable and transient periods when L-DOPA medicated PD patients experience a loss of therapeutically restored motor function, while the 'wearing off' phenomenon refers to the loss of motor function experienced towards the end of a specific L-DOPA dose period.

Substantial pre-clinical and clinical evidence has suggested that the pharmacokinetic properties of L-DOPA, and in particular the short half life of L-DOPA of around 60-90min is mainly to blame for causing these motor complications (Singh *et al.*, 2007). Under physiological conditions, nigrostriatal dopamine neurones fire continuously at a near constant rate, with burst firing only occurring briefly and transiently when reward is anticipated or when novel stimuli are encountered (Steiger, 2008). This predominant tonic firing pattern stimulates a tonic and sustained release of dopamine in the striatum, which in turn gives rise to a continuous tonic activation of striatal dopamine receptors. Because of the relatively short half-life of L-DOPA, treatment with L-DOPA fails to replicate this physiological tonic and continuous pattern of striatal dopamine receptor activation that is observed under normal conditions (Schapira, 2009). Instead L-DOPA therapy results in striatal dopamine receptors being stimulated in a non-physiological pulsatile manner, with peak and trough levels of dopamine receptor activation coinciding with peak and trough L-DOPA plasma concentrations after administration of each L-DOPA dose (Singh *et al.*, 2007). Moreover, it is believed that motor complications tend to increase with disease progression due to the increasingly denervated striatum becoming increasingly less able to effectively buffer striatal extracellular dopamine levels after L-DOPA dosing (Singh *et al.*, 2007).

1.4. Current Research Strategies aimed at Finding Improved Treatments for PD

Due to the serious shortcomings that are associated with the currently available drugs to treat PD, there is an urgent clinical need for new more effective pharmacological treatments, and enormous research efforts are currently focused on discovering and developing new treatments for PD. The four main research strategies aimed at finding new improved pharmacological treatments for the motor symptoms in PD include, the

development of approaches to provide a more continuous stimulation of striatal dopamine receptors, the development of non-dopaminergic drugs that are able to provide more effective symptomatic relief, the development of neurorestorative cell transplant therapies, and the development of neuroprotective drugs that can slow or halt disease progression. A brief overview of each of these research strategies is given below.

1.4.1. Strategies Aimed at Providing More Continuous Stimulation of Striatal Dopamine Receptors

As it is thought that the pulsatile activation of dopamine receptors by L-DOPA therapy is mainly to blame for causing L-DOPA induced motor complications, significant research efforts have been undertaken to develop treatment strategies that allows for a more continuous and constant activation of striatal dopamine receptors to be achieved (Rezak, 2007; Singh *et al.*, 2007; Steiger, 2008). One specific strategy has focused on trying to alter the pharmacokinetics of the current dopamine based drugs so as to achieve more sustained plasma concentrations. Even when co-administered with carbidopa, ~20% of an administered L-DOPA dose fails to enter the systemic circulation due to metabolism of L-DOPA by catechol-O-methyl transferase (COMT) enzymes located in the gut into 3-O-methyl-DOPA, a chemical derivative that acts as a false dopamine neurotransmitter (Rezak, 2007). By administering L-DOPA in combination not only with carbidopa, but also with a COMT inhibitor such as entacapone, the half life of L-DOPA can be extended from ~60-90min to ~3h (Olanow *et al.*, 2006). Although this increase in half life only gives rise to a relatively less pronounced pulsatile pattern of dopamine receptor stimulation rather than to a truly continuous stimulation pattern, clinical trials have shown supplementation of L-DOPA with COMT inhibitors to significantly increase ‘on’ time and also to decrease dyskinesias (Thobois *et al.*, 2005).

Moreover, most of the newer dopamine receptor agonists that are currently used to treat PD have relatively long half lives, and in most cases when used as mono-therapy they are associated with far fewer motor complications (Schapira *et al.*, 2006; Schapira, 2009). Attempts are, therefore, made to postpone treatment with L-DOPA for as long as possible, and to only supplement dopamine receptor agonist treatment with L-DOPA at a point in the disease progression when unsatisfactory therapeutic effects are achieved with the dopamine receptor agonist alone (Rezak, 2007). Additionally,

separate attempts have also been made to develop drug formulations and delivery systems that can provide more continuous plasma concentrations of the dopamine based drugs. A sustained release formulation of L-DOPA has for example been developed, but disappointingly it failed to show any benefits in reducing motor complications when tested in clinical trials (Steiger, 2008). Research efforts in this area are, however, still continuing, and an intra-intestinal L-DOPA delivery technique is currently being evaluated in clinical trials (Olanow *et al.*, 2006). Rotigotine, a new long acting dopamine receptor agonist delivered as a once daily patch has also recently been approved and shown to be effective as a mono-therapy in early PD and as an adjuvant in advanced disease (Rascol & Perez-Lloret, 2009). It, however, remains to be determined whether the latter approach offers any benefits in reducing L-DOPA induced motor complications.

1.4.2. Strategies aimed at Targeting Non-Dopaminergic Neurotransmitter Systems

Another one of the current main research strategies is aimed at developing new drugs that can provide symptomatic relief for the motor symptoms in PD by pharmacologically modulating non-dopaminergic targets in the brain. Receptors for a number of different non-dopaminergic neurotransmitter systems are localised not only to nigrostriatal dopamine neurones but also to various non-dopaminergic neural systems that make up the rest of the basal ganglia circuitry involved in motor function (Schapira *et al.*, 2006; Schapira, 2007; Fox *et al.*, 2008). It is thought that targeting of some of these receptors might provide symptomatic relief in PD either by modulating dopamine release from nigrostriatal dopamine neurones or alternatively by correcting dysfunctional signalling in neuronal pathways in the basal ganglia downstream of the degenerating nigrostriatal dopaminergic pathway. A number of non-dopaminergic drugs including, nicotinic acetylcholine receptor agonists, α_2 adrenergic receptors antagonists, and adenosine A2 receptor antagonists have all shown promise in animal models of PD, but subsequently failed to significantly improve motor symptoms in PD patients in clinical trials (Schapira, 2007; Singh *et al.*, 2007; Fox *et al.*, 2008; Schapira, 2009). Furthermore, substantial current research efforts are also aimed at investigating whether non-dopaminergic drugs might be able to reduce the motor complications induced by L-DOPA when they are co-administered with L-DOPA. For example, it is believed that glutamate hyperactivity in the striatum might be the cause of L-DOPA induced dyskinesias, and NMDA and 2-amino-3-(5-methyl-3-oxo-1,2- oxazol-4-yl)

propanoic acid (AMPA) receptor antagonists have been evaluated for their ability to reduce dyskinesias in PD patients in clinical trials, but they were shown to be ineffective (Fox *et al.*, 2008). Various subtypes of 5-hydroxytryptamine (5HT) receptors are localised throughout the basal ganglia circuitry, and a number of different drugs targeting 5HT receptors, including antagonists at the $5HT_2$, $5HT_{2A}$, $5HT_{2C}$ receptors, and agonists at $5HT_{1B}$ receptors have been shown to reduce L-DOPA induced dyskinesias in animal models, but they remain to be evaluated in clinical trials (Schapira *et al.*, 2006; Fox *et al.*, 2008).

1.4.3. Strategies Aimed at Developing Neurorestorative Cell Transplant Therapies

Over the last 30 years, substantial research efforts have been focused on developing a neurorestorative cell transplant therapy for PD. As discussed earlier, the motor symptoms in PD results from the selective degeneration of a specific subset of dopaminergic neurones that are anatomically localised within the nigrostriatal dopaminergic pathway, a distinct and well defined area of the brain. These features make PD a technically viable disease candidate for cell transplantation therapies, as only a single subset of neurones need to be transplanted into a single well defined target site within the brain. The first evidence that cell transplant therapies might be able to restore motor function in PD was provided by experiments in which allogeneic rodent adult adrenal medullary or foetal mesencephalic tissue was grafted into the dopamine depleted striatum of 6-hydroxydopamine (6OHDA) lesioned rats (Drucker-Colin & Verdugo-Diaz, 2004). Foetal ventral mesencephalic tissue was used in these experiments because it contains the embryonic dopaminergic neurones that develop into the nigrostriatal dopaminergic tract in adults. Adrenal medullary tissue, on the other hand, was used because it is primarily composed of neuroendocrine chromaffin cells that are able to synthesise, store, and release a number of different catecholamine neurotransmitters. Results from these studies demonstrated that although only a small percentage of the transplanted cells survived, a population of the surviving cells retained a dopaminergic phenotype, and these neurones sprouted nerve terminals that reinnervated the striatum (Snyder & Olanow, 2005). Importantly the transplants also alleviated the motor deficits present in the 6OHDA lesioned rats. Over the course of the following two decades, a number of both open label and double blind randomised clinical trials were subsequently carried out to assess the effectiveness of these cell transplantation approaches in PD (Snyder & Olanow, 2005). In these studies, a number

of different transplantation techniques were used to graft either allogeneic adrenal medullary tissue or foetal mesencephalic tissue obtained from aborted foetuses into the caudate putamen of PD patients. Post-mortem histological results from some of these studies demonstrated that, as was observed in the pre-clinical studies, only a small number of the transplanted cells survived in the long term (Snyder & Olanow, 2005). Importantly, some of the surviving transplanted cells were found to have retained a dopaminergic phenotype, and these surviving dopaminergic neurones sent out projections that reinnervated the striatum. However, disappointingly, although the transplants alleviated motor deficits in some individual patients in the initial open label studies, foetal mesencephalic transplants were found not to provide significant clinical benefits in all of the large double blind randomised studies (Drucker-Colin & Verdugo-Diaz, 2004). Worryingly, the transplants also induced severe and debilitating off-medication dyskinesias in a large proportion of the PD patients that received the transplants (Snyder & Olanow, 2005). A number of hypotheses have been put forward to explain both the lack of efficacy of the transplants and the dyskinesias induced by the transplants. Some researchers have argued that it is primarily technical problems that have limited the success of the trials carried out, thus far, and it is believed that the approach has the potential to offer significant clinical benefit if the transplant techniques are optimised to overcome these problems. It is, for instance, believed that the lack of efficacy of the transplants is due to an insufficient number of the transplanted cells surviving to provide a therapeutic degree of reinnervation of the striatum (Correia *et al.*, 2005). A number of different factors have also been put forward as being potential causes of the transplant-induced dyskinesias, including uneven reinnervation of the striatum by the transplanted cells, inflammation around the implantation site, and the heterologous cell composition of the transplanted tissue, which results in the transplanted tissue containing not only dopaminergic neurones but also several other cell types (Correia *et al.*, 2005). In the case of foetal mesencephalic transplants, the graft tissue often contains large populations of serotonergic neurones, and there is evidence that release of serotonin by these neurones in the striatum stimulates dysfunctional signalling in the basal ganglia circuitry that leads to the transplant-induced dyskinesias (Wakeman *et al.*, 2011). Current research efforts are, therefore, attempting to develop a transplant procedure that increases the survival of the transplanted cells, and which also eliminates or reduces the factors that are thought to induce dyskinesias.

However, even if an optimal clinically effective transplant procedure is developed, the widespread use of ventral mesencephalic transplants for the treatment of PD would be prohibited by graft tissue supply constraints, as ~6-8 aborted foetuses of a specific developmental stage is needed for each transplant procedure (Taylor & Minger, 2005). Additionally, ethical issues prevent the use of tissue from aborted foetuses in many countries. Therefore, in recent years, PD cell transplant research has focused mainly on finding better sources of graft tissue material rather than on optimising foetal mesencephalic transplant procedures. Recent findings have indicated that stem cells hold the potential of being the ideal source of graft tissue for PD transplants. Stem cells are undifferentiated progenitor cells, and it is believed that the capability of these cells not only to self-amplify but also to differentiate into a number of different cell types means that they have the potential to provide an infinite supply of dopaminergic grafting material for transplants. A number of different types of stem cells are found throughout the developing and adult body, and some are pluripotent and able to differentiate into any of the cells that make up the body, while others are multipotent, and only able to differentiate into a more limited number of cell types. A number of different types of stem cells have been demonstrated to have potential in PD transplant therapies, including embryonic stem cells (ESCs), neural stem cells (NSCs), and induced pluripotent stem cells (iPSCs).

ESCs are pluripotent stem cells that are derived from the inner cell mass of the pre-implantation blastocyst. Protocols have been developed to not only maintain and expand ESCs in culture, but also to differentiate them into neurones with a dopaminergic phenotype. When these ESC-derived dopaminergic neurones are transplanted into the dopamine depleted striatum of animals with nigrostriatal lesions, a proportion of the dopamine neurones in the grafts not only survive but also reinnervate the striatum, and, importantly, the grafts have been demonstrated to bring about a robust improvement in the motor symptoms present in the lesioned animals. A number of different protocols are currently available to differentiate ESCs from mice, monkeys, and humans into dopaminergic neurones, and, importantly, ESC-derived dopaminergic neurone transplants derived from all of the latter species have also been shown to be effective in animal models of PD, both in terms of obtaining reinnervation of the dopamine depleted striatum and alleviating motor deficits (Kawasaki *et al.*, 2000; Kim *et al.*, 2002; Takagi *et al.*, 2005; Brederlau *et al.*, 2006; Chung *et al.*, 2006; Roy *et al.*, 2006; Rodriguez-Gomez *et al.*, 2007; Sonntag *et al.*, 2007; Chiba *et al.*, 2008; Cho *et*

al., 2008; Hedlund *et al.*, 2008; Sanchez-Pernaute *et al.*, 2008; Friling *et al.*, 2009; Lonardo *et al.*, 2010; Kriks *et al.*, 2011). In the initial ESC transplant experiments, the same two main problems were encountered with ESCs derived from all of the abovementioned species. Only a small number of dopaminergic neurones in the grafts were found to survive in the long term, and this was thought to be mainly due to the initial un-optimised differentiating protocols giving rise to poor yields of dopamine neurones (Kawasaki *et al.*, 2000; Kim *et al.*, 2002; Brederlau *et al.*, 2006). The second major problem was that many of the grafts developed into teratomas after transplantation (Kawasaki *et al.*, 2000; Kim *et al.*, 2002; Roy *et al.*, 2006; Sonntag *et al.*, 2007; Chiba *et al.*, 2008). Improved differentiating protocols have, however, subsequently been developed which have overcome both of these limitations. Optimised differentiation protocols have been developed that produce a high yield of dopaminergic neurones from mice, monkey and human ESCs, and the increased dopamine neuron yields have been shown to give rise to increased survival rates after grafting (Kim *et al.*, 2002; Chung *et al.*, 2005; Roy *et al.*, 2006; Sonntag *et al.*, 2007; Chiba *et al.*, 2008; Cho *et al.*, 2008; Friling *et al.*, 2009; Lonardo *et al.*, 2010; Kriks *et al.*, 2011). Additionally, the risk of teratoma formation has been greatly reduced by using fluorescence-activated cell sorting techniques to select only cells with a committed neural lineage for transplantation, and, by doing so, greatly reducing the number of tumourigenic pluripotent stem cells that are included in a transplant (Chung *et al.*, 2006; Hedlund *et al.*, 2008; Friling *et al.*, 2009). Alternatively, teratoma formation has also been shown to be eliminated or reduced through the use of relatively long differentiation protocols which yield transplants containing primarily post-mitotic cells, and not many undifferentiated cells with tumourigenic potential (Sonntag *et al.*, 2007; Sanchez-Pernaute *et al.*, 2008; Kriks *et al.*, 2011).

NSCs are multipotent stem cells that are committed to a neural lineage, and they are found in a number of different regions of the developing and adult brain. As with ESCs, protocols have also been developed to differentiate NSCs derived from the embryonic ventral mesencephalon of rats and humans, and also form the subventricular zone (SVZ) of embryonic rats into dopamine neurone enriched cultures, and NSC-derived dopaminergic neurone transplants derived from all of the latter species have been shown to be effective in animal models of PD, both in terms of obtaining reinnervation of the dopamine depleted striatum and alleviating motor deficits (Studer *et al.*, 1998; Sanchez-Pernaute *et al.*, 2001; Shim *et al.*, 2007; O'Keeffe *et al.*, 2008; Parish

et al., 2008). A significant advantage that the NSC-derived transplants have over ESC-derived transplants is that they appear to have a very low tumourigenic potential, as no teratomas have, thus, far, been recorded in any of the studies with NSC-derived transplants. As with the ESC-derived transplants, only minimal survival of the grafted dopaminergic neurones was achieved with some of the initial NSC differentiation protocols (Studer *et al.*, 1998; Sanchez-Pernaute *et al.*, 2001; Shim *et al.*, 2007). This problem has, however, also been overcome by the recent development of optimised NSC differentiating protocols that give rise to greatly improved yields of dopaminergic neurones, which after transplant demonstrate robust and high levels of survival of functional integrated dopaminergic neurones (O'Keeffe *et al.*, 2008; Parish *et al.*, 2008).

iPSCs are produced by converting differentiated somatic cells into pluripotent stem cells. This reprogramming of somatic cells into stem cells is achieved by altering transcription factor activity in somatic cells with the use of genetic engineering techniques and also by adding a number of different de-differentiation factors to the cells (Wijeyekoon & Barker, 2009). These stem cells have the potential to become the most favourable graft tissue source, as iPCSc are able to yield autogeneic graft tissue; and this would avoid all the problems of immune rejection that are associated with not only foetal mesencephalic transplants but also with transplants carried out with ESCs and NSCs, as the currently available techniques only allow the later two stems to be derived from allogeneic sources. One group has developed a protocol that not only converts fibroblasts into pluripotent stem cells, but which subsequently also brings about the differentiation of a population of these pluripotent cells into dopamine neurones (Wernig *et al.*, 2008). Striatal transplantation of these iPSC-derived cell populations enriched for dopaminergic neurones into 6OHDA lesioned rats brought about an improvement of motor function (Wernig *et al.*, 2008). However, although some of the transplanted cells survived and also retained a dopaminergic phenotype, it was only a very small proportion of the transplanted cells, and worryingly, some of the cells were found to have developed into teratomas. Unlike the ESC and NSC techniques, optimised procedures, thus, still need to be developed for iPSCs to overcome the above two issues.

Despite the tremendous progress that has, thus, far been made, clinical trials with stem cell derived grafting tissue are, however, still a long way off, as substantial pre-clinical testing in animal models of PD would be needed not only to develop an optimal standardised grafting procedure that allows for the long term survival and

integration of a sufficient number of dopaminergic neurones into the striatum, but also to extensively evaluate the effectiveness and safety of the procedure. Importantly, it needs to be specifically demonstrated that a standardised differentiation protocol and transplantation procedure leads to robust and consistently reproducible improvements in motor function in animal models, and also that the procedure has a low risk of causing cancerous growths and other adverse effects such as dyskinesias.

1.4.4. Strategies Aimed at Finding Neuroprotective Treatments that can Slow Disease Progression

In PD, there is a progressive loss of nigrostriatal dopamine neurones over many years, with motor deficits only appearing once more than ~60% of dopamine neurones in the SNc are lost (Dauer & Przedborski, 2003). A major shortcoming of all of the currently available treatments for PD is that they only provide symptomatic relief for the motor symptoms of PD, and they do nothing to slow down the ongoing degeneration of the remaining functional dopaminergic neurones (Peterson & Nutt, 2008). The third main current research strategy aimed at finding new pharmacological treatments for PD is, therefore, aimed at developing new treatments that are able to slow down the ongoing nigrostriatal degeneration in PD. Such neuroprotective drugs have the potential to bring about the greatest therapeutic benefit, as unlike the currently available therapies, they would be able to slow down or halt disease progression. So far, most rational drug design strategies aimed at developing new neuroprotective drugs for PD have aimed at investigating the neuroprotective potential of agents that either stimulate dopamine neurone survival (***see section 1.5 below***) or drugs that counter one or more of the putative aetiological causes of nigrostriatal degeneration in PD that have been identified, thus far; including, oxidative stress, mitochondrial dysfunction, and neuro-inflammation. Many agents that counteract the putative pathological processes involved in PD have, indeed, been shown to have neuroprotective effects in animal models of PD including, for example anti-oxidants, anti-apoptotic agents, iron chelators, and inhibitors of glutamate signalling (Thobois *et al.*, 2005; Schapira, 2007; Singh *et al.*, 2007; Fox *et al.*, 2008; Schapira, 2009). A number of agents have also been tested for their neuroprotective potential in clinical trials, including the following selected examples. Coenzyme Q_{10} is a component of the electron transport chain and it has been tested in clinical trials for its neuroprotective effects based on the rationale that it might help to correct the mitochondrial dysfunction present in the PD brain (Hauser, 2010). A number

of agents with anti-oxidant properties, including vitamin E and the MAO-B inhibitors have also been tested based on the logic that they might counteract the increased levels of oxidative stress that is present in the PD SN (Hauser, 2010). However, unfortunately no treatment has, thus, far, been conclusively shown to have significant and clinically relevant neuroprotective effects in clinical trials with PD patients (Hauser, 2010). Additionally, anti-inflammatory treatments might also be able to provide neuroprotection in PD, as a number of agents with anti-inflammatory activities have been shown to have neuroprotective effects in animal models of PD, including dexamethasone, cyclo-oxygenase-2 (COX2) inhibitors, minocycline, naloxone, and vasoactive intestinal peptide (Gao *et al.*, 2003; Liu, 2006). None of these drugs have however been evaluated in clinical trials thus far, and as most of the aforementioned drugs have additional pharmacological actions that don't target inflammatory processes, it remains to be conclusively shown that their neuroprotective effects do actually stem from their anti-inflammatory effects rather than from their other actions.

1.5. The Potential of Growth Factors as Neuroprotective Treatments for PD

It has long been known that neurotrophic growth factors have the capability to stimulate the survival of neuronal cells, and that the presence of specific growth factors in the intact adult brain is essential in allowing for the survival of specific populations of neurones (Dawbarn & Allen, 2003). For this reason, substantial research efforts have focused on evaluating whether neurotrophic growth factors might have neuroprotective potential in PD, and recent pre-clinical findings have identified numerous neurotrophic growth factors that do (Peterson & Nutt, 2008). It is believed that neurotrophins will, at worse, be able to stimulate the survival and functioning of the remaining dopamine neurones, and, by doing so, potentially either halt or slow the progression of PD (Peterson & Nutt, 2008). At best, neurotrophins might also be able to stimulate the regeneration of non-functional dopamine neurones, leading to a restoration of lost motor function.

Pre-clinical experiments have identified a myriad of neurotrophins that have potential in treating PD, including fibroblast growth factor-2 (FGF2), insulin like growth factor (IGF), epidermal growth factor (EGF), transforming growth factor alpha (TGF-α), interleukins, TNF-α, IFN-γ, conserved dopamine neurotrophic factor (CDNF), brain-derived neurotrophic factor (BDNF), and glial-derived neurotrophic factor (GDNF) (Unsicker, 1994; Peterson & Nutt, 2008). Of these growth factors, GDNF has

been investigated the most thoroughly (Kirik *et al.*, 2004). In rats and monkeys, centrally administered GDNF protects nigrostriatal dopamine neurones against 6OHDA, and MPTP-induced cell death, respectively (Sullivan *et al.*, 1998; Grondin *et al.*, 2002). In an initial small clinical trial, GDNF significantly improved motor deficits in a group of PD patients when delivered directly into the putamen (Gill *et al.*, 2003). However, in a number of subsequent clinical trials, centrally delivered GDNF failed to show any benefit in late-stage PD patients (Kirik *et al.*, 2004). The lack of effect is believed to be due to GDNF not reaching its target receptors on dopamine neurones, as a result of limited diffusion from the infusion site. Thus, although there are still some technical problems to overcome to allow the effective delivery of neurotrophins, the results achieved with GDNF have provided support for the effectiveness of neurotrophins in treating PD.

1.6. Neuroprotective Potential of FGF20 in PD

Fibroblast growth factor-20 (FGF20) has recently been identified to be another growth factor that could have neuroprotective potential in PD (***see section 4.1.5 for more details***). In the rat, mRNA for FGF20 is present in the embryonic midbrain, and in the adult brain, FGF20 mRNA is localised in both the SN and the striatum (Ohmachi *et al.*, 2003; Grothe *et al.*, 2004). *In vitro*, recombinant human FGF20 protects rat ventral mesencephalic (VM) embryonic dopamine neurones against serum withdrawal, glutamate toxicity, and 6OHDA-induced cell death (Ohmachi *et al.*, 2000; Ohmachi *et al.*, 2003; Murase & McKay, 2006). Moreover, evidence from biochemical and genetic studies in humans have indicated that dysfunctioning of FGF20 signaling and also fibroblast growth factor (FGF) signaling in general might play a role in the aetiology of PD. In the SNc, the prototypic FGF family member, *FGF2* is abundantly present in post-mortem control brains, but nearly completely absent in PD brains (Tooyama *et al.*, 1994), and a number of FGF20 SNP polymorphisms have been found to be associated with an increased risk of PD (***detailed in section 4.1.5***). The above findings taken together with results from post mortem studies showing FGFR1 to be present in the remaining SNc dopamine neurones of PD patients (Walker *et al.*, 1998), provide convincing support that exogenous application of FGF20 to the nigrostriatal tract might have neuroprotective therapeutic potential in PD.

1.7. Overall Aims of this Thesis

As detailed above and expanded on in more detail in Chapter 3 (***section 4.1.5***), recent findings have demonstrated FGF20 to have neuroprotective potential in PD, and the main aim of this thesis was to further investigate FGF20's neuroprotective effects on dopamine neurones. FGF20 has previously been shown to have neuroprotective effects on dopamine neurones, *in vitro*. And two of the primary aims of this thesis were, firstly, to confirm FGF20's previously reported *in vitro* neuroprotective effects, by testing whether FGF20 is able to protect VM embryonic dopamine neurones against 6OHDA, and, secondly, to evaluate for the first time whether FGF20's neuroprotective effects on dopamine neurones are also present *in vivo*, in the partially lesioned 6OHDA rat model of PD.

Prior to carrying out the planned *in vitro* and *in vivo* neuroprotection studies with FGF20, it was important to ensure that FGF20's receptors, the fibroblast growth factor receptors (FGFRs) were, indeed, present in both of the abovementioned model systems. Therefore, in Chapter 2, immunohistochemistry studies were carried out with the aim of characterising, in detail, the colocalisation profiles of FGF20, and the FGFR1, 3, and 4 in both VM cultures, and in the nigrostriatal tract of the rat brain.

In Chapter 3, 6OHDA dose-response experiments were carried out with the aim of establishing an appropriate partially lesioned 6OHDA rat model of PD in which FGF20 could be evaluated for its neuroprotective effects on dopamine neurones, *in vivo*. Furthermore, to successfully evaluate FGF20's neuroprotective efficacy, *in vivo*, it was essential that a biologically active dose of the growth factor was tested in the planned neuroprotection study. Experiments were, thus, also carried out – in which phosphorylated extracellular regulated kinase-1/2 (phospho-ERK1/2) was used as a marker of FGF20 stimulated FGFR activation - with the aim of identifying a biologically active intra-nigrally delivered dose of FGF20.

In Chapter 4, studies were carried firstly to confirm FGF20's *in vitro* neuroprotective effects, by testing whether FGF20 is able to protect VM embryonic dopamine neurones against 6OHDA, and secondly to determine if FGF20's neuroprotective effects are also present *in vivo*, by evaluating whether FGF20 is able to protect nigrostriatal dopamine neurones in the partially lesioned 6OHDA rat model of PD that was established in Chapter 3. Evidence from a number of studies has indicated that one of the physiological roles of the endogenous FGF system in the nigrostriatal

tract is to stimulate and maintain the survival of dopamine neurones. An additional aim of Chapter 4 was to determine if the endogenous FGF system does, indeed, play a role in protecting nigrostriatal dopamine neurones by evaluating whether chronic pharmacological inhibition of FGFR signaling potentiates 6OHDA-induced nigrostriatal dopamine neurone degeneration in the rat.

In Chapter 5, cell viability studies were carried out in PC12 cells with the aim of investigating the signalling mechanisms mediating FGF20's neuroprotective effects against 6OHDA. More specifically, it was evaluated whether FGF20's neuroprotective effects are, indeed, mediated by the FGFRs, and at the intracellular level, experiments were carried out to determine if FGF20's neuroprotective effects are mediated by the extracellular regulated kinase-1/2 (ERK1/2) mitogen activated protein kinase (MAPK) pathway. The heparin sulphate proteoglycans (HSPGs) play an important role in modulating FGF signaling, and the HSPG, agrin when co-applied with FGF2, potentiates both FGF2-stimulated ERK1/2 activation and neurite outgrowth in PC12 cells. In chapter 5 it was evaluated, firstly, whether agrin is able to potentiate FGF20 induced ERK1/2 activation, and, secondly, if agrin potentiates FGF20's neuroprotective effects against 6OHDA toxicity in the PC12 cells. When taken together, it was hoped that the results generated from all of the studies undertaken as part of this thesis would further research efforts aimed at characterising the neuroprotective potential of FGF20 in the treatment of PD.

Chapter 2: Immunohistochemical Localisation of FGF20 and FGFR 1, 3, and 4 in the Rat Nigrostriatal Tract and in Ventral Mesencephalic Embryonic Dopamine Neurone Cultures

2.1. Introduction

2.1.1. The Fibroblast Growth Factor Family

The fibroblast growth factor (FGF) family is a group of structurally related polypeptide growth factors, currently composed of 23 members, FGF1-23 (Reuss & von Bohlen und Halbach, 2003). The prototypic FGFs, FGF1 and FGF2, were the first two FGFs to be discovered, and were originally called acidic and basic fibroblast growth factor, due to the acidic and basic iso-electric points associated with the proteins, respectively, and because of FGF2's mitogenic effects on fibroblasts (Rudland *et al.*, 1974; Esch *et al.*, 1985). When the FGF family was shown to contain numerous members, a nomenclature was adopted in which each FGF family member is distinguished by a numerical suffix indicating the sequential order in which it was identified. The molecular weight of the different FGF family members varies between 17-34kDa, and the family members all share a similar general peptide structure, with there being 13-71% amino acid homology between the different members. The FGFs are distributed widely throughout most tissues of both the developing and adult body, and they function to regulate a diverse range of physiological processes, including differentiation, mitogenesis, cell survival, and angiogenesis (Eswarakumar *et al.*, 2005). In the central nervous system (CNS), the FGFs play a crucial role in regulating the development of the brain during embryogenesis (Dono, 2003; Thisse & Thisse, 2005), and in the adult CNS, the FGFs have specifically been shown to regulate differentiation, neural plasticity, and neuronal survival in a number of different brain areas (Eckenstein, 1994; Reuss & von Bohlen und Halbach, 2003). In the neurogenic areas of the brain, including the subventricular zone and the subgranular zone, the FGFs play an important role in regulating neurogenesis (Dono, 2003; Reuss & von Bohlen und Halbach, 2003). Importantly, the FGFs have also been demonstrated to play a role in regulating the repair processes that are initiated after injury of the nervous system (Reuss & von Bohlen und Halbach, 2003).

2.1.2. The Fibroblast Growth Factor Receptors

The FGFs mediate their biological effects by activating their membrane bound receptor tyrosine kinases (RTKs), the FGFRs. There are four subtypes of FGFRs referred to as the FGFR-1, 2, 3, and 4, and all four subtypes are composed of ~820 amino acids (Johnson *et al.*, 1990). The FGFRs have a general structure similar to that found in most other RTKs. Thus, they consist of an extracellular N-terminal ligand binding domain, a single transmembrane domain, and an intracellular C-terminal domain containing the protein kinase catalytic activity of the receptor. A unique feature of the FGFRs is the presence of three immunoglobulin (Ig)-like domains in the extracellular C-terminal domain of the receptors (***Fig. 2.1***). The Ig-like domain closest to the N-terminal of the receptor is referred to as D1, while the middle and juxtamembrane Ig-like domains are called D2 and D3, respectively (Johnson *et al.*, 1990). The peptide sequence linking D1 and D2 is rich in acidic residues and is referred to as the acid box. There is a relatively high degree of amino acid sequence homology between the four FGFR subtypes (Eckenstein, 1994). In the D1, D2, and D3 Ig-like domains, the degree of sequence homology ranges from 19-40%, 61-79%, and 74-81% between the 4 receptor subtypes, respectively. As expected the highest degree of amino acid sequence homology (75-92%) is found in the tyrosine kinase domains of the FGFRs.

Different isoforms of each of the FGFR subtypes have been shown to exist. Each FGFR subtype is coded for by a single gene, and alternative splicing of the genes gives rise to the different isoforms. The FGFR1, 2, and 3 all exist as two prototypical FGFR isoforms, referred to as the b and c isoforms (Johnson *et al.*, 1991). The C-terminal half of the D3 Ig-like domain of the FGFRs is only coded for by a single exon. The juxtamembrane half of D3, on the other hand, can be coded for by either exon 8 or exon 9 of the FGFR gene, giving rise to the b and c isoforms of the receptor, respectively (***Fig. 2.1***). The D3 domain plays an important role in ligand binding, and accordingly the b and c isoforms display substantial differences in their affinities for the various FGF ligands (Yayon *et al.*, 1992). It appears that the FGFR4 (Johnson *et al.*, 1991) does not exist as these prototypical b and c isoforms, but 3 alternative isoforms of this receptor have nevertheless also been identified (van Heumen *et al.*, 1999; Ezzat *et al.*, 2001; Kwiatkowski *et al.*, 2008). All 3 of the additional FGFR4 isoforms have been shown to consist of C-terminal truncated forms of the FGFR4. Two of the isoforms results from the alternative splicing of intron 17 of the FGFR4 gene (van Heumen *et al.*, 1999), while one is the product of an mRNA splice variant lacking exon 16

(Kwiatkowski *et al.*, 2008). Furthermore, in addition to the membrane bound FGFRs, soluble forms of the FGFR subtypes have also been identified (Root & Shipley, 2000). Their function is not well understood, but it is thought that they might be secreted extracellularly, where they could modulate FGFR activation by competing with membrane bound FGFRs for binding of FGFR ligands.

Figure 2.1. Structure of the FGFRs

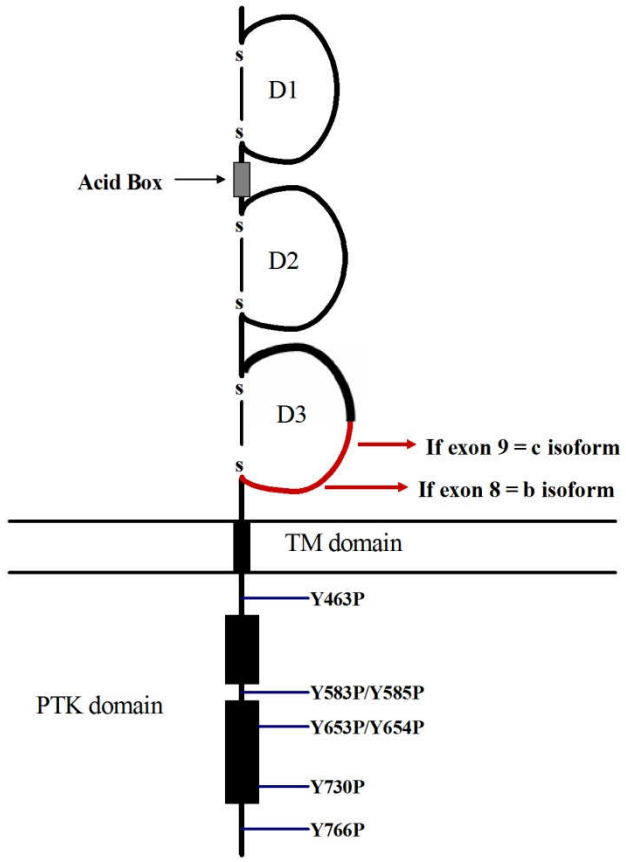

Figure 2.1. General structure of the fibroblast growth factor receptors (FGFRs). Similar to other receptor tyrosine kinases (RTKs), the FGFRs are composed of an extracellular N-terminal ligand binding domain, a single transmembrane (TM) domain, and an intracellular C-terminal domain containing the protein tyrosine kinase (PTK) activity. A distinguishing feature of the FGFRs is the presence of 3 immunoglobulin (Ig)-like domains (D1-D3) in its N-terminal domain. A run of acidic residues (the acid box) connects D1 to D2. Alternative splicing of genes coding for the FGFR1-3 subtypes give rise to b and c isoforms for each of these receptors. C-terminal tyrosine (Y) autophosphorylation sites are depicted.

2.1.3. Localisation of the FGFs in areas of the Brain other than the Nigrostriatal Tract

Of the 23 FGFs, 13 have so far been localised to the adult brain including, FGF1, FGF2, FGF4, FGF5, FGF8, FGF9, FGF10, FGF14, FGF20, FGF22, and FGF23 (Bean *et al.*, 1991; Goldfarb *et al.*, 1991; Kuzis *et al.*, 1995; Yamamoto *et al.*, 2000; Yamashita *et al.*, 2000; Nakatake *et al.*, 2001; Hajihosseini *et al.*, 2008; Shakkottai *et al.*, 2009). Of these 13, the mRNA and protein localisation profiles of only FGF1 and FGF2 have been comprehensively characterised in the rodent brain using *in situ* hybridization and/or immunohistochemistry (Gonzalez *et al.*, 1995; Kuzis *et al.*, 1995). The localisation profile of FGF10 in the mouse brain has been comprehensively studied using a genetically transfected FGF10 reporter gene system (Hajihosseini *et al.*, 2008). FGF1 and FGF2 mRNA and protein have been shown to be distributed widely throughout the brain, with both being found in nearly all areas of the brain (Gonzalez *et al.*, 1995). Additionally, FGF2 was shown to be present in nearly all cell types found in the CNS, including neurones, glial cells, ependymal and subependymal cells, endothelial cells, as well as cells that make up the meninges (Gonzalez *et al.*, 1995). FGF1, on the other hand, appears to be preferentially found in glial cells, although it is also present in some neurones (Kuzis *et al.*, 1995). FGF10 was found to be expressed in the cerebellum, thalamus, hindbrain, hippocampus, telencephalon, hypothalamus, pituitary gland, and also in ependymal cells (Hajihosseini *et al.*, 2008). In non-comprehensive studies utilising *in situ* hybridisation studies, FGF5 was localised to the hippocampus, thalamus, and the cerebral cortex (Goldfarb *et al.*, 1991), while FGF23 was localised to the ventromedial thalamic nucleus (Yamashita *et al.*, 2000). In another study, FGF14 mRNA and protein was shown to be present in granule and purkinje cells in the cerebellum (Shakkottai *et al.*, 2009).

2.1.4. Localisation of the FGFRs in areas of the Rat Brain other than the Nigrostriatal Tract

Using *in situ* hybridisation, the mRNA expression patterns of the 4 FGFRs have been comprehensively characterised in the adult rat brain in a number of studies (Wanaka *et al.*, 1990; Yazaki *et al.*, 1994; Belluardo *et al.*, 1997). The latter studies found only the FGFR1, 2, and 3 to be expressed in the rat brain, with mRNA for FGFR4 being found to be undetectable in all areas of the brain. Recent findings have, however, shown this to

be incorrect, as it has been robustly demonstrated that mRNA for the FGFR4 is abundantly present in the medial habenula (MHB), where FGFR4 mRNA is expressed in cholinergic neurones (Miyake & Itoh, 1996). In contrast to FGFR4, FGFR1, 2, and 3 have been shown to have a widespread distribution in the brain, with mRNA for all three of the receptors being present in numerous structures within the telencephalon, diencephalon, mesencephalon, metencephalon, and myelencephalon (Yazaki *et al.*, 1994; Belluardo *et al.*, 1997). All three of the receptors are particularly abundantly expressed in the lower brainstem and the cerebellum. In the diencephalon and telencephalon – with the exception of the hippocampal formation – mRNA encoding the receptors is expressed at substantially lower levels or not at all. Furthermore, mRNA for FGFR1, 2, and 3 is expressed abundantly in several physiologically and pathologically important nuclei, including the substantia nigra (SN), the locus coeruleus (LC), the dorsal raphe nucleus (DRN), and two cholinergic nuclei (the pedunculopontine and laterodorsal tegmental nuclei) (Wanaka *et al.*, 1990; Yazaki *et al.*, 1994; Belluardo *et al.*, 1997). Moreover, in most areas of the brain, FGFR1 mRNA was shown to be present predominantly in neurones, although it is also found at low levels in non-neuronal/glial tissues and cells (white matter, pia mater, the choroid plexus, and ependymal cells) (Wanaka *et al.*, 1990; Yazaki *et al.*, 1994; Belluardo *et al.*, 1997). In contrast, it appears that FGFR2 and FGFR3 mRNA is mainly found in glial cells.

Thus far, the localisation profile of only the FGFR2 *protein* has been systematically characterised in the rat brain with immunohistochemistry (Chadashvili & Peterson, 2006). In this study, the localisation profile of the FGFR2 protein was shown to be comparable to its mRNA expression profile, as the FGFR2 protein was found to be present in most areas of the brain. The FGFR2 protein was demonstrated to only be present in astrocytes in all of the areas evaluated, confirming the assertion made in previous *in situ* hybridisation studies that FGFR2 mRNA is preferentially expressed in glial cells (Wanaka *et al.*, 1990; Yazaki *et al.*, 1994; Belluardo *et al.*, 1997). Immunohistochemical studies describing localisation profiles of FGFR1, 3, and 4 in the brain are currently lacking. FGFR1 protein has, however, been reported to be present in astrocytes in the cerebral cortex (Clarke *et al.*, 2001), and in the ventral tegmental area, where FGFR1 was shown to be present in dopamine and GABAergic neurones, and also in astrocytes (Flores *et al.*, 2010). Another study has characterised the localisation of FGFR1 and 3 in the hippocampus (Ferrer & Marti, 1998). FGFR1 was shown to be

present in nearly all of the hippocampal neurones, while FGFR3 was only present in astrocytes within the hippocampus.

2.1.5. Localisation of the FGFs and the FGFRs in the Nigrostriatal Tract of the Rat Brain

An important physiological role for the FGF system in the nigrostriatal dopaminergic tract is suggested by the abundant presence of a number of FGFs and FGFRs in this pathway. Thus far, 5 of the FGF family members have been detected in the nigrostriatal tract of the brain, FGF1, 2, 8, 9, and 20. As with other areas of the brain, the localisation profiles of the prototypical FGFs, FGF1 and FGF2, within the nigrostriatal tract have been characterised the most thoroughly. FGF1 and FGF2 mRNA and protein have been localised to both the SN and the striatum (Bean *et al.*, 1991; Kuzis *et al.*, 1995; Claus *et al.*, 2004), and in the SNc, both FGF1 and 2 specifically localizes to dopamine neurones (Bean *et al.*, 1991; Claus *et al.*, 2004). In both the SN and striatum, it appears that FGF1 is mainly present in neurones, while FGF2 is found in both neuronal and glial cells (Bean *et al.*, 1991; Kuzis *et al.*, 1995; Claus *et al.*, 2004). The striatal localisation of FGF1 and 2 have been demonstrated in only the rat (Kuzis *et al.*, 1995; Claus *et al.*, 2004), while the nigral localisation has been shown in the rat, monkey, and human brain (Bean *et al.*, 1991; Kuzis *et al.*, 1995; Claus *et al.*, 2004). FGF8, 9, and 20 have only more recently been shown to be present in the nigrostriatal tract, and their localisation profiles have, thus far, been characterised less comprehensively. In the human brain, the FGF8 protein has been localised to dopamine neurones in the substantia nigra (Tanaka *et al.*, 2001), whereas the FGF9 protein has been shown to be present in the SN and in the striatum in both the human and the rat brain (Todo *et al.*, 1998). In the rat brain, FGF9 was found to be present mainly in neurones within both the SN and striatum, with only a few astrocytes staining weakly positive for FGF9, and in the human nigrostriatal tract, reactive astrocytes stained positive for FGF9 (Todo *et al.*, 1998). In the rat brain, mRNA for FGF20 has also been shown to preferentially localise to the SNc and the striatum (Ohmachi *et al.*, 2003; Grothe *et al.*, 2004).

Both *in situ* hybridisation and PCR studies have demonstrated that the mRNA transcripts encoding FGFR1, 2, and 3 are present in both the striatum and the SN (Yazaki *et al.*, 1994; Gonzalez *et al.*, 1995; Belluardo *et al.*, 1997; Claus *et al.*, 2004). In the Claus *et al.*, 2004 study, it was also specifically evaluated if FGFR4 mRNA is present in the striatum and SN, but none were detected. In the SNc and SNr, FGFR1 mRNA was present at moderately high levels in a large percentage of the neuronal cells

that were present in the area, whereas FGFR2 and 3 mRNA were expressed at low to moderate levels in a small percentage of the glial cells present in the area (Belluardo *et al.*, 1997). In the striatum, FGFR1 mRNA was not detected at all, while mRNA for both FGFR2 and 3 were detected, but again only in glial cells.

The localisation profile of the FGFR1 and 2 proteins have also been characterised by immunohistochemistry in the nigrostriatal tract. In the human brain, contrary to the previously reported mRNA expression results described above, the FGFR1 protein has been shown to be present in the SNc not only in dopamine neurones, but also in a subset of astrocytes (Walker *et al.*, 1998). In the nigrostriatal tract of the rat brain, both the FGFR1 and 2 proteins have been found to be present in the SN and the striatum (Gonzalez *et al.*, 1995; Chadashvili & Peterson, 2006; Murase & McKay, 2006). The FGFR2 protein was shown to be present exclusively in astrocytes in both the SN and the striatum. In the SN, FGFR2 was localised in astrocytes in both the SNc and SNr, and in the striatum, the FGFR2 protein was found in astrocytes within both the white and grey matter.

The immunohistochemical characterisation of the localisation profiles of the FGFRs within the nigrostriatal tract, however, remains incomplete. In the nigrostriatal tract of the rat brain, no reports have, thus far, comprehensively characterised the localisation profiles of the FGFR1, 3, and 4 proteins within the nigrostriatal tract of the rat. While in the nigrostriatal tract of the human brain, the localisation profiles of the FGFR1, 2, 3, and 4 proteins still need to be characterised in the striatum. In the human SN, only the localisation profile of the FGFR1 protein has been characterised, and the localisation profile of the FGFR2, 3, and 4 proteins, thus, still also need to be characterised comprehensively. Additionally, although FGF20 mRNA has been shown to be localised to the striatum and the SN of the rat, there are currently no published immunohistochemical studies confirming that the FGF20 protein is, indeed, present within the nigrostriatal tract.

2.2. Objectives

2.2.1. Objective 1. Characterise the Immunohistochemical Localisation Profiles of FGF20 and FGFR1, 3, and 4 in the Rat Nigrostriatal Tract and in Ventral Mesencephalic Embryonic Dopamine Neurone Cultures

In studies carried out as part of chapter 4 of this thesis, FGF20's ability to protect dopamine neurones against 6OHDA toxicity in VM cultures and in the 6OHDA lesioned rat model of PD was evaluated. Prior to carrying out these studies, it was important to ensure that FGF20's receptors, the FGFRs were, indeed, present in both of these model systems. Using immunohistochemistry, studies undertaken as part of this Chapter aimed to characterise, in detail, the colocalisation profiles of FGF20, and the FGFR1, 3, and 4 in both VM cultures, and in the nigrostriatal tract of rats. The localisation pattern of FGFR2 was not characterised because a previous study has already comprehensively described the localisation profile of this receptor within the rat nigrostriatal tract.

2.3. Methods

2.3.1. Preparation of Paraffin Wax Embedded Rat Brain Sections for Immunostaining

2.3.1.1. Paraffin Wax Embedding of Rat Brain Tissue

Naive male Sprague Dawley rats (Harlan, UK) weighing ~250g were intra-cardially perfusion fixed and their brains removed and embedded in paraffin wax using the procedure described in detail below. Rats were administered with an overdose (5mg/kg, i.p) of pentobarbital (Euthatal), and once a surgical plane of anaesthesia – tested for by the loss of a hindlimb withdrawal reflex – was reached, the rat's abdominal and thoracic cavities were exposed through a laparotomy and thoracotomy, respectively. The main blood vessels supplying the gastrointestinal tract were punctured so as to serve as an outlet for the systemic blood, which needs to be cleared out of the cardiovascular system prior to perfusion with para-formaldehyde (PFA). The rats were then intra-cardially perfused with ~200ml of ice cold PBS solution (pH7.6) to clear as much blood from the circulatory system as possible, and thereafter, with ~200ml of ice cold 4% PFA solution (dissolved in 0.9% NaCl, pH 7.6) to fix the brain *in situ*. Next, the PFA perfused brains were carefully removed from the skull and kept in a 4% PFA solution for a further 4 days at 4°C to ensure complete fixation of the entire brain. The brains were then cut to produce single blocks of brain tissue that contained both the entire SN and striatum. This was done by cutting off the cerebellum at the caudal end of the brains, and ~3cm of brain tissue at the rostral end of the brains.

The blocked rat brains were then placed into plastic cassettes and embedded in paraffin wax using a Leica automated tissue processing machine. To dehydrate the brain tissue, the brain blocks were immersed and agitated for 1x 2hr session in 90% industrial methylated spirits (IMS), and then for 3x 2hr sessions in 100% IMS, with solution changes separating each session. To clear the brains, they were next immersed and agitated in a 50% xylene: 50% IMS solution for 1x 2hr session, and then in a 100% xylene solution for 3x 2hr sessions. Next, the brains were infiltrated with paraffin wax by immersing and agitating them in a paraffin wax solution kept at between 56-58°C for 2x 2hr sessions, with solution changes separating each session. Finally, the paraffin wax embedded brains were mounted into wax blocks by positioning them in tissue moulds, filling the moulds with wax, and then leaving the moulds at 4°C to allow the wax to set into blocks.

2.3.1.2. Preparation of Nigral and Striatal Tissue Sections from the Paraffin Wax Embedded Rat Brains for Immunohistochemical Staining

8µm thick coronal sections of the wax embedded brains were cut at RT with a microtome at the rostro-caudal levels containing the SN and the striatum. For each of these areas, serial sections were taken of the entire SN and striatum, so that sections were obtained for each area from a caudal, medial, and rostral level. After cutting the sections, they were transferred into a water bath kept at ~45°C, in which they were left to float on the water surface for a few minutes until the sections had expanded fully. Sections were then transferred onto Superfrost Plus glass microscope slides, firmly pushed down against the slide using blotting paper dampened with 30% IMS, and incubated at 37°C for 1h to strengthen the adhesion of the sections to the microscope slides.

The brain sections were then prepared for immunohistochemical staining, firstly, by de-waxing and dehydrating them. Sections were immersed in 100% xylene for 2x 5min time-periods and subsequently immersed in 100% IMS for 4x 2min time-periods, with solution changes separating each immersion. The sections that were stained using the horseradish peroxidase (HRP)/diaminobenzidine (DAB) avidin-biotin complex (ABC) indirect staining method were then immersed for 10min in a 3% H_2O_2 solution (dissolved in H_2O) to inactivate any endogenous peroxidase activity. Thereafter, antigenicity was restored in the sections with the use of citric acid antigen retrieval. This was done by boiling the de-waxed sections in a citric acid (1M, dissolved in dH_2O, pH6.0) solution for ~8min in a microwave pressure cooker. After this, the sections were removed from the citric acid solution and thoroughly rinsed in dH_2O to wash away any remaining buffer solution. Excess dH_2O was removed from the slides/sections by dabbing them lightly on blotting paper, after which a PAP pen was used to apply a hydrophobic barrier around each brain section. Sections were then incubated in blocking buffer (1% bovine serum albumin (BSA) and 10% NaAz dissolved in 0.5M tris buffered saline (TBS), pH7.6) for 10min to block non-specific binding sites.

2.3.2. Culturing and Preparation of Ventral Mesencephalic Cultures for Immunofluorescence Staining

2.3.2.1. Coating of Glass Coverslips with Poly-D-lysine for Use in Cell Culture Experiments

13mm glass coverslips were coated with poly-D-lysine. Batches of ~300 coverslips were immersed and agitated in an 80% ethanol solution for 2h at RT to sterilise the coverslips. The coverslips were then rinsed 3x with sterile dH_20 to remove all traces of ethanol. Thereafter, the coverslips were immersed and agitated in a 0.1mg/ml poly-D-lysine solution (made up in dH_2O) for 3h at RT. The coverslips were then again washed 3x in dH_2O, this time to remove any unbound poly-D-lysine. The poly-D-lysine coated coverslips were then stored in dH_2O in a sealed sterile container kept in the fridge.

2.3.2.2. Preparation of VM Cell Suspension for Plating

Pregnant female time-mated rats incubating E15 rat embryos (Harlan, UK) were anaesthetised using carbon dioxide. Once the rats reached a surgical plane of anaesthesia – checked for by loss of the hindlimb reflex – a laparotomy was carried out, and the rat embryos removed and placed in a PBS solution kept on ice. Around 10-15 embryos were usually obtained from a single pregnant female rat. Under a dissecting microscope and under sterile conditions, VM brain tissue was dissected out from the developing brains of each of the individual rat embryos, and all of the individual pieces of VM brain tissue originating from the same mother were pooled together in 1ml of ice cold sterile Dulbecco's phosphate buffered saline (D-PBS). The dissected VM tissue was washed 3x with D-PBS, and then incubated in 0.25% trypsin (dissolved in D-PBS) at 37°C for 10min. 8ml of foetal bovine serum (FBS) positive (FBS+) cell culture media (Dulbecco's modified eagles medium (DMEM) Glutamax media supplemented with 10% foetal bovine serum (FBS), 100 units of penicillin, and 100g/ml of streptomycin) was added to the tissue suspension, and the suspension centrifuged for 2min at 400g. The supernatant was discarded, and the cells re-suspended in 1ml of FBS+ cell culture media. The cell suspension was triturated using a flame polished pasteur pipette until a single cell suspension was obtained.

2.3.2.3. Quantification of Cell Densities using Trypan Blue Cell Exclusion

The number of viable cells present in the 1ml VM cell suspension was then quantified using trypan blue cell exclusion. A 50µl aliquot of the 1ml VM cell suspension was pipetted into an eppendorf tube. 50µl of a 0.04% trypan blue solution was added to the 50µl of cell suspension and the resulting 100µl solution triturated to ensure that the cells were evenly distributed throughout the solution. ~50µl of the trypan blue cell suspension was then pipetted into the counting chamber of a haemocytometer, ensuring that the chamber was filled completely. The following method was then used to calculate the total number of cells that were present in the original 1ml cell suspension. Using an inverted phase contrast microscope, the number of cells present in 4 different haemocytometer counting cells were counted. These 4 counts were summed, and the resulting value multiplied by the dilution factor, which was 2 in this case. Finally, this value was then multiplied by 10000 to give the total number of cells that are present in the 1ml of cell suspension.

2.3.2.4. Plating of VM Cultures onto Poly-D-Lysine coated Glass Coverslips

In all VM cell culture experiments, cells were plated onto 13mm poly-D-lysine coated glass coverslips by transferring 500µl of cell suspension, prepared at an appropriate concentration, into each well of a 24 well tissue culture plate. To achieve this, the 1ml of cell suspension was diluted so that each 500µl of cell suspension contained the same number of cells as was desired to be present in each well. As cells were plated at a density of 300000 cells/coverslip in all of the VM culture experiments, the 1ml suspensions of cells were, thus, diluted as to give a final concentration of 300000 cells/500µl of cell suspension. The diluted cell suspension was thoroughly mixed to ensure that the cells were evenly distributed throughout the solution. Finally, the cells were then plated onto 13mm poly-D-lysine coated coverslips placed inside the wells of a 24 well NunC tissue culture plate. To do this, 500µl aliquots of the appropriately diluted cell suspensions were slowly applied to the coverslips as repeated drops, which were positioned as to ensure that the cells were distributed evenly over the entire surface of the coverslip. The plated VM embryonic neurone cultures were then left to grow in a cell culture incubator under standard conditions, 37°C, 95% humidity, and 5%CO_2, until the cultures were used, with old media being replaced with fresh media every ~3 days.

At 6 days in vitro (DIV6), cultures were fixed by incubation in ice cold 4% PFA for 10min. The cultures were then washed in TBS to remove all traces of the PFA solution, and then kept in TBS in the fridge until they were used in immunohistochemistry experiments.

2.3.3. Localisation of FGF20 and FGFR1, 3, and 4 in the Rat SN and Striatum using ABC-HRP/DAB Immunohistochemistry

In initial immunohistochemistry experiments, striatal and nigral coronal rat brain sections were stained with the horseradish peroxidase (HRP)/diaminobenzidine (DAB) avidin-biotin complex (ABC) indirect staining method to determine whether each of the antigens (FGF20, and FGFR1, 3, and 4) were present in the SN and striatum, and also to characterise the general staining pattern for each of the antigens in these regions.

2.3.3.1. Application of Primary and Secondary Antibodies

Previously prepared rat brain sections (***as detailed in section 2.3.1***) were incubated in blocking buffer (1% BSA and 10% NaAz dissolved in 0.5M TBS, pH7.6) for 10min to block non-specific binding sites. The blocking solution was removed, and to localise FGF20, sections were incubated with a rat monoclonal anti-FGF20 primary antibody (R&D systems, MAB2547, 1/50) at RT overnight. To localise FGFR1, 3, and 4, sections were incubated overnight at RT with rabbit anti-FGFR1 (sigma, F5421, 1/50), anti-FGFR3 (Santa Cruz Biotechnology, sc-9006, 1/50), or anti-FGFR4 (Santa Cruz Biotechnology, sc-123, 1/50) primary antibodies, respectively. In all cases, sections were then washed in TBS (0.5M TBS, pH7.6) for 10min to remove any unbound primary antibody, and antigen localisation visualised with the HRP/DAB/ABC method. For FGF20 staining, sections were, thus, subsequently incubated with a goat anti-rat biotinylated secondary antibody (Vectorlabs, BA-9400, 1/200) for 2h at RT. For FGFR1, 3, and 4, sections were incubated with a donkey anti-rabbit biotinylated secondary antibody (Vectorlabs, BA-1000, 1/200) for 2h at RT.

2.3.3.2. Visualisation of Staining using the HRP/DAB ABC Method

An avidin-biotin-HRP complex was freshly prepared using a Vectorlabs ABC kit (Vectorlabs Ltd., UK). This was done by mixing/diluting solution A (Avidin-OH) with

solution B (biotinylated HRP) in an appropriate ratio in TBS (10µl of solution A and B was added to every 1ml of 0.5M TBS, pH7.6). Sections were washed for 10min in TBS to remove any excess unbound secondary antibody, and then incubated for 1h in the freshly prepared avidin-biotin-HRP complex to allow the complex to conjugate to the biotinylated secondary antibody bound in the sections. Sections were washed in TBS to remove any excess unbound avidin-biotin-HRP complexes. Finally, antigen localisation was visualised by incubating the sections in a 0.05% DAB/0.03%H_2O_2 solution dissolved in TBS (0.1M TBS, pH7.6) for 10min. This results in a brown coloured stain developing in the close vicinity of the antibody-localised antigen, as the HRP enzyme converts DAB into a brown coloured water insoluble precipitate in the presence of hydrogen peroxide. Following this, sections were removed from the DAB solution and thoroughly washed in dH_2O to remove any remaining DAB solution from the slides. Sections were subsequently counterstained with haematoxylin to visualise cell nuclei. The sections were immersed in a Mayer's haematoxylin solution (0.1% haematoxylin, 5% alum, 0.02% sodium iodate, 2% acetic acid, dissolved in dH_2O) for ~ 90sec, and thereafter, the sections were thoroughly washed with dH_2O, and staining differentiated by immersing in a differentiation solution (0.5% HCl dissolved in 70% IMS) for ~60sec. Thereafter, sections were firstly dehydrated by immersing them in 100% IMS for 4x 2min time-periods, and then subsequently cleared by immersing them in 100% xylene for 2x 5min time-periods, with solution changes separating each immersion period. Glass coverslips were then finally mounted on top of the immunohistochemically stained sections using the hydrophobic mountant, dibutyl phthalate in xylene (DPX). Images of the HRP/DAB stained sections were acquired using a standard Zeiss bright field microscope fitted with an Axiocam colour camera and using Axiovision image analysis software.

2.3.4. Immunofluorescence Colocalisation Experiments in Ventral Mesencephalic Cultures and Rat Brain Sections

In all of the immunofluorescence colocalisation experiments carried out, FGF20 and FGFR1, 3, and 4 localisation were visualised using a 3 step indirect immunofluorescence method employing a biotinylated secondary antibody conjugated to a 594 fluorophore-streptavidin complex. Previously prepared rat brain sections (***as detailed in section 2.3.1***) or ventral VM cultures (***as detailed in section 2.3.2***) were incubated with blocking buffer for 10min at RT to block non-specific binding sites. The

blocking buffer was removed, and to localise FGF20, the rat brain sections or VM cultures were then incubated with a rat monoclonal anti-FGF20 primary antibody (R&D systems, MAB2547, 1/50) at RT overnight. To localise FGFR1, 3, and 4, rat brain sections or VM cultures were incubated overnight at RT with rabbit anti-FGFR1 (sigma, F5421, 1/50), anti-FGFR3 (Santa Cruz Biotechnology, sc-9006, 1/50), or anti-FGFR4 (Santa Cruz Biotechnology, sc-123, 1/50) primary antibodies, respectively. The sections or VM cultures were then washed with TBS, and for experiments with FGF20, incubated for 1hr at RT with a goat anti-rat biotinylated secondary antibody (Vectorlabs, BA-9400, 1/200). For experiments with FGFR1, 3, and 4, sections or VM cultures were incubated with a donkey anti-rabbit biotinylated secondary antibody (Vectorlabs, BA-1000, 1/200). Thereafter, in all cases, sections or VM cultures were washed with TBS and incubated for 1hr at RT with a fluorescent AlexaFluor-594 streptavidin complex (Invitrogen, S11227, 1/1000).

For FGF20 colocalisation experiments with TH, glial fibrillary acidic protein (GFAP), or ionised calcium binding adapter molecule 1 (Iba1), sections or VM cultures were washed with TBS and subsequently incubated with a rabbit polyclonal anti-TH (AB152, Millipore, 1/1000), anti-GFAP (Dako, Z0334, 1/500), or anti-Iba1 (Wako, 019-19741, 1/500) primary antibody for 1h at RT, respectively. Thereafter, sections or VM cultures were washed with TBS, and in all of the above cases, they were incubated for 1h at RT with a donkey anti-rabbit-488 fluorescent secondary antibody (Invitrogen, A21206, 1/1000) solution containing Hoechst 33258 (Sigma, B2883, 1µg/ml).

For all of the FGFR colocalisation experiments with TH, GFAP, and human neuronal protein (HuCD), sections or VM cultures were washed with TBS and subsequently incubated with a mouse monoclonal anti-TH (Chemicon, MAB318, 1/1000), anti-GFAP (Sigma, G3893, 1/1000), or anti-HuCD (Molecular Probes, A-21271, 1/1000) primary antibody at RT for 1h, respectively. Thereafter, sections or VM cultures were washed with TBS, and in all cases, they were incubated for 1h at RT with an AlexaFluor-488 goat anti-mouse fluorescent antibody (Invitrogen, A11029, 1/1000) solution containing Hoechst. The immunofluorochemically stained rat brain sections and VM cultures were then washed in TBS, and immediately mounted with glass coverslips or onto glass microscope slides, respectively, using the hydrophilic anti-fade mountant, mowiol 4-88. Fluorescence images were acquired in all cases using a Zeiss Apotome fluorescent microscope and Axiovision image analysis software. For all colocalisation experiments, 2D images were acquired from a single z plane. Three

images were acquired from each area of interest, with the first, second, and third image being taken using narrow bandpass filters for Hoechst, AlexaFluor-488, and AlexaFluor-594 fluorescent dyes, respectively. The Axiovision software automatically assigned images taken with filter set 1, 2, and 3 a green, blue and red colour, respectively. Once acquired, the three images were then saved as three separate JPEG files. Using Adobe Photoshop, the image clarity of each of the three images taken from a specific area of interest was then optimised separately by making global adjustments in the contrast, brightness, and levels of the images. Thereafter, Photoshop was used to produce a merged image from the 3 optimised images, and also to annotate the images.

'No primary antibody' control experiments were carried out with all of the abovementioned secondary antibody combinations that were used in both the immunohistochemistry and immunofluorescence experiments to confirm that the secondary antibodies themselves did not give rise to any non-specific staining when applied in the absence of any primary antibodies. Exactly the same staining protocol was followed in these control experiments to that used in the actual experiments, with the only difference being that the sections were not incubated with any of the respective primary antibody combinations, and control staining experiments were carried out with all of the respective brain/cell sample preparations in which the the antibody combinations were used, including nigral and striatal sections, and/or ventral mesencephalic cell culutres. Results from the control experiments demonstrated none of the secondary antibody combinations to produce any non-specific staining when applied in the absence of primary antibody.

2.3.5. Drugs and Chemicals

The Pentobarbital (Euthatal) was obtained from Merial Animal Health Ltd (Essex, UK). The diaminobenzidine (DAB), bovine serum albumin (BSA), Poly-D-lysine, trypan blue, sodium azide (NaAz), and the Mayers Haemotyoxylin were all purchased from Sigma-Aldrich (Dorset, UK). The foetal bovine serum (FBS), DMEM Glutamax media, and penicillin/streptomycin were all obtained from Invitrogen.

2.4. Results

In the nigrostriatal tract of rats, the localisation profiles for each of the antigens (FGF20 and FGFR1, 3, and 4) were determined in all of the main distinct anatomical areas comprising this pathway including, the striatum, the SNc, and the SNr. Striatal or nigral coronal rat brain sections were initially stained immunohistochemically using the HRP/DAB/ABC method to determine whether each of the antigens were, indeed, present in each area. These results also provided an indication of the general staining pattern present, i.e. whether there was a diffuse and/or cell specific (neuronal or glial) staining pattern. However, because the colocalisation profiles of each of the antigens were characterised in detail in later immunofluorescence experiments, in each of the abovementioned brain areas, examples of DAB stained images for only selected antigen/area combinations are shown here. Immunofluorescence colocalisation studies were then subsequently carried out to determine the specific cell types that the antigens co-localised with in each area. It was determined whether each antigen was present in the cell bodies of neuronal cells and also in specific types of glial cells, including astrocytes, microglia, and oligodendrocytes. In most cases, determinations were made based on results from colocalisation studies using markers of each cell type. Human neuronal protein (HuCD), glial fibrillary acidic protein (GFAP), and ionised calcium binding adapter molecule 1 (Iba1) were used as markers of neurones, astrocytes, and microglia respectively. In situations where appropriate antibody combinations were not available to carry out colocalisation studies, determinations were based on the distinctive morphology of positive cells. Colocalisation with oligodendrocytes was exclusively determined by the morphology of stained cells as a specific marker for these glial cells was not available – Refer to (Cammer *et al.*, 1991; Wu *et al.*, 2001; Bernstein *et al.*, 2004) for examples of the morphology of immunostained oligodendrocytes in the adult rat brain. Importantly, in the SNc and striatum it was also determined, through colocalisation experiments, whether each antigen co-localises with dopamine cell bodies and nerve terminals, respectively. Tyrosine hydroxylase (TH), the rate limiting enzyme in the dopamine synthesis pathway was used as a marker of dopamine neurones in these experiments. All of the localisation profiles that are reported for each antigen were found to be representative of the caudal, medial, and rostral levels of both the striatum and SNc. In VM cultures, immunofluorescence studies were carried out to determine whether each antigen is present in dopaminergic neurones, non-dopaminergic neurones, and astrocytes.

2.4.1. HRP/DAB Immunostaining Results

2.4.1.1. FGF20, and FGFR1, 3, and 4 are all Present in the Rat Striatum

FGF20, and FGFR1, 3, and 4 were all found to be present within the rat striatum (***Fig 2.2***). Only cells with a glial morphology stained positive for FGF20 (***Fig 2.2.A***). In contrast, both neuronal and glial cells stained positive for FGFR1, 3, and 4 (***Fig 2.2.B, 2.2.C, and 2.2D***). Additionally, for FGFR1 and FGF20, a diffuse punctuate staining pattern was also present throughout the striatum (***Fig 2.2.A, and 2.2.B***). For all of the antigens, positive cells/staining were distributed equally throughout the striatum.

Figure 2.2. Localisation of FGF20 and FGFR1, 3, and 4 in the Striatum

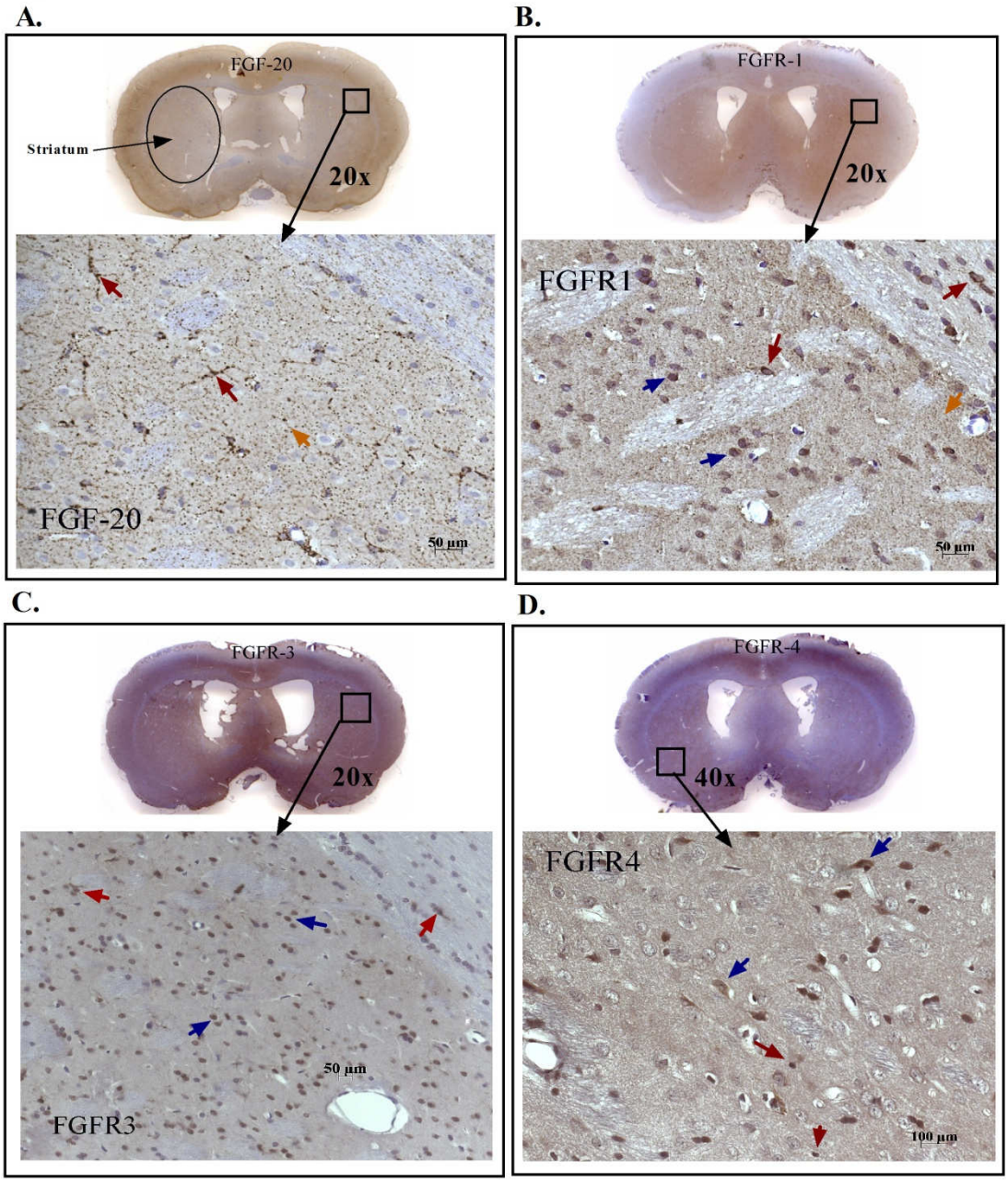

Figure 2.2. FGF20 and FGFR1, 3, and 4 were detected in the rat striatum using immunohistochemistry. By the morphology of the stained cells, it appeared that only glial cells stained positive for FGF20 (**A**), while both neuronal and glial cells stained positive for FGFR1(**B**), FGFR3 (**C**), and FGFR4 (**D**). For both FGF20 and FGFR1, a punctuate diffuse staining pattern (orange arrows) was also present throughout the striatum. Brown and blue staining: antigen visualised using DAB, and haematoxylin stained nuclei, respectively. Blue and red arrows: cells with a neuronal and glial morphology, respectively.

2.4.1.2. FGF20, and FGFR1, 3, and 4 are all Present in the Rat SN

FGFR1, 3, and 4 were all found to be present in both neuronal and glial cells in the SNc (***Fig 2.3***), and the SNr. DAB stained images from the SNr are not shown here as for most of the antigens evaluated, an equivalent staining pattern was observed in both the SNr and the SNc. FGF20, on the other hand, was present exclusively in the SNr, with no staining at all being observed in the SNc (DAB stained images of FGF20 staining in the SN is not shown as FGF20's staining pattern in the SN is most clearly illustrated by later immunofluorescence results shown in ***Fig 2.5.A***). Both neuronal and glial cells in the SNr were positive for FGF20, and a diffuse punctuate staining for FGF20 was also present throughout the SNr (this is also clearly illustrated in ***Fig 2.5.A***).

Figure 2.3. Localisation of FGFR1, 3, and 4 in the Rat SNc

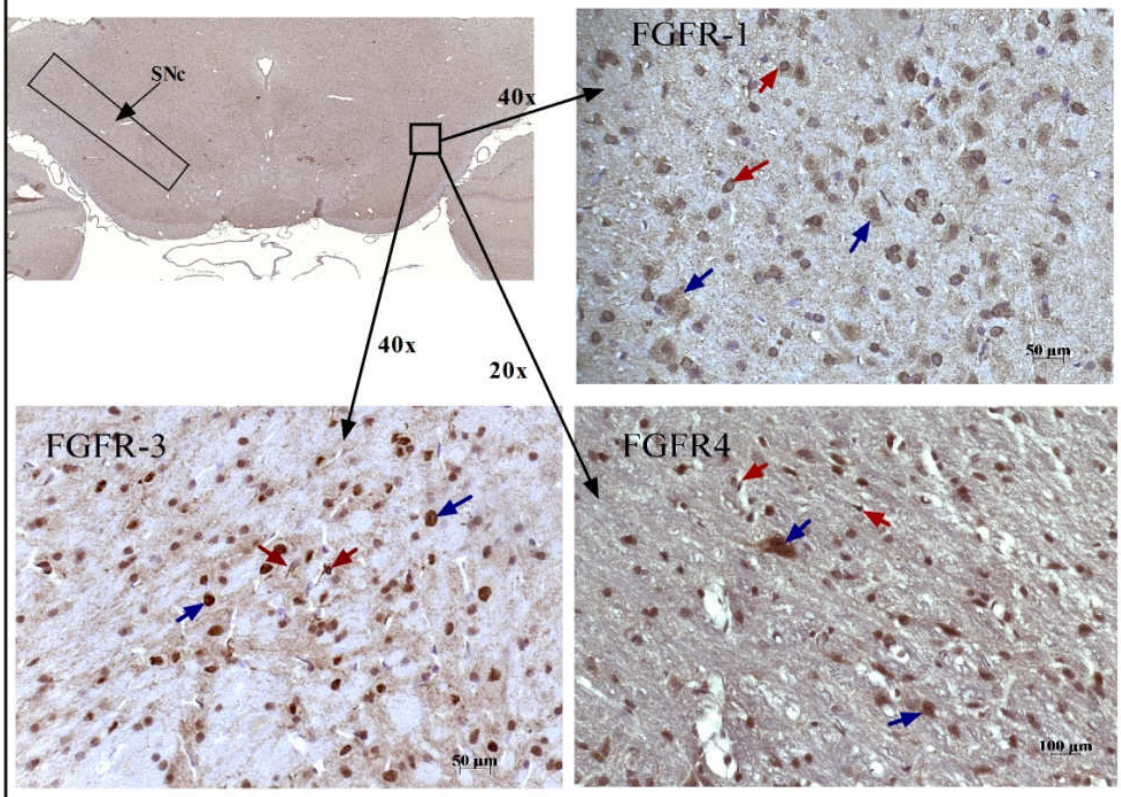

Figure 2.3. FGFR1, 3, and 4 were detected in the rat substantia nigra pars compacta (SNc) using immunohistochemistry. Both neuronal and glial cells appeared to stain positive for FGFR1, 3, and 4. Brown and blue staining: antigen visualilsed using DAB, and haematoxylin stained nuclei, respectively. Blue and red arrows: cells with a neuronal and glial morphology, respectively.

2.4.2. Immunofluorescence Results

2.4.2.1. Colocalisation Profile of FGF20 in the Rat Striatum and SN

In the striatum, FGF20 was present in astrocytes (***Fig 2.4.B***), but not in neuronal cells (based on the morphology of stained cells), oligodendrocytes (based on the morphology of stained cells), or microglia (***Fig 2.4.C***). Most of the astrocytes within the striatum appeared to be positive for FGF20, and some were more strongly positive than others. FGF20 staining was localised to only the processes of astrocytes, with no nuclear staining being observed in any of the positively stained astrocytes. A diffuse punctuate FGF20 staining pattern was present in the striatum, but it did not colocalise with striatal TH+ dopamine neurone terminals (***Fig 2.4.A***).

As mentioned earlier, FGF20 staining was completely absent in the SNc, and FGF20 was found not to co-localise with any of the dopamine neurone cell bodies in the SNc (***Fig 2.5.A***). A strong diffuse punctuate FGF20+ staining pattern was, however, present throughout the SNr, and all of the TH+ dopamine neurone dendrites extending into the SNr were surrounded by this diffuse positivity (***Fig 2.5.A***). Additionally, in the SNr, FGF20 was also present in astrocytes (***Fig 2.5.B***) and in a small number of neuronal cells (***Fig 2.5.B***, morphological determination), but not in microglia (results not shown) or oligodendrocytes (morphological determination). As in the striatum, most of the astrocytes within the SNr appeared to be positive for FGF20, and staining for FGF20 was found to be restricted to the processes of the astrocytes, with no nuclear staining being observed in any of these cells. In the few positive neurones, FGF20 was found to have a purely cytoplasmic localisation, with no nuclear staining being observed in any neurones.

Figure 2.4. FGF20 Colocalisation in the Striatum

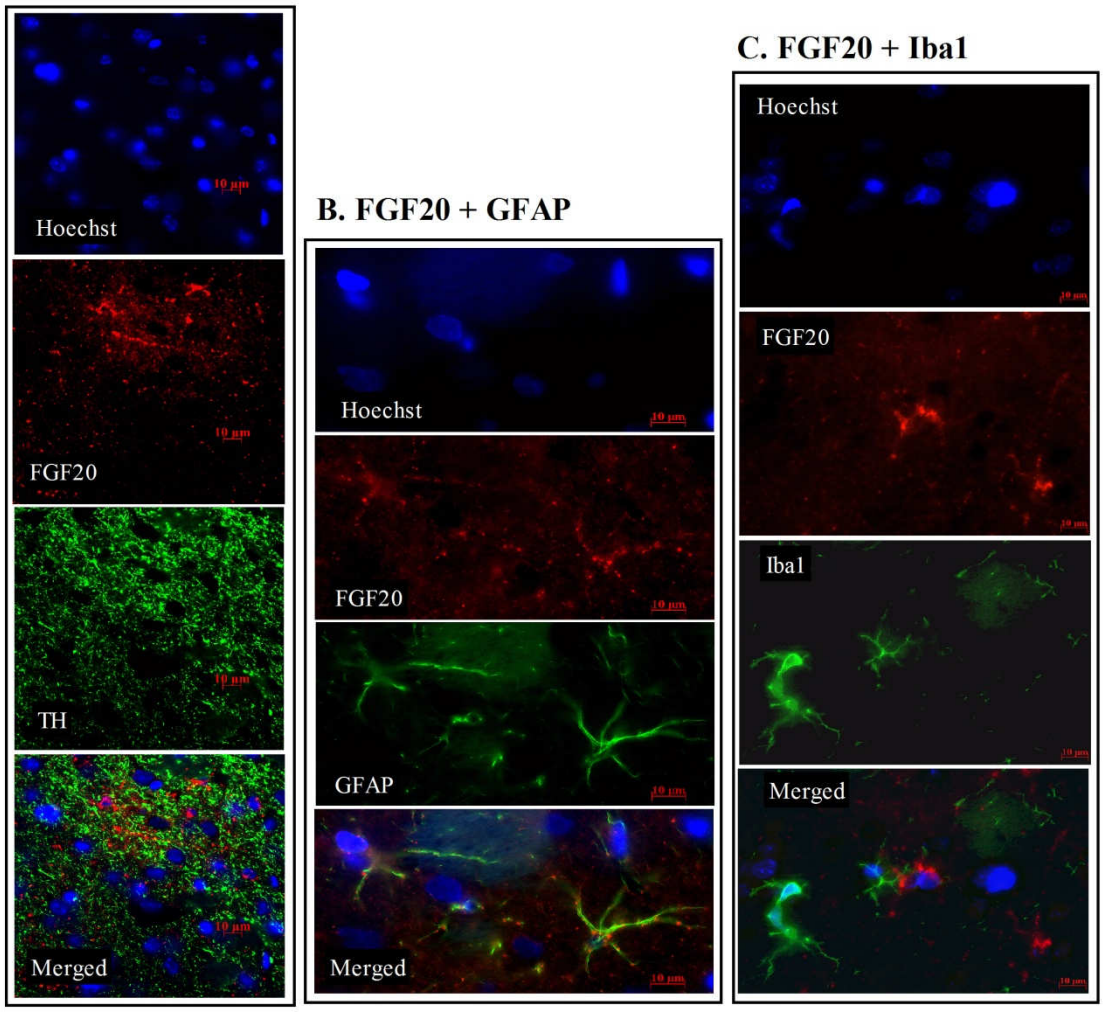

Figure 2.4. Colocalisation profile of FGF20 in the rat striatum. Diffuse punctuate staining for FGF20 in the striatum did not co-localise with TH+ nerve terminals (**A**). FGF20 colocalised with GFAP+ cells (**B**), but not with Iba+ cells (**C**). TH, GFAP, and Iba1 are markers for dopamine neurones, astrocytes, and microglia, respectively. Antigens were visualised using immunofluorescence. Images in A, B, and C were taken at 20x, 63x, and 63x magnification, respectively.

Figure 2.5. FGF20 Colocalisation in the SN

A. FGF20 + TH - SN

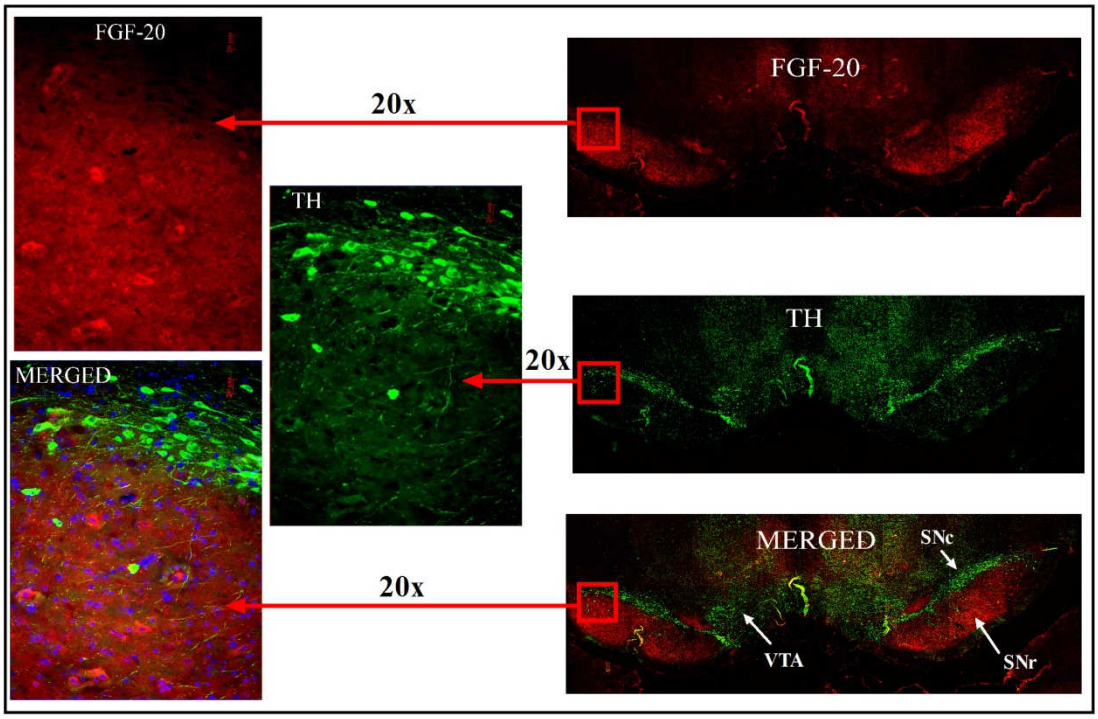

B. FGF20 + GFAP - SNr

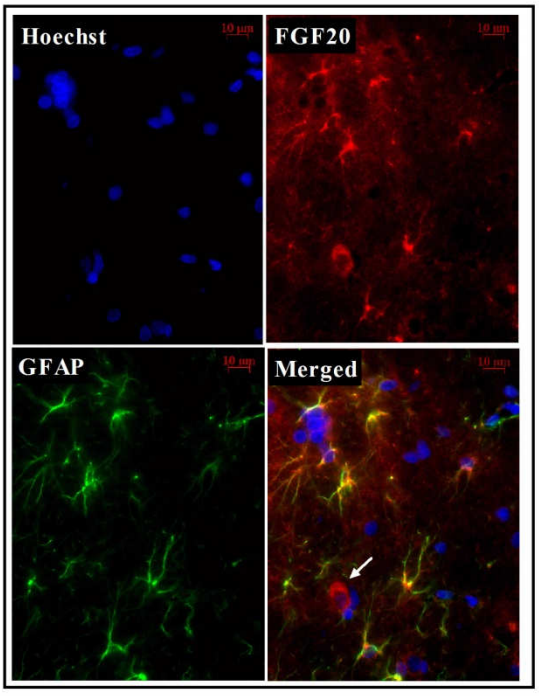

Figure 2.5. Colocalisation profile of FGF20 in the rat substantia nigra (SN). Diffuse punctuate and cell specific staining for FGF20 were locaslised throughout the substantia nigra pars reticulata (SNr), while in the substantia nigra pars compacta (SNc) FGF20 staining was completely absent (**A**). In the SNr, FGF20 colocalised with GFAP+ cells, and with cells with a neuronal morphology (white arrow) (**B**). TH and GFAP are markers for dopamine neurones and astrocytes, respectively. Antigens were visualised using immunofluorescence, and images in figure B were taken at 40x magnification. Abbreviations; VTA: ventral tegmental area.

2.4.2.2. Colocalisation Profile of FGFR1 in the Rat Striatum and SN

Within the striatum, FGFR1 was present in neuronal cells (***Fig 2.6.B***), astrocytes (***Fig 2.6.C***), and oligodendrocytes (***Fig 2.6.B&C,*** morphological determination), but not in microglia (morphological determination). A cytoplasmic staining pattern was observed for FGFR1 in both the positive neurones and glial cells, and no nuclear staining was observed in any positive cells. A diffuse punctuate FGFR1 staining pattern was present in the striatum, and it was found to colocalise with TH+ dopamine neurone terminals, but based on a purely subjective estimate, only ~40% of TH+ striatal terminals co-localised with FGFR1 (***Fig 2.6.A***).

Figure 2.6. FGFR1 Colocalisation in the Striatum

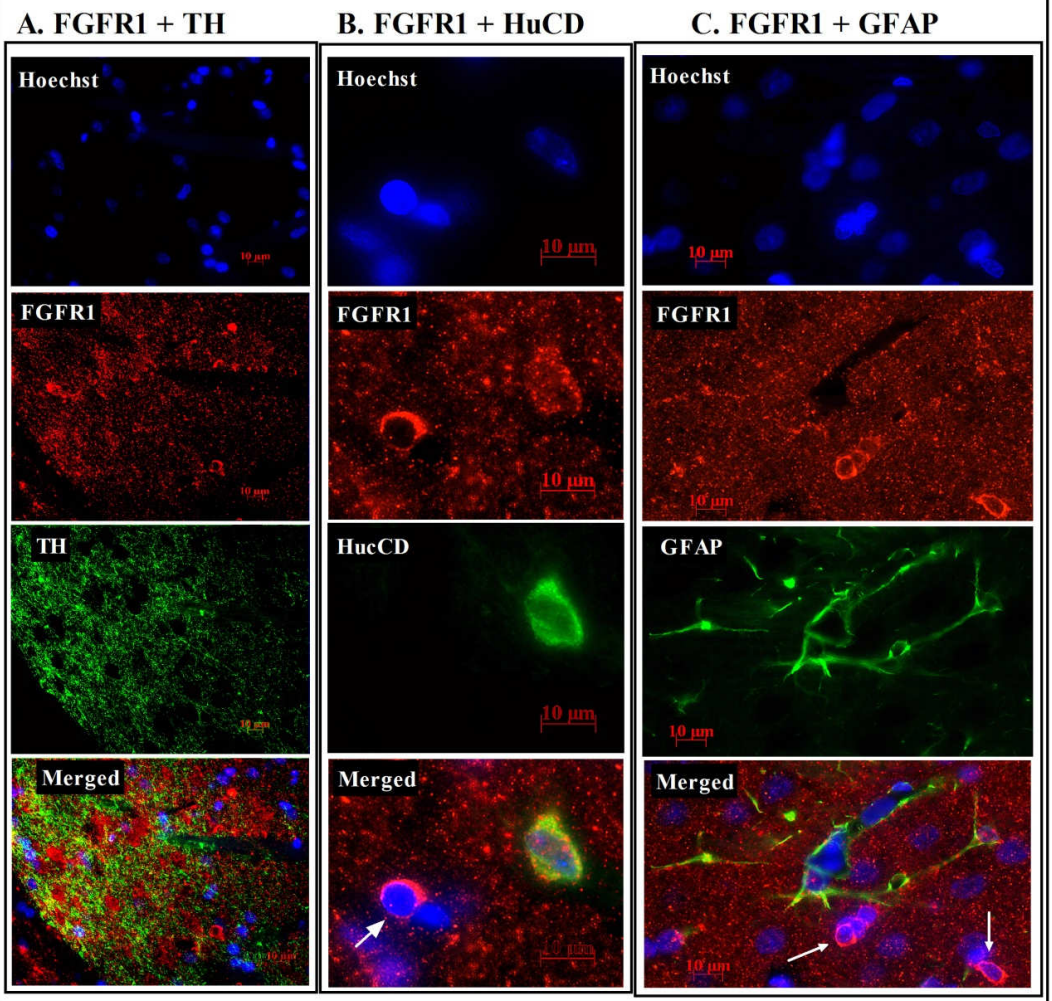

Figure 2.6. Colocalisation profile of FGFR1 in the rat striatum. Diffuse punctuate FGFR1 staining in the striatum colocalised with TH+ nerve terminals (**A**). FGFR1 colocalised with HuCD+ (**B**) and GFAP+ cells (**C**). Numerous glial cells that appeared to be oligodendrocytes were strongly FGFR1+ (**B** and **C,** white arrows). TH, HuCD, and GFAP are markers for dopamine neurones, neurones, and astrocytes, respectively. Antigens were visualised using immunofluorescence. Images in A, B, and C were taken at 20x, 63x, and 40x magnification, respectively.

In the SNc, FGFR1 was present in all TH+ dopamine neurone cell bodies (***Fig 2.7.A***), but not in astrocytes (***Fig 2.7.B***) or microglia (morphological determination). Numerous oligodendrocytes in the SNc were strongly FGFR1+ (***Fig 2.7.A&B,*** morphological determination), including some that appeared to be interacting with TH+ neurone cell bodies. Additionally, a small number of TH negative neurones in the SNc also appeared to stain positive for FGFR1 (morphological determination). A punctuate staining pattern was present in the nuclei and cytoplasm of all of the TH+ and TH- neurones in the SNc that stained positive for FGFR1. In the positive oligodendrocytes, FGFR1 staining was localised to only the cytoplasm, with no nuclear staining being observed in these cells.

In the SNr, FGFR1 was present in neurones (***Fig 2.8.A***), astrocytes (***Fig 2.8.B***), and oligodendrocytes (***Fig 2.8.A&B,*** morphological determination), but not in microglia (morphological determination). In contrast to the SNc, a purely cytoplasmic staining pattern was observed for FGFR1 in positive neurones in the SNr, with no nuclear staining being observed in these positive neurones. In the SNr, a purely cytoplasmic staining pattern was observed for FGFR1 in both the positive neurones and oligodendrocytes, with no nuclear staining being observed in any positive cells. Furthermore, FGFR1 staining was restricted to the processes of positive astrocytes, with no nuclear staining also being observed in any of these cells.

Figure 2.7. FGFR1 Colocalisation in the SNc

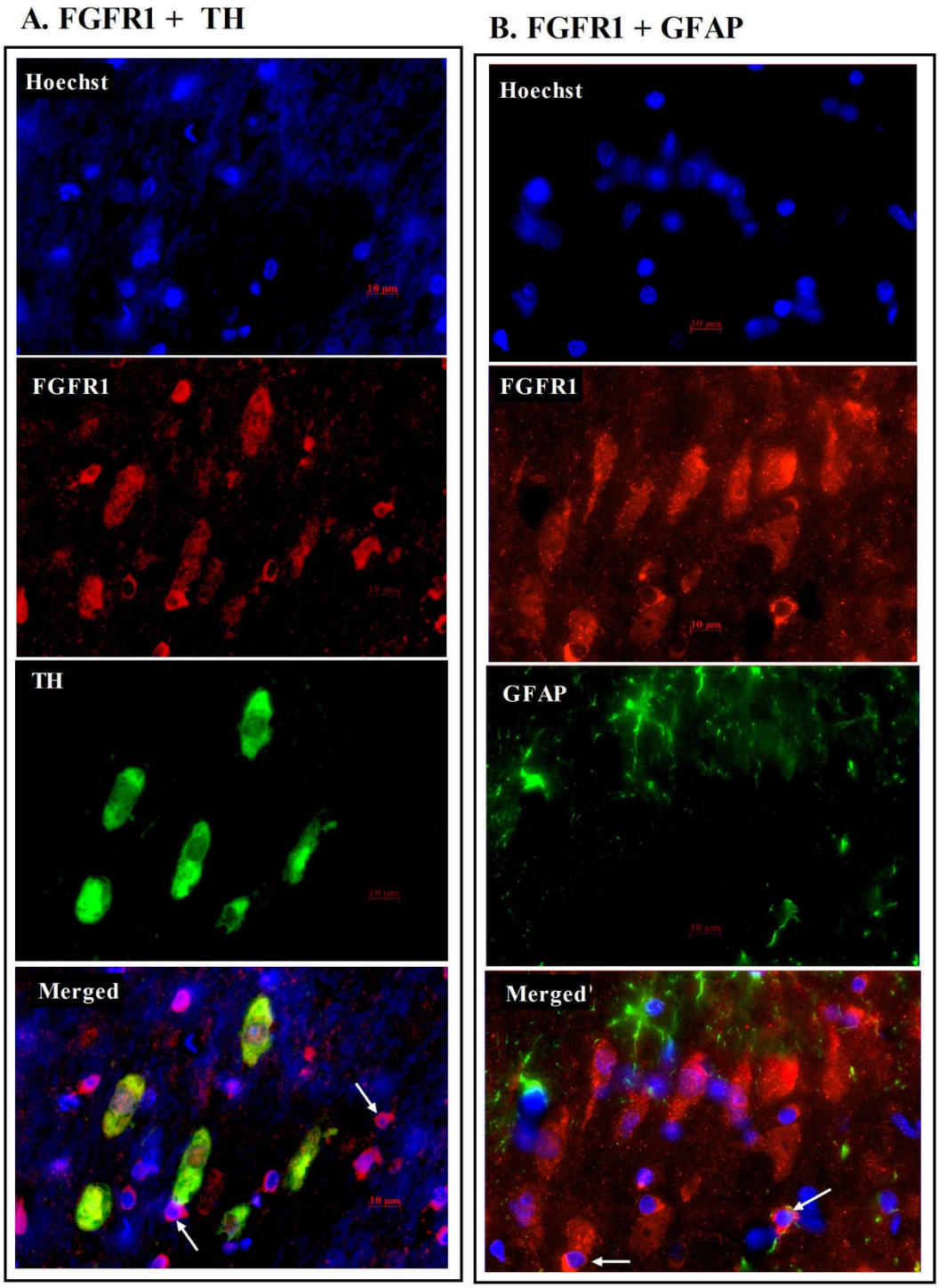

Figure 2.7. Colocalisation profile of FGFR1 in the rat substantia nigra pars compacta (SNc). FGFR1 colocalised with TH+ cells (**A**), but not with GFAP+ cells (**B**). Numerous glial cells with an oligodendrocyte morphology were strongly FGFR1+ (**A** and **B**, white arrows). TH and GFAP are markers for dopamine neurones and astrocytes, respectively. Antigens were visualised using immunofluorescence, and images were taken at 63x magnification.

Figure 2.8. FGFR1 Colocalisation in the SNr

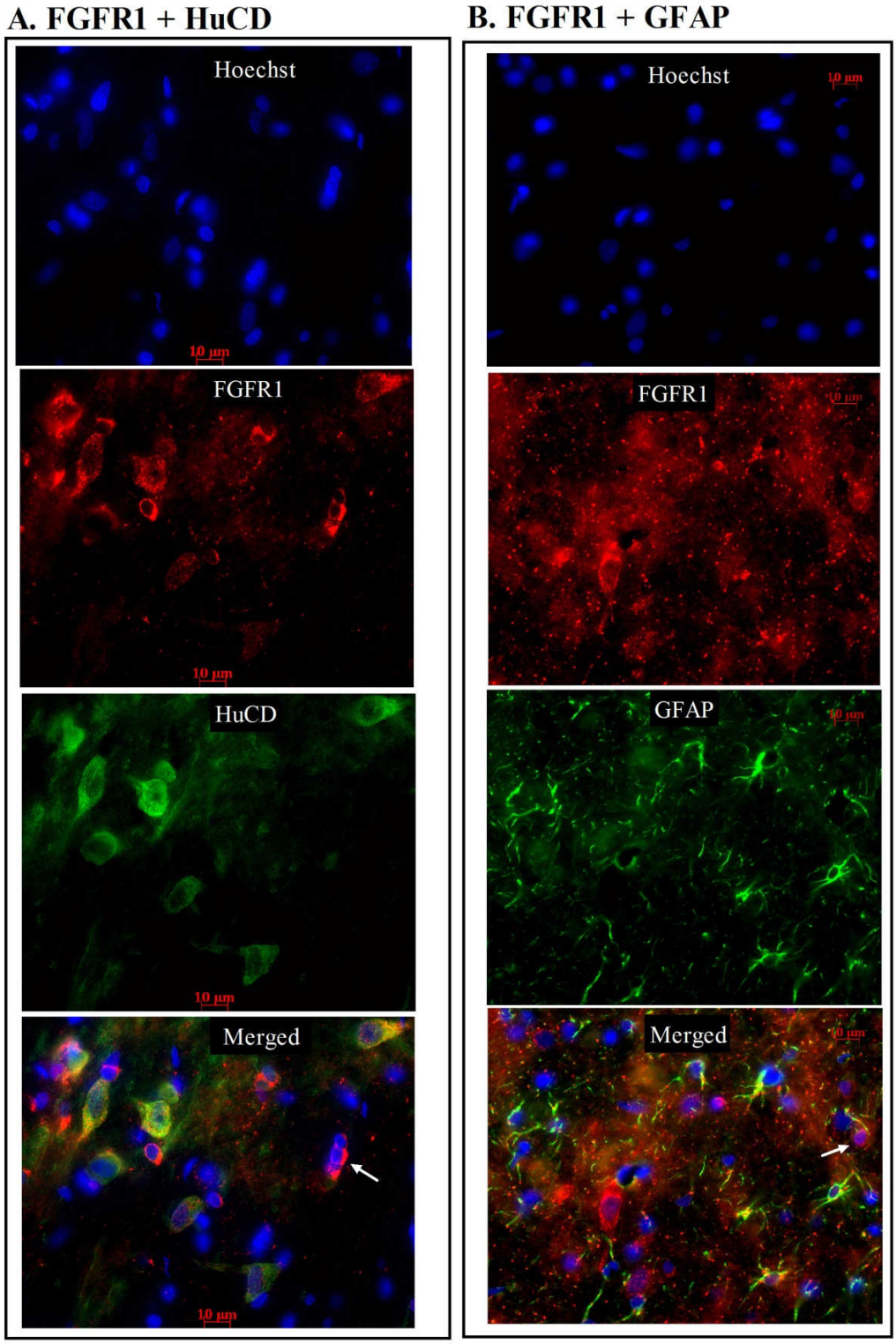

Figure 2.8. Colocalisation profile of FGFR1 in the rat substantia nigra pars reticulata (SNr). FGFR1 colocalised with HuCD+ (**A**) and with GFAP+ cells (**B**). Numerous glial cells with an oligodendrocyte morphology were strongly FGFR1+ (**A** and **B**, white arrows). HuCD and GFAP are markers for neurones and astrocytes, respectively. Antigens were visualised using immunofluorescence, and images were taken at 40x magnification.

3.4.2.3. Colocalisation Profile of FGFR3 in the Rat Striatum and SN

Within the striatum, FGFR3 was present in neurones (***Fig 2.9.A***), and in numerous oligodendrocytes (***Fig 2.9.A&B***, morphological determination), but not in astrocytes (***Fig 2.9.B***) or microglia (morphological determination). Interestingly, FGFR3 was found to only localise to the nuclei of neurones, with no staining being observed in the cytoplasm of any of the positive neurones. FGFR3 localised to only the cytoplasm of oligodendrocytes, with no nuclear staining being observed in any of these glial cells.

Figure 2.9. FGFR3 Colocalisation in the Striatum

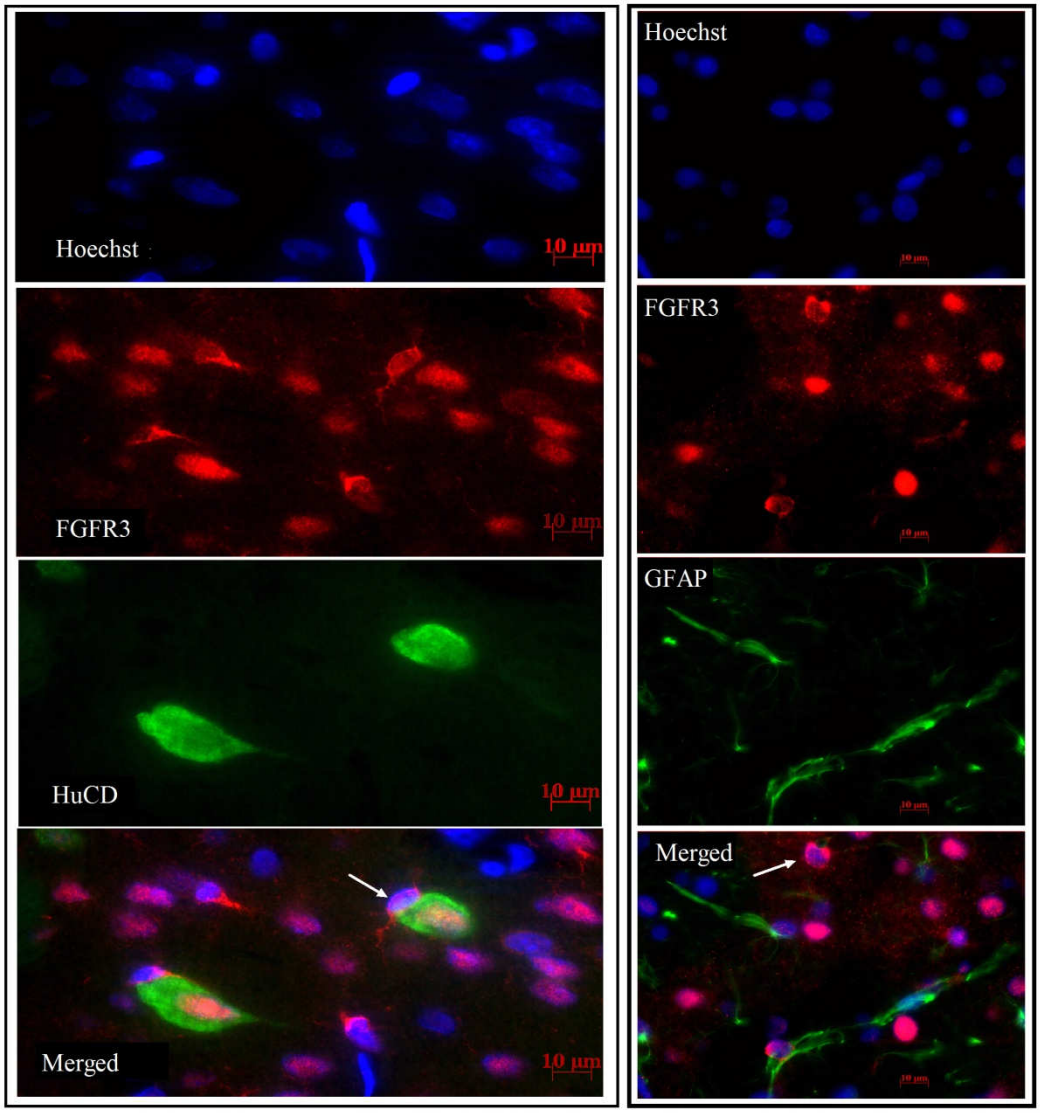

Figure 2.9. Colocalisation profile of FGFR3 in the rat striatum. FGFR3 colocalised with the nuclei of HuCD+ cells (**A**). No colocalisation was seen in GFAP+ cells (**B**), and numerous glial cells that appeared to be oligodendrocytes were strongly FGFR3+ (**A** and **B**, white arrows). HuCD, and GFAP are markers for neurones and astrocytes, respectively. Antigens were visualised using immunofluorescence. Images A and B were taken at 63x and 40x magnification, respectively.

In the SNc, FGFR3 was present in the nuclei of all TH+ dopamine neurones (***Fig 2.10.A***), and also in numerous oligodendrocytes (***Fig 2.10.A&B***, morphological determination), but not in astrocytes (***Fig 2.10.B***) or microglia (morphological determination). As with other FGFR3 positive neurones, FGFR3 staining was found to only localise to the nuclei of TH+ neurones. In oligodendrocytes, FGFR3 staining was restricted to the cytoplasm and processes of these cells.

In the SNr, FGFR3 was present in oligodendrocytes (***Fig 2.11.A&B***), and in the nuclei of neurones (***Fig 2.11.A***), but not in astrocytes (***Fig 2.11.B***) or microglia (morphological determination). Again, FGFR3 was found to only be localised to the nuclei of positive neurones, while FGFR3 staining was restricted to the cytoplasm and processes of all of the positively stained oligodendrocytes.

Figure 2.10. FGFR3 Colocalisation in the SNc

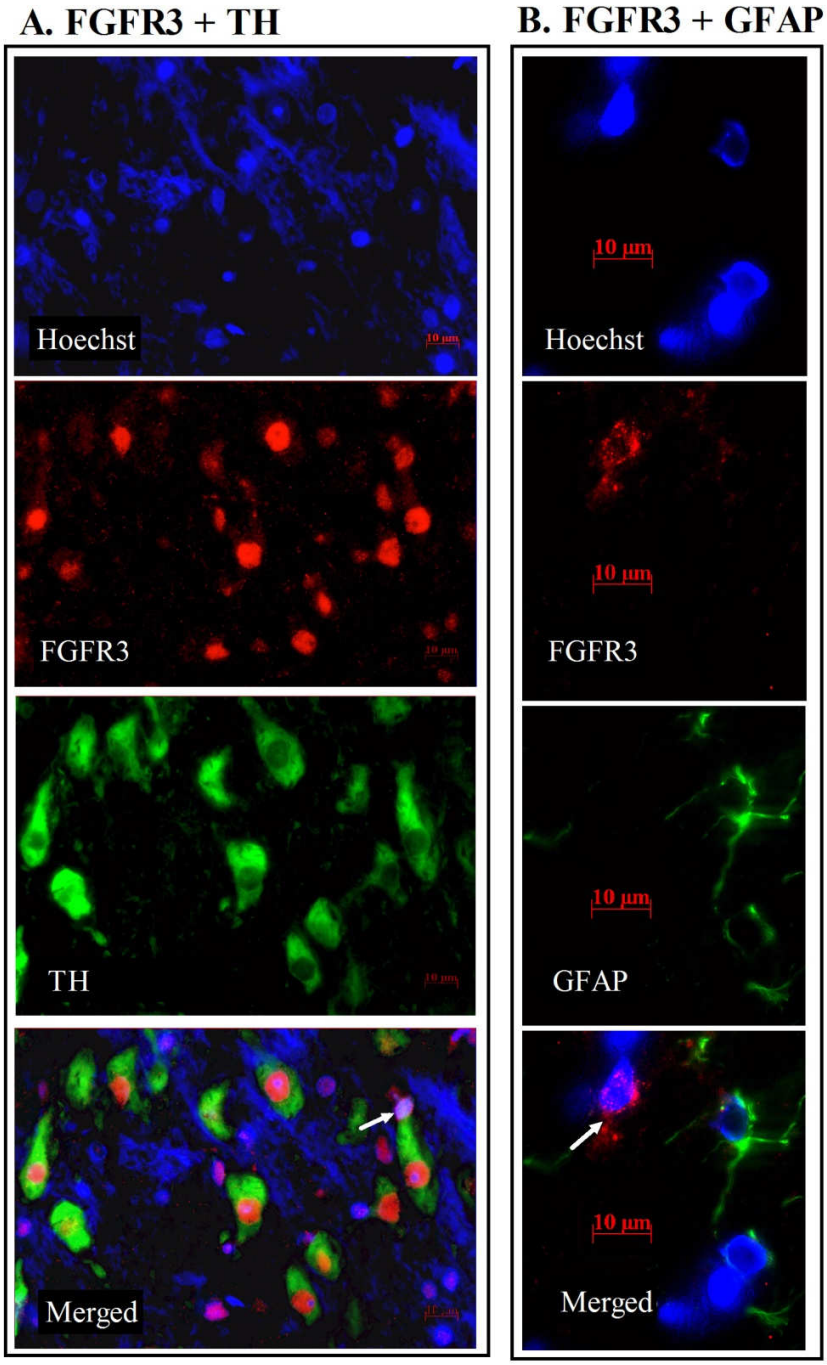

Figure 2.10. Colocalisation profile of FGFR3 in the rat substantia nigra pars compacta (SNc). FGFR3 colocalised with the nuclei of TH+ cells (**A**). No colocalisation was seen in GFAP+ cells (**B**), and numerous glial cells with an oligodendrocyte morphology were strongly FGFR3+ (**A** and **B**, white arrows). TH and GFAP are markers for dopamine neurones and astrocytes, respectively. Antigens were visualised using immunofluorescence, and images A and B were taken at 40x and 63x magnification, respectively.

Figure 2.11. FGFR3 Colocalisation in the SNr

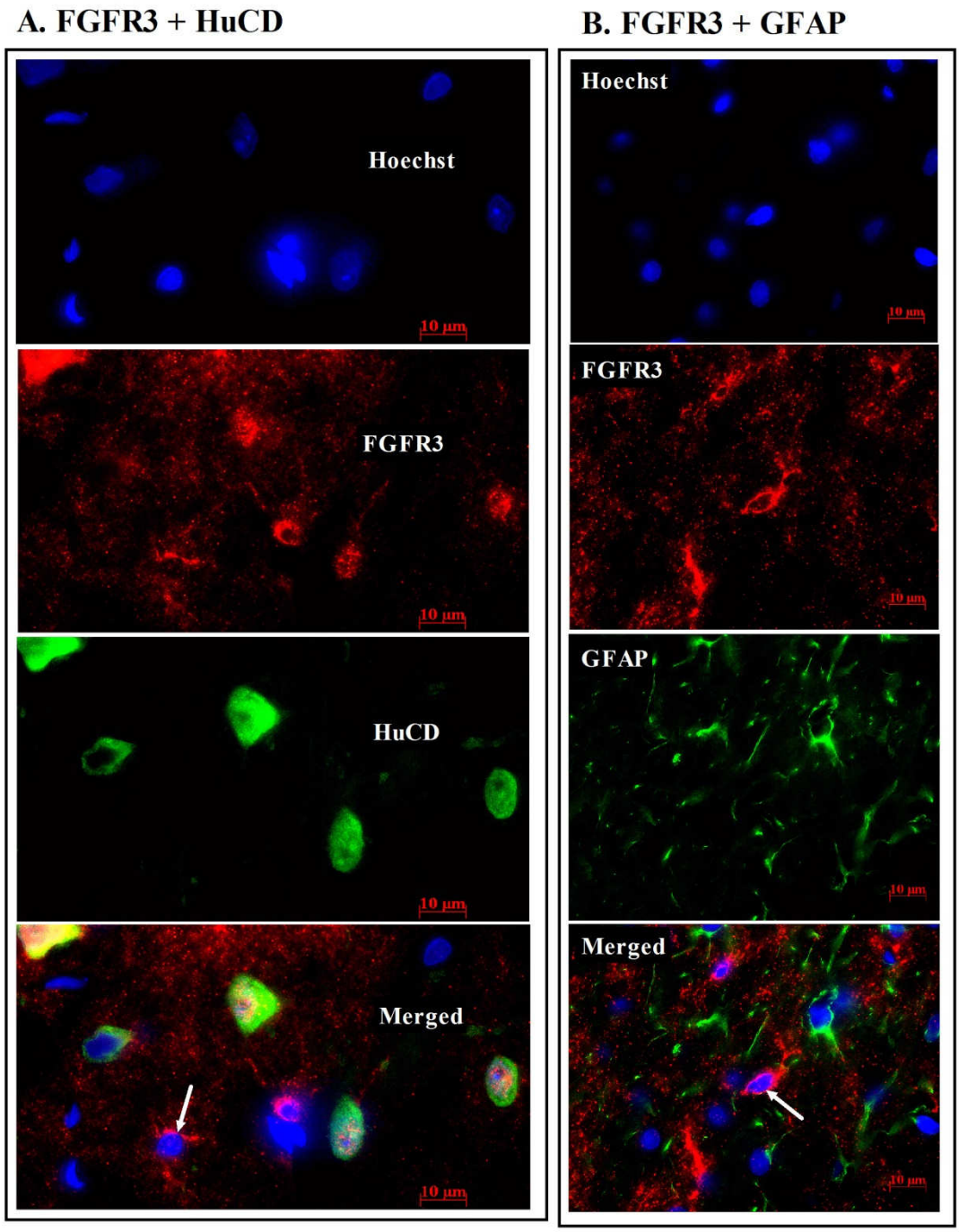

Figure 2.11. Colocalisation profile of FGFR3 in the rat substantia nigra pars reticulata (SNr). FGFR3 colocalised with the nuclei of HuCD+ cells (**A**). No colocalisation was seen in GFAP+ cells (**B**), and numerous glial cells with an oligodendrocyte morphology were strongly FGFR3+ (**A** and **B**, white arrows). HuCD and GFAP are markers for neurones and astrocytes, respectively. Antigens were visualised using immunofluorescence, and images were taken at 63x magnification.

3.4.2.4. Colocalisation Profile of FGFR4 in the MHB, Striatum and SN

A previous study has shown that, within the rat brain, FGFR4 mRNA is exclusively localised to cholinergic neurones in the medial habenula (MHB) (Miyake & Itoh, 1996). Results obtained in this study conflicts with these findings, as FGFR4 was found also to be present within the nigrostriatal tract (***Fig 2.12.A and 13***). Localisation of FGFR4 in the MHB was, therefore, characterised to provide evidence that the antibody used in this study is able to correctly detect FGFR4. In the MHB, cells with a neuronal morphology were strongly FGFR4+ (***Fig 2.12.B***). FGFR4 was found to localise to the cytoplasm of all the positive MHB neurones, and no nuclear staining was observed in any of the cells. In the striatum, FGFR4 was present in neuronal cells (***Fig 2.12.A***) and oligodendrocytes (***Fig 2.12.A***, morphological determination), but not in astrocytes (results not shown) or microglia (morphological determination). In the striatum, FGFR4 localised to the cytoplasm and processes of positive neurones and oligodendroctyes, and no nuclear staining was observed in any of the positive cells.

In the SNc, FGFR4 was present in all TH+ dopamine neurones (***Fig 2.13.A***), and also in numerous oligodendrocytes (***Fig 2.13.A,*** morphological determination). Furthermore, staining for FGFR4 was stronger in some TH+ neurones compared to others in the SNc, and small number of what appeared to be spindle shaped TH- neurones were also FGFR4+ (***Fig 2.13.A***). In the SNr, FGFR4 was present in neuronal cells (***Fig 2.13B.***) and oligodendrocytes (***Fig 2.13.B***, morphological determination), but not in astrocytes (results not shown) or microglia (morphological determination). In the SN, FGFR4 localised to the cytoplasm of positive neurones and oligodendrocytes, and no nuclear staining was observed in any of the positive cells.

Figure 2.12. FGFR4 Colocalisation in the Striatum and MHB

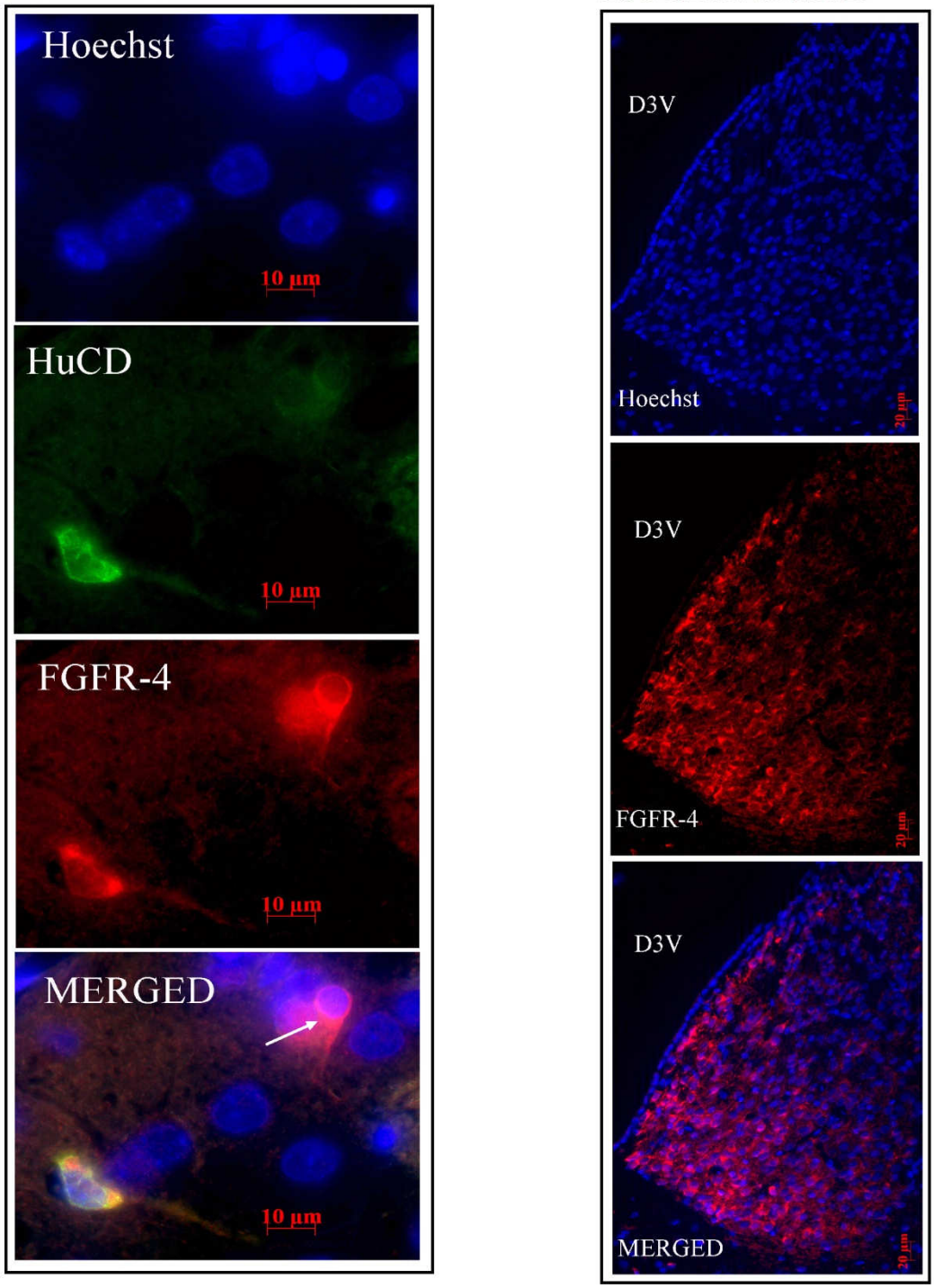

Figure 2.12. Colocalisation profile of FGFR4 in the rat striatum and medial habenular nucleus (MHB). In the striatum, FGFR4 colocalised with HuCD+ cells (**A**), and numerous glial cells with an oligodendrocyte morphology were strongly FGFR4+ (**A**, white arrows). In the MHB, cells with a neuronal morphology were strongly FGFR4+ (**B**). HuCD is a marker for neurones. Antigens were visualised using immunofluorescence, and images were taken at 63x magnification. Abbreviations; D3V: Dorsal third ventricle.

Figure 2.13. Colocalisation of FGFR4 in the SN

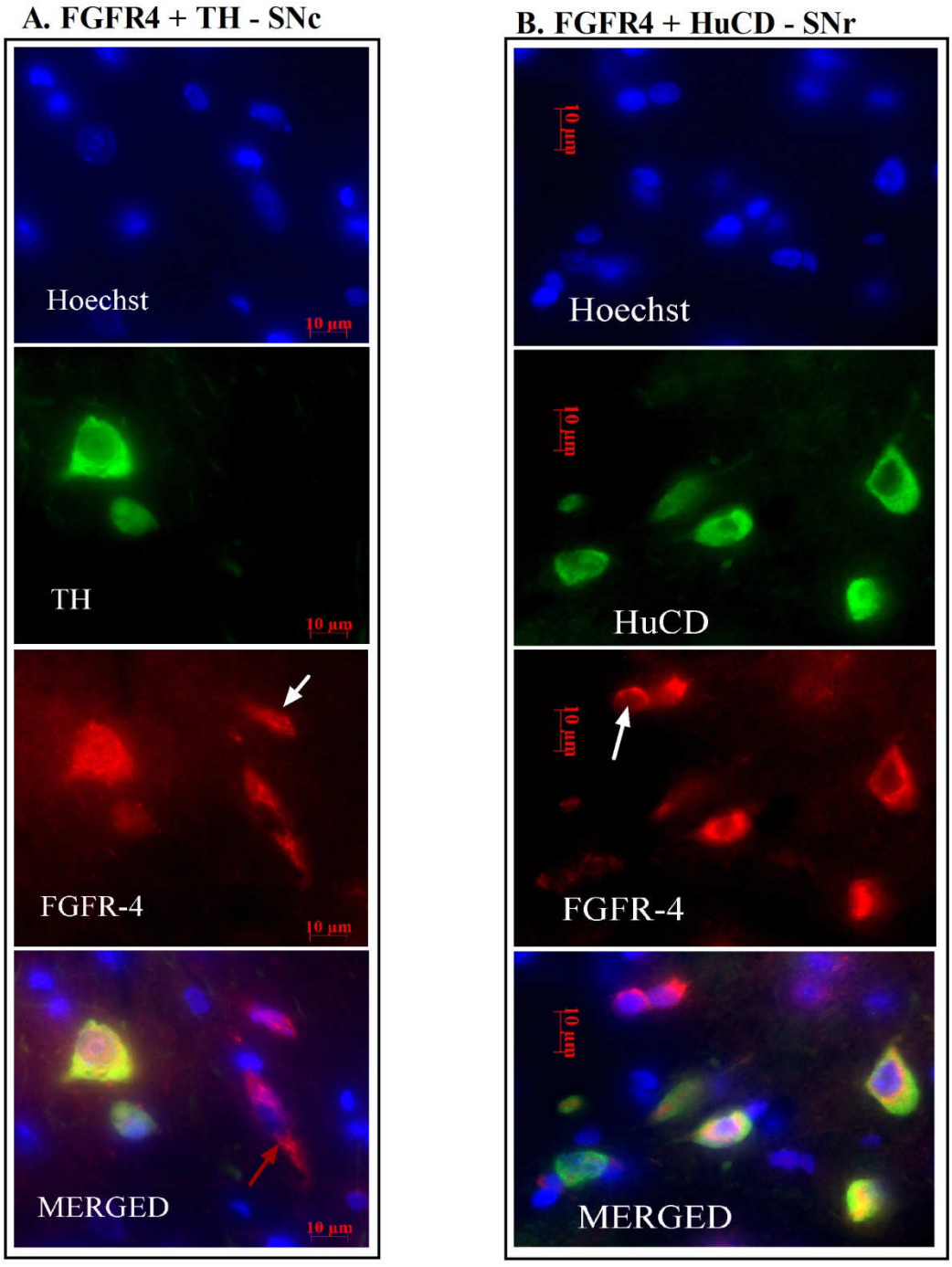

Figure 2.13. Colocalisation profile of FGFR4 in the rat substantia nigra (SN). In the substantia nigra pars compacta (SNc), FGFR4 colocalised with TH+ neurones and with cells that appeared to be spindle shaped TH- neurones (**A,** red arrow). In the substantia nigra pars reticulata (SNr), FGFR4 colocalised with HuCD+ cells (**B**), and in both the SNc and the SNr it colocalised to glial cells with a oligodendrocyte morphology (**A** and **B**, white arrows). TH and HuCD are markers for dopamine neurones and neurones, respectively. Antigens were visualised using immunofluorescence, and all images were taken at 63x magnification.

3.4.2.5. Colocalisation Profile of FGF20, and FGFR1, 3, and 4 in Ventral Mesencephalic Embryonic Cultures

FGF20 was found not to be present in any cell types in the VM cultures (results not shown). FGFR1, on the other hand, was localised not only in most of the TH+ dopaminergic neurones (***Fig 2.14.A***) and HuCD+ neuronal cells (***Fig 2.14.B***) present in the cultures, but also in most of the astrocytes (***Fig 2.14.C***). In most cases, FGFR1 was found to localise to not only the cytoplasm but also to the nucleus of the positive neurones and/or glial cells. However, in a small number of astrocytes and neurones (TH+ and HuCD+), a purely cytoplasmic FGFR1 localisation pattern was observed, with no nuclear staining being seen in these cells. Furthermore, not only FGFR1 but also FGFR3 and 4 were also present on what appeared to be neuronal precursor cells, an example of which can be seen for FGFR1 in ***Fig2.14.B*** and for FGFR3 in ***Fig 2.15.C***.

Figure 2.14. FGFR1 Colocalisation in VM Cultures

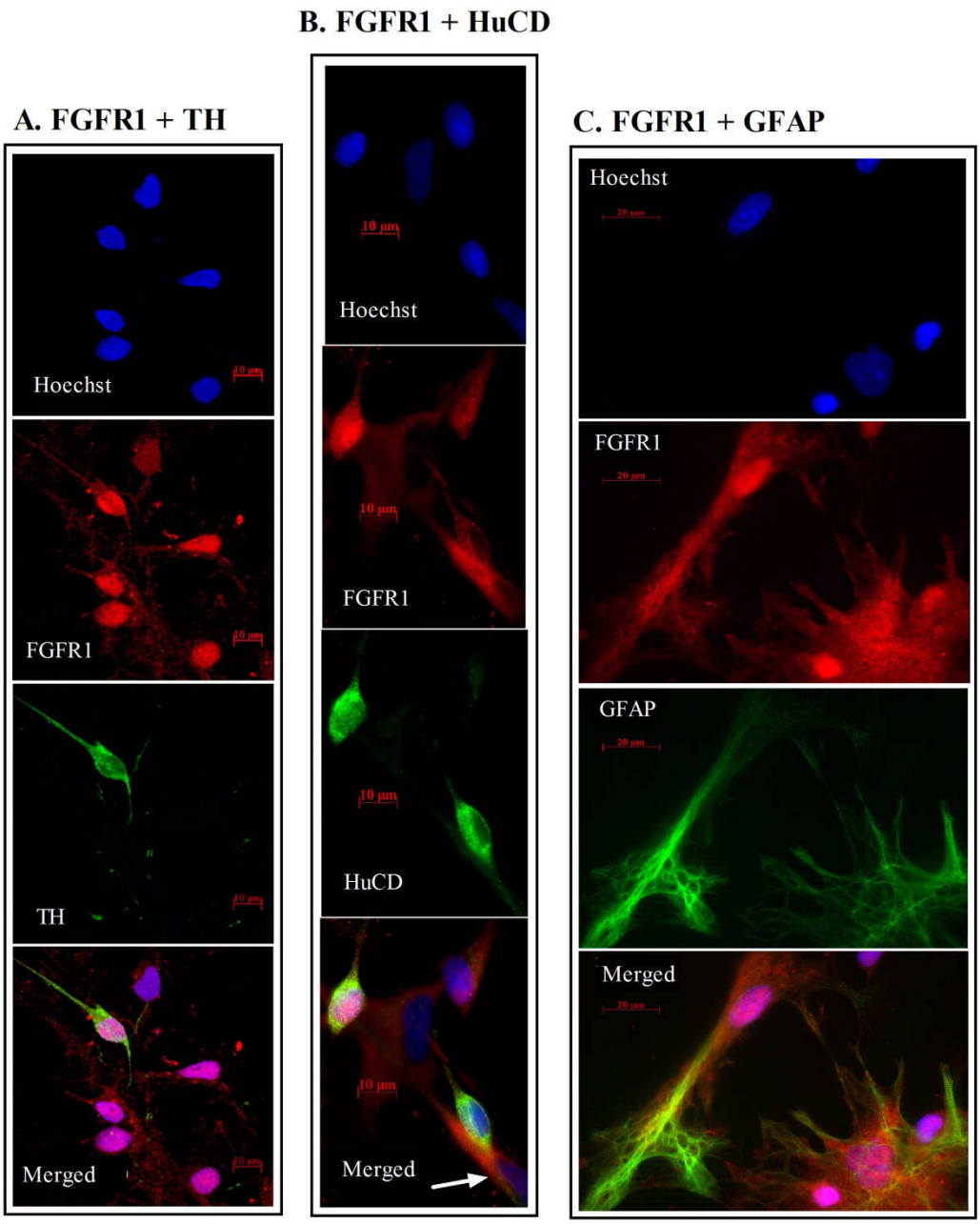

Figure 2.14. Colocalisation profile of FGFR1 in rat ventral mesencephalic (VM) embryonic dopamine neurone cultures. FGFR1 colocalised with TH+ (**A**), HuCD+ (**B**), and GFAP+ cells (**C**). Cells that appeared to be neuronal precursor cells were also strongly FGFR1 positive (**B**, white arrow). TH, HuCD, and GFAP are markers for dopamine neurones, neurones, and astrocytes, respectively. Antigens were visualised using immunofluorescence, and all images were taken at 63x magnification.

As with FGFR1, FGFR3 was also localised not only in most of the TH+ dopaminergic neurones (***Fig 2.15.A***) and HuCD+ neuronal cells present in the cultures, (***Fig 2.15.B***), but also in most of the astrocytes (***Fig 2.15.C***). In most cases, FGFR3 was found to localise to not only the cytoplasm but also to the nucleus of the positive neurones and/or glial cells. However, in a small number of astrocytes and neurones (TH+ and HuCD+), a purely cytoplasmic FGFR3 localisation pattern was observed.

FGFR4 was localised in most of the TH+ dopaminergic neurones (***Fig 2.16.A***) and HuCD+ neuronal cells present in the cultures (***Fig 2.16.B***), but, in contrast to FGFR1 and 3, it was not localised in any astrocytes (***Fig 2.16.C***). Similar to FGFR1 and 3, FGFR4 was found to localise to not only the cytoplasm but also to the nucleus of positive neurones, in most cases. However, in a small number of neurones (TH+ and HuCD+), a purely cytoplasmic FGFR4 localisation pattern was observed.

Figure 2.15. FGFR3 Colocalisation in VM Cultures

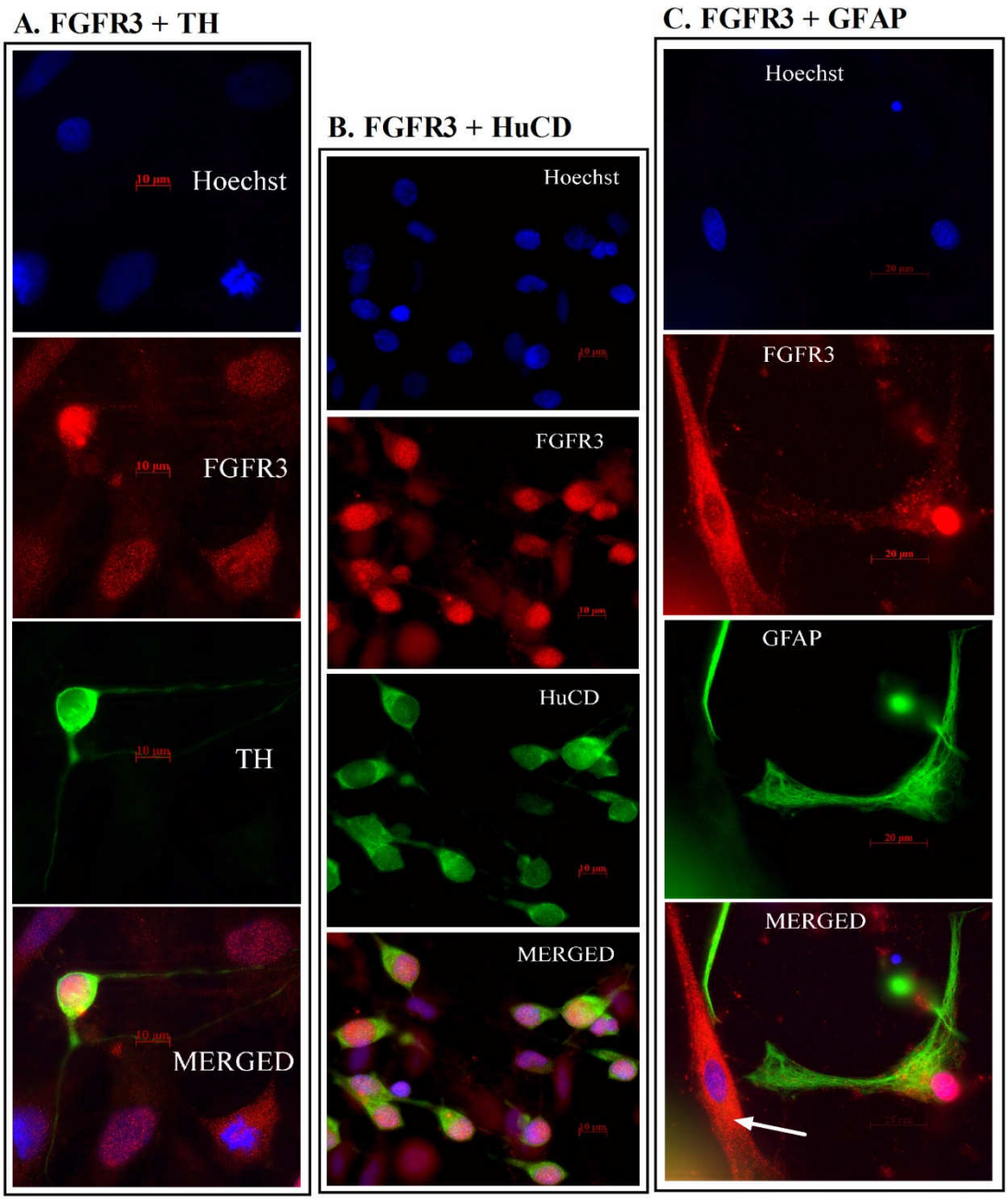

Figure 2.15. Colocalisation profile of FGFR3 in rat ventral mesencephalic (VM) embryonic dopamine neurone cultures. FGFR3 colocalises with TH+ (**A**), HuCD+ (**B**), and GFAP+ cells (**C**). Cells that appeared to be neuronal precursor cells were also strongly FGFR1 positive (C, white arrow). TH, HuCD, and GFAP are markers for dopamine neurones, neurones, and astrocytes, respectively. Antigens were visualised using immunofluorescence, and all images were taken at 63x magnification.

Figure 2.16. FGFR4 Colocalisation in VM Cultures

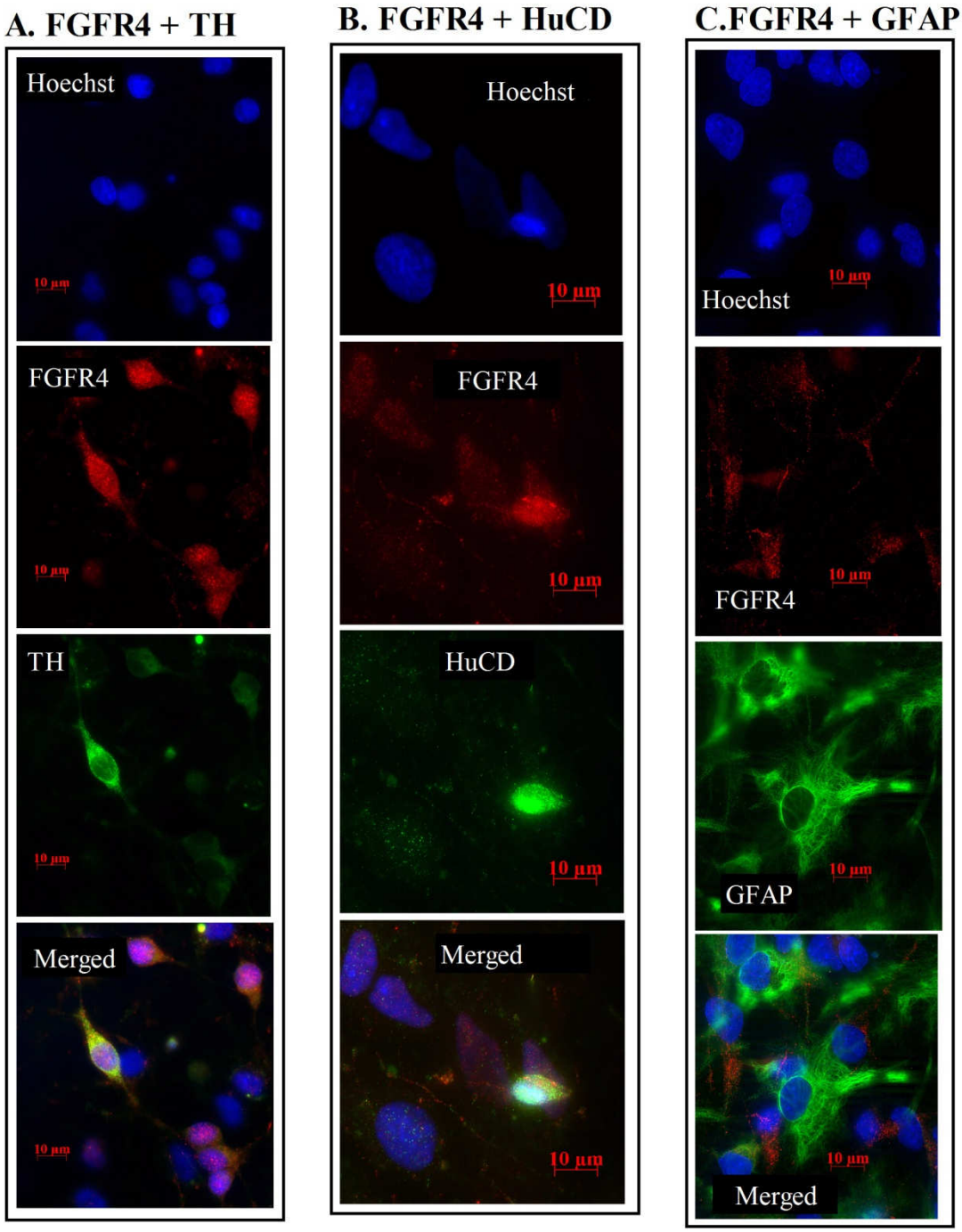

Figure 2.16. Colocalisation profile of FGFR4 in ventral mesencephalic (VM) dopamine neurone cultures. FGFR1 colocalises with TH+ (**A**), HuCD+ (**B**), but not with GFAP+ cells (**C**). TH, HuCD, and GFAP are markers for dopamine neurones, neurones, and astrocytes, respectively. Antigens were visualised using immunofluorescence, and all images were taken at 63x magnification.

Fig 2.17. Table Summarising the Colocalisation of FGF20 and FGFR1, 3, and 4 in the Rat Nigrostriatal Tract and in VM Cultures

Striatum

Antigen/Cell type	FGF20	FGFR1	FGFR3	FGFR4
Neurones (HuCD)	Negative	Positive	Positive – Nuclei only	Positive
Astroctyes (GFAP)	Positive – appears all +	Positive	Negative	Negative
Oligodendrocytes (Morphology)	Negative	Positive	Positive	Positive
Microglia (Iba1)	Negative	Negative	Negative	Negative
Diffuse staining	Positive – does not colocalise with TH	Positive - ~40% overlap with TH	Negative	Negative

Substantia Nigra pars compacta (SNc)

Antigen/Cell type	FGF20	FGFR1	FGFR3	FGFR4
Dopamine Neurones (TH)	Negative	Positive	Positive – Nuclei only	Positive
Astroctyes (GFAP)	Negative	Negative	Negative	Negative
Oligodendrocytes (Morphology)	Negative	Positive	Positive	Positive
Microglia (Iba1)	Negative	Negative	Negative	Negative
Diffuse staining	Negative	Negative	Negative	Negative

Substantia Nigra pars reticulata (SNr)

Antigen/Cell type	FGF20	FGFR1	FGFR3	FGFR4
Neurones (HuCD)	Positive	Positive	Positive – Nuclei only	Positive
Astroctyes (GFAP)	Positive	Positive	Negative	Negative
Oligodendrocytes (Morphology)	Negative	Positive	Positive	Positive
Microglia (Iba1)	Negative	Negative	Negative	Negative
Diffuse staining	Positive	Negative	Negative	Negative

Ventral Mesencephalic Cultures

Antigen/Cell type	FGF20	FGFR1	FGFR3	FGFR4
Neurones (HuCD)	Negative	Positive	Positive	Positive
Dopamine Neurones (TH)	Negative	Positive	Positive	Positive
Astroctyes (GFAP)	Negative	Positive	Positive	Negative

Fig 2.17. Table summarising the co-localisation profiles of FGF20 and FGFR1, 3, and 4 in the substantia nigra (SN) and striatum of the rat brain and in ventral mesencephalic (VM) embryonic dopamine neurone cultures as determined by immunohistochemistry. Human neuronal protein (HuCD), tyrosine hydroxylase (TH), glial fibrillary acidic protein (GFAP), ionised calcium binding adapter molecule 1 (Iba1) were used as markers of neurones, dopamine neurones, astrocytes and microglia, respectively. Co-localisation with oligodendrocytes was deteremined based on the morphology of the stained cells in all cases.

2.5. Discussion

In studies carried out as part of Chapter 4 of this thesis, FGF20's ability to protect dopamine neurones against 6OHDA toxicity in VM cultures and in the 6OHDA rat model of PD was evaluated. Prior to carrying out these studies, it was important to ensure that FGF20's receptors, the FGFRs were, indeed, present in both of these model systems. Therefore, in the current Chapter, the immunohistochemical localisation profiles of FGF20 and FGFR1, 3, and 4 were comprehensively characterised in the nigrostriatal tract of the rat brain and in VM embryonic dopamine neurone cultures.

2.5.1. Localisation of FGF20 and FGFR1, 3, and 4 in VM Cultures

In VM embryonic dopamine neurone cultures, FGF20 was found not to be localised in any of the cell types present in the culture. FGF20 has been shown to have a neurotrophic effect on VM dopamine neurone cultures when applied exogenously, with FGF20 treatment being able to greatly increase the yield of dopamine neurones derived from VM cultures (Correia *et al.*, 2007). Results generated in this study indicate that there might be a chance that FGF20 actually does not play a physiological role in the developing nigrostriatal tract, based on results from this study showing FGF20 not to be present in the DIV6 VM cultures. This would be in contrast to FGF2, which is present in both the developing (Bean *et al.*, 1992) and the adult nigrostriatal tract (***see section 2.1.5***). It has, however, been shown that certain growth factors including the FGF's are only expressed in specific areas of the developing rat brain at specific gestational periods (Powell *et al.*, 1991; Kuzis *et al.*, 1995; Monfils *et al.*, 2006). A study in which the temporal expression pattern of FGF20 in the developing midbrain is comprehensively characterised throughout embryogenesis would, thus, be needed before it could be conclusively determined whether or not FGF20 plays a role in the development of the nigrostriatal tract during embryogenesis.

FGFR1, 3, and 4 were all found to be present abundantly in a number of different cell types within the VM cultures. This is not surprising, as the FGF system has been shown to play an important role in regulating the development of the embryonic brain (Dono, 2003; Thisse & Thisse, 2005). FGFR1 and 3 had an equivalent colocalisation profile in the VM cultures, as both receptors were found to colocalise to most of the astrocytes, dopamine neurones, and non-dopaminergic neurones within the VM cultures. FGFR4, on the other hand, was found to localise to both dopaminergic

and non-dopaminergic neurones, but unlike FGFR1 and 3, FGFR4 was found not to localise to any astrocytes. For FGFR1, FGFR3, and FGFR4 a purely cytoplasmic staining pattern was observed in some astrocytes or neurones, while in others a nuclear and cytoplasmic staining pattern was observed. This indicates that all three receptors might signal through a nuclear signalling pathway in the VM cells (***see section 2.5.3 for detailed discussion***).

2.5.2. Localisation of FGF20 in the Rat Nigrostriatal Tract

In the rat brain, FGF20 was found to be present in both the SN and the striatum. In the SN, FGF20 was however, exclusively localised to the SNr, with no FGF20 staining being observed in the SNc. The results showing FGF20 not to be localised in the SNc conflicts with previously reported *in situ* hybridisation results which showed FGF20 to be exclusively localised to dopamine neurones in the SNc of the rat brain (Ohmachi *et al.*, 2000). It has been demonstrated that specific mRNA transcripts are in some cases locally translated into proteins at nerve terminals after being transported from their site of production in the cell body to nerve terminals (Giuditta *et al.*, 2008). This discrepancy might, thus, be due to FGF20 mRNA being transcribed but not translated at the level of the SNc, with FGF20 mRNA only locally being translated into protein in the striatal dopaminergic nerve terminals after being transported there. This scenario is, however, unlikely to apply to FGF20, as, if this was the case, one would expect FGF20 protein to be localised to TH+ nerve terminals in the striatum, and although a diffuse punctuate FGF20 staining pattern was observed in the striatum in this study, FGF20 was found not to co-localise to striatal TH+ nerve terminals. The only feasible explanation for this discrepancy might, thus, be that the FGF20 mRNA gets transcribed into mRNA but not translated into protein, as has been reported to occur with a number of specific mRNA transcripts in certain contexts (Honda *et al.*, 1993; Pascal *et al.*, 2008). Importantly, it also needs to be noted that the results from the Ohmachi *et al*., 2000 study showing FGF20 to be exclusively localised to nigrostriatal dopaminergic neurones are controversial, as in another study, FGF20 was shown to be predominantly expressed by non-dopaminergic cells, as a unilateral 6OHDA lesion in rats fails to attenuate FGF20 mRNA levels in both the striatum and SN of the lesioned nigrostriatal tract (Grothe *et al.*, 2004). Furthermore, results from this study also conflict with results from the Ohmachi *et al*., 2000 study in a second manner, as it was demonstrated here that FGF20 localised to the SNr and also to the striatum, whereas the Ohmachi *et al*.,

2000 study found FGF20 mRNA to be present in no other region in the rat brain apart from the SNc. In this study, a highly sensitive 3 step indirect ABC fluorescence method (***see section 2.3.4***) was used which allowed for the amplification of the FGF20 fluorescence signal. It is, thus, possible that FGF20 is expressed at a relatively low copy number in the SNr and striatum, which resulted in the *in situ* hybridisation technique in the Ohmachi *et al.*, 2000 study having an insufficient sensitivity to detect FGF20 mRNA in the SNr and striatum, and possibly other areas of the brain as well. Further support is provided for this possibility by a recent study that detected FGF20 mRNA not only in the rat SN but also in the striatum with the use of the highly sensitive PCR method (Grothe *et al.*, 2004).

Moreover, in this study, FGF20 was found to be localised to numerous astrocytes and to a very small number of neuronal cells within the SNr. Additionally, FGF20 appeared to be localised to afferent SNr nerve terminals, as a diffuse punctuate FGF20 staining pattern consistent with that observed for axon terminals was observed throughout the SNr. Although not verified in this study, it is likely that this diffuse staining localises to either glutamatergic or GABAergic nerve terminals which comprise the main afferent inputs into the SNr (Blandini *et al.*, 2000). Despite FGF20 not being present in the SNc where the cell bodies of the nigrostriatal dopamine neurones are localised, it is still feasible that endogenous FGF20 might act on dopamine neurones at the nigral level, under physiological conditions; as numerous TH+ dopamine neurone dendrites extended throughout the SNr where they were surrounded by FGF20.

As was observed in the SNr, in the rat striatum a diffuse punctuate FGF20 staining pattern consistent with that observed for axon terminals was also observed throughout the striatum. However, it appears that the diffuse FGF20 striatal staining localises with non-dopaminergic striatal afferent terminals, as the diffuse FGF20 staining did not co-localise to striatal TH+ dopamine nerve terminals. Additionally, FGF20 was also abundantly localised in most, if not all, of the astrocytes present in the striatum. The prototypical FGF family member, FGF2 also localises to striatal astrocytes (Gonzalez *et al.*, 1995), and indirect evidence from *in vitro* studies have indicated that astrocyte-derived striatal FGF2 might play an important neurotrophic role in the nigrostriatal tract by stimulating and maintaining dopamine neurone survival. In VM embryonic dopamine neurone cultures, astrocytic FGF2 release is stimulated by the activation of dopamine receptors located on the astrocytes, and this dopamine stimulated astrocyte-derived FGF2 has a neurotrophic effect on dopamine neurones in

the culture (Reuss & von Bohlen und Halbach, 2003; Li *et al.*, 2006). Results showing FGF20 to also be abundantly localised to striatal astrocytes, opens the possibility that FGF20 might be another FGF family member that acts alongside FGF2 to maintain an optimal neurotrophic environment within the rat nigrostriatal tract.

2.5.3. Localisation of FGFR1, 3, and 4 in the Rat Nigrostriatal Tract

Results from this study demonstrated FGFR1, 3, and 4 all to be present in the rat nigrostriatal tract, and there was a partial correlation between the colocalisation profiles of the different receptors. The localisation profiles of the three receptors were identical in respect to their colocalisation with oligodendrocytes and microglia within the nigrostriatal tract. FGFR1, 3, and 4 were all localised to oligodendrocytes within the SNc, SNr, and the striatum. This is not surprising, as the FGF system has been shown to play an important role in regulating the functioning of both embryonic and adult oligodendrocytes (Butt & Berry, 2000). In contrast, all three of the receptors did not localise to microglia in any of the areas examined. Furthermore, all three of the receptors were found to colocalise with TH+ dopamine neurones in the SNc, and to HuCD+ neuronal cells within the SNr, and the striatum. The sub-cellular localisation of FGFR3 in dopamine neurones and in neuronal cells, however, differed to that observed for FGFR1 and 4. For FGFR1 and 4 a cytoplasmic localisation pattern was observed in all TH+ dopamine neurones and HuCD+ neurones, while FGFR3 was exclusively localised to the nuclei of neurones in all of the nigrostriatal areas examined. The FGFRs are RTKs, and they are, therefore, traditionally considered to exist and function as classical plasma membrane receptors that signal through various second messenger systems (***detailed in section 5.1***). The nuclear staining pattern that we observed for FGFR3 is, thus, not consistent with the staining pattern that one would expect to observe for a RTK, opening the possibility that the FGFR3 nuclear staining might be non-specific or artefactual. Recent findings have, however, conclusively demonstrated that a number of plasma membrane receptors also signal through an unorthodox nuclear signalling pathway that involves the translocation of the receptors from the plasma membrane to the nucleus, and the FGFRs are a prototypical example of such receptors (Bryant & Stow, 2005). Activation of membrane bound FGFR1 by FGF2, for example, leads to the nuclear translocation of some of the FGFR1-FGF2 complexes (Bryant & Stow, 2005). This nuclear translocation has been shown to be essential in allowing FGF2's full mitogenic effects to be expressed (Bossard *et al.*, 2003). It is, however,

unlikely that the nuclear staining that we observed for FGFR3 is due to the receptor signalling through such a nuclear translocation pathway in neurones within the nigrostriatal tract. If this was the case, one would expect both nuclear and cytoplasmic staining to be observed, and exclusively nuclear FGFR3 staining was observed in neurones within the nigrostriatal tract. The nuclear localisation pattern observed for FGFR3 can, however, be explained by findings which have shown some growth factor receptors to exist as specific isoforms that localise exclusively to the nucleus of cells, where they signal through various intracrine mechanisms (Bailly *et al.*, 2000; Soulet *et al.*, 2005), and there is in fact evidence for FGFR3 existing as such an isoform. FGFR3 is most widely known to exist as the two classical b and c FGFR isoforms (Johnson *et al.*, 1991). Recent studies have, however, demonstrated another 3 additional C-terminal truncated isoforms of FGFR3 to exist, and one of these isoforms appears to be localised exclusively to the nucleus (Keegan *et al.*, 1991; Johnston *et al.*, 1995). It is, thus, possible that the nuclear FGFR3 staining represents the presence of such an exclusively nuclear localised receptor in the neurones within the nigrostriatal tract. Before such an explanation could be accepted further experiments are, however, required to ensure that the neuronal FGFR3 staining isn't artefactual or non-specific. More specifically, the FGFR3 localisation profile needs to be replicated with FGFR3 primary antibodies targeting alternative epitopes of the FGFR3 protein. Additionally, the specificity of the staining also needs to be confirmed in control experiments in which it is evaluated whether the FGFR3 staining can be blocked with the antigenic peptides used to generate the primary antibodies. Such control experiments were not carried out in this study due to us not having access to these antigenic peptides. These additional studies are particularly necessary due to the results showing FGFR3 to be localised to neuronal cells being controversial in itself, as previous studies have reported FGFR3 mRNA to be mainly localised to glial cells within the nigrostriatal tract within the rat brain (Wanaka *et al.*, 1990; Yazaki *et al.*, 1994; Belluardo *et al.*, 1997). As mentioned above, 5 isoforms of FGFR3 have, thus, far been detected, and the failure of these studies to detect FGFR3 in neuronal cells could simply be due to the primers used in their studies not being designed to detect all of the different isoforms of the FGFR3.

The findings showing FGFR1 to be localised with TH+ neurones in the SNc, and with neurones in the SNr and striatum is consistent with previous reports. Using in situ hybridisation, FGFR1 mRNA has been demonstrated to be localised to both glial and neuronal cells in the SNc, SNr, and also in the striatum (Wanaka *et al.*, 1990;

Yazaki *et al.*, 1994; Belluardo *et al.*, 1997). Using immunohistochemistry, the FGFR1 protein has also previously been shown to co-localise to dopamine neurones in the rat and human SNc (Walker *et al.*, 1998).

As mentioned earlier, in this study, FGFR4 was found to be expressed in TH+ neurones in the SNc, and also in HuCD+ neurones in the SNr and striatum. Additionally, FGFR4 was also found to be present in a small number of spindle shaped non-dopamine neurones in the SNc and in numerous oligodendrocytes in all areas of the nigrostriatal tract. These results conflict with previous studies in which FGFR4 mRNA was found to be exclusively localised to cholinergic neurones within the MHB of the rat brain (Miyake & Itoh, 1996). In order to validate that the antibody used was, indeed, appropriately detecting FGFR4, control experiments were carried out to check if the antibody used in this study was able to detect FGFR4 in neuronal cells in this area of the brain where FGFR4 mRNA has previously been reported to be present. In these experiments, neuronal cells within the MHB were found to stain strongly positive for FGFR4, thus, providing supporting evidence that the antibody was appropriately detecting FGFR4 in the rat brain. The staining detected for FGFR4 appeared to be lower in the nigrostriatal tract compared to the MHB. It is, thus, possible that the *in situ* hybridisation technique used in the Miyake *et al.*, 1996 study was sensitive enough to detect FGFR4 in the MHB where the receptor is expressed at relatively high levels, but not in other areas of the brain where it appears FGFR4 is expressed at lower levels. Moreover, like FGFR3, FGFR4 has also been shown to exist as a number of different isoforms which result from the alternative splicing of the FGFR4 gene (van Heumen *et al.*, 1999; Ezzat *et al.*, 2001; Kwiatkowski *et al.*, 2008). FGFR4 does not exist as the classical b and c FGFR isoforms, which exist for FGFR1, 2, and 3. Instead, FGFR4 has been shown to exist as 3 additional C-terminal truncated isoforms. It is, thus, also possible that the previous *in situ* hybridisation studies failed to detect FGFR4 in the nigrostriatal tract and in other areas of the brain due to the primers in their studies binding to an FGFR4 isoform that is expressed only in the MHB and not to isoforms expressed in other areas of the rat brain. Additionally, the conclusiveness of published *in situ* hybridisation studies also remain questionable based on the fact that in many cases mRNA for a specific protein is found by initial studies to be localised to only specific areas, only for later studies then to contradict this by reporting the mRNA to be localised to additional areas. This is actually the case with FGFR4, as two initial studies found no FGFR4 mRNA to be localised in the brain at all (Partanen *et al.*, 1991; Yazaki

et al., 1994), whereas a subsequent study contradicted these results by demonstrating FGFR4 to be localised in the MHB of the rat brain (Miyake & Itoh, 1996).

Of the 3 FGFRs examined in this study, only the FGFR1 was found to be localised to astrocytes within the nigrostriatal tract. In the SN, only a very small number of astrocytes were found to be present in the SNc, and FGFR1 appeared not to colocalise to any of these astrocytes. In the SNr and striatum, on the other hand, numerous astrocytes were present throughout these areas of the nigrostriatal tract, and FGFR1 co-localised to many if not all of the astrocytes present in the SNr and striatum. The results showing FGFR1 to be localised to both neurones and glial cells in the nigrostriatal tract are consistent with previous reports which demonstrated FGFR1 to be localised to both neuronal and glial cell in the SN and striatum (Wanaka *et al.*, 1990; Yazaki *et al.*, 1994; Belluardo *et al.*, 1997; Walker *et al.*, 1998).

2.5.4. Conclusion

In the current study, the colocalisation profiles of FGF20 and the FGFR1, 3, and 4 proteins in both VM cultures and in the nigrostriatal tract of the rat brain were immunohistochemically characterised. A previous study has comprehensively characterised the localisation profile of the FGFR2 protein in the rat nigrostriatal tract (Chadashvili & Peterson, 2006). The results presented in this Chapter, however, provide the first detailed account describing the localisation of the FGFR1, 3, and 4 proteins in VM cultures and in the nigrostriatal tract of the rat brain. FGFR1, 3, and 4 were demonstrated to be abundantly present within VM cultures and also throughout the nigrostriatal tract of the rat brain. In the Chadashvili & Peterson, 2006 study, FGFR2 was also shown to be present in the SN and striatum, although it was found to be exclusively localised to astrocytes. The widespread presence of all 4 of the FGFRs within the nigrostriatal tract, and more particularly, the localisation of FGFR1, 3, and 4 to nigrostriatal dopamine neurones, provide a sound anatomical rationale for investigating the neuroprotective potential that pharmacological activation of the FGF system might have in PD. Furthermore, if the FGFs are protecting dopamine neurones by directly activating FGFRs on nigrostriatal dopamine neurones, results from this study indicates that targeting the FGF system at the level of the substantia nigra, rather than the striatum, is likely to have the greatest neuroprotective potential. This is as, at the nigral level, FGFR1, 3, and 4 were found to be present in TH+ nigrostriatal

dopamine neurones within the SNc. In the striatum, on the other hand, only FGFR1 co-localises with striatal dopamine neurone terminals, and of all the TH+ striatal nerve terminals, only ~40% appear to be positive for FGFR1.

Chapter 3: Establishing a Unilateral Partially Lesioned 6OHDA Rat Model of Parkinson's Disease in which to Test FGF20 for its Neuroprotective Effects

3.1. Introduction

3.1.1. Animal Models of PD

Animal models of PD serve as essential tools in research efforts that are aimed at uncovering the pathogenic processes that cause PD, and also at finding new more effective treatments for the disease. Although numerous animal models of PD are currently available, only a selected number of these are widely used due to many of the available models having significant shortcomings that limit their use. In order for an animal model to be considered to be a representative and practically useful model, it has to fulfil three main criteria. Firstly, the aetiology that causes the induced disease state in the animal model must be representative of the ascertained or putative aetiological mechanisms that cause the disease in humans, that is, the model must have good *construct validity*. For a PD animal model to have good construct validity, the factors that induce the model must, therefore, include one or more of the putative aetiological causes of PD, which include oxidative stress, mitochondrial dysfunction, UPS dysfunction, exposure to environmental toxins, and neuroinflammation (***detailed in section 1.2***). Secondly, the model also has to have good *face validity*, meaning that the cardinal symptoms and pathological features that manifest in the animal model must reflect those observed in the clinic. A PD animal model with good face validity, must, therefore, reproduce not only the progressively developing cardinal clinical symptoms of PD, which include bradykinesia, akinesia, rigidity, and postural instability, but also the key pathological features of PD, namely, progressive nigrostriatal dopaminergic degeneration, and formation of SNCA and Ub positive LB inclusions in dopamine neurones. Thirdly, the model also has to have good *predictive validity*, which means that there has to be a good correlation between the therapeutic effects achieved by drugs in the animal model and in the clinic, and this is particularly important for models which are used in drug discovery research.

The main PD animal models that are currently available can be divided into five sub-groups based on the way in which they are induced: pharmacologically, proteasome inhibitor, pesticide, genetically, and neurotoxin induced models. In the following

sections, a brief overview of each of these sub-groups of models is given. The main aim of the current chapter is to establish an appropriate partially lesioned 6OHDA rat model of PD in which to test FGF20 for its neuroprotective effects *in vivo*. The overview given below, thus, also serves to rationalise why the 6OHDA rat model was chosen in preference to the other models by detailing the specific shortcomings that make the other models unamenable to neuroprotective studies. Additionally, all of the favourable attributes of the partially lesioned 6OHDA rat model of PD that make it particularly amenable to early stage neuroprotection studies are also highlighted.

3.1.1.1. Pharmacologically-Induced Models

Two of the most commonly used pharmacologically induced models PD include the reserpine and the haloperidol rodent models. Reserpine is a vesicular monoamine transporter inhibitor, and when systemically administered to rats, it acts to deplete vesicular stores of several catecholamine neurotransmitters in the brain, including dopamine, serotonin, and noradrenaline. Around 12h after administration, rats display the classical features of reserpine treatment, which include akinesia, ptosis, and piloerection (Betarbet *et al.*, 2002; Jenner, 2008; Duty & Jenner, 2011). The latter two signs result from the depletion of noradrenaline and serotonin, and reversal of these signs by drugs is most commonly used to screen for agents with antidepressant activity. Akinesia, on the other hand, results from the depletion of striatal dopamine stores. The reserpine rat model of PD, thus, reproduces not only the striatal dopamine deficiency observed in PD, but also the akinesia that results from striatal dopamine depletion.

Haloperidol, on the other hand, is a dopamine receptor antagonist, and, when systemically administered to rodents, it acts to inhibit striatal dopaminergic neurotransmission by inhibiting the activation of striatal dopamine receptors, and through this action it induces catalepsy and rigidity in the rodents (Duty & Jenner, 2011). The haloperidol model, thus, reproduces both the reduction in dopamine receptor activation observed in PD, and also one of the cardinal motor symptoms of PD, rigidity. In drug discovery research, the reserpine and the haloperidol rodent models of PD are widely used to identify potential new symptomatic treatments for PD by screening drugs for their ability to reverse reserpine-induced akinesia, and haloperidol-induced rigidity, respectively.

A major shortcoming associated with the pharmacologically induced models of PD includes the apparent lack of construct validity. Additionally, these models also

have poor face validity, as the disruption of striatal dopaminergic transmission induced by the drugs is only temporary, and no degeneration or pathological changes are brought about by the drugs in the nigrostriatal tract. The latter shortcoming makes these models unsuitable for use in studies aimed at finding neuroprotective agents that can protect dopamine neurones from neurodegeneration, and also for most studies investigating PD pathogenesis. These pharmacological models are, nevertheless, widely used in early stage drug discovery research aimed at finding new symptomatic treatments for PD, as these models possess excellent predictive validities, and also because the models are time and cost efficient. The reserpine rat model, for example, was the first animal model in which L-DOPA's therapeutic efficacy was demonstrated, and all of the current drugs that are currently used to treat PD clinically are effective at reversing akinesia in the reserpine rat (Duty *et al.*, 2011).

3.1.1.2. Proteasome Inhibitor Model

A number of different selective proteasome inhibitors, including epoxomicin and lactacystin, have been demonstrated to induce PD-like phenotypes when administered to rats (McNaught *et al.*, 2002; Fornai *et al.*, 2003; Emborg, 2004; Niu *et al.*, 2009). Either chronic systemic administration or single intra-cerebral (both intra-nigral and intra-striatal) injections of proteasome inhibitors have been shown to induce progressive nigrostriatal dopaminergic degeneration accompanied by progressively developing apomorphine responsive motor deficits. Additionally, SNCA and Ub positive LB-like inclusions are also observed in the dopamine neurones of the proteasome inhibitor treated rats. The proteasome inhibitor model, therefore, initially appeared to be an ideal model system as it possessed good face, construct and also good but incompletely validated predictive validity. However, disappointingly this model failed to become widely utilised due to the model having poor reproducibility (Duty & Jenner, 2011).

3.1.1.3. Genetically Induced Models

As discussed earlier in ***section 1.2***, a number of single gene mutations have been shown to be the cause of familial forms of PD. Mutations in the *SNCA* and *LRKK-2* genes are responsible for causing autosomal dominant forms of familial PD, while mutations in either the *parkin*, *PINK-1*, or *DJ-1* gene leads to autosomal recessive forms of PD. It was hoped that representative transgenic mouse models of PD could be created by

producing transgenic strains of mice with analogous mutations in the genes associated with the familial forms of PD, but disappointingly little success has been achieved thus far. Transgenic mouse strains that express either mutant PD associated forms *SNCA* or *LRRK-2* have been created and characterised, and so have knockout mice in which the *parkin*, *PINK-1*, or *DJ-1* gene have been deleted (Harvey *et al.*, 2008; Dawson *et al.*, 2010; Taylor *et al.*, 2010). Unfortunately, none of these genetic manipulations gave rise to dopamine neurone degeneration, and none of the transgenic mice strains demonstrated robust motor deficits, making these models unsuitable for use in drug discovery research. One of the transgenic mouse models overexpressing the A53T *SNCA* mutant gene that causes familial PD has, however, been shown to reproduce the LB pathology observed in PD, as dopamine neurones in the mice were found to contain Ub and SNCA positive proteinacious inclusions (Dawson *et al.*, 2010). This model might, thus, be useful for studying the processes that lead to inclusion formation. It might also be useful in a limited number of drug discovery studies that are aimed at identifying drugs that can inhibit inclusion formation.

Despite these initial disappointments, research in this area is ongoing, and attempts are currently underway to create better transgenic animal models of PD by genetically inducing some of the putative aetiological causes of PD in mice. A defect in mitochondrial respiration is thought to be one of the putative causes of sporadic PD, and, encouragingly, the selective induction of a mitochondrial defect in dopamine neurones produces a highly representative parkinsonian phenotype in the resulting mice strain, which is referred to as the mitoPARK mouse (Ekstrand *et al.*, 2007; Terzioglu & Galter, 2008; Ekstrand & Galter, 2009). The transcription factor, TFAM plays an important role in regulating the transcription of mitochondrial DNA; and selective deletion of TFAM using a conditional knockdown strategy in the MitoPARK mice leads to progressive nigrostriatal dopaminergic degeneration and the formation of inclusions in the remaining dopamine neurones. Importantly, the nigrostriatal pathology was demonstrated to be accompanied by progressively developing motor deficits, which responded to L-DOPA treatment. This model, therefore, has the potential to be an excellent research tool at it appears, from these initial reports, that the model has one of the best construct and face validity profiles of any of the currently available models. The model reproduces not only the main symptoms and pathological features of PD, but also the progressive development of these features, a character lacking in many of the models that are currently widely used. The robustness and predictive validity of the

model, however, still needs to be validated as these findings have, thus far, not been replicated by any independent groups, and no studies have thus far evaluated the predictive validity of the model.

3.1.1.4. Neurotoxin Induced Models of PD

3.1.1.4.1. Rotenone Model

Three main neurotoxin-induced models of PD are currently available, the rotenone rodent model, the MPTP model, and the 6OHDA rat model, although only the latter two models are widely used in PD research. In the rotenone rodent model, a parkinsonian-like phenotype is induced in rats by administering them with chronic systemic injections of rotenone, an organic plant root derived pesticide (Betarbet *et al.*, 2000; Beal, 2001; Betarbet *et al.*, 2002; Duty & Jenner, 2011). Rotenone is a selective mitochondrial complex 1 inhibitor, and when chronically administered to rats, it causes selective and progressive nigrostriatal dopaminergic degeneration accompanied by progressively developing apomorphine responsive motor deficits, including postural instability and bradykinesia. Additionally, rotenone also induces the formation of SNCA and Ub positive LB-like inclusions in dopamine neurones. Overall, the rotenone model, thus, fulfils all the criteria for being a highly representative model of PD, as it has good construct, face, and predictive validity, although the later remains to be comprehensively validated. However, unfortunately, the rotenone model has failed to become widely utilised due to two main shortcomings. There is significant variation in the sensitivity of different rats to the nigrostriatal toxicity of rotenone, with only ~50% of treated rats developing the described parkinsonian phenotype (Beal, 2001). In additional to this, rotenone also produces severe illness in the treated rats, with ~30% of rats dying due to peripheral toxicity (Duty & Jenner, 2011). These shortcomings unfortunately prevent this model from being successfully used in neuroprotection studies, and it limits its use to specific studies investigating PD pathogenic processes.

3.1.1.4.2. MPTP Model

The selective dopamine neurone toxin, MPTP is used to create PD models in both mice and non-human primates (NHPs), and these MPTP models represent some of the most widely used animal models of PD (Beal, 2001; Betarbet *et al.*, 2002; Emborg, 2004; Jenner, 2008; Duty & Jenner, 2011). After systemic administration, MPTP readily

crosses the blood brain barrier (BBB) and enters the CNS due to the high lipophilicity of the compound. In the CNS, MPTP gets metabolised into its active toxic metabolite, 1-methyl-4-phenylpyridium (MPP+) by MAO-B enzymes that are localised throughout the brain. MPP+ subsequently gets selectively taken up and concentrated in dopamine neurones due to MPP+ being a substrate for the dopamine transporter which is selectively expressed in dopamine neurones. Once inside the dopamine neurones, MPP+ accumulates in mitochondria, and it ultimately causes dopamine neurone degeneration by stimulating free radical production and also by inhibiting mitochondrial complex 1 activity (Beal, 2001). Due to many animal species including most rat strains being insensitive to the toxic effects of MPTP for poorly understood reasons, MPTP's use is limited to sensitive animal species, including certain strains of mice (C57 black, and Swiss Webster) and NHPs (Duty & Jenner, 2011). In mice, repeated systemic MPTP administration has been reported in some studies to cause both nigrostriatal dopamine neurone degeneration and motor deficits (Jenner, 2008). The use of the MPTP mouse model is, however, limited by the fact that MPTP induces robust nigrostriatal degeneration and motor deficits in mice only when administered at relatively high doses, which are associated with significant adverse affects and mortality (Emborg, 2004). Research carried out in the MPTP primate model of PD, on the other hand, has and still is making major contributions to PD research efforts, and it is currently considered the gold standard animal model of PD due the model having one of the best construct, face, and predictive validity profiles of any of the available models. The model is considered to have good construct validity as the mechanisms causing MPTP induced dopamine neurone degeneration, mitochondrial complex 1 inhibition and free radical production, corresponds with two of the putative aetiological causes of PD. The model is considered to have good face validity as repeated systemic administration of MPTP to NHPs causes not only selective nigrostriatal dopamine neurone degeneration but also all of the cardinal motor symptoms of PD in the primates, including akinesia, bradykinesia, rigidity, and postural stability (Beal, 2001; Duty & Jenner, 2011). An additional advantage of this model is that an equivalent degree of nigrostriatal degeneration (~70%) is induced in most MPTP primate models to that observed in early stage PD (Duty & Jenner, 2011). Importantly, the model also has excellent predictive validity, as all of the dopamine based drugs that are currently used in the clinic are also effective in the MPTP primate (Jenner, 2008). Moreover, the model has also been extensively used in research into L-DOPA induced dyskinesias (LID) as long term L-

DOPA treatment induces motor complications in MPTP treated primates that are indistinguishable from those observed in PD patients (Duty & Jenner, 2011). The model, nevertheless, does have some shortcomings, the main ones being that MPTP does not induce the formation of LB-like inclusions in most studies, and the onset of nigrostriatal degeneration achieved in the model is acute rather than progressive (Beal, 2001; Betarbet *et al.*, 2002). Furthermore, the cost and ethical issues that are associated with the use of NHPs in research limits the use of this model mainly to late stage pre-clinical drug development research.

3.1.1.4.3. 6-Hydroxydopamine Rat Model of PD

In the 6OHDA rat model of PD, the selective degeneration of the nigrostriatal dopaminergic pathway that is observed in PD is reproduced in rats with the use of the selective dopamine neurone toxin, 6OHDA. Because 6OHDA does not cross the BBB, it needs to be delivered directly to either the SNc, the medial forebrain bundle (MFB), or the striatum using stereotaxic surgery. After being introduced directly into the nigrostriatal tract, 6OHDA is actively accumulated in dopamine neurones as a consequence of 6OHDA being a substrate for both the dopamine and noradrenaline transporter proteins (Simola *et al.*, 2007). Because 6OHDA is also a substrate for the noradrenaline transporter, it induces the degeneration of not only dopamine neurones, but also noradrenergic neurones (Simola *et al.*, 2007). However, in most 6OHDA rat models of PD, intra-cerebral administration of 6OHDA leads to minimal noradrenergic nerve damage due to the 6OHDA infusion site being limited to the vicinity of the nigrostriatal dopaminergic tract, in areas of the brain that are relatively sparsely innervated by noradrenergic inputs and also not in close proximity to the noradrenergic nuclei of the brain. Additionally, in some 6OHDA rat models of PD, rats are pre-treated with a noradrenaline reuptake inhibitor such as desipramine prior to 6OHDA lesioning to limit any noradrenergic degeneration (Schwarting & Huston, 1996b). Upon entering the cytoplasm of dopamine neurones, 6OHDA is rapidly and non-enzymatically oxidised in the presence of molecular oxygen, leading to the generation of the highly reactive ROS, H_2O_2 and p-quinone (Schwarting & Huston, 1996b; Soto-Otero *et al.*, 2000). 6OHDA's cytotoxic effects on dopamine neurones, however, result not only from excessive ROS production, but also from 6OHDA-mediated inhibition of complex 1 of the mitochondrial respiratory chain (Glinka & Youdim, 1995; Glinka *et al.*, 1996; Schwarting & Huston, 1996b; Soto-Otero *et al.*, 2000).

Tyrosine hydroxylase (TH) is the rate limiting enzyme in the dopamine synthesis pathway, and because of the relatively selective localisation of TH to catecholaminergic neurones, it is often used as a marker of dopamine neurones. In the 6OHDA rat model of PD, the degree of nigrostriatal degeneration induced by 6OHDA is, therefore, quantified using TH immunohistochemistry, and in drug discovery studies, test treatments are evaluated for their ability to preserve both striatal TH levels and nigral TH+ cell counts at significantly higher levels compared to vehicle treated 6OHDA lesioned rats. Importantly, the nigrostriatal degeneration induced by 6OHDA leads to the development of motor deficits in the rats, including akinesia, postural instability, and rigidity, and these deficits can be quantified by a number of behavioural tests of motor function (Deumens *et al.*, 2002). In most studies using the 6OHDA rat model of PD, unilaterally rather than bilaterally lesioned rats are utilised as bilateral lesions produce debilitating adverse effects in the rats, including severe aphagia and adipsia. Additionally, in some studies the use of a unilateral model removes the need for a sham lesioned group, as it allows the non-lesioned contralateral nigrostriatal tract and rat paw to serve as appropriate controls for TH-immunohistochemistry and motor function results, respectively.

Motor tests that are commonly employed to quantify motor deficits in unilaterally 6ODHA lesioned rats include both tests that measure drug induced motor asymmetries, for example, the apomorphine and amphetamine induced rotation tests (Schwarting & Huston, 1996a), and tests that measure spontaneous motor function, such as the cylinder test and the adjusted stepping test (Schallert & Tillerson, 2000). In the two drug-induced rotational tests, the rotational behaviour of unilaterally 6OHDA lesioned rats is assessed after injecting the rats with either apomorphine (a D2 receptor agonist) or amphetamine (a catecholamine releasing agent). In unilaterally lesioned rats, apomorphine stimulates post-synaptic dopamine receptors on the striatal medium spiny gabaergic neurones in the striatum ipsilateral to the lesion to a much greater extent compared to the contralateral intact striatal hemisphere. This is due to the unilateral nigrostriatal lesion inducing a unilateral depletion of striatal dopamine levels, and a consequent unilateral supersensitisation of striatal dopamine receptors in the striatal hemisphere ipsilateral to the lesion. For this reason, apomorphine induces rotations in the rat that is directed ipsilateral to the lesion. Because amphetamine, on the other hand, acts to release dopamine from nerve terminals, its administration causes stimulation of dopamine receptors in the intact contralateral striatum, and only minor stimulation of

dopamine receptors in the ipsilateral denervated striatum. As a result of this, amphetamine, thus, causes the unilaterally 6OHDA lesioned rats to rotate contralaterally to the lesion.

After unilateral 6ODHA lesioning, rats develop forelimb motor asymmetry, as the unilateral degeneration of the nigrostriatal tract results in motor deficits developing in the impaired forelimb contralateral to the lesioned hemisphere, while normal motor function is retained in the unimpaired forelimb ipsilateral to the lesioned hemisphere. In the cylinder test, this asymmetry in motor deficits is quantified and used as a measure of contralateral forelimb akinesia (Schallert & Tillerson, 2000). Briefly, rats are placed inside transparent plexiglass cylinders in order to encourage exploratory rearing behaviour (***see section 3.3.2.1 for detailed methods***). By recording forelimb use during rearing movements, forelimb use preferences are then quantified; i.e., the percentage of total rears that is supported by either both forelimbs, the ipsilateral forelimb alone, or the contralateral forelimb alone is quantified. In this test, the unilateral contralateral forelimb motor deficits induced by unilateral 6OHDA lesioning results in a significantly smaller percentage of total rears being supported by both forelimbs and by the contralateral forelimb alone, while a significantly greater percentage of rears is supported by the ipsilateral forelimb alone. In the adjusted stepping test, on the other hand, the capability of rats to make balance restoring adjusting step movements with their ipsilateral or contralateral forelimbs is quantified (***see section 3.3.2.2 for detailed methods***). After unilateral 6OHDA lesioning, a significant reduction in the number of adjusted steps made by the contralateral forelimb is recorded, while the adjusted stepping ability of the forelimb ipsilateral to the lesioned hemisphere is retained. The reductions in adjusted stepping ability that are detected by this test are taken to be a quantitative measure of postural instability (Schallert & Tillerson, 2000). Importantly, it has been demonstrated that the relative size of the motor deficits that are detected by both the cylinder test and the adjusted stepping test are proportional to the degree of nigrostriatal degeneration that is present in rats (Lee *et al.*, 1996; Schallert & Tillerson, 2000).

Overall, the 6OHDA rat model of PD is considered to be one of the most representative and useful animal models of PD as the model possesses one of the best and most thoroughly validated construct, face, and predictive validities of any of the currently available models. The model has good construct validity as the mechanisms mediating 6OHDA's cytotoxic effects on dopamine neurones overlaps with some of the

putative aetiological causes of PD, namely, oxidative stress and mitochondrial complex 1 inhibition. The model also has excellent face validity as both the nigrostriatal dopamine neurone degeneration and the consequent motor deficits that are present in PD are reproduced in the model. Importantly, not only the striatal TH and dopamine depletion but also the nigral dopamine neurone degeneration that is observed in PD is robustly recreated in the 6ODHA rat model (Duty & Jenner, 2011). In addition to this, many of the other biochemical and inflammatory abnormalities that are associated with PD are also reproduced in the model (Duty & Jenner, 2011). In the 6OHDA lesioned rat brain, striatal levels of the anti-oxidant enzymes GSH peroxidase and superoxide dismutase are depleted, while nigral levels of microglial activation, TNFα, and iron are raised. Furthermore, many of the PD associated plastic changes that occur in other neural systems that make up the basal ganglia are also reproduced in the 6OHDA lesioned rat brain. These changes include increased firing of the subthalamic nucleus, increased glutamate levels and firing rate in the basal ganglia output nuclei, and also increased striatal enkephalin levels, and decreased striatal dynorphin and substance P levels. Importantly, the model also has excellent predictive validity, as all of the dopamine based drugs that are currently used in the clinic are also effective in the 6OHDA rat model of PD (Jenner, 2008).

For these reasons, the 6OHDA rat model of PD is one of the most widely used animal models of PD, and the beneficial features possessed by the model has made it useful in not only research into the pathogenesis of PD but also for testing a number of different types of potential treatments for PD. The robust and easily quantifiable motor deficits that are induced by full 6ODHA lesions and the high predictive validity of the model has resulted in the model being particularly useful in early stage pre-clinical PD research efforts that are aimed at identifying potential new pharmacological symptomatic treatments for PD. The model has additionally also been extensively used to test neurorestorative cell transplant therapies for PD (***detailed in section 1.4.3***). Moreover, after around three weeks of chronic L-DOPA treatment, unilaterally 6OHDA lesioned rats start to display dyskinesias analogous to those observed in the PD patients after long term L-DOPA treatment. The dyskinesias observed in the rats – termed abnormal involuntary movements (AIMS) - include choreiform twisting of the neck and upper body, abnormal movements of the forelimb, abnormal orolingual movements, and increased locomotor activity, with all of these abnormal movements occurring contralaterally to the lesion (Duty & Jenner, 2011). A further application of the 6OHDA

treated rat is, therefore, to study the mechanisms leading to L-DOPA induced dyskinesias, and also to identify new treatments that have the potential to alleviate L-DOPA induced dyskinesias. Furthermore, as discussed earlier, there is currently an urgent need for the development of new neuroprotective therapies for PD, and in more recent times the 6OHDA rat model of PD has also been extensively used in research efforts aimed at identifying treatments for PD that might have neuroprotective potential. The robust and easily quantifiable nigrostriatal lesion that is induced by 6OHDA has made this model particularly amenable to such neuroprotective studies, as it allows treatments that are able to protect nigrostriatal dopamine neurones against 6OHDA-induced degeneration to be identified.

3.1.1.4.4. The 6OHDA Partially Lesioned Rat Model of PD

By adjusting the dose of 6OHDA that is delivered to the nigrostriatal tract, it is possible to induce either a full or a partial nigrostriatal tract lesion in rats. In PD, there is a gradual loss of nigrostriatal dopamine neurones over many years. Motor symptoms in most cases only appear once more than ~60% of dopamine neurones in the SNc have been lost (Dauer & Przedborski, 2003), and at this point symptomatic treatment with L-DOPA is usually commenced. In most drug discovery studies, it is, therefore, preferable to use a partially lesioned 6ODHA rat model of PD as this would represent a more clinically representative model than compared to a fully lesioned model. Moreover, in drug discovery studies aimed at identifying potential neuroprotective therapies, it is essential to use a partially lesioned model in order to give the test treatment a realistic opportunity to mediate any beneficial effects, and also to more fully evaluate its therapeutic potential, and this is particularly necessary due to the onset of 6OHDA-induced nigrostriatal degeneration being relatively acute rather than progressive. The relatively high doses of 6ODHA used to induce a full lesion causes nearly all of the dopamine neurones in the lesioned nigrostriatal tract to die (Schwarting & Huston, 1996b). On the other hand, when the nigrostriatal tract is partially lesioned, by using a lower dose of 6OHDA, dopamine neurones have three possible fates. One group of dopamine neurones will undergo apoptosis or necrosis and die (Jeon *et al.*, 1995). A second group of neurones will remain alive but will lose their dopaminergic phenotype and become non-functional (Bowenkamp *et al.*, 1996). A third group of dopamine neurones will remain healthy and maintain normal functionality (Jeon *et al.*, 1995). In a partially lesioned model, a test treatment, therefore, has the opportunity to have a

therapeutic effect through 3 possible mechanisms. It can have a neuroprotective effect by preventing the neurones exposed to lethal concentrations of toxin from dying (Alexi *et al.*, 2000). Secondly, it could have a regenerative effect by restoring the damaged neurones to a functional state (Bowenkamp *et al.*, 1995). Thirdly, it can also increase the functioning of the remaining healthy neurones, providing symptomatic relief by compensating for the loss in functionality caused by the lesion (Gash *et al.*, 1995; Gash *et al.*, 1996). Another advantage offered by a partially lesioned model is that the lower 6OHDA dose used is likely to cause dopamine neurone degeneration at a slower rate compared to the higher doses used in a fully lesioned model. In a full lesion model, degenerating nigral cell bodies are found as early as 12h after the 6OHDA infusion is made (Jeon *et al.*, 1995). Some of the biological effects mediated by certain neuroprotective drugs, such as growth factors are known to take hours or even days to become apparent, as they are brought about by changes in gene transcription. A slower onset of degeneration would, thus, provide a substantial benefit when evaluating neuroprotective treatments, as it would lengthen the effective time-period in which the treatment could bring about its neuroprotective effects. However, an advantage possessed by fully lesioned 6OHDA models is that, in most cases, they induce robust motor impairments which can be easily measured by several different motor tests. The basal ganglia circuitry, however, has extensive and remarkably effective compensatory mechanisms that can maintain basal ganglia output signals at near normal levels when only a partial nigrostriatal lesion has been inflicted (Bezard *et al.*, 2003). A disadvantage of the partially lesioned 6OHDA rat model of PD, therefore, is that this model produces more subtle motor deficits which can only be detected by a number of the more sensitive motor tests.

3.2. Objectives

3.2.1. Objective 1. Establish a Unilateral Partially Lesioned 6OHDA Rat Model of PD in which to Test FGF20 for its In Vivo Neuroprotective Effects

Recent findings have shown FGF20 to have neuroprotective effects on dopamine neurones *in vitro* (***detailed in section 4.1.5***), and one of the main aims of this thesis was to evaluate whether FGF20's neuroprotective effects on dopamine neurones are also apparent, *in vivo*, in the partially lesioned 6OHDA rat model of PD (***see Chapter 4***). The first aim of the current study was to establish an appropriate partially lesioned 6OHDA rat model of PD in which to evaluate FGF20 for its ability to protect nigrostriatal dopamine neurones, *in vivo*. To accomplish this objective, 6OHDA dose-response experiments were carried out to identify an intra-nigrally delivered dose of 6OHDA that induces a ~60-80% partial nigrostriatal lesion. However, in an initial 6OHDA dose-response experiment, the infusion procedure was found to induce a substantial nigrostriatal lesion by itself. For this reason, a follow-up 6OHDA dose-response experiment was carried out in which a refined lesioning protocol was used. It is possible to induce partial unilateral 6ODHA induced nigrostriatal lesions in rats by infusing low doses of 6OHDA directly into either the substantia nigra where the nigrostriatal dopamine neurone cell bodies are located, or into the striatum where the dopamine neurone terminals are located. In the current study, nigrostriatal lesions were induced with intra-nigral rather than intra-striatal 6OHDA infusions mainly because of practical considerations. In the subsequent neuroprotection study it was planned that FGF20 would be administered supra-nigrally rather than into the striatum as immunohistochemistry results generated as part of Chapter 2 demonstrated the FGFRs to be more abundantly localised in the SN compared to the striatum. Intra-nigral 6OHDA infusions were, thus, used as this would allow both 6OHDA and FGF20 infusions to be delivered through a single dual-cannulae brain cannula.

Furthermore, because partial nigrostriatal lesions induce subtle motor deficits that are more difficult to detect than that induced by full lesions, two drug-induced motor tests (apomorphine and amphetamine induced rotations) and two spontaneous motor tests (adjusted stepping test and cylinder test) were evaluated in this study to identify tests that are capable of detecting motor deficits induced by a partial 6OHDA lesion.

3.2.2. Objective 2 - Identify a Biologically Active Dose of FGF20 to use in a Future In Vivo Neuroprotection Study

To successfully evaluate FGF20's neuroprotective efficacy *in vivo*, it is essential that a biologically active dose of the growth factor is tested. FGF20 mediates its biological effects by activating its membrane bound RTKs, the FGF receptors (FGFRs), of which there are 4 subtypes which are referred to as the FGFR1, 2, 3, and 4 (***detailed in section 2.1.2***). Several of the FGFRs are localised to nigrostriatal dopamine neurones and also to glial cells within the SN of the rat brain (***see Chapter 2***), and the anti-apoptotic and mitogenic effects stimulated by FGFR activation is mediated through the extracellular regulated kinase-1/2 (ERK-1/2) MAPK signalling pathway (Gardner & Johnson, 1996; Gu *et al.*, 2004; Khalil *et al.*, 2005). A second aim of this Chapter was to identify a biologically active intra-nigrally delivered dose of FGF20 that can be employed in the *in vivo* neuroprotection study by using phospho-ERK1/2 as a biomarker of FGF20 mediated FGFR activation.

3.3. Methods

3.3.1. Unilateral 6OHDA Nigrostriatal Tract Lesioning

3.3.1.1. Animals

Male Sprague Dawley rats, weighing between 270-300g, were obtained from Charles River (Kent, UK). The rats were maintained on a 12:12h light:dark cycle (lights on at 7 am). Room temperatures were kept at 22±2°C and room humidity at 55%. Food and water was available *ad libitum*. All animal procedures were undertaken in accordance with the UK Animals (Scientific Procedures) Act 1986.

3.3.1.2. Unilateral 6OHDA Lesioning of the Rat Nigrostriatal Tract – PROTOCOL 1

A 5µl Hamilton micro-syringe (23G) was fitted to an upright infusion pump attached to a stereotaxic frame. The inter-aural line was used as a reference point to calculate the coordinates at which the intra-nigral 6OHDA infusions had to be delivered at. The injection needle of the Hamilton syringe was, therefore, positioned so that its tip was located right in the centre of the tapered point of an ear bar that had been tightened in place on the stereotaxic frame. Once the AP and DV co-ordinates of the inter-aural line were recorded, rats were anaesthetised with a mixture of ketamine (75mg/kg, i.p.) and medetomidine (0.5 mg/kg, i.p.). Rats were pre-treated with the noradrenaline reuptake inhibitor, desipramine (25 mg/kg i.p.) and the MAO-B inhibitor, pargyline (5 mg/kg i.p.) 30min before being anaesthetised. 6OHDA is able to induce the degeneration of both dopamine and noradrenaline neurones, as 6OHDA is taken up by not only the dopamine transporter, but also by the noradrenaline transporter. Rats were therefore pre-treated with desipramine to limit any 6OHDA induced degeneration of noradrenaline neurones. The pargyline pre-treatment, on the other hand, was given to potentiate 6OHDA's toxic effect on dopamine neurones by inhibiting 6OHDA from being metabolised into an inactive metabolite by MAO-B. The anaesthetised rats were mounted in the stereotaxic frame after shaving their scalps. Their scalps were disinfected with ethanol and povidone-iodine (Betadine), and a midline incision made in the scalp after checking for the absence of a hind-limb withdrawal response. The cranium was fully exposed using retractors, and the pericranial membrane scraped away with a scalpel blade. A burr hole was made in the cranium using a 20G drill bit, and the

meninges pierced. When any bleeding had ceased, the Hamilton micro-syringe was then filled with 5µl of either a vehicle (sterile dH_2O containing 0.02% ascorbic acid) or a 6OHDA solution (1.5µg/µl, 2µg/µl, or 3µg/µl 6OHDA dissolved in vehicle). The 6OHDA solution was freshly prepared on the day of the lesioning, and it was dissolved in a 0.02% ascorbic acid solution, kept on ice, and wrapped in foil, all to minimise the inactivation of 6OHDA through auto-oxidation. Immediately after filling the micro-syringe, the needle of the Hamilton syringe was slowly lowered into the brain until the tip of the injection needle was located at the desired intra-nigral coordinates (AP, +3.7; ML, +2.0; DV, +2.2, relative to the interaural line, (Paxinos & Watson, 1993)) and intra-nigral infusions of either vehicle or 6OHDA (6, 8, or 12µg 6OHDA dissolved in 4µl of vehicle) were administered to the rats at a flow rate of 2µl/min. The syringe needle was left in place for 4min, after which the needle was removed, and the rats scalp sutured with self-dissolving polyester sutures. Rats were administered with an atipamezole (1mg/kg, s.c.) injection to reverse anaesthesia, and placed in a heated environment until recovery. Rats were given a saline injection (1ml, s.c.) to aid rehydration, and were maintained on a mashed food diet for 3 days post-surgery, or until rats started maintaining a healthy weight. A total of 44 rats were used in this experiment, with an n of 11, 12, 13, and 8 being used in the sham, 6µg, 8µg, and 12µg groups, respectively.

3.3.1.3 Unilateral Lesioning of the Rat Nigrostriatal Tract – PROTOCOL 2 (Refined Protocol)

A 5µl Hamilton micro-syringe was mounted onto an automated micro-infusion pump, and the tip of the syringe connected to a length of vinyl tubing which was, in turn, connected to a 33G stainless steel injection needle. The injection needle was fastened tightly onto a guide cannula holder which was securely fitted to the stereotaxic frame. Intra-nigral 6OHDA or vehicle infusions were then administered to the rats by using nearly exactly the same protocol as was in used in ***section 3.3.1.2***, with only 3 alterations being made. Firstly, in the current experiments intra-nigral infusions were administered to the rats using the 33G stainless steel needle described above instead of the 23G Hamilton syringe injection needle that was used in ***section 3.3.1.2***. Secondly, a 0.09% sterile saline solution containing 0.02% ascorbic acid was used as a vehicle in this study rather than the dH_2O vehicle used in previous study, and lastly, the doses of 6OHDA infused in this study differed to that used in section 3.3.1.2, as either vehicle

infusions, or 4µg, 6µg, or 8µg 6OHDA doses were administered to the rats. Thus, once the rat was mounted into the stereotaxic frame and a burr hole made in the skull, the 33G injection needle and the length of tubing to which it was connected, were filled with 5µl of either a vehicle solution (0.09% sterile saline containing 0.02% ascorbic acid) or a 6OHDA solution (1µg/µl, 1.5µg/µl, or 2µg/µl 6OHDA dissolved in vehicle). The remainder of the lesioning procedure was, however, carried out exactly as described in ***section 3.3.1.2***. A total of 26 rats were used in these experiments, with 7 rats being used in both the sham and 8µg groups, while 6 rats were used in both the 4µg and 6µg groups.

3.3.2. Behavioural Measurement of Motor Deficits in the 6OHDA Lesioned Rats

3.3.2.1. Cylinder Test

Rats were placed in a transparent cylindrically shaped plexiglass enclosure (diameter = 20cm, height = 30cm), and the rats rearing behaviour recorded in real-time by observation (***Fig 3.1***). The rearing behaviour of only a single rat was recorded at any one time. To allow the rearing behaviour of the rats to be clearly observed regardless of whether the rats were facing toward or away from an observer, a mirror was placed in an upright position against a wall, and the cylinder positioned in front of the mirror. The number of rearing postures supported by either both forelimbs, the ipsilateral (i.e. same side as the lesion) forelimb alone, or the contralateral (i.e. opposite side of the lesion) forelimb alone was then quantified. The percentage of total rearing postures supported by the ipsilateral forelimb alone was calculated, and, hereafter 'ipsilateral forelimb use alone' is taken to mean the percentage of total rears that were supported by the ipsilateral forelimb alone. In this thesis, increases in ipsilateral forelimb use alone were used as a measure of the degree of motor impairment that was present in the contralateral affected forelimb (***see section 3.4.1.3***). Cylinder test results for rats were only included in analyses if the rat reared 10 or more times in a session. Cylinder test measurements were taken 2 days (acclimatisation session) and 1 day (baseline measurements) prior to 6OHDA lesioning, and on day 5, 8, and 11 post-lesioning. Mean (±sem) ipsilateral forelimb use alone values were generated for each of the treatment groups, at each of the measurement time-points, and these results were analysed with two-way ANOVAs and Bonferroni post-hoc tests. Within the 6OHDA treatment groups, it was assessed whether ipsilateral forelimb use was significantly higher on any

of the time-points, post-lesioning when compared to baseline. Importantly, at each of the time-points, it was also assessed whether ipsilateral forelimb use was significantly different in any of the 6OHDA dose groups compared to the sham lesioned group.

Figure 3.1. Picture illustrating the cylinder test.

3.3.2.2. Adjusted Stepping Test

Rats were held with both hands, with one hand supporting the rat's hindquarters, and the other hand supporting the rat's frontal body while at the same time immobilising one of the rat's forelimbs (***Fig. 3.2***). The paw of the non-restrained forelimb was then placed on the surface of a lab bench, and the rat moved laterally at a steady pace (~90cm/45sec) along the edge of the bench, allowing the rat to make adjusting steps to regain its balance**.** The number of adjusted steps made by the rat with its ipsilateral and contralateral paws, over a distance of 90cm, was counted. Three repeat measurements were made to generate mean adjusted stepping test values for each paw. As with the cylinder test, adjusted step measurements were taken 2 days (acclimatisation session) and 1 day (baseline measurements) prior to 6OHDA lesioning, and on day 5, 8, and 11 post-lesioning. Mean (±sem) ipsilateral and contralateral adjusted step values were generated for each of the treatment groups, at each of the measurement time-points. The magnitude of the decrease in the number of adjusted steps made, post-lesioning, was

used as a measure of forelimb motor deficits. In the adjusted stepping test, two independent data sets were generated, one that included all the results for the contralateral impaired forelimb, and another that included all the results for the ipsilateral unimpaired forelimb. The two independent data sets were then separately analysed by two independent two-way ANOVA and Bonferroni analyses. For each forelimb, it was evaluated whether adjusted step measurements were significantly different on any of the time-points, post-lesioning when compared to baseline, within each of the treatment groups. Additionally, for each forelimb, it was also determined whether at each of the time-points, adjusted step measurements were significantly different in any of the 6OHDA dose groups compared to the sham lesioned group.

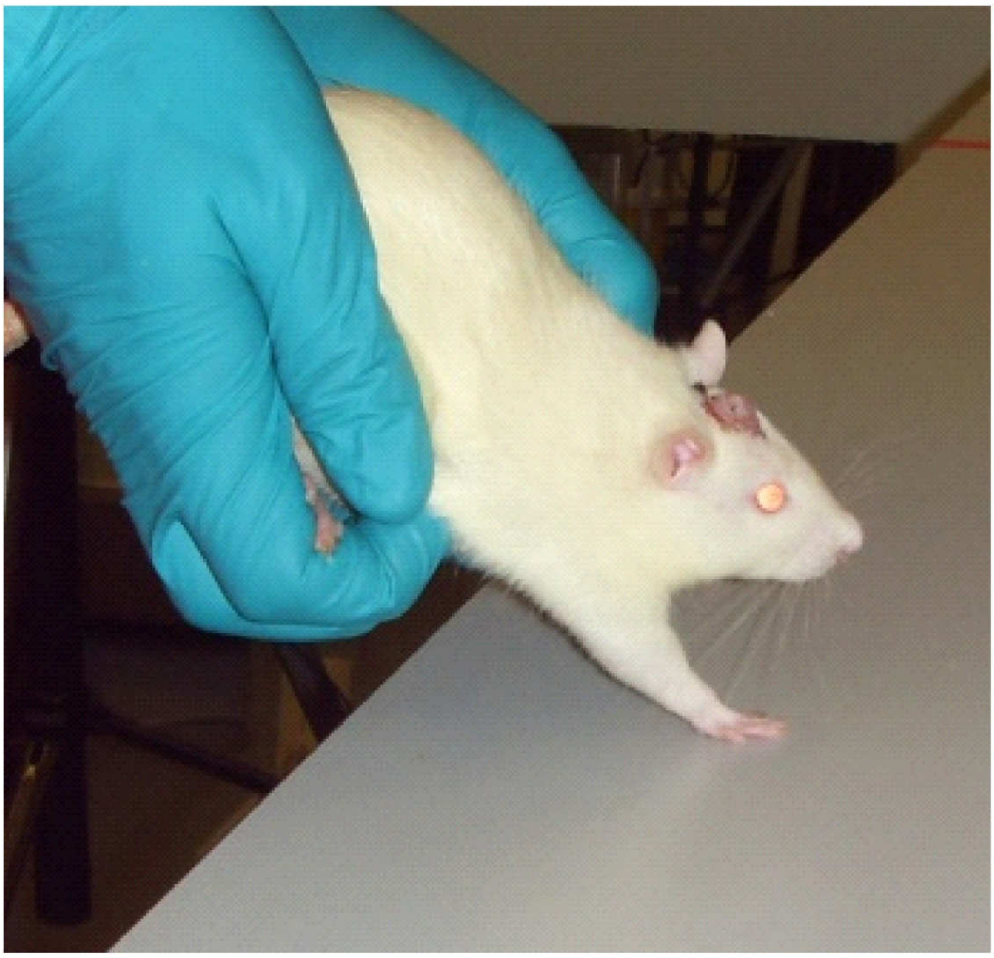

Figure 3.2. Picture illustrating the adjusted stepping test.

3.3.2.3. Drug-Induced Rotational Behaviour

Drug-induced motor behaviour was measured using rotometers and the Roto-Rat data acquisition software supplied by Med Associates Inc. (St. Albans, Vermont, USA).

Apomorphine and amphetamine-induced rotational behaviour was measured on day 14 and day 15, post-lesioning, respectively. Rats were injected with either apomorphine (1mg/kg, i.p.), or amphetamine (5mg/kg, i.p.), after which they were fitted with a harness, and placed inside a rotometer to which their harnesses were attached. Rotational behaviour was then recorded, by the Roto-Rat software, for a 70min period, post-injection. Over this period, the total number of clockwise and anti-clockwise rotations that were made by each of the rats was recorded in 5min time blocks. The mean number of net ipsiversive rotations and the mean number of net contraversive rotations made by each treatment group in each of the 5min time blocks were then calculated for the amphetamine-induced rotation and the apomorphine-induced rotation experiments, respectively. For each time block, net ipsiversive rotations were calculated by subtracting total contraversive rotations from total ipsiversive rotations, while net contraversive rotations were calculated by doing the inverse. These results were then analysed to produce two separate time-course profiles, one for the amphetamine induced mean net ipsiversive rotation 5min time block results, and another for the apomorphine-induced mean net contraversive rotation results. From these time-course profile graphs, the 25min time period after drug administration during which peak rotational behaviour occurred was then identified. For the amphetamine and the apomorphine experiment, the mean cumulative net ipsiversive or contraversive rotations made by each of the different treatment groups during this 25min time period was then calculated, respectively. Finally, these mean peak cumulative rotation results were analysed with one way ANOVA and Dunnett's post hoc test analyses, with the apomorphine and amphetamine results being analysed separately. For the amphetamine and the apomorphine experiment, it was assessed if the drug injections induced a significantly greater number of peak net ipsiversive or contraversive rotations, respectively, in any of the 6OHDA treatment groups compared to the sham lesioned group.

3.3.3. Quantification of Nigrostriatal Tract Lesions using TH Immunohistochemistry

3.3.3.1. Paraffin Wax Embedding of Rat Brain Tissue

On day 16 post-lesioning, rats were intra-cardially perfusion fixed and their brain's embedded in paraffin wax using exactly the same protocol as detailed in ***section 2.3.1.1***.

3.3.3.2. Preparation of Nigral and Striatal Tissue Sections from the Paraffin Wax Embedded Rat Brains for Immunohistochemical Staining

Paraffin wax embedded nigral and striatal brain sections were prepared for immunohistochemical staining using exactly the same protocol as that used for the HRP/DAB stained brain sections in ***section 2.3.1.2***.

3.3.3.3. Immunohistochemical Staining of Paraffin Wax Embedded Brain Sections for TH

3.3.3.3.1. Application of Primary and Secondary Antibodies

Striatal and nigral sections from the 6OHDA dose-response experiments that had been previously prepared were stained for TH. The blocking solution in which the prepared sections were still immersed in was removed, and the sections incubated with a rabbit polyclonal anti-TH primary antibody (Chemicon, AB152, 1 in 1000 dilution) overnight at RT. Sections were then washed in TBS buffer solution for 10min to remove any unbound primary antibody. In all cases, TH staining was visualised using the HRP/DAB/ABC method. Sections were, thus, subsequently incubated with a polyclonal biotinylated goat anti-rabbit secondary antibody (DAKO, E0432, 1 in 300 dilution) for 2h at RT.

3.3.3.3.2. Visualisation of TH Staining using the HRP/DAB/ABC Method

TH staining was then visualised with the HRP/DAB/ABC method and glass coverslips mounted on top of the stained sections by using exactly the same protocol as described in ***section 2.3.3.2***. The only exception is that none of the TH stained sections were counterstained with haematoxylin in this study.

3.3.3.3.3. Quantification of Nigrostriatal Tract Lesions using TH Immunohistochemistry

Digital images of the whole TH-immunostained *striatal* sections were acquired using an Epson Perfections V700 colour scanner, and densiometric analysis of the acquired images was carried out using ImageJ image analysis software. The mean grey staining densities present in the entire lesioned and non-lesioned striatal hemispheres were quantified. In these analyses, the net staining densities present in the striatal

hemispheres were calculated by subtracting background staining density measurements from the striatal density measurements. Two independent background staining measurements were generated for each section by quantifying the staining densities present in the entire ipsilateral and contralateral cerebral cortex hemispheres separately. Finally, ipsilateral and contralateral cerebral cortex background staining measurements were then subtracted from ipsilateral and contralateral striatal density measurements, respectively, to yield net striatal staining densities. The percentage staining density present in the lesioned hemispheres relative to the non-lesioned hemispheres (% TH-immunoreactivity) were then calculated for sections from the rostral (AP, +1.6), medial (AP, +0.2), and caudal (AP, -1.4) striatum (all AP coordinates are relative to bregma (Paxinos & Watson, 1993)). For each rat, mean % TH-immunoreactivity values for each of the areas were derived by analysing three adjacent sections at each level. A mean overall % TH-immunoreactivity value was then derived for each rat by averaging the three % TH-immunoreactivity values generated for each of the 3 different rostro-caudal areas. Finally, mean overall % TH-immunoreactivity values were then calculated for each of the 6OHDA and vehicle treatment groups by averaging the mean overall % TH-immunoreactivity values of all the rats in each group. Striatal TH immunohistochemistry results were analysed with one-way ANOVA and Dunnett's test post-hoc analyses to determine if striatal % TH immunoreactivity levels in any of the 6ODHA dose groups were significantly different to the sham group.

Digital images of the lesioned and non-lesioned TH-immunostained *nigral* hemispheres were acquired at 10x magnification using a Zeiss bright field microscope fitted with an Axiovision colour camera. Viable TH+ cells in the lesioned and non-lesioned SNc were counted using ImageJ image analysis software. Only intact round cells with a clear nucleus and cytoplasm having a definite ''halo'' were counted. Mean nigral TH+ cell numbers present in the lesioned and non-lesioned hemispheres were also quantified by analysing 3 sections taken from a rostral (AP, -4.8), medial (AP, -5.2), and caudal (AP, -5.8) area of the substantia nigra (all AP coordinates are relative to bregma (Paxinos & Watson, 1993)). Mean total TH+ nigral cell counts for each individual rat and for each treatment group were then calculated in the same manner as was done for the striatal TH immunohistochemistry results. Nigral TH immunohistochemistry results were analysed with two-way ANOVA and Bonferroni analyses to firstly determine whether, within each of the treatment groups, TH+ nigral cell counts were significantly different in the lesioned compared to the non-lesioned

hemisphere. Secondly, it was determined whether TH+ cell counts in the lesioned nigral hemisphere of any of the 6ODHA dose groups were significantly different compared to the sham group.

'No primary antibody' control experiments were carried out with the anti-rabbit biotinylated secondary antibody (Vectorlabs, BA-1000, 1/200) that was used in all of the TH immunohistochemistry experiments to confirm that the secondary antibody by itself did not give rise to any non-specific staining when applied in the absence of the primary anti-TH antibody. Exactly the same staining protocol was followed in these control experiments to that used in the actual experiments, with the only difference being that nigral and striatal brain sections were not incubated with anti-TH primary antibody. Results from the control experiments demonstrated the abovementioned secondary antibody not to produce any non-specific staining when applied in the absence of primary antibody.

3.3.4. FGF20 Dose Finding Experiments

3.3.4.1. Acute Intra-Nigral FGF20 Infusions

Intra-nigral FGF20 infusions were delivered to the brains of rats using a nearly identical procedure to that followed for the 6OHDA infusions in lesioning protocol 1 (***see section 3.3.1.2***). Briefly, naive male Sprague Dawley rats weighing around ~270g were anaesthetised, mounted onto a stereotaxic frame, their skulls exposed, and a burr hole drilled in their skull. Using a 5µl Hamilton 23G micro-syringe, freshly prepared FGF20 artificial cerebrospinal fluid (aCSF) vehicle solution (148mM NaCl, 3mM KCl, 1.4mM CaCl2, 0.8mM MgCl2, 1.5mM HPO4, 0.2mM NaH2PO4, 100ng/ml of rat serum albumin, pH7.4) or FGF20 (100ng and 1µg dissolved in 4µl of vehicle) infusions were delivered at exactly the same intra-nigral coordinates as that used for 6OHDA (AP, +3.7; ML, +2.0; DV, +2.2, relative to the interaural line (Paxinos & Watson, 1993)). In contrast to the 6OHDA dose-response study, the rats in this study were not allowed to recover after the intra-nigral FGF20 infusions were delivered. Instead, the rats were intra-cardially para-formaldehyde perfusion fixed 30min after the FGF20 infusions were made, and their brains removed. Paraffin wax embedded blocks of brain tissue containing the entire SN from each of the rat brains were then prepared, and serial 8µm thick coronal nigral sections were then cut with a microtome, so that sections were obtained from the entire SN using the same protocols as detailed in ***section 2.3.3.1 and***

2.3.3.2. A total of 6 rats were used in these experiments, with 2 rats being used in the vehicle and each of the different FGF20 dose groups.

3.3.4.2. Immunostaining of Nigral Sections for Phospho-ERK1/2 and Quantification of Nigral Phospho-ERK1/2 Positive Cells

Nigral sections from the FGF20 dose finding study that had been previously prepared for immunohistochemical staining using the procedure in ***section 2.3.1*** were stained for phospho-ERK1/2. As detailed later in ***section 3.2.2***, the mitogenic and anti-apoptotic effects stimulated by FGFR1 activation is mediated through the ERK1/2 signalling pathway, and phospho-ERK1/2 (activated form of ERK1/2) was, therefore, used as a marker of FGFR activation in this study. The blocking solution in which the prepared sections were still immersed in was removed, and the sections incubated with a rabbit anti-phospho-ERK1/2 (Santa Cruz Biotechnology, sc-101761, 1/250) primary antibody at RT overnight. Next, sections were washed in TBS to remove any unbound primary antibody, and incubated with a donkey anti-rabbit biotinylated secondary antibody (Vectorlabs, BA-1000, 1/200) for 2h at RT. Thereafter, phospho-ERK1/2 staining was visualised with the HRP/DAB/ABC method and glass coverslips mounted on top of the stained sections by using exactly the same protocol as described in ***section 2.3.3.2***. The only exception is that none of the stained sections were counterstained with haematoxylin in this study.

Digital images of the phospho-ERK1/2-immunostained nigral sections were acquired at 10x magnification using a Zeiss bright field microscope fitted with an Axiovision colour camera. Phospho-ERK1/2 positive cell numbers at the nigral FGF20 infusion sites were counted using ImageJ image analysis software. Net phospho-ERK positive cell counts were calculated by subtracting contralateral from ipsilateral cell counts, and mean phospho-ERK1/2 cell numbers for each rat were derived by analysing 6-9 adjacent nigral sections taken from the infusion sites within the substantia nigra. No statistical analysis was carried out on these results as only an ‘n’ of 2 rats were used in each group.

3.3.5. Drugs and Chemicals

FGF20 was obtained from Peprotech (Rocky Hill, N.J), and pentobarbital (Euthatal) was obtained from Merial Animal Health Ltd (Essex, UK). The Betadine was purchased

from LE West Ltd. (Barking, UK). Ketamine HCl (Vetlar), medetomidine HCl (Domitor), and atipamezole HCl (Antisedan) were all obtained from Pfizer (Sandwich, UK). 6-OHDA-HBr, L-ascorbic acid, desipramine HCl, pargyline HCl, apomorphine hydrochloride hydrate, D-amphetamine sulphate and all the other chemicals were obtained from Sigma-Aldrich (Dorset, UK).

3.4. Results

3.4.1. Nigrostriatal Dopaminergic Lesions and Motor Deficits Induced in Rats using Lesioning Protocol 1

3.4.1.1. Dose-Dependent Reductions in Nigral TH+ Cell Counts and Striatal TH Levels Induced by Intra-Nigral Infusions of 6OHDA

A 6OHDA dose-response experiment was carried out in rats to identify an intra-nigrally delivered dose of 6OHDA that induces a partial nigrostriatal tract lesion. Unilateral intra-nigral 6OHDA infusions dose-dependently reduced both striatal TH levels and nigral TH+ cell numbers in the lesioned nigrostriatal tracts (***Fig 3.3 and 3.4***).

Striatal TH levels were reduced in the ipsilateral (lesioned) hemispheres of all of the 6OHDA dose groups, and surprisingly also in the sham lesioned group when compared to the contralateral striatal hemispheres (***Fig 3.3.B***). Quantitative results showing the % ipsilateral striatal TH levels (relative to the contralateral hemisphere) that were present in the different groups are shown in ***Fig 3.3.A***. In the sham lesioned group, striatal TH levels were reduced in the ipsilateral striatum by ~25% compared to the contralateral striatum. The 6OHDA infusions produced a significant dose-dependent reduction in striatal TH levels ($p<0.001$), with the 6µg and 8µg 6OHDA doses inducing partial losses of ipsilateral striatal TH levels of ~55% and ~60%, respectively, while the 12µg dose induced a complete 100% loss of striatal TH levels. All of the 6OHDA doses induced a significantly bigger loss of striatal TH levels when compared to the sham lesioned group ($p<0.05$).

Similarly, the absolute number of TH+ cells were significantly lower in the lesioned SNc of all the groups, including the sham lesioned group, compared to the non-lesioned SNc (***Fig 3.4.A***, $p<0.01$). Worryingly, in the sham lesioned group, TH+ cell numbers in the lesioned SNc was ~50% lower compared to the non-lesioned SNc. Again, 6OHDA reduced nigral TH+ cell numbers in a dose-dependent manner ($p<0.01$). In the 6µg, 8µg and 12µg 6OHDA groups, TH+ cell numbers in the lesioned SNc were

~75%, ~80% and ~100% lower than in the non-lesioned SNc ($p<0.01$). All three 6OHDA doses reduced TH+ cell numbers in the lesioned hemisphere to a greater degree compared to vehicle ($p<0.01$).

Figure 3.3. Reductions in Striatal TH Induced by 6OHDA using Lesioning Protocol 1

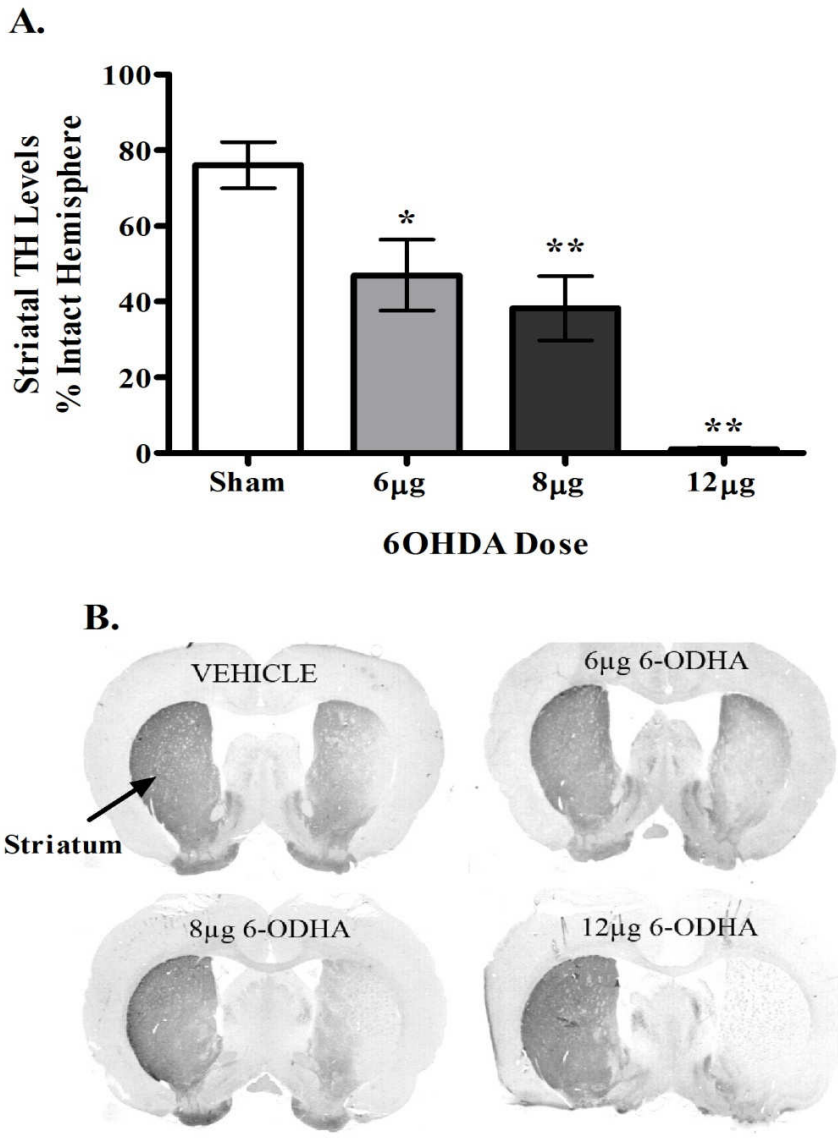

Figure 3.3. Reduction in striatal TH levels (**A**) induced by unilateral intra-nigral infusions of a range of 6OHDA doses or vehicle (sham) delivered using lesioning protocol 1. Data points represent mean±sem, and n=8-13 for each group. *$p<0.05$ and **$p<0.01$ compared to the sham lesioned group. Representative examples of TH-immunostained coronal sections from the medial striatum of each group (**B**). Abbreviations; TH: tyrosine hydroxylase, 6OHDA: 6-hydroxydopamine.

Figure 3.4. Reductions in Nigral TH+ Cells Induced by 6OHDA using Lesioning Protocol 1

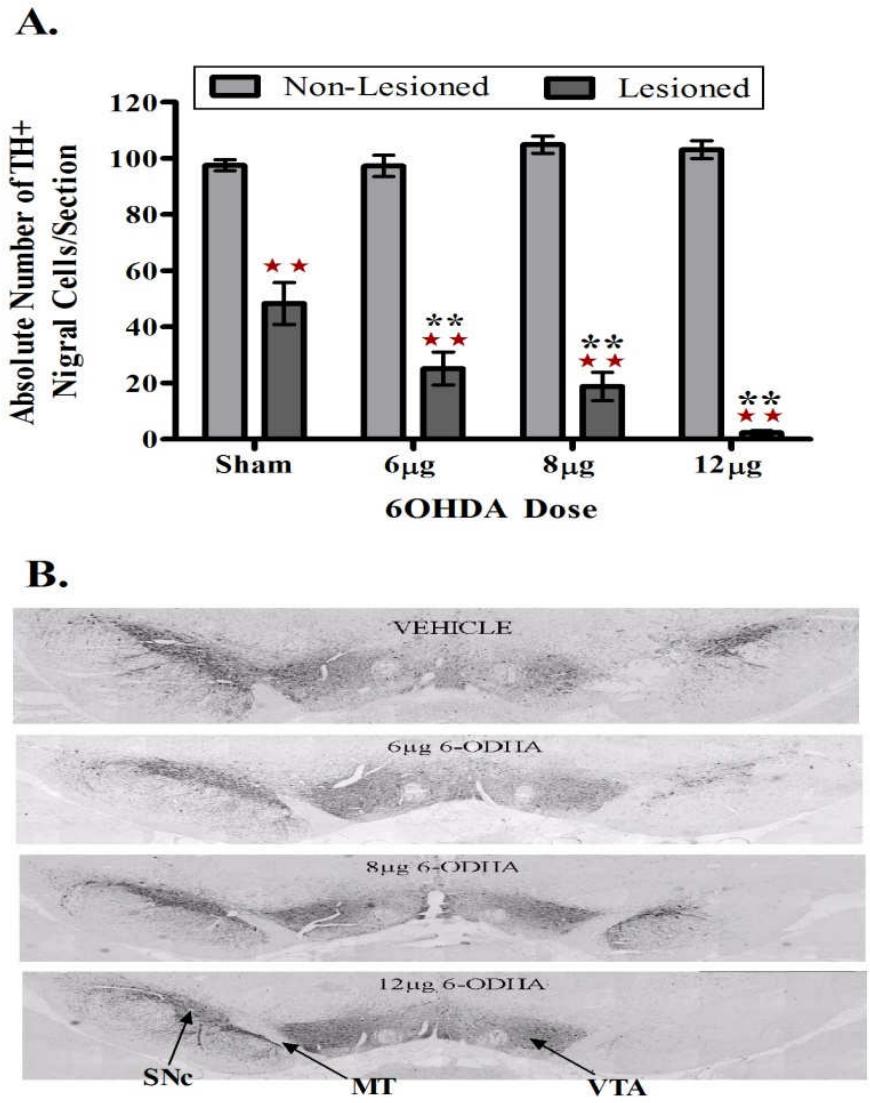

Figure 3.4. Reduction in TH-positive nigral cell numbers (**A**) induced by unilateral intra-nigral infusions of a range of 6OHDA doses or vehicle (sham) delivered using lesioning protocol 1. Data points represent mean±sem, and n=8-13 for each group. ★★$p<0.01$ compared to the non-lesioned contralateral SNc of the same group. **$p<0.01$ compared to lesioned SNc of the sham lesioned group. Representative examples of TH-immunostained coronal sections from the medial SNc of each group (**B**). Abbreviations; TH: tyrosine hydroxylase, 6OHDA: 6-hydroxydopamine, SNc: substantia nigra pars compacta, MT: medial terminal nucleus of the accessory optic tract, VTA: ventral tegmental area.

3.4.1.2. Drug-Stimulated Motor Asymmetry Detected in Rats Lesioned using Protocol 1

Amphetamine stimulated a time-dependent increase in net ipsiversive rotations in all of the 6OHDA dose groups, and also in the sham lesioned group (***Fig 3.5.A***). Peak net ipsiversive rotations occurred in the 25 to 50min time-period, post-amphetamine injection (***Fig 3.5.A***). In this period, amphetamine induced ~40 cumulative net ipsiversive rotations in the sham lesioned group (***Fig 3.5.B***). The 6OHDA infusions brought about a dose-dependent increase in amphetamine-induced cumulative net ipsiversive rotations during this period (***Fig 3.5.B***, $p<0.01$). Amphetamine induced ~115, ~220, and ~355 net ipsiversive rotations in the 6µg, 8µg and 12µg 6OHDA groups, respectively. Amphetamine-induced net ipsiversive rotations were, however, only significantly higher in the 8µg and 12µg 6OHDA groups compared to the sham lesioned group ($p<0.05$ and $p<0.01$, respectively).

Apomorphine stimulated a time-dependent increase in net contraversive rotations in all of the 6OHDA dose groups, but not in the sham lesioned group (***Fig 3.6.A***). In the 6OHDA groups, peak net contraversive rotations occurred during the 15 to 40min time period, post-apomorphine injection (***Fig 3.6.A***). During this period, apomorphine failed to induce any mean peak net contraversive rotations in the sham group, while in the 6µg, 8µg and 12µg 6OHDA groups, apomorphine induced mean peak net contraversive rotations of ~20, ~8, and ~68, respectively (***Fig 3.6.B***). However, net apomorphine-induced contraversive rotations were only significantly greater in the 12µg fully lesioned rats compared to the sham lesioned rats ($p<0.05$).

Figure 3.5. Rotational Behaviour Stimulated by Amphetamine in Rats Lesioned using Protocol 1

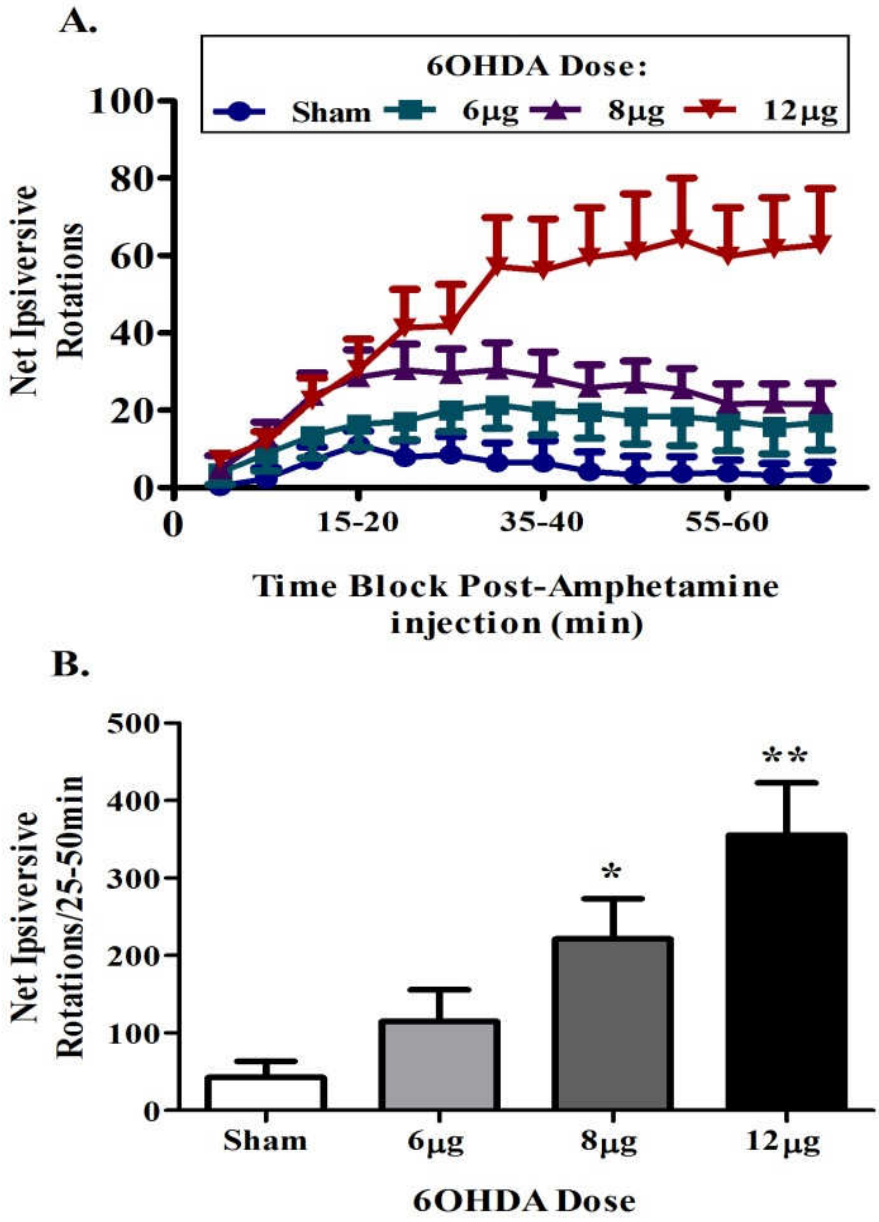

Figure 3.5. Rotational behaviour stimulated by amphetamine (5mg/kg, i.p) in rats which received unilateral intra-nigral infusions of a range of 6OHDA doses or vehicle (sham) delivered using lesioning protocol 1. Rotations were quantified in 5min time-blocks. Results are expressed as time-course profiles of the mean net ipsiversive rotations made over a 70min period post-drug injection (**A**), and as the mean cumulative net rotations made during the 25-50min period in which peak rotational behaviour occurred (**B**). Data points represent mean±sem, and n=8-13 for each group.*$p<0.05$ and **$p<0.01$ compared to sham.

Figure 3.6. Rotational Behaviour Stimulated by Apomorphine in Rats Lesioned using Protocol 1

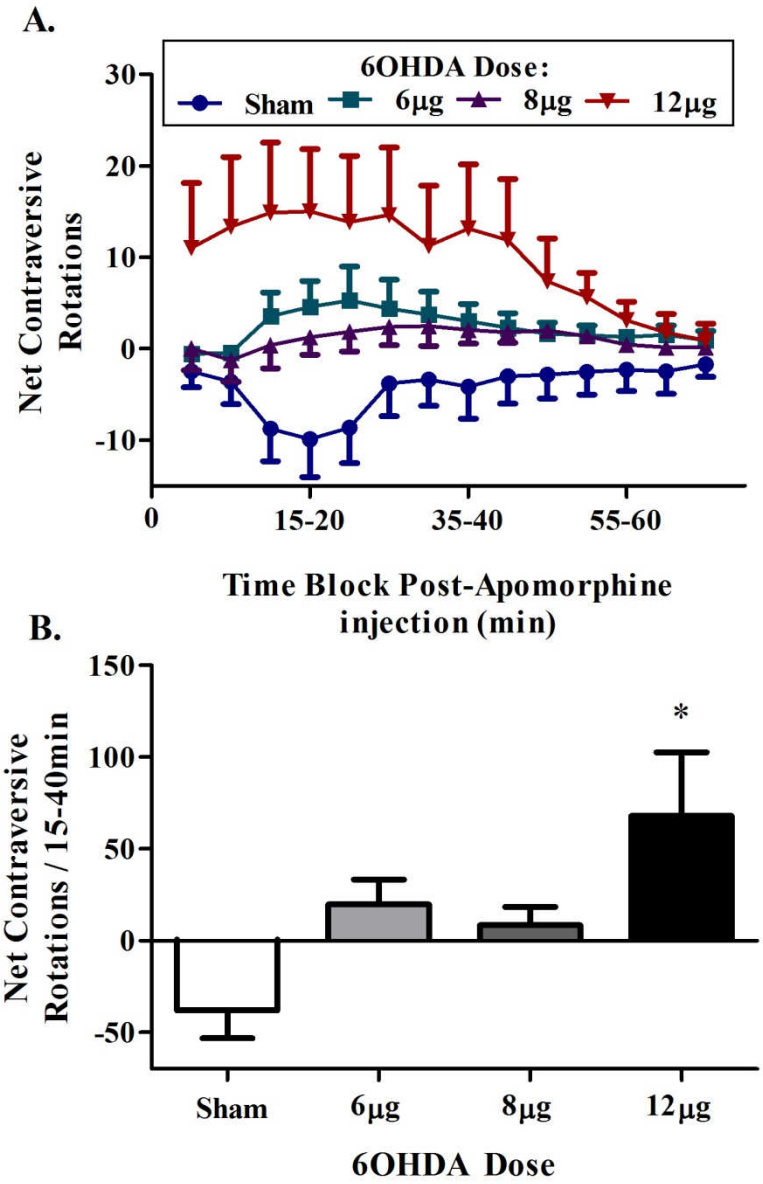

Figure 3.6. Rotational behaviour stimulated by apomorphine (1mg/kg, i.p) in rats which received unilateral intra-nigral infusions of a range of 6OHDA doses or vehicle (sham) delivered using lesioning protocol 1. Rotations were quantified in 5min time-blocks. Results are expressed as time-course profiles of the mean net contraversive rotations made over a 70min period post-drug injection (**A**), and as the mean cumulative net rotations made during the 15-40min period in which peak rotational behaviour occurred (**B**). Data points represent mean±sem, and n=8-13 for each group.*$p<0.05$ compared to sham.

3.4.1.3. Motor Deficits Detected by the Cylinder Test in Rats Lesioned using Protocol 1

In the cylinder test, the majority of the rats in all of the groups mainly used both of their forelimbs to support themselves in a rearing position at baseline (***Fig 3.7.A***), with a mean of ~60-80% of total rears being supported by both forelimbs in the different groups. A much smaller % of total rearing postures were supported by the ipsilateral or contralateral forelimb alone (~7-22% of total rears) (***Fig 3.7.A***). These baseline results showed that the rats in all of the treatment groups had no preference for using one of their forelimbs over another, which demonstrates that no forelimb asymmetry was present in any of the groups at baseline.

The forelimb motor deficits induced by a unilateral 6OHDA lesion can be expressed in a number of different ways. After a unilateral 6OHDA lesion, the affected contralateral paw will be used on far fewer occasions. This will be reflected in the results by the % of total rears being supported by the contralateral forelimb alone and by both forelimbs decreasing after lesioning. The % of total rears supported by the ipsilateral forelimb alone, on the other hand, will increase. Forelimb motor deficits can, therefore, be quantified by assessing the decrease in the % of total rears supported by the contralateral forelimb alone after lesioning. Alternatively, motor deficits can be quantified by measuring the increase in the % of total rears that are supported by the ipsilateral forelimb alone after lesioning. By analysing the raw data showing the absolute number of rears made by all of the rats in the different groups, one finds that each rat on average made ~23 total rears at baseline. A total of 44 rats were used in this study, and 27 of these rats only reared 0-3 times using their contralateral forelimb alone at baseline. For these 27 rats it would, therefore, not have been possible to calculate a meaningful decrease in the % of total rears supported by the contralateral forelimb alone after lesioning. For this reason, forelimb motor deficits were measured in this study by assessing the increases in the % of total rears supported by the ipsilateral forelimb alone (% ipsilateral forelimb use alone) that occurred after lesioning. Thus, hereafter, significant increases in % ipsilateral forelimb use post lesioning is taken to be a measure of the degree of motor deficits that were present in the contralateral forelimbs of the rats.

Significant contralateral forelimb motor deficits were, in this way, detected by the cylinder test in the sham lesioned group, and in all of the 6OHDA dose groups at multiple time-points, post lesioning, when compared to baseline (***Fig 3.7.B***). The 12µg

group failed to respond in the cylinder test on day 5, post-lesioning, precluding the use of a two-way ANOVA to analyse these results. Instead, cylinder test results for this study were analysed by a number of separate independent one-way ANOVA and Dunnett's test post hoc analyses to determine if in any of the treatment groups significantly greater motor deficits were present at any of the time-points post lesioning when compared to baseline. Additionally, results from each of the time-points were also analysed with independent one-way ANOVA analyses to assess whether motor deficits were significantly greater in any of the 6OHDA dose groups when compared to sham at each of the time-points.

In the sham lesioned group, significant motor deficits were detected by the cylinder test on day 5 and 8 post-lesioning ($p<0.01$), but not on day 11. In the sham group, ipsilateral forelimb use alone increased from ~20% at baseline to ~45-60% post-lesioning. Significant motor deficits were present in all of the 6OHDA dose groups at all of the time-points, post-lesioning, when compared to baseline ($p<0.01$). In the 6µg group, ipsilateral forelimb use alone increased from ~18% at baseline to ~57-62% at post-lesioning time-points, while in the 8µg group it increased from ~13% to ~72-90%. The biggest increase in motor deficits were, however, observed in the 12µg group, in which ipsilateral forelimb use alone increased from ~8% at baseline to ~96-99% post-lesioning.

As mentioned, the cylinder results were also analysed to determine if the 6OHDA treatments induced a significantly greater degree of forelimb motor deficits at each of the different time-points, post-lesioning, compared to the sham lesioned group. The motor deficits detected by the cylinder test in the 6µg 6OHDA group were found not to be significantly greater than that detected in the sham lesioned group, on all of the time-points post-lesioning. The motor deficits detected in the 8µg group were significantly greater than the sham lesioned group on day 8 and 11, post-lesioning ($p<0.01$ and $p<0.05$, respectively), but not on day 5. In the 12µg group, motor deficits were significantly greater than the sham group on both day 8 and 11, post-lesioning ($p<0.01$).

Figure 3.7. Motor Deficits Detected by the Cylinder Test in rats Lesioned using Protocol 1

A. Cylinder test - Forelimb use at Baseline

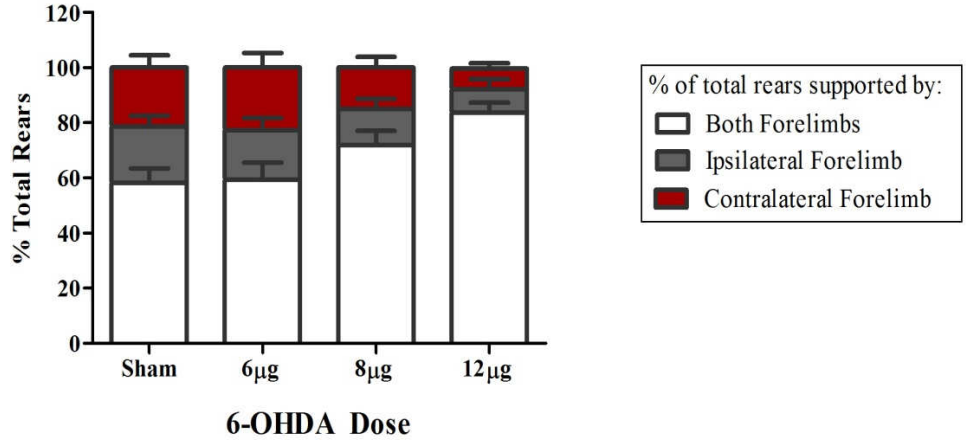

B. Cylinder test - Unilateral Impairments in forelimb use Post-Lesioning

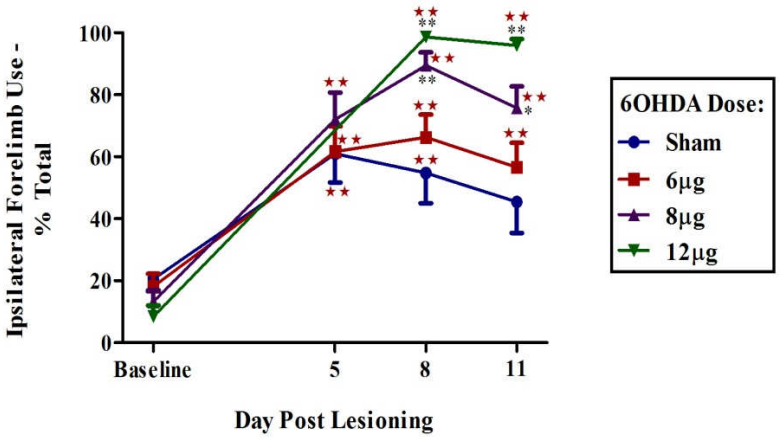

Figure 3.7. Forelilmb motor function as measured by the cylinder test. **A.** The percentage of total rears supported by the rats using either both forelimbs, their ipsilateral forelimb alone, or their contralateral forelimb alone at baseline. **B.** Unilateral deficits in forelimb motor function detected by the cylinder test in rats which received unilateral intra-nigral infusions of a range of 6OHDA doses or vehicle (sham) delivered using lesioning protocol 1. Increases in ipsilateral forelimb use alone, post-lesion, was used as a measure of the degree of motor impairment that was present in the contralateral impaired forelimb. Cylinder test results for the 12µg group are absent on day 5 due to a failure of the rats to respond. Data points represent mean±sem, and n=8-13 rats for each group. ★★$p<0.01$ compared to baseline. *$p<0.05$, and ** $p<0.01$ compared to sham.

3.4.1.4 Motor Deficits Detected by the Adjusted Stepping Test in rats Lesioned using Protocol 1

The adjusted stepping test detected no motor deficits in the unaffected ipsilateral forelimbs of any of the treatment groups (***Fig 3.8.B***). At baseline, the different treatment groups made ~21-23 adjusted steps with their ipsilateral forelimbs, and in all of the groups there were no significant differences between the number of ipsilateral adjusted steps made at any of the time-points post-lesioning when compared to baseline. There were also no significant differences between the number of ipsilateral adjusted steps made by the different groups at each of the different time-points.

At baseline, the different treatment groups made ~19-23 adjusted steps with their contralateral forelimbs, and the adjusted stepping test also failed to detect any significant motor deficits in the affected contralateral forelimbs of the sham and 6µg 6OHDA groups at any of the time-points post-lesioning, when compared to baseline (***Fig 3.8.A***). Significant contralateral forelimb motor deficits were, however, detected in the 8µg and 12µg 6OHDA groups ($p<0.05$). In the 8µg group, contralateral forelimb measurements were ~22% lower on day 5 post-lesioning when compared to baseline ($p<0.01$), and importantly, these deficits were also significantly different to sham at this time-point ($p<0.01$). The reductions in contralateral adjusted step measurements observed on day 8 and 11, post-lesioning in the 8µg group were, however, found not to be statistically significant. In the 12µg 6OHDA group, significant contralateral motor deficits were detected at all 3 time-points, post-lesioning, with adjusted step measurements being reduced by ~61-94% on post lesioning time-points when compared to baseline ($p<0.01$), and importantly, the motor deficits in the 12µg 6OHDA group were also significantly greater to that present in the sham lesioned group at all of the time-points, post-lesioning ($p<0.01$).

Figure 3.8. Motor Deficits Detected by the Adjusted Stepping Test in rats Lesioned using Protocol 1

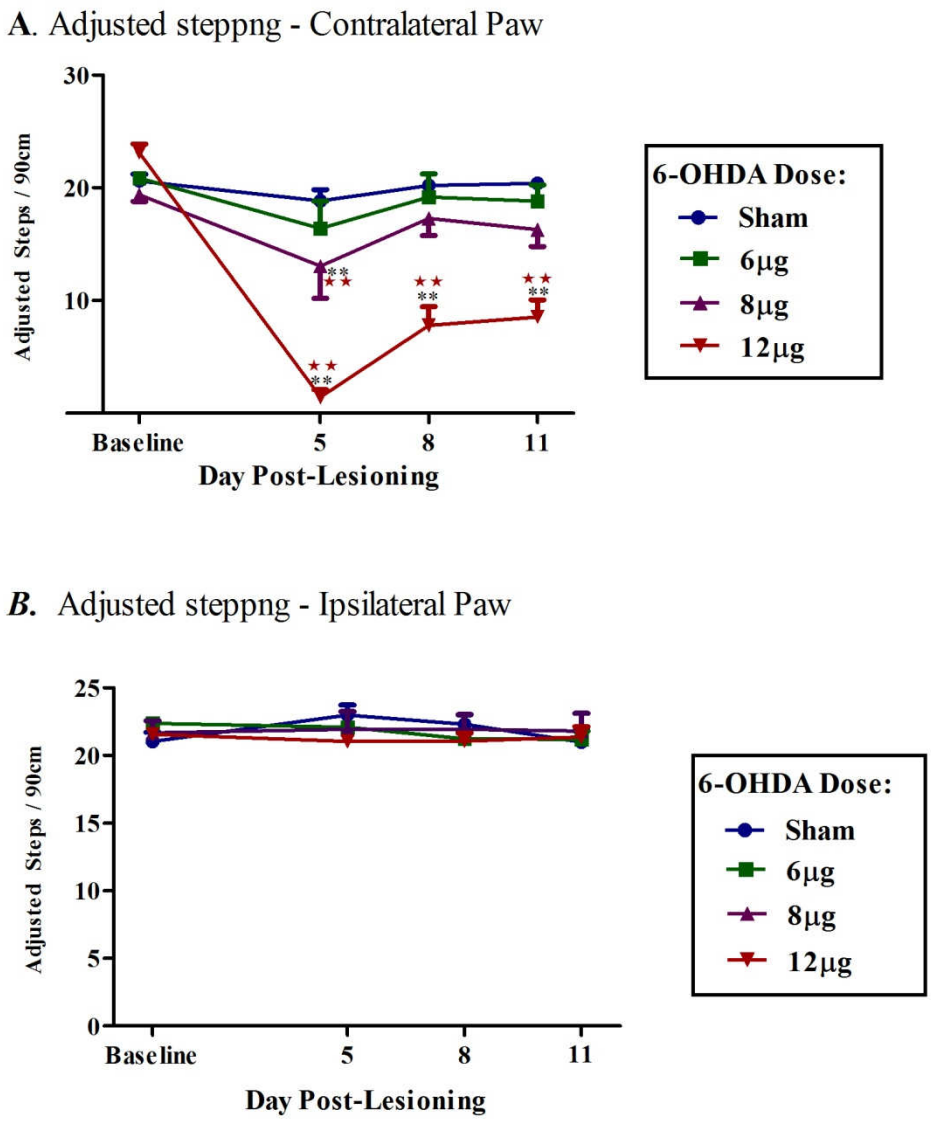

Figure 3.8. Unilateral deficits in forelimb motor function detected by the adjusted stepping test in rats which received unilateral intra-nigral infusions of a range of 6OHDA doses or vehicle (sham) delivered using lesioning protocol 1. The number of adjusted steps made by the contralateral (impaired) and ipsilateral (unimpaired) forelimb over a 90cm distance is shown in **A** and **B**, respectively. Decreases in the number of adjusted steps made after lesioning was used as a meaure of forelimb motor impairment. Data points represent mean±sem, n=8-13 rats for each group.★★$p<0.01$ compared to baseline.** $p<0.01$ compared to sham.

3.4.2. Nigrostriatal Dopaminergic Lesions and Motor Deficits Induced in Rats using Lesioning Protocol 2

3.4.2.1. Dose-Dependent Reductions in Nigral TH+ Cell Counts and Striatal TH Levels Induced in Rats using Lesioning Protocol 2

In the first 6OHDA dose-response experiment that was carried out as part of this Chapter, a substantial nigrostriatal lesion was found to be present in the sham lesioned group. With the aim of identifying an intra-nigral infusion procedure that produces minimal nigrostriatal tract degeneration by itself, a second follow-up 6OHDA dose-response experiment was carried out in which vehicle and 6OHDA infusions were delivered using a refined protocol (***protocol 2, see section 3.3.1.3 for method***).

In this study, no reductions in striatal TH levels were found to be present in the ipsilateral striatum of the sham group when compared to the contralateral striatum (***Fig 3.9.A&B***). This represents a substantial improvement when compared to the first study, where a substantial ~25% striatal lesion was present in the sham group. The unilateral intra-nigral 6OHDA infusions, however, induced a significant dose-dependent reduction in striatal TH levels in the lesioned hemispheres when compared to the contralateral striata (***Fig 3.9.A***), with the 6µg, and 8µg 6OHDA doses inducing nearly complete striatal TH loss of ~90% and ~95%, respectively, while the 4µg dose induced a desirable ~65% partial loss of striatal TH. All of the 6OHDA doses induced a significantly bigger loss of striatal TH compared to the sham lesioned group ($p<0.01$).

Figure 3.9. Reductions in Striatal TH Induced by 6OHDA using Lesioning Protocol 2

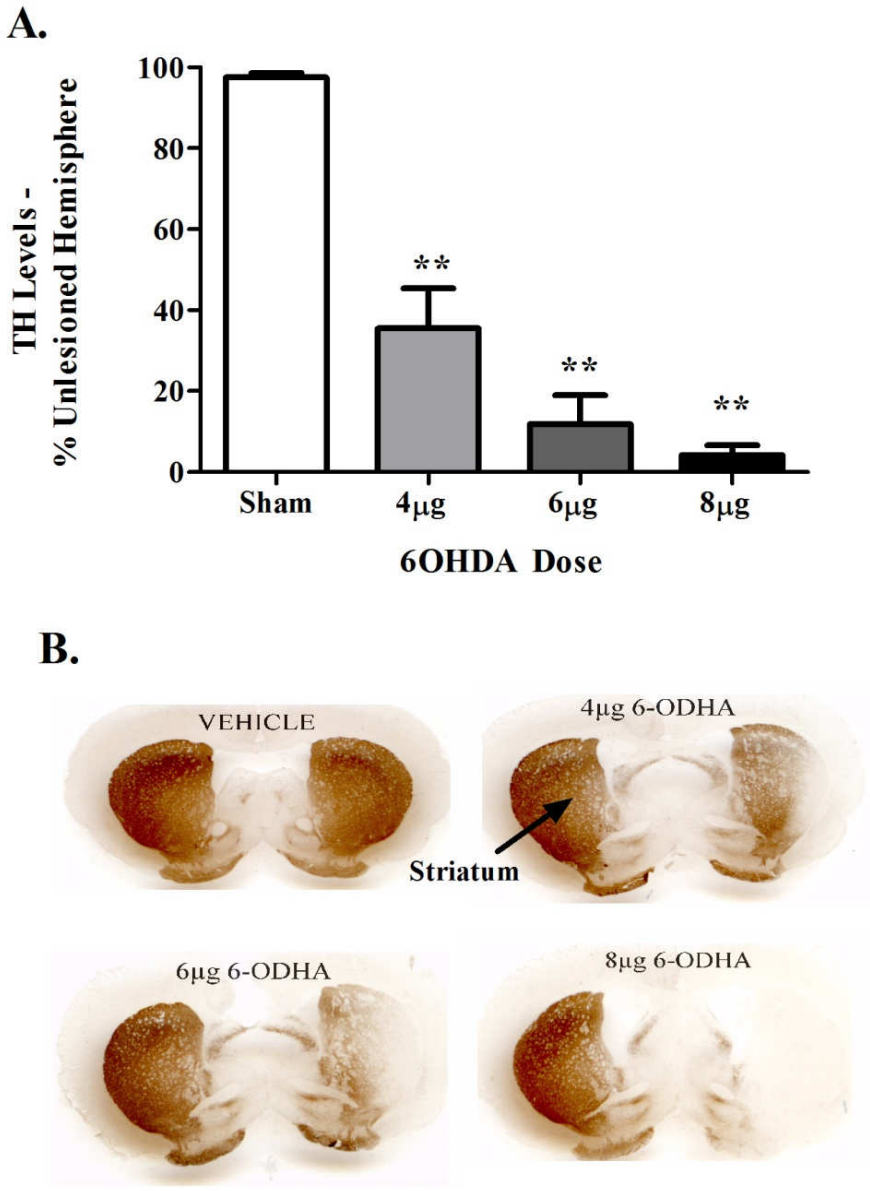

Figure 3.9. Reduction in striatal TH levels (**A**) induced by unilateral intra-nigral infusions of a range of 6OHDA doses or vehicle (sham) delivered using lesioning protocol 2. Data points represent mean±sem, and n=6-7 for each group. **p<0.01 compared to the sham lesioned group. Representative examples of TH-immunostained coronal sections from the medial striatum of each group (**B**). Abbreviations; TH: tyrosine hydroxylase, 6OHDA: 6-hydroxydopamine.

Nigral TH+ cell count results are shown in ***Fig 3.10***. Although nigral TH+ cell numbers were found to be significantly lower in the ipsilateral SNc of the sham lesioned group compared to the contralateral SNc ($p<0.05$), cell numbers were only reduced by a negligible ~10% (***Fig 3.10.A***). The refined lesioning procedure, thus, also caused a substantially smaller degree of nigral TH+ cell loss compared to the original procedure, which induced an ~50% reduction in TH+ cells in the ipsilateral SNc. The 6OHDA doses also induced a dose-dependent loss of ipsilateral nigral TH+ cells (***Fig 3.10.A***). The 6µg and 8µg 6OHDA doses induced a nearly complete loss of TH+ nigral cells, with TH+ cell numbers in the lesioned SNc being ~92% and ~95% lower compared to the non-lesioned SNc in the two groups, respectively ($p<0.01$ in all cases). The 4µg dose, on the other hand, produced a desirable partial ~80% loss of nigral TH+ cells in the lesioned compared to the non-lesioned SNc. All three of the 6OHDA doses induced a significantly greater degree of TH+ cell loss in the lesioned SNc compared to that present in the sham lesioned group ($p<0.01$).

Figure 3.10. Reductions in Nigral TH+ Cells Induced by 6OHDA using Lesioning Protocol 2

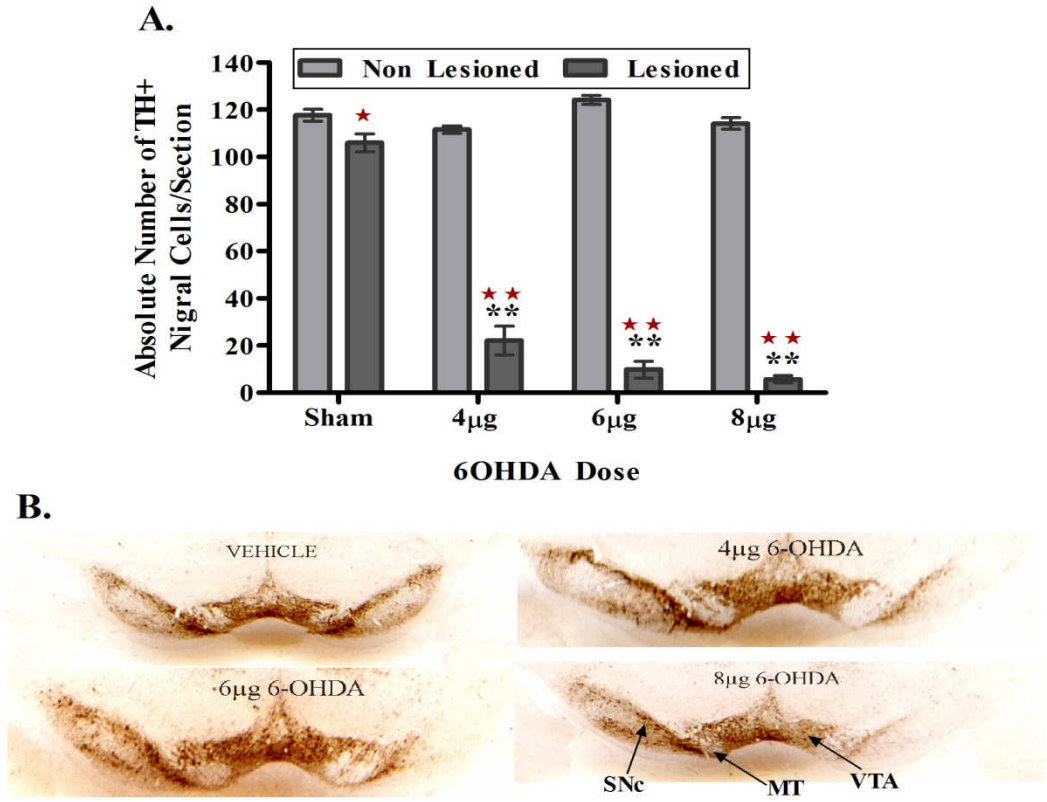

Figure 3.10. Reduction in TH-positive nigral cell numbers (**A**) induced by unilateral intra-nigral infusions of a range of 6OHDA doses or vehicle (sham) delivered using lesioning protocol 2. Data points represent mean±sem values, and n=6-7 for each group. ★★$p<0.01$ and ★$p<0.05$ compared to the non-lesioned contralateral SNc of the same group. **$p<0.01$ compared to lesioned SNc of the sham lesioned group. Representative examples of TH-immunostained coronal sections from the medial SNc of each group (**B**). Abbreviations; TH: tyrosine hydroxylase, 6OHDA: 6-hydroxydopamine, SNc: substantia nigra pars compacta, MT: medial terminal nucleus of the accessory optic tract, VTA: ventral tegmental area.

3.4.2.2. Drug-stimulated Motor Deficits Detected in Rats Lesioned using Protocol 2

In contrast to the first study, in which both the apomorphine and the amphetamine rotation tests were used to assess motor asymmetry, only the amphetamine rotation test was used in this study. The apomorphine test was not used in this study because it was demonstrated to have an insufficient sensitivity to detect motors deficit in partially lesioned rats in the previous study.

Amphetamine stimulated a time-dependent increase in net ipsiversive rotations in all of the 6OHDA dose groups (***Fig 3.11.A***). However, in contrast to the first study, amphetamine stimulated no net ipsiversive rotations in the sham lesioned group (***Fig 3.11.A***). The minimal amount of nigrostriatal damage induced by the refined lesioning procedure, thus, gave rise to substantially lower motor deficits being detected in this test in the sham lesioned group, as ~40 cumulative amphetamine-induced rotations were recorded in the sham group in the first study. Peak net ipsiversive rotations occurred in the 40 to 65 min time-period, post-amphetamine injection (***Fig 3.11.A***). In this period, amphetamine induced no cumulative net ipsiversive rotations in the sham lesioned group, while the 6OHDA infusions brought about a dose-dependent increase in amphetamine-induced cumulative rotations (***Fig 3.11.B***, $p<0.01$), with ~220, ~222, and ~579 net ipsiversive rotations being recorded in the 4µg, 6µg and 8µg 6OHDA groups, respectively. Rotations were found to be significantly higher in all of the 6OHDA dose groups when compared to the sham lesioned group ($p<0.5$ in all cases).

Figure 3.11. Rotational Behaviour Stimulated by Amphetamine in Rats Lesioned using Protocol 2

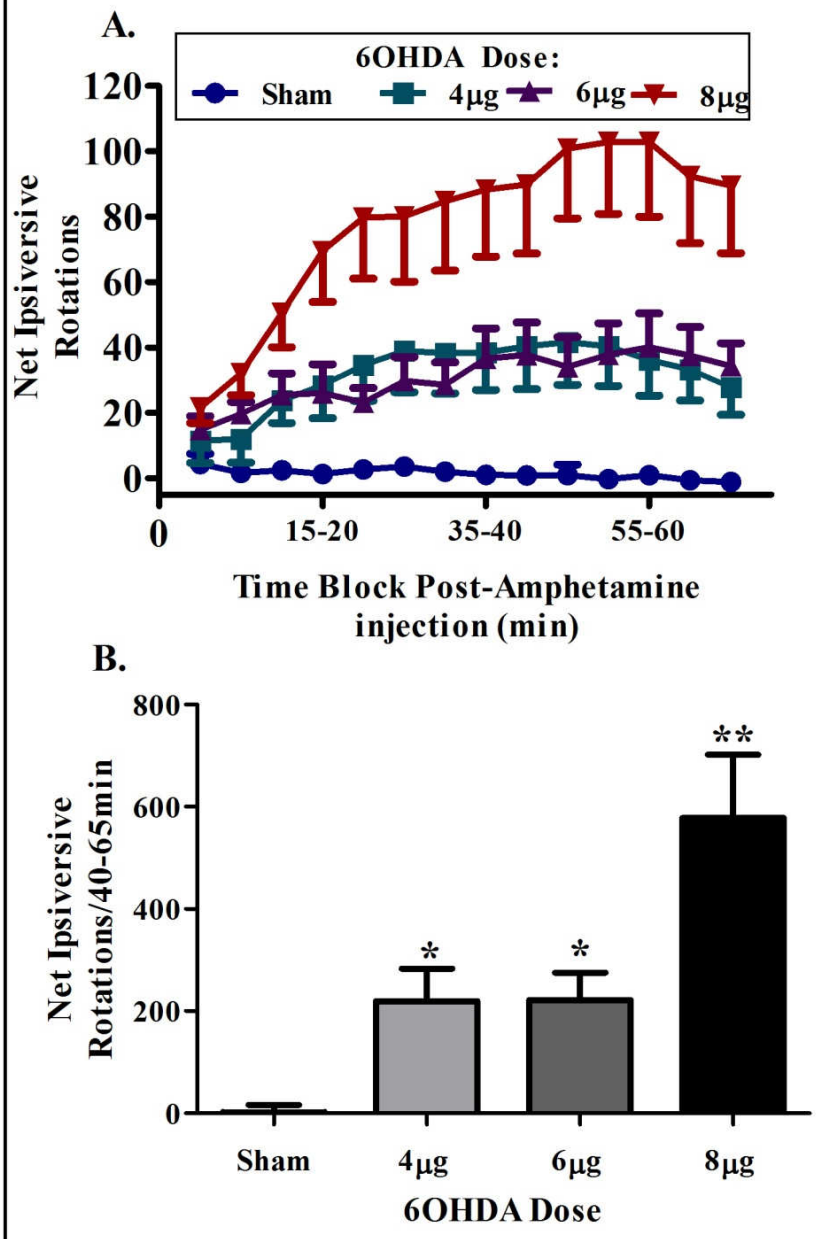

Figure 3.11. Rotational behaviour stimulated by amphetamine (5mg/kg, i.p) in rats which received unilateral intra-nigral infusions of a range of 6OHDA doses or vehicle (sham) delivered using lesioning protocol 2. Rotations were quantified in 5min time-blocks. Results are expressed as time-course profiles of the mean net ipsiversive rotations made over a 70min period post-drug injection (**A**), and as the mean cumulative net rotations made during the 25-50min period in which peak rotational behaviour occurred (**B**). Data points represent mean±sem, and n=6-7 for each group.*$p<0.05$ and **$p<0.01$ compared to sham.

3.4.2.3. Motor Deficits Detected by the Cylinder Test in Rats Lesioned using Protocol 2

The cylinder test failed to detect any significant motor deficits in the contralateral forelimb of the sham lesioned group at any of the time-points, post-lesioning, when compared to baseline (***Fig 3.12***). Significant contralateral forelimb motor deficits were, however, detected in all of the 6OHDA groups at all of the time-points, post-lesioning, when compared to baseline (***Fig 3.12***, $p<0.05$ in all cases). In the 4µg group, ipsilateral forelimb use alone increased from ~13% at baseline to ~74-91% at post-lesioning time-points. In the 6µg group, ipsilateral forelimb use alone increased from ~6% at baseline to ~88-95% post-lesioning, while in the 8µg group it increased from ~17% to ~86-88%. Importantly, at all of the time-points, post-lesioning, the motor deficits detected in all of the 6OHDA groups were found to be significantly greater to that detected on the equivalent day in the sham lesioned group ($p<0.05$ in all cases).

Figure 3.12. Motor Deficits Detected by the Cylinder Test in rats Lesioned using Protocol 2

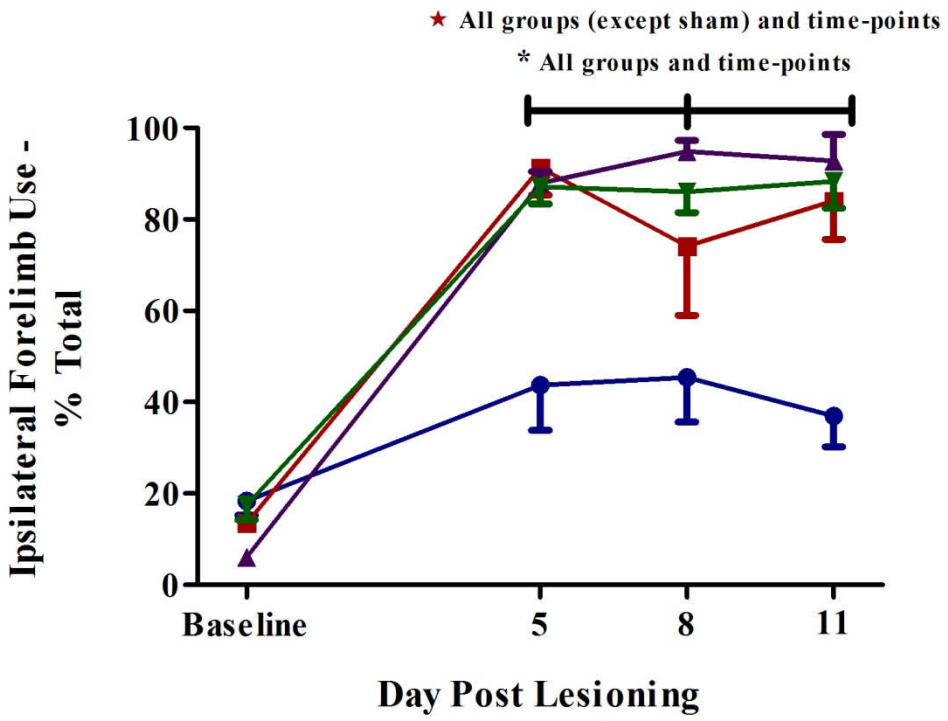

Figure 3.12. Unilateral deficits in forelimb motor function detected by the cylinder test in rats which received unilateral intra-nigral infusions of a range of 6OHDA doses or vehicle (sham) delivered using lesioning protocol 2. Increases in ipsilateral forelimb use alone, post-lesion, was used as a measure of the degree of motor impairment that was present in the contralateral impaired forelimb. Data points represent mean±sem, and n=6-7 rats for each group. ★$p<0.05$ compared to baseline, and *$p<0.05$ compared to sham.

3.4.2.4. Motor Deficits Detected by the Adjusted Stepping Test in Rats Lesioned using Protocol 2

The adjusted stepping test detected no motor deficits in the unaffected ipsilateral forelimbs (***Fig 13.3.B***). At baseline, the different treatment groups made ~23-24 adjusted steps with their ipsilateral forelimbs, and in all of the groups there were no significant differences between the number of ipsilateral adjusted steps made at any of the time-points post-lesioning when compared to baseline. There were also no significant differences between the number of ipsilateral adjusted steps made by the different groups at each of the different time-points.

At baseline, the different treatment groups made ~22-23 adjusted steps with their contralateral forelimbs, and significant contralateral forelimb motor deficits were detected in all of the treatment groups, including the sham group (***Fig 13.3.A***). In the sham and 4µg 6OHDA groups significant contralateral motor deficits were detected on day 8 and 11 ($p<0.05$ in all cases), but not on day 5, post-lesioning, when compared to baseline. In the sham group, adjusted step measurements were ~17-19% lower at the latter post-lesioning time points compared to baseline, while in the 4µg group they were ~21-23% lower. In the 6µg and 8µg 6OHDA groups, significant contralateral forelimb motor deficits were detected at all of the time-points, post-lesioning, when compared to baseline. In the 6µg group, adjusted step measurements were ~20-28% lower on post-lesioning time points compared to baseline ($p<0.05$ in all cases), while in the 8µg group they were ~35-42% lower ($p<0.01$ in all cases). The motor deficits in only the 6µg and 8µg 6OHDA groups were, however, found to be significantly greater to that present in the sham lesioned group. In the 6µg group, motor deficits were only significantly greater compared to sham on day 5 post-lesioning ($p<0.05$), whereas in the 8µg 6OHDA group, motor deficits were significantly greater to that present in the sham lesioned group at all time-points, post-lesioning ($p<0.01$).

Figure 3.13. Motor Deficits Detected by the Adjusted Stepping Test in rats Lesioned using Protocol 2

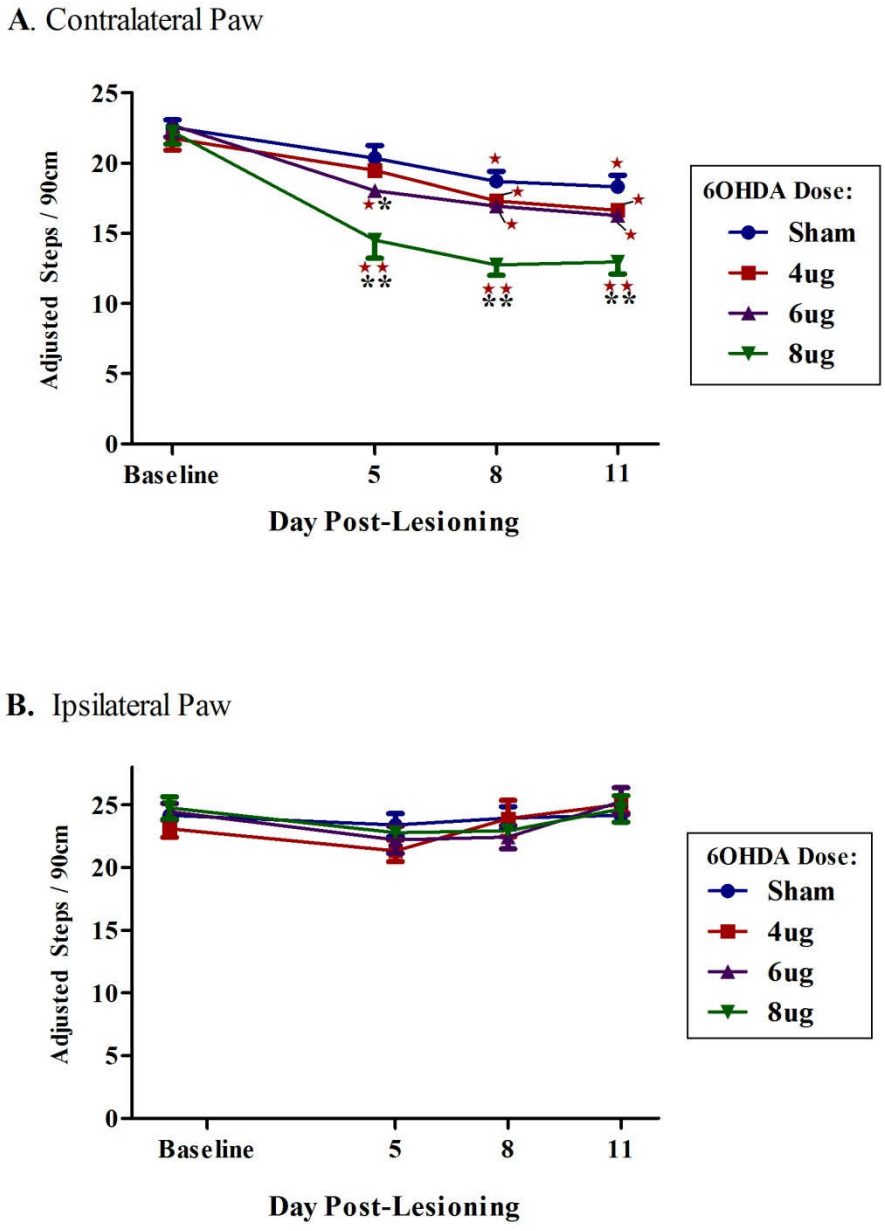

Figure 3.13. Unilateral deficits in forelimb motor function detected by the adjusted stepping test in rats which received unilateral intra-nigral infusions of a range of 6OHDA doses or vehicle (sham) delivered using lesioning protocol 2. The number of adjusted steps made by the contralateral (impaired) and ipsilateral (unimpaired) forelimb over a 90cm distance is shown in **A** and **B**, respectively. Decreases in the number of adjusted steps made after lesioning was used as a meaure of forelimb motor impairment. Data points represent mean±sem, n=6-7 rats for each group. ★$p<0.05$ and ★★$p<0.01$ compared to baseline. * $p<0.01$ and **$p<0.01$ compared to sham.

3.4.3. ERK1/2 Activation Stimulated by Intra-Nigral Infusions of FGF20

Only a relatively small number (~5-25) of phospho-ERK1/2 positive cells were present in the contralateral control nigral hemispheres (***Fig 3.14.B***). Intra-nigral infusions of not only FGF20 but also vehicle produced a substantial increase in phospho-ERK1/2 positive cell numbers around the nigral infusion site relative to the equivalent area in the contralateral hemisphere (***Fig 3.14.A&B***). This is qualitatively demonstrated in the images in ***Fig 3.14.B***, which show a substantially greater number of round brown stained phospho-ERK1/2 positive cells to be present in the ipsilateral relative to the contralateral hemispheres. Quantitative analysis of the results revealed there to be a trend towards FGF20 increasing net phospho-ERK1/2 positive cell numbers in a dose-dependent manner, as ~81, ~93, and ~113 phospho-ERK1/2 positive cells were present in the vehicle, 100ng, and 1µg groups, respectively (***Fig 3.14.A***). However, statistical tests could, unfortunately, not be used to test for significant differences between groups, as an 'n' of only 2 was used in each group. Moreover, substantial phospho-ERK1/2 activation was observed in cells all along the cannulae tracts (examples no shown).

Figure 3.14. Change in phospho-ERK1/2-Positive Cell Numbers Stimulated by Intra-Nigral FGF20 Infusions

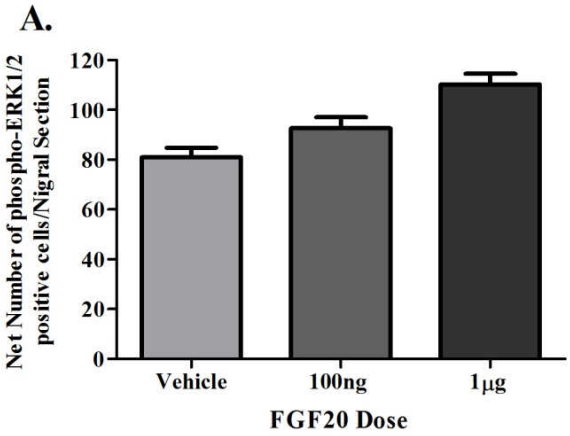

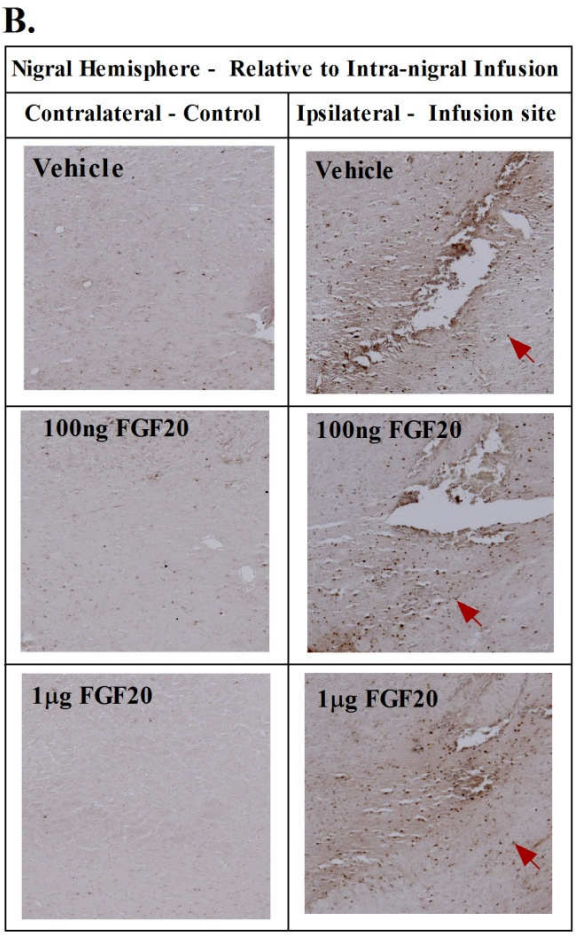

Figure 3.14. Change in net phospho-ERK1/2 (phosphorylated extracellular regulated kinase-1/2)-positive cell numbers induced by unilateral intra-nigral infusions of FGF20 or vehicle (**A**). n=2 for each group, and 6-9 coronal sections from each rat were used to calculate mean±sem values. **B**. Representative example images of the ipsilateral nigral infusion sites and of the corresponding contralateral nigral control areas taken from phospho-ERK1/2 immunostained nigral sections from each of the groups. Red arrows: Brown DAB stained phospho-ERK1/2 positive cells.

3.5. Discussion

3.5.1. Nigrostriatal Dopaminergic Lesions and Motor Deficits Induced in Rats using Lesioning Protocol 1

One of the main aims of this thesis was to evaluate whether FGF20 has neuroprotective effects on dopamine neurones, *in vivo*, in the partially lesioned 6OHDA rat model of PD. In this study, 6OHDA dose-response experiments were carried out to identify an intra-nigrally delivered dose of 6OHDA that induces an appropriate partially lesioned 6OHDA rat model of PD in which FGF20 could be evaluated for its neuroprotective effects. In an initial experiment, 6OHDA induced a dose-dependent loss of nigrostriatal dopamine neurones, with a 6µg and 8µg 6OHDA dose inducing a partial nigrostriatal lesion, whilst a 12µg dose induced an undesirable full lesion. However, unexpectedly and worryingly, in this initial study, the vehicle infusion alone caused a fairly substantial nigrostriatal lesion, reducing striatal TH levels by around ~25%**,** and TH+ nigral cell numbers by around ~50% when compared to the non-lesioned hemisphere. This indicated that the injection procedure itself caused some degree of nigrostriatal degeneration. Therefore, it follows that a substantial degree of nigrostriatal degeneration in the 6OHDA treatment groups can, thus, be attributed to the injection procedure rather than the selective toxic effects mediated by 6OHDA. The bulk of this damage is likely to be caused by the mechanical disruption induced by the insertion of the injection needle into the brain. Because there is a risk of 6OHDA forming a precipitate when dissolved in saline, the toxin was delivered in a dH_2O vehicle solution in this initial study. The vehicle also contained 0.02% ascorbate, which was added to prevent the oxidative inactivation of 6OHDA prior to it being infused. It is, thus, also likely that the dH_20 vehicle caused some cell death as a result of it disrupting the osmotic conditions at the injection site. The osmotic damage caused by the vehicle infusion is, however, likely to be limited as very small volumes (4µl) were delivered into the SNc. As ascorbate is a non-toxic substance with anti-oxidant properties, it is unlikely that it contributed to any cell death, especially at the very low concentrations at which it was present.

Although the aetiology of PD remains incompletely understood, there is evidence that a number of factors including mitochondrial dysfunction, oxidative stress, ubiquitin proteasome system dysfunction, and exposure to environmental toxins contribute to the development of PD. The dopaminergic cell death in PD is, however,

almost certainly not caused through mechanical or osmotic insults. There is, on the other hand, evidence that 6OHDA might induce dopamine neurone cell death through similar mechanisms that are at work in PD, as 6OHDA has been shown to induce dopamine neurone death by impairing the functioning of mitochondria, and/or through the generation of oxidative stress (Blum *et al.*, 2001). In order to produce the most clinically relevant model of PD possible, it would, therefore, be desirable to minimise the amount of dopaminergic degeneration that is induced by insults other than the 6OHDA toxin. Furthermore, it is also possible that mechanical and/or osmotic insults might cause the affected dopamine neurones to die immediately or at a very rapid rate. This might hinder the therapeutic potential of a treatment as it would reduce the number of dopamine neurones on which it could successfully have a beneficial effect. Moreover, although it was not investigated whether the infusion procedure inflicted damage on other non-dopaminergic cells around the infusion site, it is highly likely that the procedure also induced significant non-specific damage to non-dopaminergic cells not only in the SNc, but also in nearby regions, such as the SNr. Such non-specific damage to other cells would act to further reduce the practical usefulness of the model by reducing not only the face validity but potentially also the predictive validity of the model. For this reason, a second 6OHDA dose-response experiment was carried out in which the experimental design was refined so as to minimise the non-specific damage induced by the infusion procedure.

In neuroprotection studies carried out with the 6OHDA rat model of PD, a treatment's neuroprotective effects on dopamine neurones are assessed by determining if it preserved nigrostriatal dopamine neurones after 6OHDA lesioning. It is, however, also important to evaluate if any protection of dopamine neurones, offered by a treatment, also translates into a preservation of motor function after lesioning. Therefore, with the aim of identifying appropriate behavioural tests to use in future neuroprotection studies, a number of behavioural tests of motor function were assessed to identify tests that are sensitive enough to detect the relatively mild motor deficits that manifest in partially lesioned 6OHDA rats. Although the protocol used here induced unacceptable levels of 6OHDA-independent non-specific nigrostriatal damage, the behavioural results obtained from these rats are still useful in guiding the decision on which motor test to use in the future neuroprotection study. Of course, as with the nigrostriatal lesions, it is important for any motor deficits that are detected in a group of 6OHDA lesioned rats to be significantly greater compared to that detected in the vehicle

group. This will ensure that a neuroprotective treatment has a window of opportunity to demonstrate a significant preservation of motor function at an equivalent level to that seen, for example, in the vehicle group.

The motor tests evaluated in the initial 6OHDA dose response experiment included two drug-induced tests, the amphetamine and apomorphine-induced rotational tests, and two spontaneous tests of motor function, the adjusted stepping test and the cylinder test. Both the cylinder test and the amphetamine-induced rotations were sensitive enough to detect significantly greater motor asymmetry/deficits in not only the fully lesioned but also the partially lesioned rats. The adjusted stepping test detected significant motor deficits in the fully lesioned rats, and there was also a strong trend towards this test detecting significantly greater motor deficits in the 8µg partially lesioned group compared to the sham lesioned group. The apomorphine-induced rotational test, on the other hand, detected significant motor asymmetry in the fully lesioned rats, but in the partially lesioned rats it failed to detect any motor deficits. The detection of motor deficits in the 8µg partially lesioned group by the amphetamine-induced rotational test but not by the apomorphine-induced rotational test is consistent with the literature, as a >90% depletion of striatal TH has been shown to be required for apomorphine to stimulate robust rotational behaviour (Schwarting & Huston, 1996a). Amphetamine, on the other hand, has been demonstrated to stimulate rotational behaviour when striatal TH is depleted by ≥50% (Schwarting & Huston, 1996a). Based on these results, only the amphetamine rotational test, the cylinder test, and the adjusted stepping test were selected to be further assessed in the subsequent refined 6OHDA dose-response study.

3.5.2. Nigrostriatal Dopaminergic Lesions and Motor Deficits Induced in Rats using Lesioning Protocol 2

In the initial 6OHDA dose-response experiment that was carried out, a substantial nigrostriatal lesion was found to be present in the sham lesioned group. With the aim of identifying an infusion procedure that produces minimal nigrostriatal tract degeneration by itself, a second follow-up 6OHDA dose-response experiment was carried out in which vehicle and 6OHDA infusions were delivered using a refined protocol (protocol 2). It was concluded that the substantial lesion in the sham lesioned group observed in the first study was most likely the result of a relatively large (23G) injection needle and a non-physiological dH_2O vehicle solution being used. For this reason, in the second

study, a much smaller 30G injection needle and a physiological 0.09% saline vehicle solution were, thus, used instead when administering the intra-nigral 6OHDA infusions.

TH immunohistochemistry results from this second study demonstrated these refinements to have successfully reduced the non-specific damage induced by the procedure to negligible levels. Using the refined infusion protocol, vehicle infusions induced only a minimal degree of nigrostriatal degeneration, with no significant reduction in striatal TH levels and only an ~10% reduction in nigral TH+ cell counts being detected in the sham group. This represents a substantial improvement, as in the first study a significant ~25% striatal and ~50% nigral lesion was observed in the sham lesioned group. Importantly, in this study, the 6OHDA infusions induced a dose-dependent degeneration of nigrostriatal dopamine neurones in the rats. However, both the 6µg and 8µg doses of 6ODHA induced an undesirable nearly complete nigrostriatal lesion of ~90%, and ~95%, respectively. The 4µg dose of 6OHDA, on the other hand, induced a desirable partial ~60-80% nigrostriatal lesion. Thus, based on the immunohistochemistry results, the 4µg dose of 6OHDA was considered to be the most appropriate dose to use in subsequent *in vivo* neuroprotection studies with FGF20.

Surprisingly, using the refined protocol, 6OHDA had a much more pronounced potency at inducing nigrostriatal degeneration when compared to the first study, as equivalent 6OHDA doses caused substantially greater nigrostriatal dopamine neurone loss in the second study compared to the first. In the first study, for example, an 8µg dose of 6OHDA induced only ~60% nigrostriatal lesion, while in the second study, this same dose induced a nearly complete ~95% lesion. This is unexpected, particularly because the infusion procedure used in the first study was shown itself to induce a substantial degree of nigrostriatal degeneration, whereas the infusion procedure in the second study only caused minimal damage in the sham group. One possible explanation for this could be that the modified vehicle solution used in the second study somehow acted to enhance the potency of 6OHDA. This discrepancy is, however, more likely to have been caused by two different batches of 6OHDA being used in the studies. The 6OHDA-HBr stock powder used to prepare the 6OHDA working solutions in the first study was ~3 years old, whereas a newly purchased batch of 6OHDA was used in the second study. As 6OHDA is known to be a fairly labile compound, the 6OHDA stock solution used in the first study might have contained substantially reduced amounts of active non-oxidised 6OHDA compared to the fresh batch of 6OHDA used in the second study.

In addition to the histological analyses, three different motor tests, the amphetamine-induced rotational test, the cylinder test, and the adjusted stepping test were also evaluated with the aim of identifying motor tests that are sensitive enough to detect motor deficits in partially lesioned 6OHDA rats. As expected, the minimal nigrostriatal tract damage induced by the vehicle infusions in this study resulted in only minimal motor deficits being detected in the sham group. Both the amphetamine-induced rotational test and the cylinder test failed to detect significant motor deficits/asymmetry in the sham lesioned group at any of the time-points post-lesioning when compared to baseline, while the adjusted stepping test detected significant but relatively small reductions in motor function of ~10-15% in the sham lesioned group. Importantly, the 6OHDA infusions induced a dose-dependent increase in motor deficits in the rats. As discussed earlier, full nigrostriatal dopaminergic lesions have been documented to produce robust motor deficits in rats that are relatively easily quantifiable by several motor tests (Schwarting & Huston, 1996a). In this study, a nearly complete nigrostriatal lesion was induced by both the 6µg and the 8µg 6OHDA doses, and consistent with literature reports, all of the tests evaluated detected motor deficits significantly greater than that present in the sham lesioned rats, in both the 6µg and 8µg groups. Of the two spontaneous motor function tests, it appeared that the cylinder test had the greatest sensitivity, as the cylinder test detected significant motor deficits in the ~90% lesioned 6µg group on all of the time-points post-lesioning, whereas the adjusted stepping test detected motor deficits significantly greater than the sham group on only day 5, post-lesioning. Consequently, in the 4µg partially lesioned rats, motor deficits significantly greater than that observed in the sham group were detected by the amphetamine-induced rotational test and the cylinder test, but not by the adjusted stepping test. As mentioned above, of all of the 6OHDA doses tested in the second study, only the 4µg dose induced an appropriate ~60-80% nigrostriatal dopaminergic lesion. Therefore, a 4µg intra-nigrally delivered dose of 6OHDA was used in the subsequent *in vivo* neuroprotection studies with FGF20. As the adjusted stepping test was found not to have a sufficient sensitivity to detect the less pronounced motor deficits that were present in the partially lesioned 4µg group, this test was not used in the neuroprotection study. The cylinder test and the amphetamine-induced rotational test, on the other hand, were both employed, as both of these tests detected significantly greater motor deficits in the 4µg group compared to the sham lesioned group.

3.5.3. Identifying a Biologically Active Intra-Nigrally Delivered Dose of FGF20

By using phospho-ERK1/2 as a marker of FGF20 stimulated FGFR activation, an attempt was made to identify a biologically active intra-nigrally delivered dose of FGF20. In this pilot study, it was anticipated that either no or very low phospho-ERK1/2 positive cell numbers would be observed in the vehicle group, while substantially higher phospho-ERK1/2 activation levels would be induced by a biologically active dose of FGF20. This would have allowed a biologically active dose to be identified through a qualitative analysis of the results. Instead, results from these experiments revealed that both the FGF20 and the vehicle infusions stimulated a substantial increase in phospho-ERK1/2 activation at the infusion site. There was a trend towards FGF20 increasing phospho-ERK1/2 activation further in a dose-dependent manner. Statistical tests could, however, not be carried out to establish if there were significantly higher phospho-ERK1/2 activation levels in the FGF20 groups, as only an n of 2 was used in each group.

As increased phospho-ERK1/2 activation was observed not only at the infusion sites, but also all the way along the cannulae tracts, it appears that phospho-ERK1/2 activation is being stimulated by the mechanical damage caused by the insertion of the injection needle. Moreover, it has previously been reported that the intra-hippocampal implantation of a microdialysis probe itself induces a substantial upregulation of FGF2 mRNA and protein around the site of implantation (Humpel *et al.*, 1994). It is, thus, likely that the mechanical damage induced by a foreign object being inserted into the brain stimulates the release of numerous signalling molecules in the brain tissue surrounding the inserted object. These signalling molecules would then stimulate the activation of numerous signalling pathways in the tissue surrounding the implantation site. Therefore, it could be anticipated that it would be difficult to study the effect of an intra-cerebrally infused test agent on signalling events in a specific brain area, if the signalling events are activated extensively or to a supra-maximal level by the damage alone. As FGF2 is a potent agonist at the FGFRs (Ornitz *et al.*, 1996; Ford-Perriss *et al.*, 2001; Eswarakumar *et al.*, 2005; Zhang *et al.*, 2006; Heinzle *et al.*, 2011), and it has been shown to be upregulated by the implantation process (Humpel *et al.*, 1994), it is likely that signalling pathways activated by the FGFRs will fall in such a category in areas where FGFRs are expressed. The failure of these experiments to detect a biologically active dose of FGF20 could, thus, potentially be attributed to the

complications outlined above. However, it could also simply be due to a big enough dose of FGF20 not having been tested in these experiments.

Although there are no published reports of FGF20 being tested for any central nervous system effects *in vivo*, several studies have investigated the pharmacologic activities mediated *FGF2* when it is delivered to the central nervous system through continuous infusion. These studies reported FGF2 to have mitogenic (Kuhn *et al.*, 1997; Kojima & Tator, 2002; Ohta *et al.*, 2006), and neuroprotective (Srivastava *et al.*, 2008) effects at a dose rate of 0.36µg/day. Moreover, pilot studies undertaken in this lab to probe the neuroprotective effects of FGF20 in rats bearing a full nigrostriatal tract lesion showed that FGF20, delivered over 6 days at a slightly higher dose rate of 2.5µg/day, provided some protection against losses of both striatal TH immunoreactivity and nigral TH+ cell numbers (unpublished results). Therefore, as the dose finding experiments failed to identify a biologically active dose, a range of FGF20 doses, including the 2.5µg/day dose used in the previous pilot study, were evaluated in the *in vivo* neuroprotection study in Chapter 4.

3.5.4. Conclusion

An intra-nigral infusion procedure that induces a negligible degree of non-specific nigrostriatal degeneration by itself was successfully developed in this study. The use of an injection needle with the smallest possible gauge and also a physiological vehicle solution, in the infusion procedure, was demonstrated to be essential in minimising non-specific nigrostriatal degeneration. The refined 6OHDA lesioning procedure was used in 6OHDA dose-response experiments to identify an intra-nigrally delivered dose of 6OHDA that induces a partial ~60-80% lesion of the nigrostriatal tract in rats. Of all the doses of 6OHDA tested, only the 4µg 6OHDA dose produced an appropriate partial nigrostriatal dopaminergic lesion, while both the 6µg and the 8µg doses induced an undesirable near complete lesion. Of the four motor tests evaluated, only the cylinder test and the amphetamine-induced rotational test detected significant motor deficits in the 4µg partially lesioned rats. Thus, in the *in vivo* neuroprotection study carried out in Chapter 4, it was evaluated if FGF20 could protect against a partial nigrostriatal lesion induced by a 4µg intra-nigrally delivered dose of 6OHDA. The cylinder test and the amphetamine-induced rotational test were selected to be used to assess if FGF20 improves the motor deficits induced by the partial nigrostriatal lesion. Since the FGF20 dose finding experiments failed to successfully identify a biologically active intra-

nigrally delivered dose of FGF20, a range of FGF20 doses based on preliminary findings from an earlier pilot study were used in the study.

Chapter 4: Neuroprotective Effects of Fibroblast Growth Factor-20 on Dopamine Neurones

4.1. Introduction

4.1.1. Protective and Regenerative Effects mediated by the FGF System

In both the peripheral organs and the nervous system, several FGF family members protect numerous tissues from injury, and in many cases they also stimulate the regeneration of the injured tissues. Peripherally, FGFs have been shown to have a protective and/or regenerative effect on the heart, cartilage, and on endothelial cells. FGF1 and FGF2 protect the heart from ischaemic reperfusion injury both *in vivo* and *ex vivo*, with a single FGF pre-treatment preserving myocardial tissue and cardiac function (Detillieux *et al.*, 2004). In the damaged knee joint, FGF2 stimulates cartilage repair when it is delivered by FGF2 overexpressing chondrocytes implanted into the knee joint (Cucchiarini *et al.*, 2005; Jungnickel *et al.*, 2006), while, *in vitro*, FGF2 protects endothelial cells against both serum withdrawal (Karsan *et al.*, 1997) and hypoglycaemia (Han *et al.*, 2005). Additionally, FGF2 has also been shown to stimulate skin wound healing (Obara *et al.*, 2005).

FGFs have been reported to have protective and/or regenerative effects in a number of different types of nervous system tissues, not only, *in vitro*, in immortalised and primary neurone cultures, but also, *in vivo*, in both the peripheral and central nervous system. FGF2 and FGF8 protect SKHMC neuroblastoma cells from oxidative stress (Mark *et al.*, 1999), while both FGF2 and FGF4 protect SHSY5Y cells from nitric oxide toxicity (Wagle & Singh, 2000). Hippocampal primary neurone cultures are protected from glutamate toxicity by FGF2 (Lenhard *et al.*, 2002), and from oxidative stress by both FGF2 and FGF4 (Detillieux *et al.*, 2004). Additionally, FGF2 protects primary cerebellar neurones from ethanol induced cell death (Luo *et al.*, 1997), and it also has neurotrophic effects on a number of different primary motor neurone cell cultures (Grothe & Wewetzer, 1996). *In vivo*, in the peripheral nervous system, FGF2 protects hypoglossal neurones against lesioning (Grothe & Wewetzer, 1996), and the facial nerve against axotomy (Cuevas *et al.*, 1995), while in another study FGF2 enhanced the reinnervation of muscle after transection of the motor nerves innervating the muscle. FGF1 and FGF2 also promotes the survival and regeneration of the injured sciatic nerve (Laird *et al.*, 1995; Grothe & Wewetzer, 1996; Jacques *et al.*, 1999; Ohta

et al., 2004), with FGF1 not only promoting regeneration but also the electrophysiological functioning of the regenerated nerve (Wang *et al.*, 2003). *In vivo*, in the CNS, FGFs also promote the survival and regeneration of a number of different injured brain structures. FGF2, when either exogenously applied or delivered by adenoviral overexpression, increases the survival and regeneration of the optic nerve after injury (Blanco *et al.*, 2000; Sapieha *et al.*, 2003). FGF2 application also protects the hippocampus against a kainite-induced lesion (Tretter *et al.*, 2000), and it stimulates increased survival of neurones in the dorsal lateral geniculate nucleus after axotomy (Agarwala & Kalil, 1998). Furthermore, both FGF2 and FGF18 protects against cerebral ischaemic brain injury, with both FGFs reducing the infarct size and also preserving motor function (Li & Stephenson, 2002; Ellsworth *et al.*, 2004). Thus, there is a wealth of evidence demonstrating the FGF system to play an important protective and/or regenerative role in many different tissues of the body.

4.1.2. Neurotrophic Effects of the FGFs on Dopamine Neurones

The FGF system also plays an important physiological role in the nigrostriatal dopaminergic tract. All of the FGFRs and 5 of the 23 FGFs - FGF1, FGF2, FGF8, FGF9, and FGF20 - are expressed by one or more cell type in the nigrostriatal tract, with all being localised to dopamine neurones (***detailed in section 2.1.5***). Furthermore, in Chapter 2 of this thesis, using immunohistochemistry, FGF20 and FGFR1, 3, and 4 were demonstrated to be localised abundantly in not only dopaminergic neurones, but also in a number of other cell types throughout the nigrostriatal tract of the rat brain. In VM embryonic dopamine neurone cultures, the FGFR1, 3, and 4 proteins were also shown to localise to a number of different cell types present in these cultures. Evidence from a number of studies has indicated that the endogenous FGF system plays an important role in maintaining the survival of not only embryonic VM developing dopamine neurones, but also nigrostriatal dopamine neurones in the intact adult brain. *In vitro*, FGF2 stimulates survival and neurite outgrowth in VM embryonic rat dopamine neurones, while in human embryonic dopamine neurone cultures, FGF2 stimulates increased survival and increased TH expression (Silani *et al.*, 1994). FGF8 also has neurotrophic effects on VM embryonic rat dopamine neurones, and treatment of VM cultures with FGF8 neutralising antibody decreased TH+ cell survival (Roussa *et al.*, 2004), while in another study, inhibition of FGFR activation enhanced reserpine induced cell death of VM embryonic dopamine neurones (Murase & McKay, 2006).

Additionally, in VM embryonic cultures, FGF2 has also been shown to regulate extracellular dopamine levels by stimulating increased dopamine uptake by both dopamine neurones and astrocytes (Silani *et al.*, 1994; Inazu *et al.*, 1999). Moreover, findings from several *in vitro* studies have provided indirect evidence that astrocyte-derived striatal FGF2 might play an important neurotrohpic role in maintaining the survival of nigrostriatal dopamine neurones in the intact brain. *In vitro*, astrocytic FGF2 release is stimulated by the activation of dopamine receptors located on the astrocytes. Both dopamine itself and the non-selective dopamine receptor agonist, apomorphine are capable of upregulating FGF2 release in astrocytes, and this dopamine receptor stimulated, astrocyte-derived FGF2 has a neurotrophic effect on dopamine neurones in culture (Reuss & von Bohlen und Halbach, 2003; Li *et al.*, 2006). Selective activation of the D1 or D2 dopamine receptors are capable of upregulating FGF2 expression in astrocytes through a cAMP/PKA and ERK1/2-dependent pathway, respectively (Li *et al.*, 2006). Based on these findings, it has been suggested that a retrograde trophic positive feedback pathway exists in the intact striatum. That is, dopamine released from nigrostriatal dopamine neurone terminals in the striatum acts on astrocytes to increase their release of striatal FGF2, which in turn mediates a neurotrophic effect on dopamine neurones. There is, however, currently no confirmatory evidence available from any *in vivo* studies that such a dopamine driven trophic feedback pathway actually exists under physiological conditions. However, if it does exist, *in vivo*, pharmacological activation of this neurotrophic pathway alone is insufficient to protect nigrostriatal dopaminergic neurones in the PD brain from ongoing degeneration, as clinical trials have demonstrated the commonly used dopamine receptor agonists to be ineffective in slowing down disease progression in PD (Hauser, 2010). Nevertheless, the postulated general neurotrophic role of the FGF system in the nigrostriatal system has been confirmed by an *in vivo* study in mice, in which transfection of nigrostriatal dopamine neurones with a FGFR1 mutant lacking a functional kinase domain resulted in ~20% reduction in nigral TH+ cell numbers, and also a decrease in striatal levels of TH and the dopamine metabolite, 3,4-dihydroxyphenylacetic acid (DOPAC) (Corso *et al.*, 2005).

4.1.3. Role of the FGF system in the Lesioned Nigrostriatal Tract

In the rat, 6OHDA lesioning of the nigrostriatal dopaminergic tract induces a robust increase in FGF2 mRNA and protein levels within the SN and the striatum (Chadi *et al.*,

1994; Agarwala & Kalil, 1998), and this increase has been shown to be caused by a substantial upregulation of FGF2 expression by activated astrocytes throughout the basal ganglia (Chadi & Gomide, 2004). This is thought to be a protective response initiated by the brain to try and counteract the degenerative effects mediated by 6OHDA. Moreover, an unidentified factor(s) derived from the adrenal glands has a permissive effect on this 6OHDA-induced upregulation of FGF2, as this effect was completely abolished by adrenalectomy in the rat (Chadi *et al.*, 2008).

Interestingly, FGF2 protein is nearly completely absent in the SNc of PD patients (Tooyama *et al.*, 1994), whereas the FGFR1 is reported to be present in the remaining SNc dopamine neurones of PD patients (Walker *et al.*, 1998). These findings suggest that the loss of FGF2 might contribute to the degeneration of dopamine neurones in PD, while the presence of the FGFR1 in the SNc of PD patients provides support that activation of the FGF system might have therapeutic potential in PD.

4.1.4. Neuroprotective Effects of the FGFs on Dopamine Neurones

In vitro, FGF2 protects VM dopamine neurones against 6OHDA, MPP^+, rotenone, and glutamate-induced cell death (Park & Mytilineou, 1992; Mayer *et al.*, 1993a; Otto & Unsicker, 1993; Casper & Blum, 1995; Hou *et al.*, 1997; Grothe *et al.*, 2000; Hsuan *et al.*, 2006). Several *in vivo* studies have shown both FGF1 and FGF2 to have robust neuroprotective effects on nigrostriatal dopaminergic neurones in a number of different animal models of PD. In mice, continuous intracerebroventricular (icv) delivery of FGF2 protected nigrostriatal dopamine neurones against MPTP-induced nigrostriatal degeneration, and it also completely reversed MPTP-induced bradykinesia in the mice (Chadi *et al.*, 1993). In rats, implantation of FGF2 overexpressing fibroblasts into the striatum protected against 6OHDA-induced dopamine neurone cell death, and it also alleviated 6OHDA-induced motor deficits (Shults *et al.*, 2000). Intra-striatal delivery of FGF1 has also been shown to preserve striatal TH immunoreactivity in the 6OHDA lesioned rat (Jin & Iacovitti, 1995). In the MPTP primate model of PD, icv infusions of FGF2 increased dopamine neurone survival and function, and it also alleviated MPTP-induced motor deficits (Fontan *et al.*, 2002). Importantly, in the latter study, FGF2 had superior neuroprotective effects (more potent and prolonged) on dopamine neurones than compared to GDNF, the current gold standard neurotrophin used in the experimental treatment of PD. Other FGF members, apart from FGF1 and FGF2, have

also been reported to have either neurotrophic and/or neuroprotective effects on dopamine neurones, including FGF9 and FGF20 (***FGF20's neuroprotective effects are detailed in section 4.1.5 below***). FGF9 protects VM dopamine neurones against MPP^+, *in vitro*, while, *in vivo*, it protects nigrostriatal dopamine neurones from MPP^+ toxicity in the rat (Huang *et al.*, 2009). It has been conclusively demonstrated that FGF2's neurotrophic and neuroprotective effects are not specific to dopamine neurones, as FGF2 also has trophic and neuroprotective effects on glial cells and on a number of other types of neurones, including GABAergic and cholinergic neurones (***detailed in section 4.1.1 and*** (Otto & Unsicker, 1993; Sensenbrenner, 1993; Bouvier & Mytilineou, 1995a)). This raises the possibility that, if FGF2 is used as a treatment for PD, it might cause adverse effects – potentially malignant growth and dysregulated functioning of non-dopamine neurones.

There is substantial direct and indirect evidence from both cell culture and *in vivo* experiments indicating that the neurotrophic and neuroprotective effects mediated by FGF2 on dopamine neurones are at least partially mediated through an astrocyte-dependent indirect mechanism. *In vitro*, astrocyte proliferation is essential in allowing FGF2's protective effects on VM dopamine neurone cultures against 6OHDA and MPP^+ (Park & Mytilineou, 1992; Hou *et al.*, 1997). Similarly, FGF2's neurotrophic effects on human and rat embryonic dopamine neurone cultures are also dependent on astrocyte proliferation (Mayer *et al.*, 1993a; Silani *et al.*, 1994). It, thus, appears that FGF2 stimulates the release of neurotrophin(s) from astrocytes, which in turn have neurotrophic and/or neuroprotective actions on dopamine neurons. Accordingly, the supernatant derived from FGF2 stimulated astrocyte cultures stimulates differentiation and increased dopamine uptake in dopamine neurone cultures (Gaul & Lubbert, 1992), while in another study, FGF2's neurotrophic effects on VM dopamine neurone cultures have been shown to be mediated by transforming growth factor-B (TGF-β) (Krieglstein *et al.*, 1998). Furthermore, *in vitro*, the neuroprotective effects of FGF2 on embryonic hippocampal neurones against glutamate toxicity are inhibited by GDNF neutralising antibodies (Lenhard *et al.*, 2002), while, *in vivo*, FGF2's neuroprotective effects on hippocampal neurones against a kainate lesion are completely dependent on FGF2 stimulated activin A release (Tretter *et al.*, 2000). However, it appears that FGF2 stimulated astrocyte derived factor(s) only partly mediate FGF2's neurotrophic effects, as FGF2's neurotrophic effects on VM dopamine neurone cultures have in another

study been shown to be partly mediated by a direct action on dopamine neurons (Mayer *et al.*, 1993a).

Furthermore, FGF2 also has the potential to increase the success of grafting therapies in PD. In the nigrostriatal-lesioned rat, co-grafting of embryonic dopamine neurones with FGF2 overexpressing fibroblasts or Schwann cells increased both the survival and fiber outgrowth of the grafted dopamine neurons (Takayama *et al.*, 1995; Roceri *et al.*, 2001). It also significantly improved motor deficits compared to the grafting of dopamine neurones alone. Another study has assessed the effectiveness of either FGF2 pretreatments or multiple icv infusions on dopamine neurone graft survival (Mayer *et al.*, 1993b). Although both approaches improved graft survival and motor deficits, the icv infusions had substantially greater and more prolonged neurotrophic effects. Moreover, FGF2 can also be used to increase the success of grafting therapies by using it to increase the yield of dopamine neurones in embryonic dopamine neurone graft preparations, as FGF2 prolongs the proliferation and delays the differentiation of embryonic dopamine precursor cells (Bouvier & Mytilineou, 1995b).

4.1.5. Neuroprotective effects of FGF20 on Dopamine Neurones and its Potential as a Treatment for PD

FGF20 has recently been identified to be another FGF family member that could have neuroprotective potential in PD. FGF20 is a 211 amino acid polypeptide with a predicted molecular weight of ~23 kDa (Kirikoshi *et al.*, 2000; Ohmachi *et al.*, 2003). In the rat brain, FGF20 mRNA has been shown be localised in both the SN and the striatum (Ohmachi *et al.*, 2003; Grothe *et al.*, 2004); and in Chapter 2, using immunohistochemistry, FGF20 protein was demonstrated to be abundantly present in both the SN and the striatum of the rat brain (***see section 2.4.1.1 and 2.4.2.1***). Moreover, results generated in Chapter 2 demonstrated FGF20 to be exclusively localised to the SNr in the SN, with no FGF20 staining being observed in the SNc. These results conflicts with the previously reported *in situ* hybridisation results which showed FGF20 to be exclusively localised to dopamine neurones in the SNc of the rat brain (Ohmachi *et al.*, 2000), and reasons for this discrepancy are discussed in detail in ***section 2.5.2***. *In vitro,* recombinant human FGF20 protects VM embryonic dopamine neurones against serum withdrawal, glutamate toxicity, and 6OHDA-induced cell death (Ohmachi *et al.*, 2000; Ohmachi *et al.*, 2003; Murase & McKay, 2006). In the Murase & McKay, 2006 study, FGF20 was shown to preferentially protect calbindin negative

dopamine neurones in the VM cultures. These calbindin negative dopamine neurones are preferentially lost in PD patients (Gibb, 1992), and they are also more sensitive to dopamine neurone toxins (German *et al.*, 1992). Calbindin is an intracellular calcium binding protein that plays an important role in buffering intracellular calcium levels. It is, thus, believed that the increased sensitivity of this subset of calbindin negative dopamine neurones is due to them having a reduced capacity to maintain intracellular calcium levels within a non-toxic range.

Moreover, like FGF2, FGF20 also has the potential to improve the success of PD grafting therapies, as FGF20 stimulates the differentiation of rodent, monkey, and human embryonically derived neuronal stem cells into dopamine neurones. In one study, FGF20 treatment stimulated a ~5 fold increase in the yield of human embryonic stem cell (hESC)-derived dopamine neurones (Correia *et al.*, 2007), while in another study, co-administration of FGF20 and FGF2 increased the yield of hESC derived dopamine neurones (Shimada *et al.*, 2009). Similarly, co-application of FGF20 and FGF2 also induced the differentiation of monkey embryonic neuronal stem cells into a dopaminergic phenotype (Takagi *et al.*, 2005). These monkey ES-derived dopamine neurones were subsequently shown to alleviate MPTP-induced motor deficits and to increase striatal F-dopa uptake (an index of striatal dopamine neurone terminal density) when transplanted into the putamen of MPTP monkeys (Takagi *et al.*, 2005). Furthermore, co-culturing of nurr1 overexpressing murine neural stem cells (NSC) with FGF20 overexpressing Schwann cells stimulated the differentiation of the NSC cells into dopamine neurones (Grothe *et al.*, 2004). When these NSC-derived dopamine neurones were co-transplanted with FGF20 overexpressing Schwann cells in rodent grafting experiments, a greater number of the transplanted cells were found to have maintained their dopaminergic phenotype when compared to control transplants.

Results from a number of genetic studies in humans have indicated that FGF20 might play a role in the aetiology of PD, as 8 single nucleotide polymorphisms (SNPs) in the *FGF20* gene have been found to increase the risk of PD, thus far. Alleles of the rs12720208, rs1721100, rs1989754, rs1721082, rs1799836, rs10888125, rs11203822, and the ss20399678 *FGF20* gene SNPs have all been shown to be associated with an increased risk of developing PD (van der Walt *et al.*, 2004; Satake *et al.*, 2007; Gao *et al.*, 2008; Mizuta *et al.*, 2008; Wang *et al.*, 2008; Wider *et al.*, 2009; de Mena *et al.*, 2010). Interestingly, some of these *FGF20* gene risk alleles have been shown to interact with *MAO-B* and *SNCA* PD risk alleles to synergistically increase the overall risk of PD

(Gao *et al.*, 2008; Mizuta *et al.*, 2008). These genetic findings are, however, controversial and still not conclusive, as a number of conflicting reports have found no association between some of the abovementioned *FGF20* gene SNPs and PD. For example, for the rs12720208 SNP, one study found an association with PD to exist (Wang *et al.*, 2008), but two reports failed to find an association (Wider *et al.*, 2009; de Mena *et al.*, 2010). For the rs1989754 SNP, there are two studies which found an association (van der Walt *et al.*, 2004; Wang *et al.*, 2008), and an equal number which found no association (Clarimon *et al.*, 2005; Satake *et al.*, 2007). Further independent replicate studies are also needed to confirm the association of the rs1799836 (Gao *et al.*, 2008), rs10888125 and rs11203822 (Wang *et al.*, 2008), and the ss20399678 SNPs (van der Walt *et al.*, 2004), as an association for each of these SNPs have only been reported by a single study. An association of the rs1721082 SNP with PD has been confirmed in two independent studies (Gao *et al.*, 2008; Wang *et al.*, 2008). However, the evidence for an association with PD is, by far, the most conclusive for the rs1721100 SNP. Five independent studies have found the rs1721100 SNP to be associated with PD (van der Walt *et al.*, 2004; Satake *et al.*, 2007; Gao *et al.*, 2008; Mizuta *et al.*, 2008; Wang *et al.*, 2008), while only one study has found no association (Clarimon *et al.*, 2005) .

In the Wang *et al.*, 2008 study, in which an association was identified between the T allele of the rs12720208 *FGF20* gene and PD, the authors also investigated the biological mechanism through which this SNP might increase PD risk. It was discovered that the rs12720208 SNP lies within a sequence that is a predicted binding site for the microRNA, miR-433. By binding specifically to its binding sites on target mRNA strands, miR-433 acts to inhibit the translation of the target mRNA into protein. In the rs12720208 C allele, the miR-433 binding site is intact, whereas, in the rs12720208 allele that is associated with PD, the T allele, the miR-433 binding sequence is disrupted. It was, thus, proposed that the T allele would give rise to higher levels of FGF20 protein, as miR-433 would be unable to suppress the translation of FGF20 mRNA into protein. This hypothesis was then substantiated by evidence from a number of studies. Using a luciferase reporter gene assay, miR-433 was shown to strongly inhibit the translation of the C allele, but not the T allele in a fibroblast cell line. In a second study, miR-433 suppressed translation of FGF20 in two fibroblast cell lines, one homozygous and the other heterozygous for the C allele, and as expected, this inhibition was greater in the fibroblast cell line that was homozygous for the C allele. Furthermore, in humans, FGF20 protein levels were shown to be higher in the brains of

T allele carriers when compared to C allele carriers. Lastly, in SHSY5Y cells, it was also demonstrated that FGF20 upregulates SNCA. Based on these finding, the authors proposed that the T allele of rs12720208 increases PD risk by increasing FGF20 protein levels – through disinhibition of mRNA translation – which in turn stimulates increased production of the SNCA protein, and overproduction of SNCA is widely believed to play a role in PD pathology. Additionally, another study found the rs12720208 SNP to be associated with increased hippocampal FGF20 expression in human post-mortem brains (Lemaitre *et al.*, 2010); and using a quantitative neuroanatomical magnetic resonance imaging (MRI) technique, they also demonstrated the rs12720208 SNP to be associated with increased hippocampal volume in healthy volunteers. These reported findings however remain controversial, both the association of the rs127202 SNP with PD risk and also its association with increased FGF20 and SNCA protein levels, as several conflicting reports have subsequently been published. As mentioned earlier, only the Wang *et al*., 2008 study has found an association between the rs12720208 *FGF20* gene SNP and PD, while two other independent studies have contradicted their findings, reporting no association between rs12720208 and PD (Wider *et al.*, 2009; de Mena *et al.*, 2010). Additionally, in the Wider *et al*., 2009 study, FGF20 protein levels were measured in human brain tissue by immunoblot, and no association was found between FGF20 protein levels and the rs12720208 SNP. No association was also found between FGF20 and SNCA protein levels in human brain tissue samples in this study. Furthermore, although the Lemaitre *et al*., 2010 study found the rs12720208 SNP to be associated with increased hippocampal FGF20 expression and hippocampal volume, they detected no abnormalities in the morphology of the SN in both young and old rs12720208 T allele carriers. Nevertheless, although the findings from the Wang *et al*., 2008 study remain inconclusive and controversial, it highlights the fact that there is a possibility that administration of exogenous FGF20 could potentially exaggerate rather than attenuate nigrostriatal degeneration. The wealth of evidence demonstrating activation of the FGF system to mediate protective and regenerative effects rather than degenerative effects on not only nigrostriatal neurones but also on many other tissues argues strongly against the theory that overexpression of FGF20 promotes nigrostriatal degeneration.

4.2. Objectives

On balance, the evidence outlined above, provides convincing support for FGF20 having neuroprotective therapeutic potential in the treatment of PD. In the current Chapter, studies were carried out to further investigate the neuroprotective effects that FGF20 has on dopamine neurones in pre-clinical model systems. Additionally, it was also evaluated whether the endogenous FGF system plays a role in protecting nigrostriatal dopamine neurones, *in vivo*, against 6OHDA induced toxicity.

4.2.1. Objective 1. Evaluate if FGF20 Protects VM Embryonic Dopamine Neurones against 6OHDA Toxicity

In Chapter 2, using immunohistochemistry, FGFR1, 3, and 4 were demonstrated to be present in VM dopamine neurones, and others have shown FGF20 to protect VM embryonic dopamine neurones against serum withdrawal, glutamate toxicity, and 6OHDA. The first objective of the current study was to confirm results from the Murase & McKay, 2006 study which demonstrated FGF20 to protect VM dopamine neurones against 6OHDA, *in vitro*. A VM embryonic dopamine neurone culture system was established, and neuroprotection experiments carried out in the VM cultures with FGF20 to evaluate whether it is able to protect VM dopamine neurones against 6OHDA-induced dopaminergic cell loss.

4.2.2. Objective 2. Evaluate if FGF20 has Neuroprotective Effects on Dopamine Neurones in the Partially Lesioned 6OHDA Rat Model of PD

In Chapter 2, using immunohistochemistry, FGFR1, 3, and 4 were shown to be present in nigrostriatal dopamine neurones in the adult rat brain. Thus far, there are, however, no published studies that have investigated whether FGF20's neuroprotective effects on dopamine neurones are also present, *in vivo*, in animal models of PD. In the current study it was, therefore, evaluated if FGF20 is able to protect nigrostriatal dopamine neurones in the partially lesioned 6OHDA rat model of PD. In a previous study carried out in our laboratory, a supra-nigral bolus injection of FGF20 failed to protect nigrostriatal dopamine neurones from 6OHDA (unpublished findings). The temporal pattern in which growth factors activate their receptors often plays an important role in determining their biological effects. In order to effectively mediate their neurotrophic actions some neurotrophins, for example, need to stimulate their receptors continuously

rather than intermittently (Peterson & Nutt, 2008). In the current study, it was evaluated whether FGF20 has neuroprotective effects on dopamine neurones in the partially lesioned 6OHDA rat model of PD when continuously delivered to the SN by osmotic mini-pumps over a more chronic time-period. The partially lesioned 6OHDA rat model of PD that was used in this study was the one that was established in Chapter 3, in which a 4µg intra-nigrally delivered dose of 6OHDA induced an optimal ~60-80% nigrostriatal lesion.

In the *in vivo* neuroprotection study, FGF20 was chronically delivered directly to the substantia nigra of rats over the course of 7 consecutive days with the use of osmotic mini-pumps. As these mini-pumps were implanted subcutaneously in the rats, the as yet undelivered FGF20 treatment reserve solutions were kept at ~37°C for the course of the 7 day delivery period. An *in vitro* stability study was, therefore, carried out with the aim of determining how long FGF20 retains its biological activity when kept in solution at 37°C.

4.2.3. Objective 3. Evaluate whether the Endogenous FGF System Plays a Role in Protecting Nigrostriatal Dopamine Neurones against 6OHDA Toxicity in the Rat

The FGF system plays an important physiological role in both the developing and the intact adult nigrostriatal dopaminergic system. A number of the FGF family members and all of the FGFRs are present in the nigrostriatal tract (***detailed in section 2.1.5 and Chapter 2***). Evidence from a number of studies have indicated that one of the main roles of the endogenous FGF system in the nigrostriatal tract is to stimulate and maintain the survival of dopamine neurones. In embryonic VM cultures, the FGFs stimulate the survival of dopamine neurones, and in the adult rat, downregulation of FGFR1 in dopamine neurones causes a partial degeneration of nigrostriatal dopamine neurones (***detailed in section 4.1.2***). Moreover, there is also convincing indirect evidence indicating that the endogenous FGF system acts to protect the nigrostriatal tract against 6OHDA induced dopamine neurone cell death. 6OHDA lesioning of the nigrostriatal tract causes a robust upregulation of FGF2 at all levels of the nigrostriatal tract, and exogenous administration of FGF2 protects dopamine neurones against 6OHDA toxicity both *in vitro*, and in animal models of PD (***detailed in section 4.1.4***). It is, thus, likely that the increased endogenous production of FGF2 stimulated by 6OHDA lesioning would also have a protective effect on the toxin exposed dopamine neurones in a similar manner as when exogenous FGF2 is applied. Moreover, evidence

from biochemical and genetic studies in humans have indicated that dysfunctioning of the FGF system might play a role in the aetiology of PD. FGF2 protein is nearly completely absent in the SNc of PD patients (Tooyama *et al.*, 1994), and a number of FGF20 SNPs have been found to be associated with an increased risk of PD (***detailed in section 4.1.5***).

In the current study, experiments were carried out to evaluate whether the endogenous FGF system does, indeed, play a role in protecting nigrostriatal dopamine neurones by evaluating whether chronic pharmacological inhibition of FGFR signaling potentiates 6OHDA-induced nigrostriatal dopamine neurone degeneration in the rat. Partial 6OHDA nigrostriatal lesions were induced in rats, and it was evaluated whether chronic systemic administration of the FGFR inhibitor, PD173074 was able to potentiate the nigrostriatal degeneration induced by the partial 6OHDA lesion.

4.3. Methods

4.3.1. Neuroprotection Studies in Ventral Mesencephalic Embryonic Dopamine Neurone Cultures

4.3.1.1. Preparation of VM Cultures

VM cultures were prepared from rat embryos using the same protocol detailed in ***section 2.3.2***.

4.3.1.2. Immunohistochemical Characterisation of the VM Cultures

Immunohistochemical experiments were carried out to quantify the percentage of total cells in the VM cultures that were neurones, dopaminergic neurones, or GABAergic neurones. In these experiments neuronal nuclei (NeuN), TH, and glutamate decarboxylase-67 (GAD67) were used as markers of neurones, dopaminergic neurones, and GABAergic neurones, respectively. Additionally, VM cultures were also stained for glial fibrillary acidic protein (GFAP), a marker of astrocytes, in order to determine whether astrocytes are present in the VM cultures.

Naive days *in vitro*-6 (DIV6) VM cultures were PFA fixed. DMEM FBS+ media was removed from the cultures, after which the cultures were washed with TBS, and then fixed by incubating the cultures in ice cold 4% PFA (dissolved in D-PBS, pH7.6) for 10min at RT. The PFA-fixed cell cultures were washed with TBS and the cultures then incubated for 10min in a 3% hydrogen peroxide solution (dissolved in H_2O) to inactivate any endogenous peroxidase activity. Thereafter, cultures were washed with TBS, and incubated in blocking/permeabilisation buffer (1% BSA, 10% NaAz, and 0.1% Tween20 dissolved in 0.5M TBS, pH7.6) for 10min to block non-specific binding sites and also to permeabilise cell membranes. To detect NeuN, TH, GAD67, and GFAP, VM cultures were then incubated with rabbit polyclonal anti-NeuN (Millipore, ABN78, 1/5000), anti-TH (Chemicon, AB152, 1/1000), anti-GAD67 (Santa Cruz Biotechnology, sc-28376, 1/500), and anti-GFAP (DAKO, Z0334, 1/1000) primary antibody overnight at RT, respectively. Thereafter, cultures were washed with TBS to remove any unbound primary antibody. In all cases, cultures were then incubated with a donkey anti-rabbit biotinylated secondary antibody (Vectorlabs, BA-1000, 1/200) for 1h at RT. Finally, staining was then visualised with the HRP/DAB/ABC method and the stained coverslips mounted onto glass microscope slides with DPX using the same

protocol as described in ***section 2.3.3.2***. The only exception is that the procedure was carried out on the VM coverslips rather than brain sections.

To calculate the percentages of NeuN+, TH+, and GAD67+ cells that were present in the immunostained cultures, digital images of the immunostained coverslips were taken at 10x magnification at 10 randomly selected areas on each of the coverslips using a Zeiss light microscope fitted with an Axiocam colour camera. The total number of positive cells and haematoxylin stained nuclei present in the 10 images were then quantified using ImageJ image analysis software. The percentage of the total number of cells present in the cultures that were positive for the different markers were then calculated by dividing the total number of cells on an immunostained coverslip that were positive for a specific antigen by the total number of haematoxylin stained nuclei present in the same coverslip. The percentage total cell values generated for each of the different markers was derived from one coverslip.

4.3.1.3. FGF20 Neuroprotection Experiments in the VM Cultures

FGF20 (100 and 500ng/ml) or FGF20's vehicle (DMEM Glutamax serum free media containing 10ng/ml rat serum albumin) treatments were freshly prepared and applied to the VM cultures on DIV6 for 24h, with all treatments being applied as 500µl volumes to each individual coverslip. Immediately after the FGF20 treatment period, on DIV7, the FGF20 treatment solutions were removed, and the cells were then exposed to either 6OHDA (40, 50, or 60µM depending on the sensitivity of the culture, see paragraph below for more details) or 6OHDA's vehicle (serum free media containing 0.02% ascorbic acid) for 4h. Final 6OHDA concentrations were applied to the cultures by adding 50µl of a 10x more concentrated 6OHDA stock solution directly to 450µl of serum free media previously added to each well. All the stock concentrations of 6OHDA were dissolved in a 0.2% ascorbate solution (dissolved in PBS, pH7.6) to limit the inactivation of 6OHDA by auto-oxidation. At the end of the 6ODHA exposure period, the 6OHDA treatment solutions were replaced with normal FBS+ media. The cells were then kept in FBS+ media until the morning of DIV8, at which point they were fixed. The DMEM FBS+ media was removed from the cultures, after which the cultures were washed with D-PBS, and then fixed by incubating the cultures in ice cold 4% PFA (dissolved in D-PBS, pH7.6) for 10min. Thereafter, the PFA solution was removed, and the cultures washed with D-PBS to remove all traces of the PFA.

In preliminary 6OHDA dose response experiments, different VM culture preparations were found to have varying sensitivities to 6OHDA toxicity. After carrying out a number of repeat experiments, it was determined that depending on the sensitivity of the culture, a dose of between 40-60µM 6OHDA induced an ~50-80% reduction in VM TH+ cell numbers. To accommodate for this variability in sensitivity to 6OHDA, all FGF20 neuroprotection experiments were carried out in parallel in cells treated with either a 40, 50 or 60µM concentration of 6OHDA. Results from only the 6OHDA concentration groups that caused ~50-80% of cell death were then selected for inclusion in analyses.

4.3.1.4. Immunocytochemical Staining of the VM Cultures for TH and Quantification of TH+ Neurones

The PFA-fixed VM cultures were immunocytochemically stained for the dopamine neurone marker, TH using the HRP/DAB ABC indirect staining method. Coverslips were immersed for 10min in a 3% H_2O_2 solution (dissolved in dH_2O) to inactivate any endogenous peroxidase activity present in the cultures. The hydrogen peroxide solution was removed, the cultures washed with TBS, and the cultures were then incubated in blocking/permeabilisation buffer (1% BSA, 10% NaAz, and 0.1% Tween20 dissolved in 0.5M TBS, pH7.6) for 10min to block non-specific binding sites and also to permeabilise cell membranes. The blocking solution was removed, and the cultures incubated overnight in rabbit anti-TH primary antibody (Chemicon, AB152, 1/1000) at RT. Thereafter, the primary antibody solution was removed, the cultures washed with TBS, and the cultures were then incubated for 2h in secondary biotinylated goat anti-rabbit secondary antibody (Vectorlabs, BA-1000, 1/200) at RT. In all cases, staining was then visualised with the HRP/DAB/ABC method and the stained coverslips mounted onto glass microscope slides with DPX using the same protocol as described in ***section 2.3.3.2***. The only exceptions are that the procedure was carried out on the VM coverslips rather than brain sections, and the cultures in this study were not counterstained with haematoxylin.

To quantify the total number of TH+ dopamine neurones that were present in each of the VM culture coverslips, images of the entire TH immunostained coverslips were taken at 10x magnification using a Zeiss light microscope fitted with an Axiocam colour camera. The total number of TH+ neurones on each coverslip was then counted blind using the image analysis program, ImageJ. For each treatment group, mean

(±sem) TH+ cell count values were derived from results from 3 independent repeat experiments, and in each repeat experiment, each treatment group comprised of 3-5 coverslips. Mean TH+ cell count results were analysed with a one way ANOVA and Bonferroni post hoc tests. In these analyses, it was evaluated whether TH+ cell counts were significantly different in any of the treatment groups compared to control, or whether cell counts in the FGF20 + 6ODHA treatment groups were significantly different from that in the vehicle + 6OHDA treatment group.

4.3.2. Neuroprotection Studies with FGF20 in the Partially Lesioned 6OHDA Rat Model of Parkinson's Disease

4.3.2.1. Animals

Male Sprague Dawley rats were sourced and maintained exactly as described in ***section 3.3.1.1***.

4.3.2.2. Preparation of Osmotic Mini-pumps and Brain Cannulae for Implantation

In the *in vivo* FGF20 neuroprotection study, experiments were carried out to investigate whether FGF20 is capable of protecting nigrostriatal dopamine neurones against a partial 6OHDA lesion when it is chronically delivered directly to the substantia nigra of the rats. The chronic supra-nigral FGF20 infusions were delivered by subcutaneously implanted osmotic mini-pumps that were connected to chronically implanted supra-nigral brain infusion cannulae. Special dual-barrelled brain cannulae were used, which were composed of two cannulae embedded immediately adjacent to one another in a single plastic support mould. One of the two cannulae served as a regular guide cannula (26G) through which an injection needle could be inserted to deliver an intra-nigral infusion of 6OHDA, while the second cannula served as an infusion cannula (30G) to which an osmotic pump containing a FGF20 treatment solution could be connected. Three different FGF20 treatment groups were included in the study, a FGF20 vehicle group, a 1µg/day FGF20 group, and a 2.5µg/day group, and Alzet 1007D osmotic mini-pumps (Alzet Osmotic Pumps, DURECT Corporation, Cuperto, US) were used to deliver the treatments. The 1007D osmotic pump model delivers treatment solutions continuously at a rate of 0.5µl/hr over a period of 7 days. For the 1µg/day and 2.5µg/day treatment groups, the mini-pumps were, thus, filled with solutions containing FGF20 at a concentration of 83.4ng/ml, and 208ng/ml, respectively. The two different

FGF20 concentrations were freshly prepared by dissolving lyophilised FGF20 powder (Peprotech Inc., NJ, US) in an aCSF vehicle solution (148mM NaCl, 3mM KCl, 1.4mM CaCl2, 0.8mM MgCl2, 1.5mM HPO4, 0.2mM NaH2PO4, pH7.4) to which 100ng/ml of rat serum albumin was added to act as a carrier protein for FGF20 (hereafter referred to as FGF20 vehicle). For the vehicle group, mini-pumps were filled with FGF20 vehicle solution only. All of the mini-pumps were filled with 84µl of freshly prepared treatment solution, and a metal flow moderator tube was then inserted into the outflow channel of the pumps. Prior to filling the pumps, ~5cm lengths of plastic PVC-60 tubing (ID=0.72mm, PlasticsOne tubing obtained from Bilaney Consultants Ltd., UK, Kent) were firmly connected to the osmotic pump infusion cannulae of all of the dual-barrelled cannulae. An appropriate FGF20 treatment solution was then flushed through the tubing until the entire piece of tubing and also the attached osmotic pump infusion cannula were completely filled with the solution. Thereafter, the remaining free end of the PVC tubing filled with treatment solution was then connected to an appropriate osmotic mini-pump by fitting it over the flow moderator tube of the mini-pump. At this point, the osmotic mini-pump/infusion cannulae sets were ready for implantation. All of the above steps were undertaken under sterile conditions.

4.3.2.3. Implantation of the Osmotic Pump/Brain Cannulae Sets

Using stereotaxic surgery, the dual cannulae were implanted unilaterally at a supra-nigral location in the brain of the rats. The dual-cannulae were implanted at coordinates which resulted in the tip of the osmotic pump infusion cannula being positioned ~2mm directly above the substantia nigra (AP, +3.7; ML, +2.0; DV, +2.6, relative to the interaural line (Paxinos & Watson, 1993)). As the guide cannulae on the dual-cannulae were positioned directly adjacent to the osmotic pump infusion cannulae, the guide cannulae were also positioned supra-nigrally at the implantation coordinates used. The tip of the guide cannulae, however, only extended 2mm into the brain, as the guide cannulae only served as an entrance site for an injection needle through which an intra-nigral infusion of 6OHDA could be delivered at a later time-point.

The following procedure was used to implant the rats with the dual-cannulae and the osmotic mini-pumps that accompanied each of the cannulae. A brain cannula – along with the osmotic mini-pump that was connected to it - was fastened onto a guide cannulae holder, which was, in turn, fitted to a stereotaxic frame. The inter-aural line was used as a reference point to calculate the coordinates at which each of the cannulae

had to be implanted at. The osmotic pump infusion cannulae were, therefore, positioned so that their tips were located right in the centre of the tapered point of an ear bar that had been tightened in place on the stereotaxic frame. Once the AP and DV co-ordinates of the inter-aural line were recorded, rats were anaesthetised with a mixture of ketamine (75mg/kg, i.p.) and medetomidine (0.5 mg/kg, i.p.). Rats were mounted in the stereotaxic frame after shaving their scalps. Their scalps were disinfected with ethanol and povidone-iodine (Betadine), and a midline incision made in the scalp after checking for the absence of a hind-limb withdrawal response. The cranium was fully exposed using retractors, and the peri-cranial membrane scraped away with a scalpel blade. The tips of the osmotic pump infusion cannulae were then aligned with the midline of the rat's skull, and the midline coordinates recorded. The AP, DV, and ML starting coordinates were then used to calculate the coordinates at which the cannulae needed to be implanted. A burr hole was made in the cranium at the point where the cannulae had to be lowered into place, and the exposed meninges pierced. When any bleeding had ceased, the cannulae were then lowered slowly into the brain until the tips of the cannulae were located at the desired DV coordinates (see above for coordinates). Two support screws were then screwed into place in locations immediately to the front and side of the cannulae. The implanted cannulae were then secured in place by encasing the support screws and cannulae together in a single mound of dental cement. After the dual-cannulae were successfully implanted, the osmotic mini-pumps that were connected to the implanted cannulae were implanted subcutaneously on the rostral hindback of the rat. Using the rostral end of the incision site on the skull as an entry point, a subcutaneous cavity was created in the rostral hindback of the rat with a blunt dissection scissor. The osmotic mini-pumps were then inserted into the cavity, and once the pumps were in place, the rats were removed from the stereotaxic frame. ~2-3 sutures were then inserted on either side of the implanted cannulae, so that the skin firmly enclosed the implanted cannulae, its cement encasing, and also the vinyl tubing connecting it to the osmotic pumps. Only small openings were left in the skin to allow access to the guide cannulae, and through this opening, metal stilettes were inserted into the guide cannula to maintain their patency. Rats were then administered with an atipamezole (1mg/kg, s.c.) injection to reverse the anaesthesia, and placed in a heated environment until recovery. Rats were given a saline injection (1ml, s.c.) to aid rehydration, and were maintained on a mashed food diet for 3 days post-surgery, or until rats started maintaining a healthy weight. A total of 26 rats were used in these

experiments, with 6 rats being used in both the 1µg/day and 2.5µg/day FGF20 groups, while 10 rats were used in the vehicle treated 6OHDA lesioned group.

4.3.2.4. Partial Unilateral Lesioning of the Nigrostriatal Tract with 6OHDA

One day after implantation of the supra-nigral cannulae and the connected mini-pumps, the nigrostriatal tracts of the rats were partially lesioned with 4µg intra-nigral 6OHDA infusions. The implanted osmotic mini-pumps commenced the supra-nigral delivery of their loaded FGF20 treatment solutions at their maximal 0.5µl/hr rate as soon as they had been heated to ~37°C. The lesions were, thus, carried out after the rats had been pre-treated for 1 day with the different FGF20 treatments. 30min before the 6OHDA infusions were delivered, the rats were pre-treated with the noradrenaline reuptake inhibitor, desipramine (25 mg/kg i.p.), and MAO-B inhibitor, pargyline (5 mg/kg i.p.) as previously described in ***section 3.3.1.2***. Under isoflurane anaesthesia, 4µg 6OHDA infusions were then delivered directly into the substantia nigra's of the rats. A 5µl Hamilton micro-syringe was mounted onto an automated micro-infusion pump, and the tip of the syringe connected to a length of vinyl tubing which was, in turn, connected to a 33G stainless steel injection needle. The injection needle and the length of tubing to which it was connected, were then filled with 5µl of a 1µg/µl 6OHDA solution. The 6OHDA solution was freshly prepared on the day of the lesioning, and it was dissolved in a 0.02% ascorbic acid solution, kept on ice, and wrapped in foil, all to minimise the inactivation of 6OHDA through auto-oxidation. The injection needle loaded with 6OHDA solution was then inserted into the brains of the rats through the supra-nigrally positioned guide cannulae, and an intra-nigral (AP, +3.7; ML, +2.0; DV, +2.2, relative to the inter-aural line, (Paxinos & Watson, 1993)) 6OHDA (4µg 6OHDA dissolved in 4µl of vehicle) infusion was then delivered at a flow rate of 2µl/min. The injection needle was left in place for 4min after the infusion had finished, after which the needle was removed, and the rats were then allowed to recover from the anaesthesia in a heated environment.

4.3.2.5. Measuring Motor Deficits with the Cylinder Test

In Chapter 3, both the cylinder test and the amphetamine rotation test were identified as being appropriate motor tests to use in the *in vivo* neuroprotection study due to them having sufficient sensitivities to detect motor deficits in partially lesioned rats.

However, because the project licence that was used for the experiments in Chapter 3 did not permit the implantation of osmotic mini-pumps, the *in vivo* neuroprotection experiments in this chapter were carried under a different project licence that included the later procedure, but not the amphetamine induced rotation test. For this reason, only the cylinder test was used to measure motor function in this study. Motor function was measured using the cylinder test 3 days (acclimatisation session) and 2 days (baseline measurements) prior to 6OHDA lesioning, and on day 5, 8, and 11 post-lesioning according to exactly the same protocol used in ***section 3.3.2.1***. Cylinder test results were also analysed in the same manner as described in the latter section, with the only exception being that the results in this study were analysed to determine whether ipsilateral forelimb use was significantly different in any of the FGF20 dose groups compared to the vehicle treated 6OHDA lesioned group at each of the time-points.

4.3.2.6. Quantification of Nigrostriatal Tract Lesions using TH Immunohistochemistry

On day 12 post-lesioning, rats were intra-cardially PFA perfusion fixed and the degree of nigrostriatal degeneration present in each of the different groups was then quantified with TH immunohistochemistry using exactly the same protocols as employed in ***section 3.3.3***. TH immunohistochemistry results were analysed in exactly the same manner as in ***section 3.3.3.3.3***, with the only exception being that the results in this study were analysed to determine whether striatal % TH immunoreactivity levels and nigral TH+ cell counts in the FGF20 dose groups were significantly different to the vehicle treated 6OHDA lesioned group.

4.3.3. FGF20 Stability Study

In the FGF20 stability study, ERK1/2 phosphorylation assays were carried out in PC12 cells to determine how long FGF20 retains its biological activity in solution when kept at 37°C. ERK1/2 activation was used as a measure of FGF20's biological activity in this study as FGF20 was found to stimulate ERK1/2 phosphorylation in PC12 cells in preliminary experiments.

4.3.3.1. Maintenance of PC12 cells

A PC12 cell line was obtained from Prof. Britta Eickholt (King's College London), and the cells cultured according to the following protocol. The PC12 cells were grown in 75cm^2 filter-capped plastic NunC tissue culture flasks in FBS+ DMEM media (DMEM Glutamax media supplemented with 10% FBS, 100 units of penicillin, and 100g/ml of streptomycin). The cells were grown in a cell culture incubator under standard conditions, 37°C, 95% humidity, and 5%CO_2. When cells reached a confluency of ~80-100%, the cells were diluted and split into a new flask(s) to yield cultures with ~5x lower densities. To split the cells, the DMEM FBS+ media in which the cells were bathed in was removed, and the cells washed 2x in ~5ml sterile D-PBS solution, and the cells detached with trypsin. 1ml of trypsin solution (0.05% trypsin dissolved in EDTA) was added to each 75cm flask, and the cells left to incubate in the trypsin solution for 5-10min. The flasks were agitated to dislodge any remaining attached cells, and 4ml of DMEM FBS+ media added to each flask to inactivate trypsin's enzymatic activity. The diluted cell suspension was tritriated thoroughly, and 1ml of the suspension transferred into a new tissue culture flask. ~12ml of DMEM FBS+ media was added to the new flask, and the solution swirled around thoroughly to ensure the cells are evenly distributed throughout the flask. The flask containing the diluted cell suspension was then placed back into the cell culture incubator. The cells were then left to grow again until they reached ~80-100% confluency, at which point they were either used in experiments, or split again. Around 2x every week old media was removed and replaced with fresh media.

4.3.3.2. Preparation and Handling of FGF20 Stock Solution

A FGF20 test stock solution was prepared fresh from stock powder at the same concentration (208ng/µl) as that used for the highest dose group in the *in vivo* neuroprotection study. The FGF20 solution was made up in a sterile eppendorf tube, and it was dissolved in exactly the same aCSF vehicle solution (148mM NaCl, 3mM KCl, 1.4mM CaCl2, 0.8mM MgCl2, 1.5mM HPO4, 0.2mM NaH2PO4, 100ng/ml rat serum albumin, pH7.4) used in the *in vivo* neuroprotection study. The ability of the FGF20 test solution to stimulate ERK1/2 phosphorylation in PC12 cells was then measured immediately after the solution was freshly prepared (D0 measurements). Thereafter, the test solution was kept in an incubator at 37°C, and the ability of the

FGF20 solution to stimulate ERK1/2 activation was then tested daily over the course of the following 7 consecutive days using the protocol detailed in the following sections.

4.3.3.3. Application of FGF20 to PC12 cells at each of the Time-Points

PC12 cells were grown in 75cm^2 tissue culture flasks in FBS+ DMEM media until they were ~80-100% confluent. At this point, the FBS+ media was removed from the flasks, and replaced by FBS- DMEM media, in which the cells were kept in overnight. FBS contains a number of different exogenous growth factors, many of which are likely to stimulate ERK1/2 phosphorylation in the PC12 cells. The cells were, therefore, kept in serum free media overnight, so that the lowest possible baseline ERK1/2 phosphorylation levels could be achieved in the un-stimulated cultures. After the overnight serum withdrawal period, the FBS- DMEM media was removed from the flasks. A 200ng/ml FGF20 solution - previously prepared from the same test stock FGF20 solution that was kept at 37°C – was then applied to the flask of PC12 cells for 5min. A 200ng/ml concentration of FGF20 was shown in preliminary ERK1/2 phosphorylation studies to represent a supra-maximal FGF20 concentration. To generate un-stimulated baseline (control) ERK1/2 phosphorylation measurements, on day 0, a FBS- solution containing only FGF20's vehicle was added to a separate flask of serum-starved PC12 cells for 5min. In all cases, FGF20 was dissolved in serum free DMEM media, and FGF20 and control treatments were delivered as 5ml volumes to each flask.

4.3.3.4. Preparation of Cell Lysates from the Stimulated PC12 Cells

In all cases, immediately after the application of the last test treatment, the treatment solutions were removed from the flasks, and 250µl of lysis buffer added to each flask to lyse the cells. Each ~250µl of lysis buffer consisted of 200µl of RadioImmunoPrecipitation Assay (RIPA) buffer to which 50µl of phosphatase inhibitor stock solution (phosphatase inhibitor set 3, Calbiochem), and 2.5µl of protease inhibitor stock solution (protease inhibitor set 1, Calbiochem) was added. The flasks were then kept on ice for 10min and agitated at intervals during this period to ensure all the cells in the flasks were completely lysed. The cell lysate in each of the flasks were then thoroughly mixed by trituration, and 400µl of the cell lysate was then pipetted into appropriately labelled ependorf tubes. 100µl of loading buffer (4% SDS, 10% 2-

mercaptoethanol, 20% glycerol, and 0.004% bromophenol blue dissolved in 0.125M Tris HCl buffer) was added to each 400µl cell lysate sample, and the resulting solution mixed thoroughly and heated for 10min at 95°C. The cell lysate samples were then stored at -20°C in the freezer.

4.3.3.5. Quantification of ERK1/2 Phosphorylation using Western Blot Analyses

The level of ERK1/2 activation stimulated by each of the different treatments was quantified in Western blot experiments. The cell lysate samples were thawed, and the proteins in the samples separated according to molecular weight with sodium dodecyl sulphate polyacrylamide gel (SDS-PAGE) electrophoresis. SDS-PAGE gels were freshly prepared in gel moulds so as to contain an ~2cm stacking gel (3% polyacrylamide, 10%SDS, and 10% APS) positioned on top of a larger ~5cm separating gel (10% polyacrylamide, 10% SDS, and 10% APS). The gels were mounted into an electrophoresis tank, and the tank filled with running buffer (0.2M glycine and 10%SDS dissolved in 0.25M TBS, pH7.6). 20µl of each of the different cell lysate samples were then loaded into the gel wells. 4µl of molecular weight marker solution (RPN800E full-range colour molecular weight markers, GEHealthcare) was also loaded into one of the remaining empty wells in the same gel. The samples were then run firstly for 20min at 120V in order to line up the protein samples at the top of the separating gel, and then for a further ~90min at 160V until the dye wavefront diffused out of the gel. After removing the gels from the tanks, the stacking gel portion of the gel was discarded, while the separating gel containing the separated protein samples were immersed and agitated in transfer buffer solution (0.2M glycine and 20% methanol dissolved in 0.25M TBS, pH7.6) for 10min. Pieces of nitrocellulose membrane were soaked in dH_2O for 5min to activate them, and thereafter soaked for a further 5min in transfer buffer. The nitrocellulose membrane and acrylamide gel were then layered on top of one another and sandwiched together between layers of blotting paper in a transfer cassette. The transfer cassette was inserted into an electrophoresis tank together with an ice pack, and the tank filled with transfer buffer. Finally the proteins were transferred out of the gel and onto the nitrocellulose membrane by running the transfer for ~60min at 160V. After this, the nitrocellulose membranes containing the separated protein samples were retrieved from the transfer cassettes and washed for 10min in a TBS-Tween solution (0.1% Tween-20 dissolved in 0.25M TBS, pH7.6).

The phospho-ERK1/2 protein bands that were present on the membranes were visualised and quantified using an indirect immunofluorescence method utilising fluorescent secondary antibodies and an Odyssey infrared fluorescence imager. To block non-specific binding sites, the membranes were immersed and agitated in a blocking solution (5% low fat milk powder, 0.1%Tween-20, 0.25M TBS, pH7.6) for 1h at RT. The milk blocking solution was removed, and the membranes incubated overnight in the fridge with a rabbit polyclonal anti-phospho-p44/42 (phospho-ERK1/2) primary antibody (Cell Signalling, 4370, 1/10000) solution made up in blocking solution. The membranes were then washed 3x with a TBS-Tween wash solution (0.1%Tween-20, 0.25M TBS, pH7.6) to remove any excess unbound primary antibody. In all of the Western blot experiments, the housekeeping protein, Glyceraldehyde-3-phosphate dehydrogenase (GAPDH) was used as a loading control. Membranes were, thus, next incubated with mouse anti-GAPDH primary antibody (Abcam, ab9484, 1/5000) for 1h at RT. Membranes were again washed 3x in TBS-Tween, and the membranes then incubated simultaneously with IRDye-800CW goat anti-mouse (Licor Biosciences, 926-32210, 1/1000) and IRDye 680LT donkey anti-rabbit secondary (Licor Biosciences, 926-32212, 1/1000) antibodies for 1h at RT. Membranes were washed 3x with TBS-Tween, and the phospho-ERK1/2 and GAPDH bands were then visualised using a Odyssey Li-COR infrared fluorescent imager (Licor Biosciences). The approximate molecular weight of each of the bands on a membrane was estimated by reference to the MW ladder, and used to determine the identity of each band. GAPDH has a predicted MW of ~40kDa, and the bands with a MW of ~40kDa, ~42kDa, and ~44kDa were, thus, taken to represent the bands for GAPDH, phospho-p42, and phospho-p44, respectively. Band densities were quantified using a tool in the Odyssey application software. The density measurement tool allows you to highlight a specific band of interest, and it then automatically generates the optical density measurement for the selected band. All phospho-ERK1/2 band density measurements were normalised by dividing the density measurements of each phospho-ERK1/2 band by the density measurement of the corresponding GAPDH band.

4.3.4. Studies to Evaluate Whether Pharmacological Inhibition of the FGFRs is able to Potentiate 6OHDA Induced Nigrostriatal Degeneration in the Rat

In this study experiments were carried out to investigate whether the selective FGFR inhibitor, PD173074 is able to potentiate the nigrostriatal dopamine neurone degeneration and/or motor deficits induced by a partial 6OHDA lesion when it is administered chronically by s.c. injections.

4.3.4.1. Animals

Male Sprague Dawley rats were sourced and maintained exactly as described in ***section 3.3.1.1***.

4.3.4.2. Chronic Subcutaneous Administration of PD173074

Three groups of rats were dosed daily for 8 days with either PD173074's vehicle (10%DMSO, 10%PEG200 dissolved in PBS, pH7.6, s.c), or with one of two doses of PD173074 (1mg/kg or 2mg/kg, s.c, dissolved in vehicle). The daily PD173074 treatments were started 3 days prior to 6OHDA lesioning, and continued for 5 consecutive days thereafter. The PD173074 treatment solutions were prepared fresh each day under sterile conditions. A total of 26 rats were used in these experiments, with 8 rats being used in both the vehicle and 1mg/kg PD173074 groups, while 7 rats were used in the 2mg/kg PD173074 group.

4.3.4.3. Partial Unilateral 6OHDA Lesioning of the Nigrostriatal Tract of the PD173074 Treated Rats

Three days after the daily PD173074 injections had commenced, and on the fourth PD173074 treatment day, the nigrostriatal tract of the rats were partially lesioned with a 4µg intra-nigral 6OHDA infusion using nearly exactly the same protocol as described in **section 3.3.1.3**. The only exception is that rather than infusing the rats with vehicle or a range of 6OHDA doses, all rats received a 4µg intra-nigrally delivered dose of 6OHDA in the current study. On day 6 post-lesioning, rats were administered with an overdose of pentobarbital, and intra-cardially perfusion fixed with PFA (ice cold 4% PFA dissolved in 0.9% NaCl, pH 7.6).

4.3.4.4. Measurement of Motor Deficits in the PD173074 treated 6OHDA Lesioned Rats using The Adjusted Stepping and The Cylinder Test

Motor function was measured using both the cylinder test and the adjusted stepping test according to exactly the same protocols as used in ***section 3.3.2.1*** and ***section 3.3.2.2***, respectively. Both tests were carried out 2 days (acclimatisation session) and 1 day (baseline measurements) before the PD173074 injections started, and on day 3 and 5 post-lesioning. Cylinder test and adjusted stepping test results were analysed in the same manner as described in ***section 3.3.2.1*** and ***section 3.3.2.2***, respectively, with the only exception being that the results in this study were analysed to determine whether motor deficits were significantly different in any of the PD173074 dose groups compared to the vehicle treated 6OHDA lesioned group at each of the time-points.

4.3.4.5. Measurement of Amphetamine-Induced Rotational Behaviour in the PD173074 treated 6OHDA Lesioned Rats

Amphetamine-induced rotations were measured on day 6 post-lesioning using exactly the same protocol as described in ***section 3.3.2.3***. Results were also analysed in nearly exactly the same manner as in the latter section, with the only exceptions being that peak net ipsiversive rotations were calculated for a 45min time-period, and results were analysed to determine if peak net ipsiversive rotations in the PD173074 dose groups were significantly different to the vehicle treated 6OHDA lesioned group.

4.3.4.6. Quantification of Nigrostriatal Tract Lesions using TH Immunohistochemistry in the PD173074 Treated Rats

On day 7 post-lesioning, rats were intra-cardially PFA perfusion fixed and the degree of nigrostriatal degeneration present in each of the different groups was then quantified with TH immunohistochemistry using exactly the same protocols as employed in ***section 3.3.3***. TH immunohistochemistry results were analysed in exactly the same manner as in the latter section with the only exception being that the results in this study were analysed to determine whether striatal TH levels and nigral TH+ cell counts in the PD173074 dose groups were significantly different to the vehicle treated 6OHDA lesioned group.

4.3.5. Drugs and Chemicals

PD173074 was obtained from Tocris Bioscience Ltd (UK, Bristol). Rat serum albumin was purchased from Sigma Aldrich Ltd (UK, Dorset), and all other drugs and chemicals were obtained from the same suppliers detailed in ***section 3.3.5***, or from Sigma Aldrich Ltd. (UK, Dorset).

4.4. Results

4.4.1. Neuroprotection Study with FGF20 in VM Cultures

4.4.1.1. Immunohistochemical Characterisation of the Embryonic VM Cultures

VM embryonic cultures at DIV6 were immunohistochemically characterised to define the cell populations that made up the culture. NeuN, TH, GAD67, and GFAP were used as markers of neurones, dopamine neurones, GABAergic neurones, and astrocytes, and all of these cell types were found to be present in the cultures (***Fig 4.1***). Neuronal cells made up ~45% of the total population of cells present in the culture, with TH+ dopamine neurones and GAD67+ GABAergic neurones making up ~3.5%, and ~7.4% of the total cell population, respectively. Astrocytes were present in large numbers, and they were ubiquitously distributed throughout the whole culture.

Figure 4.1. Immunohistochemical Characterisation of a VM Culture Preparation used in Neuroprotection Experiments with FGF20

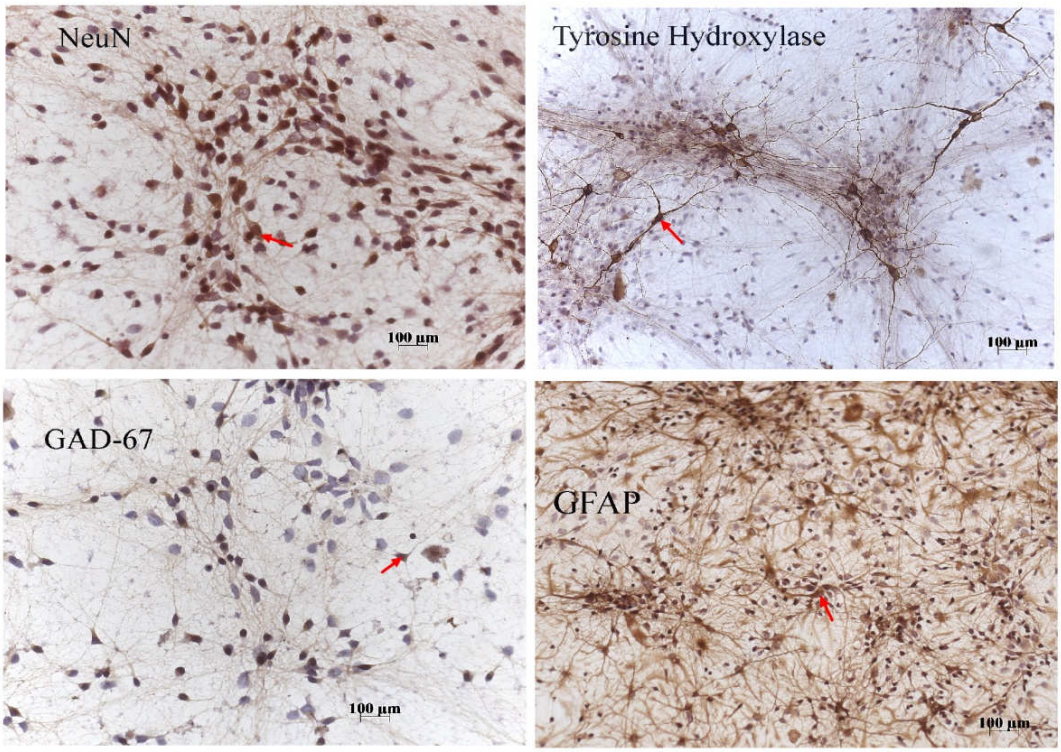

Figure 4.1. Immunohistochemical characterisation of the cell types present in a ventral mesencephalic (VM) embryonic dopamine neuron culture preparation used in neuroprotection experiments with FGF20. Cultures were fixed on DIV6, and stained for NeuN, TH, GAD-67, and GFAP, markers of neurones, dopamine neurones, GABAergic neurones, and astrocytes, respectively. All of the mentioned cell types were present in the cultures. Red arrows: Brown DAB immunostained positive cells. Blue: Haematoxylin stained nuclei.

4.4.1.2. FGF20 Protects VM Dopamine Neurones against 6OHDA Toxicity

FGF20 protected VM embryonic TH+ dopamine neurones against 6OHDA toxicity (***Fig 4.2***). The mean TH+ cell count in the control group was ~990, and in the vehicle + 6OHDA group, TH+ cell numbers were reduced to ~425, a cell count that was found to be significantly lower compared to the control group ($p<0.01$). In the 100ng/ml and 500ng/ml FGF20 + 6OHDA treatment groups, mean TH+ cell counts were preserved at ~850 and ~904, respectively. In the vehicle + 6OHDA group, TH+ cell numbers were, thus, reduced by ~67% relative to the control group. Both FGF20 concentrations provided a significant protection against this cell death ($p<0.05$), with TH+ cell counts only being reduced by ~15% and ~9% in the 100ng/ml and 500ng/ml FGF20 + 6ODHA treatment groups compared to control, respectively. Furthermore, in both the FGF20 treatment groups, TH+ cell numbers were preserved at control levels, as there was no significant difference between the number of TH+ cells present in both of the FGF20 treatment groups compared to the control group.

Figure 4.2. FGF20 Protects VM Dopaminerigc Neurones against 6OHDA Toxicity

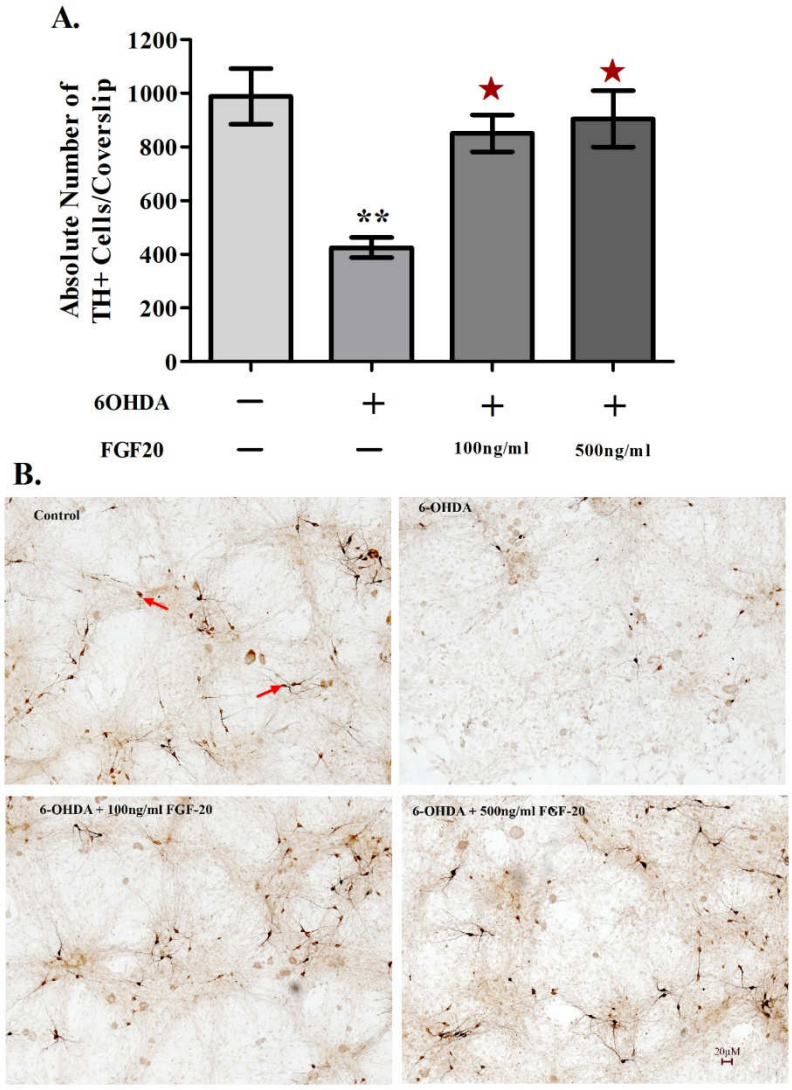

Figure 4.2. FGF20 concentration-dependently protected ventral mesencephalic (VM) embryonic dopamine neurones against 6OHDA toxicity (**A**). Cultures were treated with FGF20 for 24h on DIV6, exposed to 6OHDA (40-60µM, depending on culture sensitivity) for 4h on DIV7, and on DIV8, cultures were fixed and stained for tyrosine hydroxylase (TH), a marker of dopamine neurones. Data points represent mean±sem values calculated from data generated in 3 independent repeat experiments. 3-5 coverslips were used per treatment group in each of the independent experiments. **B.** Representative examples of TH immunostatined cultures from the different groups are shown at 10x magnification.**p<0.01 compared to control, and ★p<0.05 compared to 6OHDA + FGF20 Vehicle.

4.4.2. Neuroprotection Studies with FGF20 in the Partially Lesioned 6OHDA Rat

4.4.2.1. FGF20 Protects Nigrostriatal Dopamine Neurones against 6OHDA in Rats

Neuroprotection studies were carried out to evaluate if FGF20 is able to protect nigrostriatal dopamine neurones in the partially lesioned 6OHDA rat model of PD. Chronic supra-nigral infusions of FGF20 dose-dependently protected dopamine neurones against a partial nigrostriatal lesion induced by a 4µg intra-nigral 6OHDA infusion (***Fig 4.3 and 4.4***). The 2.5µg/day but not the 1µg/day FGF20 dose preserved both striatal TH levels (***Fig 4.3***) and nigral TH+ cell numbers (***Fig 4.4***) at significantly higher levels compared to the vehicle treated 6OHDA lesioned group.

In the vehicle treated 6OHDA lesioned group, striatal TH levels in the lesioned striatum was ~54% lower compared to the non-lesioned contralateral striatum, while in the 2.5µg/day group, striatal TH levels in the lesioned striatum was only ~33% lower vs. the contralateral striatum (***Fig 4.3***). Striatal TH levels were, thus, preserved at ~21% higher levels in the 2.5µg/day group compared to the vehicle treated 6OHDA group. Striatal TH levels in the 1µg/day FGF20 dose group was ~48%, levels equivalent to that in the vehicle treated 6OHDA lesioned group.

In the vehicle treated 6OHDA lesioned group, TH+ cell numbers were reduced by ~71% in the lesioned SNc compared to the non-lesioned contralateral hemisphere, while in the 2.5µg/day group nigral cell counts were reduced by only ~50% compared to the non-lesioned SNc (***Fig 4.4***). Nigral cell counts were, thus, preserved at ~18% higher levels in the 2.5µg/day treatment group compared the vehicle treated group. In the 1µg/day FGF20 group, nigral cell counts in the lesioned hemisphere were reduced by ~68% to levels equivalent to that present in the vehicle treated 6OHDA lesioned group.

Figure 4.3. FGF20 Preserves Striatal TH Levels in Partially 6OHDA Lesioned Rats

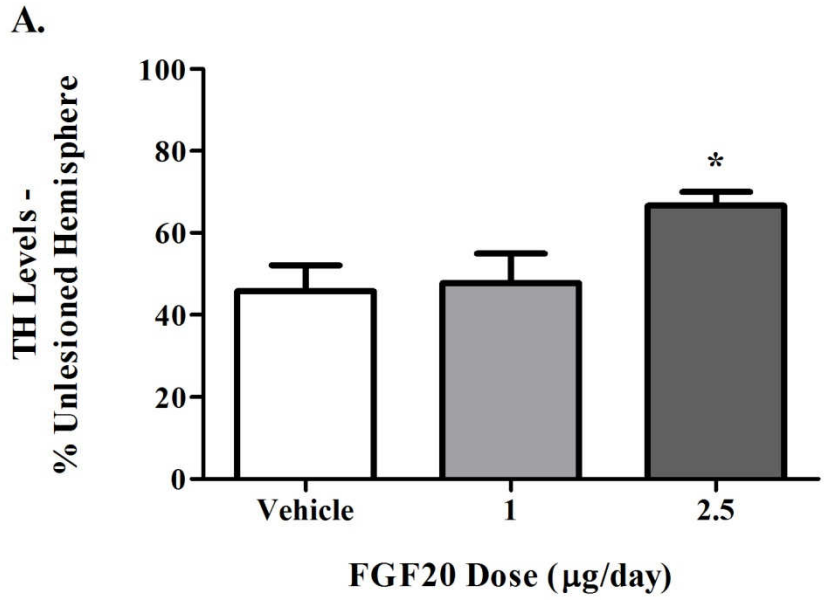

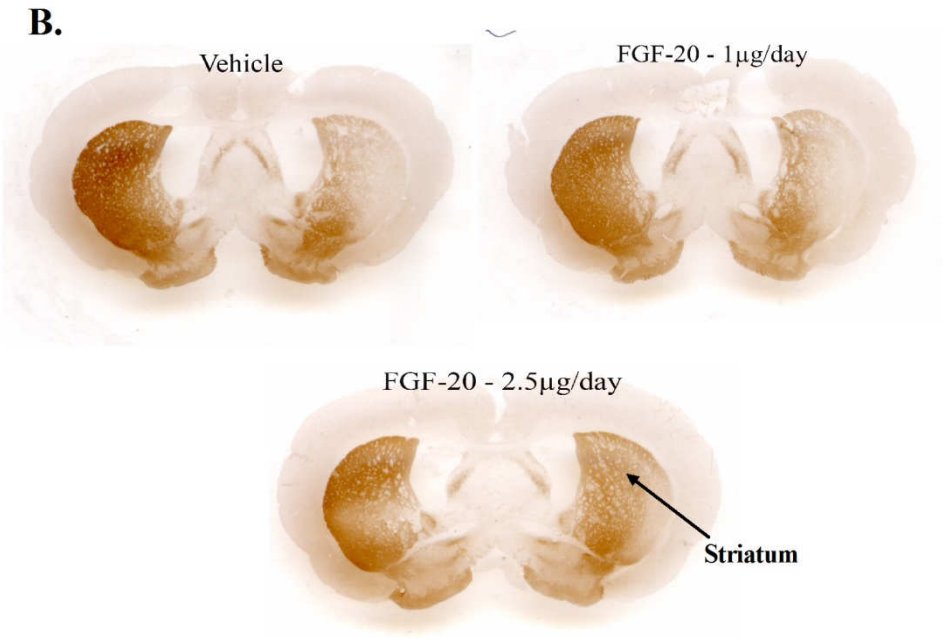

Figure 4.3. Chronic supra-nigral infusion of FGF20 dose-dependently preserved striatal tyrosine hydroxylase (TH) levels in partially 6OHDA lesioned rats. Partial lesions were induced by 4µg unilateral intra-nigral 6OHDA infusions (**A**). FGF20 treatments were delivered with osmotic mini-pumps, and were commenced 1 day prior to lesioning and continued for 6 days thereafter. **B.** Representative examples of TH-immunostained coronal sections from the medial striatum of each group. Data points represent mean±sem, and n=6-10.

Figure 4.4. FGF20 Protects Nigral TH+ Dopaminergic Neurones against a Partial 6OHDA Nigrostriatal Lesion in Rats

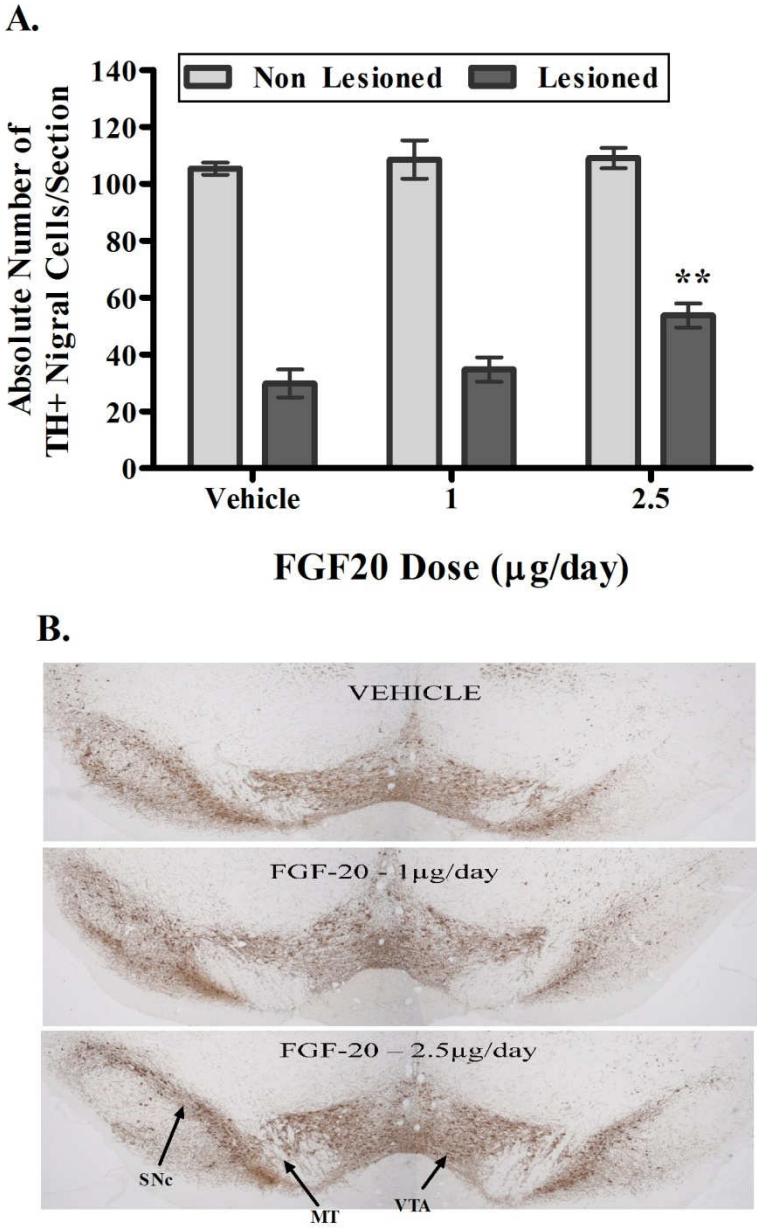

Figure 4.4. Chronic supra-nigral infusion of FGF20 dose-dependently protected nigral tyrosine hydroxylase positive (TH+) dopaminergic neurones against a partial nigrostriatal 6OHDA lesion in rats (**A**). Partial lesions were induced by 4µg unilateral intra-nigral 6OHDA infusions. FGF20 treatments were delivered with osmotic mini-pumps, and were commenced 1 day prior to lesioning and continued for 6 days thereafter. **B.** Representative examples of TH-immunostained coronal sections from the medial SNc of each group. Data points represent mean±sem, and n=6-10. Abbr.; SNc: substantia nigra pars compacta, MT: medial terminal nucleus of the accessory optic tract, VTA: ventral tegmental area.

4.4.2.2. Effects of FGF20 on the Motor Deficits Induced by a Partial 6OHDA Lesion in Rats

The cylinder test was used to assess whether chronic FGF20 treatment reduces the motor deficits induced by a partial 6OHA lesion in rats. Both of the FGF20 doses failed to preserve motor function at significantly higher levels compared to the vehicle treated 6OHDA lesioned group (***Fig 4.5***). There was, however, a strong trend towards motor deficits being lower in the 2.5µg/day FGF20 group compared to vehicle, at all of the time-points, post-lesioning. At baseline, ipsilateral forelimb use alone (as a % of total forelimb use) was ~13%-20% in the different groups, and at this time-point there were no significant differences in ipsilateral forelimb use between the groups. In the vehicle group, ipsilateral forelimb use increased to ~45-68% on post-lesioning time-points, while in the 2.5µg/day FGF20 treatment group, ipsilateral forelimb use increased to only ~28-46%. Motor deficits in the affected contralateral forelimb were, thus, ~16-24% lower in the 2.5µg/day FGF20 group compared to vehicle on post-lesioning time-points, although these differences were found not to be statistically significant. In the 1µg/day FGF20 group, ipsilateral forelimb use increased to ~44-59% on post-lesioning time-points, which represented equivalent increases to that observed in the vehicle treated rats. Furthermore, in the vehicle group, ipsilateral forelimb use was significantly higher at all of the time-points, post-lesioning, when compared to baseline levels ($p<0.05$), while, in the 2.5µg/day treatment group, on the other hand, ipsilateral forelimb use was not significantly higher at any of the time-points, post-lesioning, when compared to baseline levels. In the 1µg/day group, ipsilateral forelimb use was significantly higher compared to baseline levels on day 5 and 8 ($p<0.05$), but not day 8, post-lesioning.

Figure 4.5. Effect of FGF20 Treatment on the Motor Deficits Detected by the Cylinder Test in Partially 6OHDA Lesioned Rats

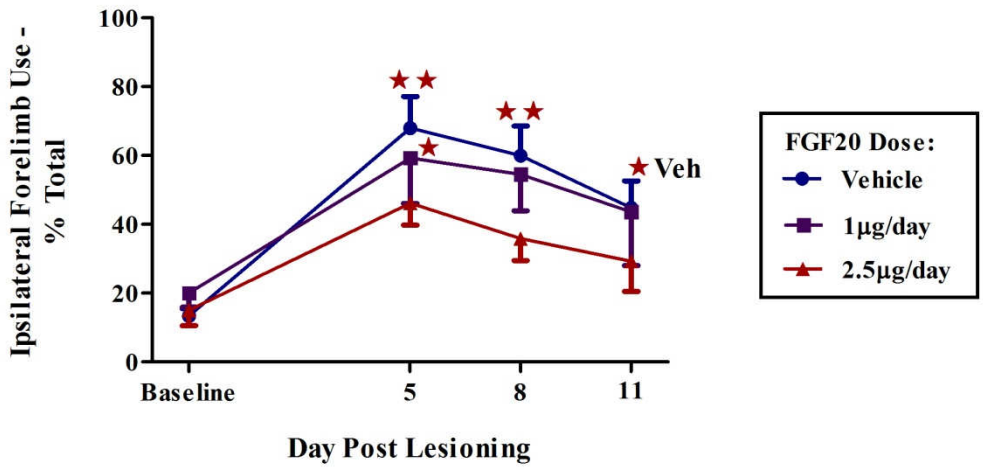

Figure 4.5. Effect of chronic supra-nigral FGF20 treatment on the forelimb motor deficits detected by the cylinder test in partially 6OHDA nigrostriatal lesioned rats. Nigrostriatal lesions were induced with 4µg unilateral intra-nigral 6OHDA infusions. FGF20 treatments were delivered with osmotic mini-pumps, and were commenced 1 day prior to lesioning and continued for 6 days thereafter. Increases in ipsilateral forelimb use alone, post-lesion, was used as a measure of the motor impairment present in the impaired contralateral forelimb. Data points represent mean±sem, and n=6-9 for each group. ★★$p<0.01$ and ★$p<0.05$ compared to baseline.

4.4.3. Stability of FGF20's Biological Activity when kept at 37°C

ERK1/2 phosphorylation experiments were carried out in PC12 cells to determine how long FGF20 retains its biological activity when kept at 37°C. Results from this study indicated that FGF20 only retains its biological activity for up to a maximum of 3 days or 72h when it is kept in solution at 37°C (***Fig 4.6***). In the un-stimulated control group, normalised phospho-ERK1/2 band densities were around ~0.17-0.36 arbitrary units. FGF20 stimulated ERK1/2 activation at levels higher than that observed in the control on day 0, when a freshly prepared FGF20 solution was applied to the cells, and also on day 1 and 2, at which points the FGF20 solution had been at 37°C for 1 and 2 days, respectively. FGF20 stimulated an ~2-4.8 fold increase in ERK1/2 activation on day 0, 1, and 2 compared to control, as phospho-ERK1/2 band densities were ~0.53-0.77 on the latter time-points. At all subsequent time-points, FGF20, however, failed to stimulate ERK1/2 activation at levels greater than that observed in the control group, as phospho-ERK1/2 band densities of ~0.06-0.26 were detected on the D3-D6 time-points.

Figure 4.6. Biological Stability of FGF20 when kept at 37°C

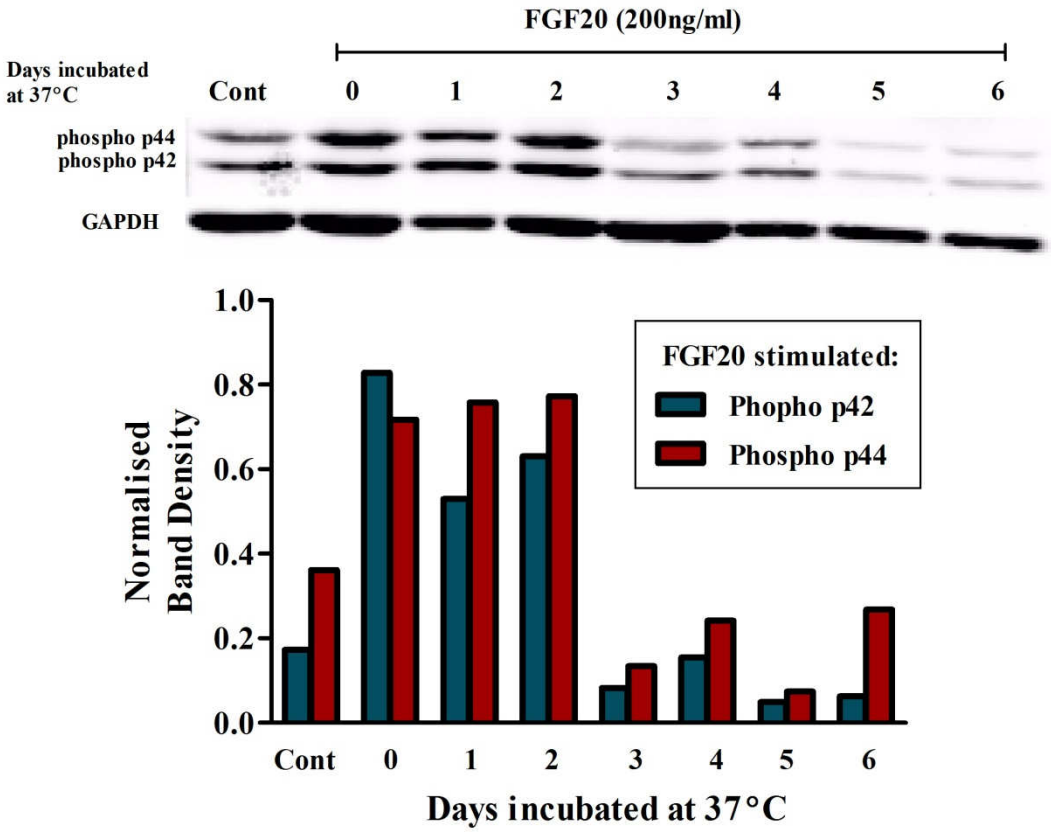

Figure 4.6. FGF20's biological activity remains intact for up to a maximum of 3 days when kept at 37°C. A 208ng/ml FGF20 solution (dissolved in aCSF+100ng/ml rat serum albumin) was kept at 37°C and its biological activity tested daily over the course of 7 days. FGF-20's biological activity was measured by quantifying its ability to stimulate extracellular regulated kinase-1/2 (ERK1/2, p42/p44) activation/phosphorylation in PC12 cells. ERK1/2 phosphorylation was measured using Western blot analysis. All phosho-ERK1/2 (phospho p42/p44) band densities were normalised by adjusting them to corresponding GAPDH loading control bands. n = 1 at all time-points.

4.4.4. Effects of PD173074 in Partially Lesioned 6OHDA Rats

4.4.4.1. Effect of PD173074 on 6OHDA-induced Nigrostriatal Degeneration in Rats

The FGFR antagonist, PD173074, was evaluated for its ability to potentiate 6OHDA-induced nigrostriatal dopamine neurone degeneration in partially lesioned rats. In the vehicle treated group, the 4µg intra-nigral 6OHDA infusions successfully induced partial unilateral nigrostriatal lesions in the rats (***Fig 4.7 & 4.8***). Chronic subcutaneous PD173074 administration, however, failed to significantly potentiate the partial nigrostriatal dopamine neurone degeneration induced by a 4µg intra-nigral infusion of 6OHDA (***Fig 4.7 & 4.8***). There was, however, a strong trend towards striatal TH levels being lower in both the PD173074 groups compared to the vehicle treated 6OHDA

lesioned rats (***Fig 4.7***). Additionally, there was also a trend towards nigral TH+ cell numbers being lower in the 2mg/kg group compared to the vehicle group (***Fig 4.8***).

In the vehicle treated group, TH levels in the lesioned striatum was ~53% lower compared to the non-lesioned contralateral striatum, while in the 1 and 2mg/kg PD173074 groups, TH levels in the lesioned striatum was ~63% and~ 67% lower compared to the contralateral striatum, respectively (***Fig 4.7***). Thus, striatal TH levels were ~10% and ~14% lower in the 1 and 2mg/kg PD173074 groups compared to the vehicle group, respectively, although these differences were found not to be statistically significant.

At the nigral level, TH+ cell numbers were reduced by ~71% in the lesioned SNc of the vehicle group compared to the non-lesioned contralateral hemisphere, while in the 2mg/kg PD173074 group, nigral cell counts were reduced by ~84% compared to the non-lesioned SNc (***Fig 4.8***). Nigral cell counts were, thus, ~13% lower in the 2mg/kg PD173074 group compared the vehicle treated 6OHDA lesioned group, although this difference was found not to be statistically significant. Nigral TH+ cell counts in the lesioned SNc of the 1mg/kg group were ~75% lower compared to the non-lesioned SNc, which represents a similar reduction to that observed in the vehicle treated 6ODHA lesioned rats.

Figure 4.7. Effect of Chronic PD173074 Treatment on the Striatal TH Depletion Induced by a Partial 6OHDA Nigrostriatal Lesion in Rats

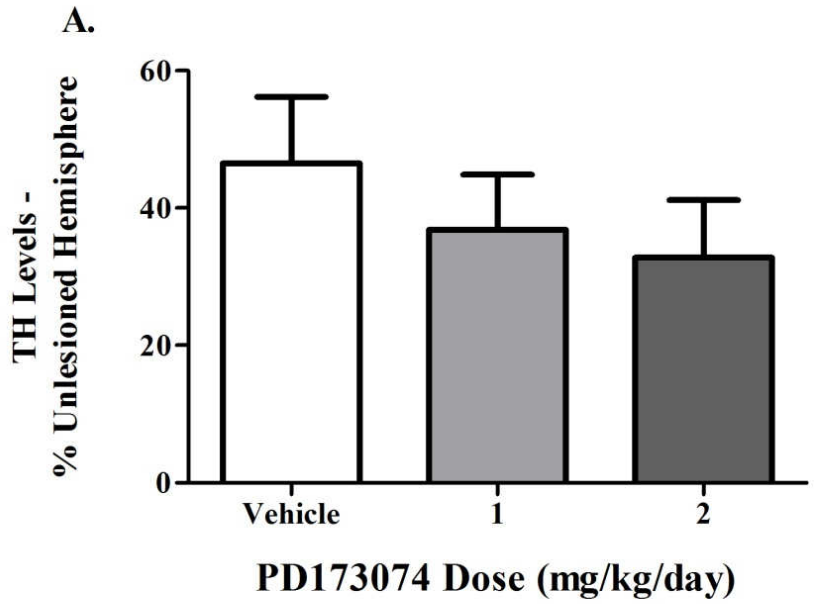

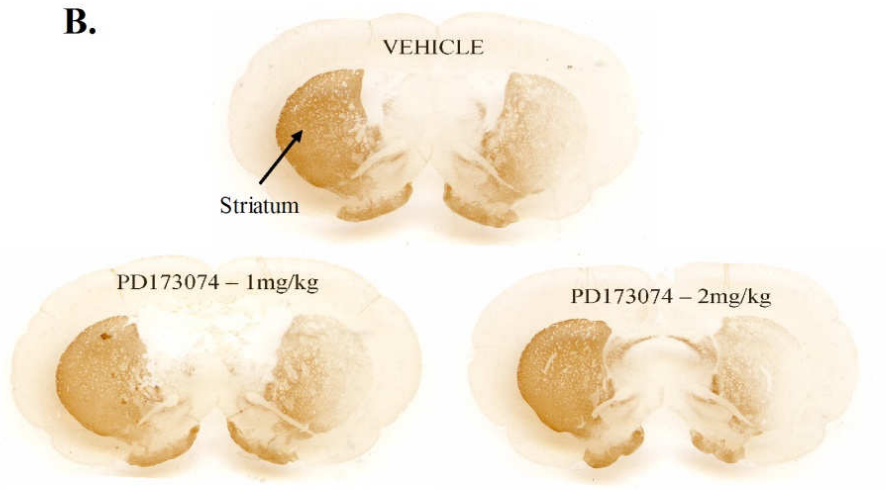

Figure 4.7. Effect of chronic systemic administration of the FGFR inhibitor, PD173074 on the partial depletion of striatal TH induced by 4μg intra-nigral 6OHDA infusions in rats (**A**). Daily subcutaneous PD173074 injections were started 3 days prior to 6OHDA lesioning, and continued for 5 days thereafter. **B.** Representative examples of TH-immunostained coronal sections from the medial striatum of each group. Data points represent mean±sem, and n=7-8 for each group.

Figure 4.8. Effect of Chronic PD173074 Treatment on the Loss of Nigral TH+ Neurones Induced by a Partial 6OHDA Nigrostriatal Lesion in Rats

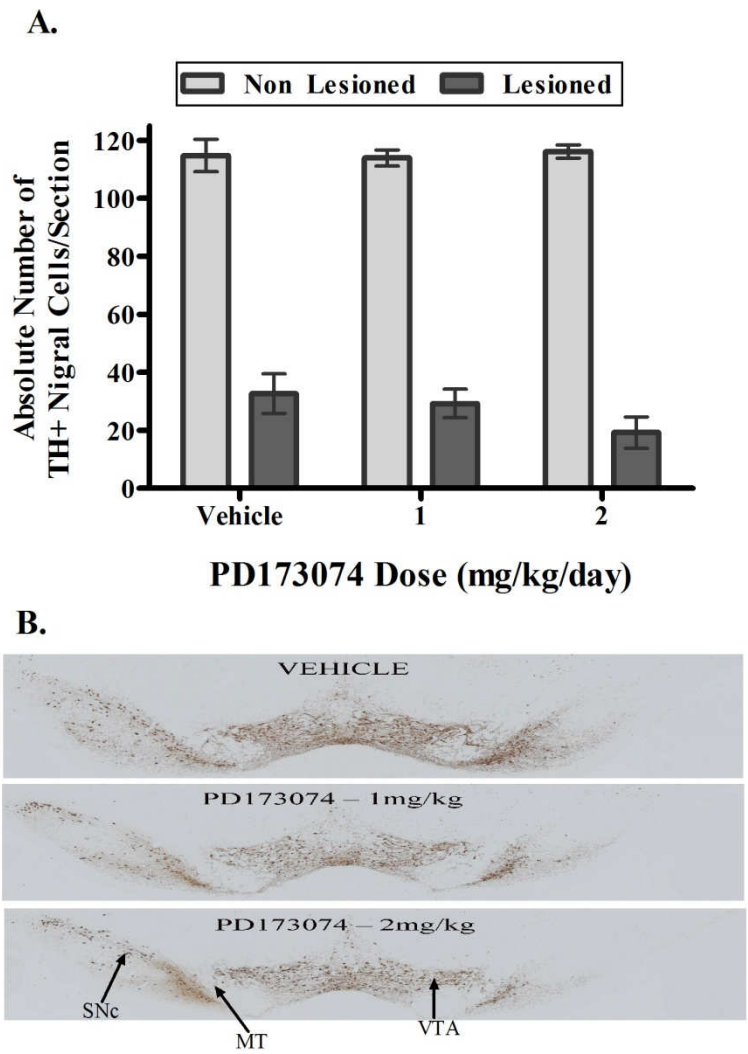

Figure 4.8. Effect of chronic systemic administration of the FGFR inhibitor, PD173074 on the partial loss of nigral tyrosine hydoxylase positive (TH+) neurones induced by 4 µg intra-nigral 6OHDA infusions in rats (**A**). Daily subcutaneous PD173074 injections were started 3 days prior to 6OHDA lesioning, and continued for 5 days thereafter. **B.** Representative examples of TH-immunostained coronal sections from the medial SNc of each group. Data points represent mean±sem, and n=7-8 for each group.

4.4.4.2 Effect of PD173074 on the Rotations Stimulated by Amphetamine in Partially Lesioned 6OHDA Rats

Chronic PD173074 administration failed to significantly potentiate the ipsiversive rotations stimulated by amphetamine in partially lesioned 6OHDA rats (***Fig 4.9***). There was however a strong trend towards amphetamine-induced rotations being higher in both the 1mg/kg and 2mg/kg PD173074 groups compared the vehicle treated 6OHDA lesioned rats. Amphetamine stimulated a time-dependent increase in net ipsiversive rotations in all of the treatment groups (***Fig 4.9.A***). Peak net ipsiversive rotations occurred in the 25 to 70min time-period, post-amphetamine injection (***Fig 4.9.A***). Amphetamine induced ~411, ~444 net cumulative ipsiversive rotations in the 1 and 2mg/kg PD173074 groups, respectively, while only ~251 rotations were recorded in the vehicle treated 6OHDA lesioned group (***Fig 4.9.B***). Amphetamine-induced rotational behaviour was, thus, ~1.6 and ~1.8 fold higher in the 1mg/kg and 2mg/kg groups compared to the vehicle group, although these differences were found not to be statistically significant.

Figure 4.9. Effect of Chronic PD173074 Treatment on the Rotational Behaviour Stimulated by Amphetamine in Partially 6OHDA Lesioned rats

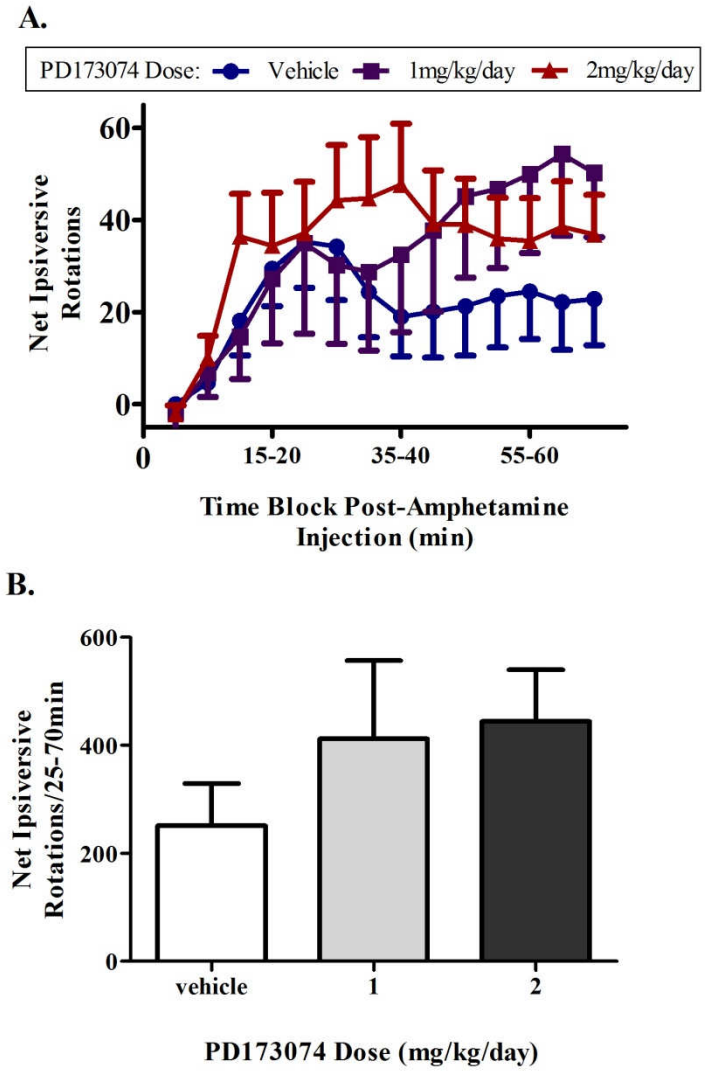

Figure 4.9. Effect of chronic systemic administration of the FGFR inhibitor, PD173074 on the rotational behaviour stimulated by amphetamine (5mg/kg, i.p) in unilateral partially 6OHDA lesioned rats. Unilateral nigrostriatal lesions were induced with 4 μg intra-nigral 6OHDA infusions. Daily subcutaneous PD173074 injections were started 3 days prior to 6OHDA lesioning, continued for 5 days thereafter, and amphetamine rotations measured at day 6, post-lesioning. Rotations were quantified in 5min time-blocks, and results are expressed as time-course profiles of the mean net ipsiversive rotations made over a 70min period post-amphetamine injection (**A**) and as the mean cumulative net ipsiversive rotations made during a 45min period in which peak rotational behaviour occurred (**B**). Data points represent mean±sem, and n=7-8 for each group.

4.4.4.3. Effect of PD173074 on the Motor Deficits detected by the Adjusted Stepping and Cylinder Test in Partially Lesioned 6OHDA Rats

In the cylinder test, no significant differences in motor deficits were found to exist between the groups at any of the time-points (***Fig 4.10***). There was, however, a trend towards motor deficits (% increases in ipsilateral forelimb use alone) being greater in both the 1mg/kg and 2mg/kg PD173074 groups compared to vehicle, at all of the time-points, post-lesioning (***Fig 4.10***). At baseline, ipsilateral forelimb use alone was ~9-13% in the different treatment groups. In all of the treatment groups, ipsilateral forelimb use was significantly higher on all of the post-lesioning time-points when compared to baseline ($p<0.01$). In the vehicle treated 6OHDA lesioned group, ipsilateral forelimb use increased to 63-70% on post-lesioning time-points, while in the 2mg/kg PD173074 group, ipsilateral forelimb use increased to ~77-85%. In the 1mg/kg PD173074 group, ipsilateral forelimb use increased to ~77% post-lesioning. Motor deficits detected by the cylinder were, thus, ~15% higher in the 2mg/kg PD173074 group, and 7-14% higher in the 1mg/kg group compared to the vehicle treated 6OHDA lesioned group. These differences were, however, found not be statistically significant.

Figure 4.10. Effect of PD173074 Treatment on the Motor Deficits Detected by the Cylinder Test in Partially 6OHDA Lesioned Rats

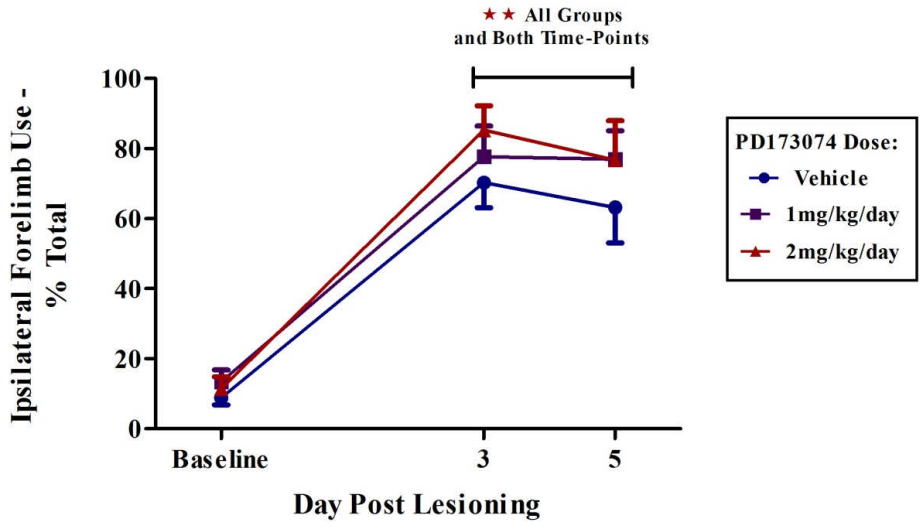

Figure 4.10. Effect of chronic systemic administration of the FGFR antagonist, PD173074 on the forelimb motor deficits detected by the cylinder test in partially 6OHDA lesioned rats. Nigrostriatal lesions were induced with 4µg unilateral intra-nigral 6OHDA infusions, and daily subcutaneous PD173074 injections were started 3 days prior to 6OHDA lesioning, and continued for 5 days thereafter. Increases in ipsilateral forelimb use alone, post-lesion, was used as a measure of the motor impairment present in the impaired contralateral forelimb. Data points represent mean±sem, and n=7-8 for each group. ★★$p<0.01$ compared to baseline.

PD173074 significantly potentiated the motor deficits detected by the adjusted stepping test in unilateral partially lesioned 6OHDA rats (***Fig 4.11***). At baseline, the different treatment groups made ~17-18 adjusted steps with their contralateral forelimbs, and significant motor deficits were detected in the affected contralateral forelimbs of all of the three groups at both time-points, post-lesioning, when compared to baseline (***Fig 4.11***). In the vehicle group, contralateral forelimb measurements were ~17% lower on post-lesioning time-points when compared to baseline ($p<0.01$). In the 1mg/kg/day and 2mg/kg/day PD173074 groups, contralateral forelimb measurements were ~28% and 22% lower on post-lesioning time-points, respectively, when compared to baseline ($p<0.01$), and at both time-points post-lesioning, adjusted step measurements were significantly lower in the two PD173074 treatment groups compared to the vehicle treated 6OHDA lesioned rats ($p<0.05$).

Figure 4.11. Effect of PD173074 Treatment on the Motor Deficits Detected by the Adjusted Stepping Test in Partially 6OHDA Lesioned Rats

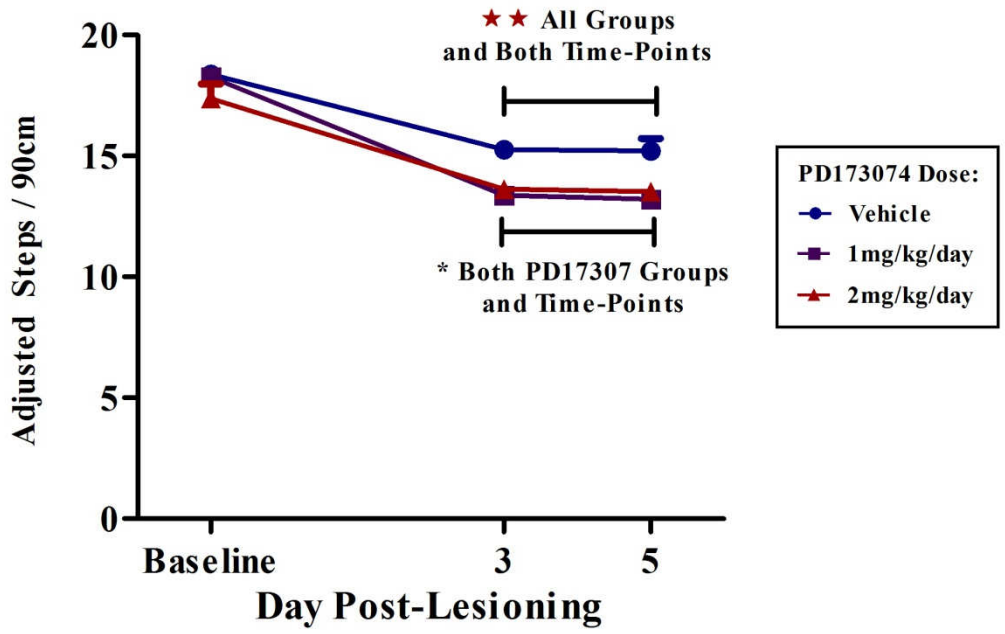

Figure 4.11. Effect of chronic systemic administration of the FGFR antagonist, PD173074 on the contralateral forelimb motor deficits detected by the adjusted stepping test in partially 6OHDA lesioned rats. Nigrostriatal lesions were induced with 4µg unilateral intra-nigral 6OHDA infusions, and daily subcutaneous PD173074 injections were started 3 days prior to 6OHDA lesioning, and continued for 5 days thereafter. Decreases in the number of adjusted steps made by the contralateral forelimb, after lesioning, was used as a measure of forelimb motor impairment. Data points represent mean±sem, and n=7-8 for each group. ★★$p<0.01$ compared to baseline, and *$p<0.05$ compared to vehicle.

4.5. Discussion

Recent findings have indicated that FGF20 might have neuroprotective potential in the treatment of PD. In immunohistochemistry experiments carried out in Chapter 2 of this thesis, FGFR1, 3, and 4 were shown to be localised to dopamine neurones in VM embryonic cultures, and in the rat nigrostriatal tract, while others have shown FGF20 to protect primary VM embryonic dopamine neurones, *in vitro*, against serum withdrawal, glutamate toxicity, and 6OHDA (***detailed in section 4.1.5***). In the current study a number of experiments were carried out to further investigate FGF20's neuroprotective effects on dopamine neurones. *In vitro*, it was firstly evaluated if FGF20 is able to protect VM embryonic dopamine neurones against 6OHDA, and in a subsequent *in vivo* study it was evaluated whether FGF20 is able to protect nigrostriatal dopamine neurones in the partially lesioned 6OHDA rat model of PD. Lastly, in a separate *in vivo* study, experiments were carried out to evaluate whether the endogenous FGF system in the nigrostriatal tract is able to protect dopamine neurones against injury, by evaluating whether pharmacological inhibition of FGFR activation is able to potentiate 6OHDA-induced nigrostriatal degeneration in the rat.

4.5.1. Neuroprotective Effects of FGF20 on Dopamine Neurones in VM Embryonic Cultures

Results from the *in vitro* neuroprotection study confirm the findings from the Murase & McKay, 2006 study which showed FGF20 to protect VM dopamine neurones against 6OHDA. Two concentrations of FGF20 (100 and 500 ng/ml) were tested for their ability to protect VM dopamine neurones against 6OHDA, and both of these concentrations preserved TH+ cell numbers at control levels. A maximal protective effect was, thus, achieved with the 100ng/ml concentration of FGF20, with negligible further benefits resulting from the higher 500ng/ml concentration. In this study, concentrations of FGF20 lower than 100ng/ml were not tested. Results from the Murase & McKay, 2006 study have, however, shown that an even lower concentration of FGF20 of 10ng/ml can provide maximal protection against 6OHDA induced dopamine neurone cell death in the VM culture system. Based on these findings, the 500ng/ml concentration tested in this study represents an excessively high concentration of FGF20. The results showing the 500ng/ml FGF20 concentration to provide an equivalent magnitude of protection compared to the 100ng/ml concentration, therefore,

serves to demonstrate that FGF20 does not mediate any toxic effects when applied at relatively high concentrations.

In Chapter 2, FGFR1, 3, and 4 immunoreactivity was shown to be present in VM dopamine neurones, and FGFR1 and 3 were also found to be localised to astrocytes in the cultures. Additionally, although there are currently no reports demonstrating FGFR2 to be present in VM cultures, this receptor is also likely to be present in the VM cultures, as FGFR2 has been shown to be abundantly and ubiquitously expressed in the developing mouse midbrain through E9.5 to E16 (Ford-Perriss *et al.*, 2001). Based on these results and also on previous findings showing FGF20 to be a relatively non-selective agonist of the different FGFR subtypes (Zhang et al, 2006), FGF20's neuroprotective effects could, thus, potentially be mediated through any of the FGFR subtypes in the VM cultures. The presence of the FGFR1 and 3 in astrocytes within the VM cultures also leaves open the possibility that FGF20's neuroprotective effects might be either partly or wholly mediated through an indirect astrocyte dependent mechanism. As the neuroprotective effects of *FGF2* on VM dopamine neurones have been shown to be mediated at least partly through an astrocyte-dependent mechanism **(*detailed in section 4.1.4***), it is likely that FGF20 might also be mediating its protective effects through a similar mechanism, especially as FGF20 and FGF2 are both relatively non-selective agonists at all of the FGFRs (Ornitz *et al.*, 1996; Ford-Perriss *et al.*, 2001; Eswarakumar *et al.*, 2005; Zhang *et al.*, 2006; Heinzle *et al.*, 2011).

4.5.2. Neuroprotective Effects of FGF20 on Dopamine Neurones in the Partially Lesioned 6OHDA Rat Model of PD

After confirming FGF20 to have neuroprotective effects on dopamine neurones, *in vitro*, in the VM cultures, experiments were subsequently carried out to evaluate whether FGF20 is also able to protect nigrostriatal dopamine neurones *in vivo*, in the 6OHDA rat model of PD. In this study, it was evaluated whether FGF20 is able to protect nigrostriatal dopamine neurones against a partial 6OHDA lesion when chronically delivered directly into the SN with the use of osmotic mini-pumps. The results from this study show for the first time that FGF20 is able to protect nigrostriatal dopamine neurones, *in vivo*, in the 6OHDA rat model of PD. FGF20 preserved nigrostriatal neurones in a dose-dependent manner, with a 1µg/day dose failing to provide any protection, while a 2.5µg/day dose preserved both striatal TH levels and nigral TH+ cell counts at significantly higher levels compared to the vehicle treated

6OHDA lesioned rats. The prototype FGF family member, FGF2 has in a number of studies been shown to have similar neuroprotective effects on dopamine neurones in the 6OHDA rat model of PD (***detailed in section 4.1.4***). As FGF20 and FGF2 are both relatively non-selective FGFR agonists (Ornitz *et al.*, 1996; Ford-Perriss *et al.*, 2001; Eswarakumar *et al.*, 2005; Zhang *et al.*, 2006; Heinzle *et al.*, 2011), it is, thus, not surprising that FGF20 also has protective effects in the 6OHDA rat model of PD. The significant preservation of nigrostriatal dopamine neurones in the 2.5µg/day group resulted in motor function being preserved in this group, as the motor deficits detected by the cylinder test were lower in 2.5µg/day group compared to the vehicle treated 6OHDA lesioned rats at all time-points, post-lesioning. This preservation of motor deficits was, however, not statistically significant, but based on the strong trend towards the motor deficits being lower in the 2.5ug/day on all time-points, post-lesioning, it is probable that the lack of significance is the result of insufficient 'n' numbers being used in this study.

Taken together, these findings provide further support that pharmacological activation of the FGF system in the nigrostriatal tract could potentially provide neuroprotection in PD. A myriad of other growth factors have previously been shown to have neuroprotective effects on dopamine neurones in the 6OHDA rat model of PD, including not only other members of the FGF family such as FGF1 and FGF2, but also GDNF, BDNF, CDNF and many others (***detailed in section 1.5 & 4.1.2***). Results from the current study, however, do not suggest that FGF20 would offer superior therapeutic effects in PD as a neuroprotective treatment compared to these other neurotrophins. First of all, based on the moderate magnitude of the neuroprotective effect obtained with FGF20 in this study, it is unlikely that FGF20 would have superior neuroprotective efficacy than FGF2 or many of the other neurotrophins. In the current study, FGF20 preserved nigrostriatal dopaminergic neurones at ~18-21% higher levels compared to vehicle treated 6OHDA lesioned rats, whereas a number of other growth factors, including GDNF, FGF2, and IGF-1 have been shown to preserve nigrostriatal dopaminergic neurones by ~40-70% in similar experimental contexts to that used in this study (Kearns & Gash, 1995; Guan *et al.*, 2000; Shults *et al.*, 2000; Fox *et al.*, 2001). Furthermore, in a previous *in vitro* study, FGF20's neuroprotective effects were reported to be selective for dopamine neurones in VM cultures (Ohmachi *et al.*, 2003). It was suggested that this apparent selectivity for dopamine neurones would potentially impart an advantage on FGF20 over other neuroprotective growth factors, in a

therapeutic setting, as the increased relative selectivity of FGF20 for dopamine neurones would likely result in it having less side effects, as many of the other growth factors have been documented to non-selectively protect a number other cell types, including glial cells, GABAergic neurones, and cholingergic neurones (Hyman *et al.*, 1994; Krieglstein, 2004), at least *in vitro*. Findings from the VM neuroprotection study and also from others, however, contradict the notion that FGF20 specifically protects dopamine neurones *in vitro*. Although the protective effects of FGF20 on non-dopaminergic neurones were not quantified in the VM study, it was obvious that FGF20 non-selectively protected the integrity of the VM culture as a whole. In the vehicle treated 6OHDA groups, it could be observed that 6OHDA consistently caused large portions of the VM cultures to detach, whereas in the FGF20 treated cultures, only very limited cell detachment was observed. As dopamine neurones only made up ~3.5% of the culture, such extensive preservation of the VM cultures as to make it obviously apparent could only reflect FGF20 also having a protective effect on other non-dopaminergic cells that made up the cultures. The contention that FGF20 has a non-selective neuroprotective effect on VM cultures is also supported by a previous study which showed FGF20 to inhibit apoptosis in non-dopaminergic neurones in human embryonic stem cell derived dopamine neurone cultures (Correia *et al.*, 2007). Furthermore, results from Chapter 2 showing the FGFRs to be present in non-dopaminergic neurones and glial cells in VM cultures together with the fact that FGF2 - a FGF family member with an equivalent selectivity for the FGFR subtypes to FGF20 - has non-selective protective effects in VM cultures argues against the likelihood of FGF20 having a selective effect on dopamine neurones.

There have, thus far, been no comprehensive efforts to distinguish which of the many neurotrophins with neuroprotective effects on dopamine neurones have the greatest neuroprotective potential in PD. A study comparing the relative neuroprotective efficacy of the most studied neurotrophins under the same experimental conditions, *in vivo*, are, thus, needed. The results from such a comparative study would then allow the identification of the neurotrophins and the neurotrophin receptors with the greatest neuroprotective potential in PD, allowing future research efforts to be focused on targeting the most promising neurotrophin systems. Furthermore, it would also be interesting to evaluate if a more efficacious neuroprotective effect might be obtained if two or more different classes of neurotrophins that are known to have neuroprotective effects on dopamine neurones are applied in combination.

In the current study, FGF20 was evaluated for its neuroprotective effects in a partially lesioned 6OHDA rat model of PD instead of a fully lesioned model. This was done not only because a partially lesioned model is considered a more clinically representative model, but also because a partial lesion model is likely to give a neuroprotective test treatment a greater opportunity to mediate any beneficial effects compared to a full lesion model. As detailed in ***section 3.1.1.4.4***, a test treatment has the opportunity to have a therapeutic effect through 3 possible mechanisms in a partially lesioned model. It could have a neuroprotective effect by preventing the neurones exposed to lethal concentrations of toxin from dying (Alexi *et al.*, 2000). Secondly, it could have a regenerative effect by restoring any damaged neurones to a functional state (Bowenkamp *et al.*, 1995). Thirdly, it could also increase the functioning of any remaining healthy neurones, providing symptomatic relief by compensating for the loss in functionality caused by the lesion (Gash *et al.*, 1995; Gash *et al.*, 1996). In the *in vivo* neuroprotection study, FGF20 was infused directly into the SN of the rats for 7 consecutive days, with the FGF20 infusions commencing one day prior to 6OHDA lesioning. As the delivery of FGF20 infusions were started one day prior to lesioning, it is possible that the 2.5µg/day FGF20 treatment preserved nigrostriatal dopamine neurones by having a neuroprotective effect on the nigrostriatal dopamine neurones. That is, FGF20 quite likely affected changes in the dopamine neurones, during the period before and close to when the lesioning was carried out, which made them more resistant to the toxic cell death inducing effects of 6OHDA, consequently resulting in less nigrostriatal dopamine neurones ultimately succumbing to 6OHDA-induced cell death. As the FGF20 infusions continued for 6 days post-lesioning, it is possible that the increased number of TH+ neurones observed in the 2.5ug/day group compared to vehicle could also have been the result of FGF20 stimulating the regeneration and restoration of the dopaminergic phenotype in the population of damaged but still viable nigrostriatal dopaminergic neurones which lost their dopaminergic phenotype. Results from the FGF20 stability studies, however, suggest that the preservation of the nigrostriatal dopamine neurones mediated by FGF20 is unlikely to be due to a regenerative effect mediated by FGF20. In the neuroprotection study, the osmotic mini-pumps were implanted subcutaneously, and this meant that the FGF20 treatment solutions would have been kept at a temperature of 37°C for the duration of the 7 day infusion period. As *FGF2* has been shown to have a relatively short half-life of ~24h when kept at 37°C and neutral pH (Gospodarowicz *et al.*, 1986), there was a concern

that the same might apply to FGF20, which would mean that FGF20 might have lost its biological activity during the delivery period. For this reason, a stability study was carried out to determine how long FGF20 retains its biological activity when kept at 37°C. These studies were unfortunately carried out after rather than before the *in vivo* neuroprotection study due to the facilities to carry out the study only being available at a later time. In the stability experiments, ERK1/2 phosphorylation assays were carried out to ascertain how long FGF20 retains its ability to stimulate ERK1/2 activation in PC12 cells when it is kept at 37°C. Results from the study suggest that FGF20 only retains its biological activity for up to 3 days, at most, when kept at 37°C. Based on these results, it is, thus, likely that the beneficial effects mediated by the 2.5µg/day FGF20 dose were brought about by actions stimulated by FGF20 on only the first 2 or 3 days immediately after the mini-pumps were implanted, and it is likely that FGF20 actually had no further pharmacological effect at later time-points. As this would have resulted in FGF20 only having a relatively acute pharmacological effect before and immediately around the time of lesioning, it is likely that the preservation of nigrostriatal dopamine neurones represents primarily a neuroprotective effect mediated by FGF20 rather than a regenerative effect. Further investigations are, thus, needed to specifically investigate whether FGF20 has any regenerative capabilities. This could be evaluated in experiments in which the FGF20 treatments are only commenced a number of days after lesioning, at a time-point after which most degeneration has already occurred. In the rat, *FGF2* has been demonstrated to stimulate not only the survival but also the regeneration of a number of different nerves after injury, including the sciatic nerve and motor nerves in the peripheral nervous system, and the optic nerve in the CNS (***detailed in section 4.1.1***). Based on these findings, there is a reasonable chance that FGF20 might be able to stimulate such a regenerative response in the lesioned nigrostriatal tract. Furthermore, results showing FGF20 to upregulate TH activity and expression in VM dopaminergic neurones *in vitro* (Bao *et al.*, 2005; Murase & McKay, 2006; Shimada *et al.*, 2009) suggests that FGF20 would, indeed, also be able to bring therapeutic benefits through such a regenerative mechanism. Moreover, this ability of FGFR activation to stimulate an upregulation of TH in dopamine neurones, leaves open the possibility that an FGF based treatment could provide therapeutic benefits not only by preventing dopamine neurones from degenerating but also by augmenting the functioning of any remaining functional dopamine neurones. As rats in the *in vivo* study were culled at day 11 post-lesioning, and possibly ~9 days after FGF20 last mediated a pharmacological effect, it is

unlikely that the increased levels of striatal TH levels in the 2.5µg/day FGF20 treatment group was partly due FGF20 stimulating increased TH synthesis in the remaining functional nigrostriatal dopamine neurones.

Moreover, a number of approaches could be used in future studies to attempt to successfully deliver biologically active FGF20 treatments to the nigrostriatal tract over more chronic time-periods in order to evaluate whether a chronic FGF20 treatment period provides for a greater neuroprotective effect than the more acute ~2 day treatment period that is likely to have been achieved in the current study. Some recent stability studies with FGF20 have shown that FGF20's thermal stability in solution can be enhanced by formulating FGF20 in a vehicle solution containing either heparin (Fan *et al.*, 2007) or arginine sulfate (Maity *et al.*, 2009). The development of a specific formulation of FGF20 that maintains its biological activity at 37°C for ~ 7 days would, thus, potentially allow FGF20 to be successfully evaluated when administered over a more chronic time-period using the same osmotic mini-pump based approach as used in this study. Alternatively, a genetic engineering based delivery approach, in which nigral cells are transfected with an FGF20 overexpressing viral vector, could potentially also allow for the effective chronic delivery of FGF20. Support for the effectiveness of the latter approach is provided by results which demonstrated GDNF to have superior neuroprotective effects in animal models of PD when delivered by a viral vector delivery system when compared to intra-nigral infusions (Kirik *et al.*, 2004).

The mechanism through which FGF20 and other FGF's mediate their neuroprotective effects on dopamine neurones, *in vivo*, in the 6OHDA rat model of PD has, thus far, not been studied. In immunohistochemistry studies carried out as part of Chapter 2, FGFR1, 3, and 4 immunoreactivity was shown to be localised to most if not all of the dopamine neurones in the SNc. This indicates that FGF20 might be mediating its neuroprotective effects through a direct mechanism by activating FGFRs on dopamine neurones. A previous study comprehensively characterised the localisation profile of the FGFR2 protein within the nigrostriatal tract, and although FGFR2 was found to be present in the SN and the striatum, it was exclusively localised to astrocytes. Any direct neuroprotective effects mediated by FGF20 on dopamine neurones is, thus, likely not to be mediated through activation of FGFR2. Additionally such a direct neuroprotective effect is also unlikely to be mediated through the FGFR3, as although FGFR3 was found to be localised to nigral dopamine neurone cell bodies, it was exclusively localised to dopamine neurone nuclei; making it unlikely that exogenously

applied FGF20 would stimulate neuroprotective effects through activation of FGFR3. Any direct FGF20 stimulated neuroprotective effect is, thus, likely to be mediated through activation of either FGFR1 or FGFR4.

There is substantial direct and indirect evidence from both cell culture and *in vivo* experiments indicating that the neurotrophic and neuroprotective effects mediated by *FGF2* on dopamine neurones are at least partially mediated through an astrocyte-dependent indirect mechanism (***detailed in section 4.1.4***). Immunohistochemical results from Chapter 2 leaves open the possibility that FGF20's neuroprotective effects on nigrostriatal dopamine neurones, *in vivo*, might also be either partially or completely being brought about through an indirect glial-mediated mechanism. FGFR1, 3, and 4 were all demonstrated to be abundantly present in oligodendrocytes in the SN. Additionally, FGFR1 was found to be localised to astrocytes in the SNr (Walker *et al.*, 1998), while others have shown FGFR2 to be present in astrocytes within the SNc and SNr (Chadashvili & Peterson, 2006). It is therefore feasible that FGF20 might be indirectly protecting dopamine neurones by activating FGFRs on oligodendrocytes and/or astrocytes, and that the events stimulated in the glial cells then acts to indirectly protect the dopamine neurones. Based on the localisation profile of the different FGFRs, any such astrocyte-dependent effects would involve stimulation of the FGFR1 and/or FGFR2, while an oligodendrocytes-dependent effect, could be mediated by either the FGFR1, 3, and/or 4.

The relatively widespread distribution of the FGFRs to non-dopaminergic neurones and also to glial cells throughout not only the nigrostriatal tract, but also the rest of the brain, raises the prospect that therapeutic targeting of the FGF system in PD through a pharmacological means could potentially lead to a number of unwanted adverse effects. Based on the pharmacology of the FGFs, a number of likely adverse effects could be anticipated to result from chronic systemic treatment with FGFR agonists. The FGFs are capable of stimulating changes in the metabolic pathways of neuronal cells. For example, FGF2 and FGF20 have been shown to stimulate the upregulation of TH expression and activity in dopamine neurone cultures (Bao *et al.*, 2005; Murase & McKay, 2006; Shimada *et al.*, 2009). In the remaining dopamine neurones in the degenerating nigrostriatal tract of PD patients, such an upregulation of TH is likely to be beneficial. The FGFs have, however, also been shown to stimulate alterations in the biochemical processes in a number of non-dopaminergic neurones, including cholinergic and GABAergic neurones (Sensenbrenner, 1993). It is, thus,

possible that a pharmacological therapy targeting the FGF system could lead to various adverse effects resulting from the treatment stimulating a dysregulation of either dopaminergic or non-dopaminergic brain systems. As mentioned earlier, FGFR1, 3, and 4 were all shown to be abundantly present in oligodendrocytes in the nigrostriatal tract, and there is evidence that activation of the FGFRs on oligodendrocytes in the adult brain might lead to deleterious rather than beneficial consequences, as several studies have reported FGF2 to stimulate a demyelinatory response in oligodendrocytes in the intact adult brain (Goddard *et al.*, 1999; Goddard *et al.*, 2001; Butt & Dinsdale, 2005a, b). Furthermore, as activation of the FGF system is pro-mitogenic, another obvious concern is that a systemic FGFR agonist therapy would be likely to increase the risk of cancers developing not only in the brain, but also in the peripheral organs, where the FGFRs are also relatively ubiquitously present (Heinzle *et al.*, 2011). There is, indeed, some evidence that excessive FGFR signaling could cause cells to become cancerous. FGF20 stimulates DNA synthesis and cell proliferation in a number of different immortalised cell lines, and FGF20 overexpressing fibroblasts become transformed two weeks after being transfected with the *FGF20* gene, and the transfected cells develop into rapidly growing tumours after s.c implantation into mice (Jeffers *et al.*, 2001).

4.5.3. Effect of Chronic Pharmacological Inhibition of the FGFRs on 6OHDA-Induced Nigrostriatal Degeneration and Motor Deficits in the Rat

Previous findings have demonstrated the FGF system to play an important neurotrophic role in sustaining the survival of nigrostriatal dopamine neurones in the intact adult brain (***detailed in section 4.1.2***). Indirect evidence also indicates that the upregulation of the FGF system in the nigrostriatal tract after 6OHDA lesioning in the rat might serve as an endogenous protective response which promotes the survival of 6OHDA exposed nigrostriatal dopamine neurones (***detailed in section 4.1.3***). It is important to gain a better understanding about the role that the FGF system plays in physiological and pathological contexts in the nigrostriatal tract, as there is some evidence that dysfunctioning of the FGF system might contribute to nigrostriatal degeneration in PD (***detailed in section 4.1.3 & 4.1.5***). In the current study, experiments were carried out in the 6OHDA rat model of PD to directly investigate whether the endogenous FGF system does, indeed, protect nigrostriatal dopamine neurones against 6ODHA-induced cell death. It was evaluated whether this is the case by testing whether chronic pharmacological inhibition of FGFR activation through systemic administration of the

non-selective FGFR antagonist, PD173074 is able to potentiate the nigrostriatal degeneration induced by a partial 6OHDA lesion in the rat. Results from this study suggest that the endogenous FGF system does provide a degree of protection against 6OHDA toxicity in the 6OHDA rat model of PD.

Based on a previous study showing a 1mg/kg/day dose of PD173074 to completely inhibit FGF-induced corneal revascularization, *in vivo*, in mice (Mohammadi *et al.*, 1998), a 1 and a 2 mg/kg/day PD173074 dose was used in this study. A similar PD173074 dosing schedule to that used in the Mohammadi *et al*., 1998 study was also employed in the current study. PD173074 or vehicle treatments were commenced 3 days prior to lesioning and continued for 5 days thereafter. It was evaluated whether the PD173074 treatments were able to potentiate not only 6OHDA-induced degeneration of the nigrostriatal tract but also 6OHDA-induced motor deficits. The TH immunohistochemistry results showed there to be a trend towards striatal TH levels being lower in both of the PD173074 dose groups when compared to the vehicle treated 6OHDA lesioned rats, while TH+ nigral cell counts, on the other hand, were lower in the 2mg/kg but not the 1mg/kg PD173074 dose group when compared to vehicle. These differences were, however, moderate in size, and not statistically significant. The lower striatal TH density in the 1mg/kg group, and the lower striatal TH density and nigral TH+ cell counts in the 2mg/kg group manifested behaviourally in the rats, as more severe motor deficits were detected in both of the PD173074 dose groups. Three motor tests were used to quantify the motor deficits in the rats, amphetamine-induced rotations, the cylinder test, and the adjusted stepping test, and all three of the tests detected larger motor deficits in the PD173074 treated groups compared to the control rats. Again, most of these differences were, however, moderate in size and not statistically significant. The only exception was the adjusted stepping results which showed motor deficits in both PD173074 groups to be significantly greater compared to the vehicle treated 6OHDA lesioned rats, at all of the time-points post-lesioning. Taken together, although the PD173074 treatments failed to cause a statistically significant potentiation of the 6OHDA-induced nigrostriatal degeneration; the strong trend towards all of the measures of nigrostriatal lesion size and also motor function being consistently lower in the 2mg/kg PD173074 group, strongly suggests that the endogenous FGF system plays a protective role in the nigrostriatal dopaminergic tract. The inability of this study to detect statistically significant differences is most likely the result of insufficient ‘n’ numbers being used in the study, as each treatment group included only

~7-8 rats. Recent statistical studies have shown that an 'n' of between 15-30 per group could potentially be required in some *in vivo* neuroprotection studies in order for the study to have sufficient power to detect true statistically significant effects (Dr Malcolm Macleod, University of Edinburgh, Internal seminar). Further studies using higher 'n' number are, thus, needed in order to conclusively determine whether the endogenous FGF system protects nigrostriatal dopamine neurones against 6OHDA toxicity.

Furthermore, the TH immunohistochemistry results demonstrated striatal TH levels but not TH+ nigral cell counts to be lower in the 1mg/kg PD173074 group compared to the vehicle treated 6OHDA rats. This might be taken to indicate that this lower dose failed to actually potentiate the 6OHDA-induced loss of nigrostriatal dopamine neurones. Instead it is possible that the 1mg/kg dose only induced a downregulation of TH in the remaining nigrostriatal dopamine neurones. It has been demonstrated that FGF20 and FGF2 are able to stimulate the upregulation of TH expression and activity in TH+ dopamine neurones *in vitro* (Bao *et al.*, 2005; Murase & McKay, 2006; Shimada *et al.*, 2009), and based on these findings, it would, thus, be expected that TH levels would be downregulated if endogenous FGFR activation was inhibited. On the other hand, the fact that both striatal TH levels and nigral TH+ cell counts were lower in the 2mg/kg PD173074 group suggests that this higher dose of PD173074 might have actually potentiated the 6OHDA-induced dopamine neurone cell death.

Moreover, the magnitude of the potentiation of 6OHDA-induced nigrostriatal degeneration brought about by the 2mg/kg dose of PD173074 was only moderate. Striatal TH levels and nigral TH+ cell counts in the 2mg/kg PD173074 group were only ~14% and ~13% lower compared to the vehicle treated 6OHDA lesioned rats, respectively. However, the dose-response profile of PD173074 was not fully characterised in this study and no pharmacokinetic results for PD173074 are available. It, thus, cannot be ruled out that these modest potentiating effects are due to a sub-maximal dose of PD173074 - which failed to completely block FGFR activation in the nigrostriatal tract - being used in this study. In a future study it, thus, needs to be evaluated whether 6OHDA-induced neurodegeneration could be potentiated more substantially by a higher dose of PD173704. As mentioned earlier, a 1 and 2mg/kg dose of PD173074 was selected to be used in this study based on results from a previous study showing a 1mg/kg/day dose of PD173074 to completely inhibit FGF-induced corneal revascularization, *in vivo*, in mice (Mohammadi *et al.*, 1998). It is, however,

possible that a higher systemically administered dose of PD173074 is required to effectively block FGFRs in the brain when compared to the retina of the eye. Although a blood-retinal barrier, similar to the blood brain barrier does also exist, the blood-retinal barrier has been shown to provide a less stringent barrier to systemically administered drugs, and it is, thus, possible that a lower concentration of PD173074 accumulates in the brain compared to the retina after a systemic administration of the drug. Results from pharmacokinetic studies characterising the brain penetrance of PD173074 at the concentrations tested in this study would be needed to determine whether optimal brain concentrations of the drug were achieved. If it is, indeed, the case that optimal brain concentrations of PD173074 could not be achieved due to the drug having poor brain penetrance, this problem could easily be overcome by delivering PD173074 directly into the brain using either icv or intra-nigral/striatal infusions.

Alternatively, the relatively modest potentiating effect achieved by blocking FGFR signaling could potentially be due to the existence of redundancy in the neurotrophic systems of the nigrostriatal tract. This is likely to be the case, as several other neurotrophic growth factors and their receptors are localised to the nigrostriatal tract, including GDNF, BDNF, and neurotrophin-3 (Gall *et al.*, 1992; Howells *et al.*, 2000). Furthermore, endogenous GDNF and BDNF have both been demonstrated to be required to maintain the survival of dopamine neurones in the intact adult brain. In one study, conditional knockdown of GDNF in mice caused a selective and extensive degeneration of monoaminergic neurones in the adult mouse brain, with the dopaminergic neurones in the SNc being severely affected, as an ~40% reduction in striatal GDNF lead to a significant ~60% loss of TH+ nigral cells relative to wild type mice (Pascual *et al.*, 2008). In rats, downregulation of BDNF expression in the nigrostriatal tract with intra-nigral BDNF anti-sense oligonucleotide infusions induced an ~40% loss of nigral TH+ neurones, as well as motor deficits (Porritt *et al.*, 2005).

In summary, results from the current study showed that there was a trend towards PD173074 potentiating both 6OHDA-induced nigrostriatal degeneration and motor deficits. These results suggest that the endogenous FGF system might play a role in protecting the nigrostriatal dopaminergic tract, but the failure of these results to reach statistical significance, however, means that these results cannot be taken to conclusively demonstrate this. Further studies using higher ‘n’ numbers and/or a PD173074 dosing regime that has been proven to yield optimal brain concentrations are

needed before it could be more conclusively decided whether the FGF system does, indeed, play a protective role in the nigrostriatal tract.

4.5.4. Conclusion

In the current study, experiments were carried out to further investigate the neuroprotective effects of FGF20 on dopamine neurones. *In vitro*, FGF20 was shown to protect VM dopaminergic neurones against 6OHDA toxicity, confirming previously published findings. Results from this study also demonstrate, for the first time, that FGF20 is able to protect dopamine neurones, *in vivo*, in the partially lesioned 6OHDA rat model of PD. Importantly, *in vivo*, FGF20 not only protected nigrostriatal dopaminergic neurones against 6OHDA-induced degeneration, but it also preserved motor function to some extent in the 6OHDA lesioned rats. In a separate *in vivo* study, experiments were carried out to investigate whether pharmacological inhibition of FGFR activation is able to potentiate 6OHDA-induced nigrostriatal degeneration in the rat, and results from this study suggests that the endogenous FGF system might play a protective role in the nigrostriatal tract. Taken together, these findings provide further support for the neuroprotective potential of FG20 in PD.

Chapter 5: Signalling Pathways Mediating FGF20's Neuroprotective Effects Against 6ODHA in PC12 Cells

5.1. Introduction

5.1.1. The Fibroblast Growth Factor Receptors

As detailed in ***section 2.1.2***, there are 4 subtypes of FGFRs referred to as the FGFR1, 2, 3, and 4. Briefly, the FGFRs have a general structure similar to that found in most other RTKs. Thus, they consist of an extracellular N-terminal ligand binding domain, a single transmembrane domain, and an intracellular C-terminal domain containing the protein kinase catalytic activity of the receptor. A unique feature of the FGFRs is the presence of 3 Ig-like domains in the extracellular N-terminal domain (***Illustrated in Fig 2.1***). The Ig-like domain closest to the N-terminal of the receptor is referred to as D1, while the middle and juxtamembrane Ig-like domains are called D2 and D3, respectively (Johnson *et al.*, 1990). Different isoforms of each of the FGFR subtypes have been shown to exist, with the FGFR1, 2, and 3 all existing as two prototypical FGFR isoforms, referred to as the b and c isoforms (***detailed in section 2.1.2***). It appears that the FGFR4 (Johnson *et al.*, 1991) does not exist as these prototypical b and c isoforms, but 3 alternative isoforms of this receptor has nevertheless also been identified thus far (van Heumen *et al.*, 1999; Ezzat *et al.*, 2001; Kwiatkowski *et al.*, 2008).

5.1.2. FGFR Activation

FGFR activation occurs through the same mechanism as utilised by most typical RTKs (Schlessinger, 2000). The FGFR exists as a monomer in its inactivated state. Binding of a FGFR ligand to the extracellular ligand binding domain of the receptor stimulates receptor dimerisation to occur. The intracellular C-terminal tyrosine kinases of each of the monomers then proceed to autophosphorylate tyrosine residues on the C-terminal of its neighbouring FGFR monomer. Seven tyrosine autophosphorylation sites have been identified on the FGFR1, Tyr463, Tyr583, Tyr585, Tyr653, Tyr654, Tyr730, and Tyr766 (Mohammadi *et al.*, 1992; Mohammadi *et al.*, 1996) (***Illustrated in Fig 2.1***)**.** These phosphotyrosine residues then serve as binding sites for src homology 2 (SH2) domain containing proteins through which numerous protein complexes are recruited to the activated receptor; ultimately facilitating the activation of numerous intracellular downstream signalling pathways. A unique feature associated with FGFR activation is

that cell surface heparin sulphate proteoglycans (HSPGs) interact with both FGF ligands and the FGFRs, and by doing so, they modulates FGFR signalling (***detailed in section 5.1.6***).

5.1.3. FGFR Signalling Mechanisms

The FGFRs employ many of the classical intracellular signalling pathways used by other RTKs to bring about changes in cellular functioning. The signalling events initiated by the FGFR1 have, thus far, been the most thoroughly studied, and the overview of FGFR signalling given below will be limited to only this receptor.

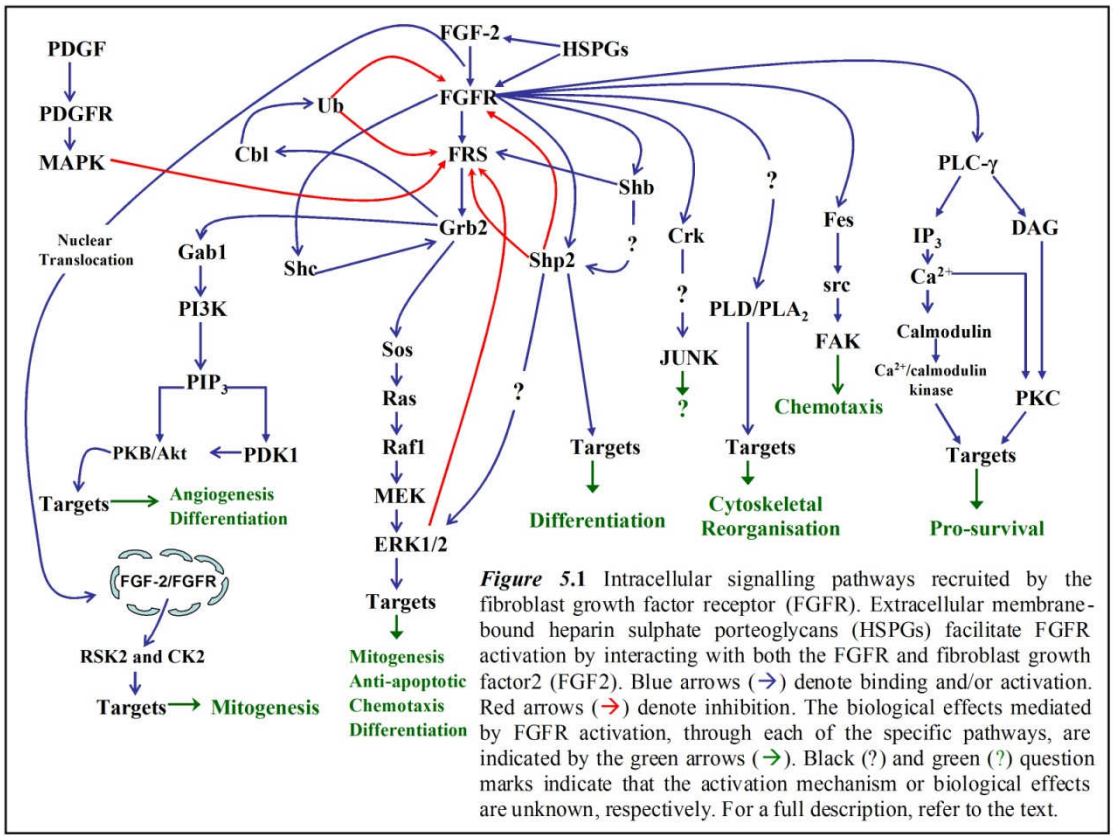

Figure 5.1 Intracellular signalling pathways recruited by the fibroblast growth factor receptor (FGFR). Extracellular membrane-bound heparin sulphate porteoglycans (HSPGs) facilitate FGFR activation by interacting with both the FGFR and fibroblast growth factor2 (FGF2). Blue arrows (→) denote binding and/or activation. Red arrows (→) denote inhibition. The biological effects mediated by FGFR activation, through each of the specific pathways, are indicated by the green arrows (→). Black (?) and green (?) question marks indicate that the activation mechanism or biological effects are unknown, respectively. For a full description, refer to the text.

FGFR1 activation has been shown to lead to the activation of phospholipase C-γ (PLC-γ), mitogen activated protein kinase (MAPK) pathways, phosphatidylinositol 3-kinases (PI-3K), tyrosine phosphatase non receptor type II (Shp2/PTPN11), and protein kinase B/RAC-alpha serine/threonine protein kinase (PKB/Akt)-dependent signalling pathways. More recently FGFR1 activation has also been found to lead to the activation of the lipid kinases, phospholipase A_2 (PLA_2) and phospholipase D (PLD), and the non-receptor tyrosine kinases, src, and Jun N-terminal kinase (JNK). FGFR1 also signals through a novel mechanism involving the nuclear translocation of membrane bound

FGFR1-FGF2 complexes. The mechanisms through which FGFR1 recruits some of these signalling pathways have been well characterised and they are described below. The specific FGFR-mediated biological effects that have been attributed to each of the different pathways are also discussed. These pathways are schematically illustrated in ***Fig 5.1***.

5.1.3.1. Recruitment of PLC-γ-dependent Pathways

Autophosphorylation of Tyr766 in the C-terminal of the FGFR1 creates a binding site for PLC-γ (Mohammadi *et al.*, 1991). Once bound to this site, PLC-γ becomes activated through FGFR1-mediated tyrosine phosphorylation. Activated PLC-γ then converts membrane bound phosphatidylinositol-(4,5)-bisphosphate (PIP_2) into the 2^{nd} messengers, inositol-(3,4,5)-trisphosphate (IP_3) and diacylglycerol (DAG). IP_3 activates IP_3 receptors on the endoplasmic reticulum, and mobilises calcium from intracellular stores. Ca^{2+} binds to and activates calmodulin, which in turn activates Ca^{2+}/calmodulin dependent kinases. The concurrent binding of DAG and Ca^{2+} to a regulatory site on the serine/threonine kinase, protein kinase C (PKC) leads to its activation. Once activated, the latter two effector proteins of the PLC-γ signalling pathway subsequently bring about changes in cellular functioning by phosphorylating and altering the activity of a range of target proteins, including ion channels, receptors, enzymes, and transcription factors (Schlessinger, 2000). PLC-γ dependent signalling events have been shown not to contribute to the mitogenic, differentiating, and chemotactic effects mediated by FGFR activation (Mohammadi *et al.*, 1992; Clyman *et al.*, 1994; Spivak-Kroizman *et al.*, 1994b). PLC-γ activation does, however, play a role in the anti-apoptotic/pro-survival effects mediated by the FGFR1 (Wert & Palfrey, 2000a). In its inactive state, PLC-γ is normally found in the cell cytosol. Its recruitment to the plasma membrane is essential in allowing it to interact with its SH2 domain binding sites on the activated FGFR1 and for its subsequent activation (Schlessinger, 2000). This recruitment is facilitated by FGFR1-mediated activation of the phospholipid kinase, phoshatidylinositol-3-Kinase (PI3K) (see below).

5.1.3.2. Recruitment of Grb2, Shc, and Shp2

The FGFR substrate 2 (FRS2) docking proteins, FRS2α and FRS2β are constitutively complexed to the juxtamembrane C-terminal domain of the FGFR1 through their

binding to phosphotyrosine residues (Ong *et al.*, 2000). FRS2α and FRS2β have both got N-terminal myristyl groups which anchor them to the inner leaf of the plasma membrane (Ong *et al.*, 2000). Within their structures, both of these signalling proteins have also got multiple tyrosine phosphorylation sites, which, once phosphorylated by an activated FGFR1, serve as binding sites for signalling proteins (Ong *et al.*, 2000). However, as none of the signalling proteins recruited by FGFR1-bound FRS2β have been identified, only the signalling proteins recruited by FRS2α are discussed below. The adaptor protein, growth factor receptor-bound protein 2 (Grb2) is one of several proteins that bind phosphotyrosine residues on FRS2α (Ong *et al.*, 2001). FGFR1 activation, however, also leads to the recruitment of Grb2 by two further indirect pathways. The adaptor protein, src homology 2 domain containing (Shc) binds to Tyr766 of the activated FGFR1 and becomes phosphorylated (Klint *et al.*, 1995). Grb2 in turn binds to phosphotyrosine residues on Shc through its SH2 domain. Alternatively, Grb2 can be recruited indirectly by binding of its SH2 domain to phosphotyrosine residues on the protein phosphatase, Shp2 (Hadari *et al.*, 1998). Shp2 is recruited to the FGFR1 signalling complex through its binding to phosphorylated FRS proteins. In addition to recruiting Grb2, Shp2 also has both negative and positive regulatory influences on FGFR1 signalling. Shp2 attenuates FGFR1 signalling by dephosphorylating phosphotyrosine residues on the autophosphorylated receptor, but, at the same time, Shp2 activity is also required for maximal FGFR1-mediated activation of the MAPK pathway (Hadari *et al.*, 1998). The mechanism through which Shp2 facilitates MAPK activation is, however, unknown. Shp2 has been shown to play a role in mediating some of FGFR1's effects on cell differentiation (Hadari *et al.*, 1998).

5.1.3.3. Activation of PI3K

Subsequent to Grb2 binding, GRB2-associated-binding protein 1 (Gab1) is recruited to the growing signalling complex through binding of its SH3 domain to a proline rich motif on Grb2 (Ong *et al.*, 2000). Gab1's assembly with FRS2α/Grb2 allows it to become phosphorylated by the FGFR1. The phosphotyrosine residues created on Gab1 then serve as specific binding sites for the SH2 domain of P13K, recruiting it to the membrane bound receptor complex (Ong *et al.*, 2000). A conformational change is induced in PI3K by its binding to Gab1, leading to the activation of the lipid kinase activity present in PI3K, which proceeds to generate PIP_2, and PIP_3 from membrane bound phosphatidylinositol phosphate (PIP). The PIP_3 ultimately recruits PLC-γ to the

plasma membrane through the binding of PLCγ's pleckstrin homology (PH) domain to the membrane bound PIP_3 generated by PI3K.

5.1.3.4. Recruitment of the Akt/PKB Pathway

Additionally, this FRS2α/Grb2/PI3K pathway also brings about the activation of the anti-apoptotic protein kinase B (PKB)/Akt signalling pathway (Ong *et al.*, 2000). Membrane bound PIP_3 serves as a binding site for the PH domains of the protein serine/threonine kinases, phosphoinositide dependent protein kinase (PDK1) and PKB/Akt. Binding of PDK1 to PIP_3 activates it, allowing it to proceed to phosphorylate its target protein, PKB. Threonine phosphorylation of PKB by PDK1, however, only partially activates it, and a second serine phosphorylation – carried out by either PDK2 or PKC – is required for PKB to become fully activated (Schlessinger, 2000). Activated PKB plays an important role in mediating growth factor stimulated pro-survival effects by activating and inactivating various anti-apoptotic and pro-apoptotic effector systems, respectively (Schlessinger, 2000). For example, PKB phosphorylates and deactivates the pro-apoptotic factors, Bad and caspase 9, and it indirectly upregulates an NF-κB-dependent program of gene expression. As of yet, the PKB signalling pathway has only been shown to contribute to FGFR's effects on angiogenesis and cell differentiation (Chen *et al.*, 2000; Forough *et al.*, 2005).

5.1.3.5. Recruitment of the MAPK Pathway

MAPK pathways play a major role in mediating the mitogenic effects of most growth factor receptors, and this pathway has also been shown to be activated by the FGFR1 (Schlessinger, 2000). Tyrosine phosphorylation of FRS docking proteins bound to the FGFR1 leads to the recruitment of multiple Grb2/ son of sevenless (sos) complexes via the binding of their SH2 domains to phosphotyrosine residues on the FRS proteins (Kouhara *et al.*, 1997). Sos is a guanosine nucleotide exchange factor, and its recruitment to the plasma membrane brings it into contact with its target signalling protein, the monomeric G-protein-like protein, $p21^{ras}$ (ras). Sos stimulates the exchange of guanosine diphosphate (GDP) for guanosine triphosphate (GTP) on ras causing it to become activated. In its active form, ras-GTP phosphorylates and activates the MAP kinase kinase kinase (MAPKKK), Raf-1 (Spivak-Kroizman *et al.*, 1994a). Raf-1 then phosphorylates and activates the MAP kinase kinase (MAPKK), MEK1/2, which in turn

phosphorylates and activates the MAP kinases (MAPK), ERK1/2 (Kuslak & Marker, 2007). Ultimately ERK1/2 brings about its mitogenic effects by phosphorylating and modifying the activity of numerous target proteins, including transcription factors, gene expression coactivators/corepressors, and histone acetylases and deacetylases. ERK1/2 activation is crucial in mediating the mitogenic, anti-apoptotic, chemotactic, and differentiating actions stimulated by FGFR1 in a number of different cell types (Gardner & Johnson, 1996; Kuo *et al.*, 1997; Nakamura *et al.*, 2001; Shono *et al.*, 2001; Gu *et al.*, 2004; Khalil *et al.*, 2005; Yang *et al.*, 2008). Furthermore, FGFR1-mediated activation of the ERK1/2 signalling pathway has been shown to be potentiated by the recruitment of two further docking proteins, SH2 domain-containing adapter protein B (Shb) and p38 (crk), to the activated FGFR1. Shb is recruited to the receptor by binding of its SH2 domain to Tyr766 of the FGFR1 (Cross *et al.*, 2002). Once bound, Shb becomes activated through FGFR1-mediated phosphorylation. Activated Shb then serves to potentiate FGFR1-mediated ERK1/2 activation by increasing FRS phosphorylation and by facilitating Shp2 recruitment and activation through an unknown mechanism (Cross *et al.*, 2002). Crk, on the other hand, binds to Tyr463 of the FGFR1 through its SH2 domain, and this binding is also followed by its phosphorylation-induced activation (Larsson *et al.*, 1999). Through an unknown mechanism, Crk acts to facilitate FGFR1-mediated activation of ERK1/2 and JNK. FGFR1's mitogenic effects have been shown to be partly dependent on Crk recruitment and activation (Larsson *et al.*, 1999).

5.1.3.6. Activation of PLA_2, PLD, and src

Recent studies have shown that FGFR activation also leads to the activation of the cytoplasmic non-receptor kinase, src (Kanda *et al.*, 2006), and the two phospholipases, PLA_2 and PLD (Cross *et al.*, 2000). Phosphorylation and activation of src is mediated indirectly by the non-receptor kinase, Fes, which in turn is activated by the FGFR1. Src is known to play an important role in modulating cell migration by activating focal adhesion proteins (FAKs), and src has, indeed, been shown to mediate the chemotactic effects stimulated by FGFR activation (Kanda *et al.*, 2006). Additionally, FGFR1's effect on differentiation is also dependent on src activation (Kuo *et al.*, 1997; Klint *et al.*, 1999). As with PLC-γ, FGFR-mediated recruitment of PLA_2 and PLD is dependent on Tyr766 phosphorylation of the receptor, but the exact mechanism by which these two lipases are activated remains poorly characterised. FGFR-mediated activation of

PLA_2 and PLD plays an important role in cytoskeletal reorganization stimulated by the FGFR1 (Cross *et al.*, 2000).

5.1.4. Intracellular Signalling by Nuclear-Translocated FGFR-FGF2 Complexes

Interestingly, in recent years it has become apparent that, in addition to utilising these classical signalling pathways, the FGFR1 also signals through an unorthodox nuclear signalling pathway which involves the translocation of FGFR1-FGF2 complexes to the cell nucleus (Bryant & Stow, 2005). This nuclear translocation has been shown to be essential in allowing FGFR1's full mitogenic effects to be expressed (Bossard *et al.*, 2003). The signalling events initiated by nuclear translocated FGFR1-FGF2 complexes are, however, not well characterised. Recent evidence suggests that they might bring about their mitogenic effects by modulating the activity of the nuclear kinases, ribosomal S6 kinase 2 (RSK2), and casein kinase II (CK2) (Bailly *et al.*, 2000; Soulet *et al.*, 2005).

5.1.5. Negative Regulation of FGFR1 Signalling

To allow for the physiological control of cell growth and differentiation, it is essential for growth factor mediated mitogenic signals to be attenuated or terminated appropriately. A number of mechanisms that negatively regulate FGFR1 signalling have been identified. The ubiquitin ligase, casitas b-lineage lymphoma (Cbl) has been shown to be recruited to the activated FGFR1 through its binding to Grb2 (Wong *et al.*, 2002), which in turn has been complexed to the receptor via its binding to FRS. The subsequent ubiquitination of both the FGFR1 and receptor bound FRS proteins ultimately leads to the internalisation and proteasomal digestion of the FGFR1 signalling complex, terminating signalling by the receptor (Wong *et al.*, 2002). Furthermore, there is also a negative feedback component in the MAPK pathway activated by the FGFR1. ERK1/2 phosphorylates several threonine residues on FRS2α (Lax *et al.*, 2002). This drastically reduces the rate at which tyrosine residues on FRS2α are phosphorylated, which leads to a decrease in Grb2 recruitment, and an ablation of all FRS/Grb2-dependent signalling cascades activated by the FGFR1. Moreover, FGFR1 signals have also been shown to be inhibited by negative crosstalk between MAPK pathways activated by other receptors. For example, activation of the platelet derived growth factor receptor by platelet derived growth factor stimulates the activation of a

MAPK that phosphorylates and inhibits the function of FGFR1-complexed FRS2α (Lax *et al.*, 2002).

5.1.6. Role of Heparin Sulphate Proteoglycans (HSPGs) in FGFR Signalling

Extracellular membrane bound HSPGs play an important role in FGFR signalling. HSPGs consist of a protein core structure to which a variable number of heparin sulphate side chains are linked (Yanagishita & Hascall, 1992). In addition to this, HSPGs also contain oligosaccharide side chains. In early studies characterising FGF2's binding sites on cells, it was discovered that, in addition to its high affinity FGFR binding sites, FGF2 also bound to a distinct low affinity, high capacity binding site (Moscatelli, 1987). This low affinity binding site was later found to be membrane bound HSPGs (Yayon *et al.*, 1991).

Subsequently, it was shown that most of the FGF2 secreted into the extracellular space is not found in its soluble form. Instead, FGF2 was predominantly localised in the extracellular matrix (ECM) where it is specifically bound to HSPG (Baird & Ling, 1987; Vlodavsky *et al.*, 1987; Folkman *et al.*, 1988). Some findings suggested that this HSPG-FGF2 complexing functioned to stabilise FGF2 in its active form, as HSPG binding protected FGF2 against denaturation and proteolytic degradation (Gospodarowicz & Cheng, 1986). ECM binding may also act to restrict the diffusion of secreted FGF2, and by doing so, ensure it acts locally in an autocrine or paracrine manner. It was later shown that soluble FGF2 and FGF2-heparin sulphate molecules could be liberated from the ECM by the action of the enzymes, heparinase and plasmin, respectively (Rifkin & Moscatelli, 1989). Importantly, it was shown that the soluble FGF2-heparin sulphate complexes were still able to activate the FGFR. This lead to the proposal that HSPGs might provide a storage site for secreted FGF2 in the ECM. Through the action of heparinase and plasmin – both of which are endogenous enzymes - the stored FGF2 could then be gradually released to mediate its effects over a prolonged period. Strong support for this proposal is provided by two studies (Flaumenhaft *et al.*, 1989; Prats *et al.*, 1989), in which FGF2 was shown, *in vitro*, to stimulate prolonged activation of plasminogen activator which persisted even after the cells were washed with PBS as to remove any unbound FGF2. However, when the cells were pre-treated with heparinase so as to strip the cells of HSPGs prior to FGF2 application, only transient stimulation of plasminogen activator was observed.

Soon after, it became apparent that, in addition to these passive roles in FGF2 signalling, HSPGs also had more active roles. In Chinese hamster ovary cells, the presence of HSPGs were shown to be essential for binding of FGF2 to the FGFR1, as inhibition of HSPG synthesis abolished FGF2 binding (Yayon *et al.*, 1991). FGF2's mitogenic effects in fibroblasts are also completely abolished by inhibition of HSPG synthesis (Rapraeger *et al.*, 1991). These inhibitory effects were completely reversed by the application of exogenous heparin sulphate. HSPGs, thus, appeared to have a permissive role in allowing the expression of FGF2's biological effects. Subsequently, the presence of HSPGs has been reported to be a prerequisite in allowing the expression of a number of different biological effects mediated by FGF2 in several different cell types (Lundin *et al.*, 2003). HSPGs have been shown to achieve this facilitation of FGF2 signalling by increasing the affinity of FGF2 for the FGFRs (Roghani *et al.*, 1994). Additionally, its presence also facilitates FGFR dimerisation (Spivak-Kroizman *et al.*, 1994a), and it increases FGFR kinase activity (Lundin *et al.*, 2000). Crystallographic studies have demonstrated HSPGs to form a ternary complex with both FGF2 and the FGFR, and by doing so, it acts to stabilise FGF2-FGFR interactions (Pellegrini, 2001).

Evidence from recent studies, however, indicates that HSPGs, in some situations, might have a relative rather than an absolute effect on FGF2 signalling. In the absence of HSPGs, FGF2 alone stimulated maximal activation of two of FGFR's downstream signalling proteins, Shp2 and Crk (Lundin *et al.*, 2003). FGF2 alone was also able to stimulate MAPK activation, but unlike the prolonged activation stimulated when HSPGs are present, only transient MAPK activation was induced in the absence of HSPGs. In another study, the absence of HSPGs had no effect on FGF2's mitogenic effects on Balb/c3T3 cells (Fannon & Nugent, 1996). It is, thus, likely that HSPGs are essential in allowing the activation of only some of the signalling pathways recruited by FGFR1 activation. These results also indicate that the specific biological effects of FGF2 that require HSPGs varies between cell types, as HSPGs are essential in facilitating FGF2's mitogenic effects in fibroblasts, while HSPGs are not needed at all for FGF2 to stimulate mitogenesis in Balb/c3T3 cells.

It has been postulated that in the absence of HSPGs, the FGFR1 takes up a conformation in which only a limited number of its C-terminal tyrosine phosphorylation sites are accessible to the tyrosine kinase activity of the receptor (Lundin *et al.*, 2003). When the receptor becomes activated, in the absence of HSPGs, autophosphorylation of

these limited tyrosine residues recruits a limited number of FGFR1 signalling pathways, which in turn only gives rise to a limited number of FGF2-stimulated biological effects. However, when HSPGs are present, they interact with FGFR1 as to bring about a conformational change in the receptor which exposes additional tyrosine phosphorylation sites in the receptors C-terminal. Autophosphorylation of these tyrosine residues creates binding sites for the recruitment of additional signalling pathways, which in turn stimulates the extra biological effects observed only when HSPGs are also present. Support for this idea is provided by the Lundin *et al., 2003* study, in which FGF2 recruited a differential set of signalling pathways depending on whether HSPGs were present or not. When HSPGs were present, FGF2 stimulated the phosphorylation of both Tyr463 and Tyr766 on the FGFR1. In contrast, when HSPGs were not present, FGF2 only stimulated the phosphorylation of Tyr463.

Moreover, it has also been proposed that HSPGs might help to bring about the differential biological effects mediated by FGF2 in different tissues (Faham *et al.*, 1998). The heparin sulphate side chains of HSPGs consist of linear polysaccharide chains composed of repeating sulphated disaccharide units (Yanagishita & Hascall, 1992). The existence of several different disaccharide building blocks, with varying spatial sulphation patterns, gives rise to a large number heparin sulphate polymer subtypes. The use of different heparin sulphate subtypes in the biosynthesis of HSPGs, in turn, gives rise to numerous HSPG subtypes. A specific sequence of amino acids in FGF2's structure acts as a binding site for the sulphate groups on heparin sulphate molecules (Pellegrini, 2001). This binding site selectively binds only to heparin sulphate molecules containing a specific sulphation pattern (Faham *et al.*, 1998). It is, thus, possible that by varying the expression profile of HSPG subtypes, cells can regulate the amplitude and/or nature of the biological response stimulated by FGF2.

5.1.7. Signalling Pathways Mediating the Neuroprotective Effects of the FGFs on Dopamine Neurones

The neuroprotective effects mediated by both FGF2 and FGF20 on primary dopamine neurones, *in vitro,* have been demonstrated to be mediated through both the ERK1/2 and PI3K intracellular signalling pathways. The neuroprotective effects of FGF2 against rotenone-induced cell death have been shown to be inhibited by selective ERK1/2 and PI3K inhibitors in SH-SY5Y cells (Hsuan *et al.*, 2006), while the neuroprotective effects of FGF20 on rat VM embryonic dopamine neurones against 6OHDA toxicity

was also inhibited by selective ERK1/2 and PI3K inhibitors (Ohmachi *et al.*, 2003; Murase & McKay, 2006). Furthermore, FGF2's protective effects, on the other hand, have also been demonstrated to be mediated through gap junctions, as FGF2 upregulated the expression of specific gap junction proteins, and inhibitors of gap junction synthesis abolished FGF2's neuroprotective effects in human embryonic dopamine neurone cultures (SiuYi Leung *et al.*, 2001). In Chapter 3 of this thesis, FGF20 was shown to protect dopamine neurones both *in vitro,* in VM cultures and *in vivo,* in the 6OHDA rat model of PD. In the current study, further *in vitro* experiments were carried out, this time in PC12 cells, an immortalised catecholaminergic cell line, to further investigate the signalling mechanisms mediating FGF20's neuroprotective effects.

5.1.8. PC12 Cells as an In Vitro Model of Dopamine Neurones in which to Investigate the Signalling Mechanisms Mediating the Neuroprotective Effects of FGF20

The PC12 cell line is an immortalised catecholaminergic neuronal cell line originally derived from a rat adrenal pheochromocytoma (Greene & Tischler, 1976), and it is widely used as an *in vitro* model of dopamine neurones due to the dopaminergic phenotype of the cells. PC12 cells contain all of the enzymes of the anabolic and catabolic dopamine metabolism pathways, including TH, dopa decarboxylase, dopamine-B-hydroxylase, MOA, and COMT (Greene & Tischler, 1976; Muller-Ostermeyer *et al.*, 2001), as well as dopamine (Shi *et al.*, 2007). Additionally, the cells also contain the dopamine reuptake transporter (Kadota *et al.*, 1996), the plasma membrane transporter protein responsible for the uptake of extracellular dopamine into the cell, as well as the vesicular monoamine transporter, the vesicular membrane protein that is responsible for the uptake of dopamine into intracellular vesicles (Liu *et al.*, 1994). Furthermore, PC12 cells are vulnerable to most of the toxins that are commonly used to cause dopamine neurone degeneration in cell and animal models of PD, including 6OHDA and MPP^+ (Gelinas & Martinoli, 2002; Lee *et al.*, 2005; Kavanagh *et al.*, 2006; Meng *et al.*, 2007; Mnich *et al.*, 2010). Consequently, PC12 cells are widely used in neuroprotection studies to identify treatments that are able to protect against this neurotoxin-induced cell death, with the hope that the identified treatments will also have protective effects in animal models of PD, and ultimately also in PD patients. Thus far, PC12 cells do appear to be a representative model, as there is a good correlation

between *in vitro* and *in vivo* findings. For instance, FGF1, FGF2, and GDNF all have neuroprotective effects in PC12 cells (Boniece & Wagner, 1993; Bouleau *et al.*, 2007; Su *et al.*, 2007; Li *et al.*, 2008; Rodriguez-Enfedaque *et al.*, 2009) and also on dopamine neurones in animal models of PD (***detailed in section 1.5***). Additionally, the PC12 cell line also serves as a good *in vitro* system in which to investigate the signalling pathways and mechanisms mediating the protective effects of FGFs. A functioning FGF signalling system is present in PC12 cells. FGF2 mRNA and protein are found in PC12 cells, and mRNA for the FGFR1, 3, and 4 but not the FGFR2 are present in the cells (Foehr *et al.*, 1998; Muller-Ostermeyer *et al.*, 2001). FGFs stimulate a number of biological responses in PC12 cells, including cell differentiation and neurite outgrowth (Neufeld *et al.*, 1987; Renaud *et al.*, 1996; Hadari *et al.*, 1998; Lin *et al.*, 1998; Kim *et al.*, 2003; Jeon *et al.*, 2010), and many of the classical FGFR signalling pathways described above are recruited after stimulation of FGFRs in PC12 cells, including the ERK1/2 MAPK, PI3K, and PLCγ pathways (Sigmund et al., 1990; Kremer et al., 1991; Spivak-Kroizman et al., 1994b; Foehr et al., 1998; Hadari et al., 1998; Karlsson et al., 1998; Raffioni et al., 1999; Wert & Palfrey, 2000a; Kawamata et al., 2001). Importantly, both FGF1 and FGF2 have been shown to have neurotrophic and neuroprotective effects on PC12 cells. Both FGF1 and FGF2 increase the survival of PC12 cells in serum free conditions (Renaud *et al.*, 1996; Muller-Ostermeyer *et al.*, 2001; Kawamata *et al.*, 2003), while FGF1 protects PC12 cells against cell death induced by the chemotherapeutic agent, etoposide (Bouleau *et al.*, 2007; Rodriguez-Enfedaque *et al.*, 2009), while FGF2 has been shown to protect PC12 cells against hypoxia-induced cell death (Boniece & Wagner, 1993). The neurotrophic effects of FGF2 on PC12 cells have in one report been shown to be mediated through both the ERK1/2 and PKCδ signalling pathways (Wert & Palfrey, 2000a), FGF1's protective effects against etoposide has been shown to be dependent on the nuclear translocation of FGF1 (Rodriguez-Enfedaque *et al.*, 2009), and also on FGF1s ability to reduce p53 activity (Bouleau *et al.*, 2007).

As detailed above, the HSPGs play an important role in modulating FGF signalling, and, importantly, PC12 cells have been demonstrated to be an appropriate *in vitro* model in which to study the influence of HSPGs on the biological and signalling events stimulated by the FGFs. PC12 cells produce HSPGs (Gowda *et al.*, 1989), and the signalling responses and biological effects mediated by FGF application in PC12 cells can be altered by co-administering FGF with the glycosaminoglycan, heparin, and

also with exogenous HSPGs. Heparin has been shown to potentiate FGF1 and FGF2 stimulated neurite outgrowth in PC12 cells (Damon *et al.*, 1988), and the HSPG, agrin when co-applied with FGF2 potentiates both FGF2-stimulated ERK1/2 activation and neurite outgrowth in PC12 cells (Kim *et al.*, 2003). Because of all of the favourable attributes detailed above, PC12 cells were chosen as a model system in which to study the signalling mechanisms mediating the neuroprotective effects of FGF20 against 6OHDA toxicity.

5.2. Objectives

5.2.1. Objective 1. Evaluate if FGF20 Protects PC12 cells against 6OHDA Toxicity

Surprisingly, there are currently no published studies which have evaluated if the FGFs are able to protect PC12 cells against any of the dopamine neurone toxins. The first objective of this Chapter was, therefore, to evaluate if FGF20 is able to protect PC12 cells against 6OHDA toxicity. Using immunohistochemistry, it was firstly evaluated whether the FGFR1, 3, and 4 proteins were present in the PC12 cell line, and using ERK1/2 phosphorylation assays it was determined whether any FGFRs present in the cells were functional. Cell viability experiments were then subsequently carried out to determine if FGF20 is able to protect the PC12 cells against 6OHDA induced cell death.

5.2.2. Objective 2. Identify the Signalling Pathways Mediating FGF20's Neuroprotective Effects against 6OHDA Toxicity in PC12 cells

The second objective of this Chapter was to investigate the signalling pathways that mediate FGF20's protective effects against 6OHDA in the PC12 cells. At the receptor level, it was evaluated if FGF20's protective effects are, indeed, mediated through the FGFRs, and at the intracellular level, it was determined if FGF20's protective effects are mediated through the ERK1/2 MAPK pathway.

5.2.3. Objective 3. Evaluate if the Heparin Sulphate Proteoglycan, Agrin is able to Potentiate the Neuroprotective Effects of FGF20 against 6OHDA in PC12 cells

FGF20 has been shown to be secreted from cells, *in vitro*, despite the fact that FGF20 lacks a classical N-terminal secretory signal, as FGF20 could be detected in the cell culture media of FGF20 overexpressing NIH 3T3 fibroblasts (Jeffers *et al.*, 2001). Importantly, in the later study, a pool of FGF20 could be released from the ECM of the fibroblast cultures by treating the cultures with suramin, a compound that acts to disrupt the weak interactions that forms between a number of FGFs and HSPGs. Thus, like the prototypical FGFs, it appears, FGF20 also interacts with HSPG in the ECM. No studies have, however, thus far, investigated the modulatory effects that HSPGs have on the signalling and biological effects stimulated by FGF20. The third objective of this chapter was to investigate whether agrin is capable of modulating the signalling and biological effects mediated by FGF20 in PC12 cells. It was firstly evaluated whether

agrin is able to potentiate FGF20 induced ERK1/2 activation, and, secondly, if agrin potentiates FGF20's neuroprotective effects against 6OHDA toxicity in the PC12 cells.

5.3. Methods

5.3.1. Maintenance of PC12 cells

PC12 cells were cultured and maintained according to exactly the same protocol detailed in ***section 4.3.3.1***.

5.3.2. Plating of PC12 Cells for Cell Viability Studies

For all of the PC12 cell experiments, cells were grown in 75cm^2 NunC plastic flasks until ~80-100% confluent, at which point they were plated into 24 well NunC plastic tissue culture plates. The DMEM FBS+ media in which the cells were bathed in was removed, and the cells washed by rinsing them 2x in ~5ml sterile D-PBS solution. Trypsin was then used to detach the cells from the flasks. 1ml of trypsin solution (0.05% trypsin dissolved in EDTA) was added to each 75cm^2 flask, and the cells left to incubate in the trypsin solution for 5-10min in a cell culture incubator until most of the cells were fully detached. The flasks were agitated to dislodge any remaining attached cells, and 4ml of DMEM FBS+ media added to each flask to inactivate the enzymatic activity of trypsin. The 5ml cell suspension was then transferred from the flask into a 15ml sterile centrifuge tube, and the cells centrifuged at 400g for 2min to create a cell pellet. The supernatant media suspension was poured off and the cell pellet re-suspended in 1ml of DMEM FBS+ media, and the suspension triturated thoroughly with a pipette to ensure that the cells were evenly distributed throughout the suspension. The number of viable cells present in the 1ml cell suspension was then quantified by trypan blue cell exclusion using the protocol detailed in ***section 2.3.2.3***.

The 1ml of cell suspension was then diluted so that each 500µl of cell suspension contained the same number of cells as was desired to be present in each well. In all cases, PC12 cells were plated at a density of 50000 cells/well, and the 1ml suspension of cells was, thus, diluted as to give a final concentration of 50000 cells/500µl of suspension. The diluted cell suspensions were thoroughly mixed to ensure that the cells were evenly distributed throughout the solution. Finally, the cells were plated either onto 13mm poly-D-lysine coated coverslips (***method for poly-D-lysine coating of coverslips is detailed in section 2.3.2.1***) placed inside the wells of a NunC 24 well tissue culture plate, or alternatively directly into the wells of 24 well NunC tissue culture plates. To do this, 500µl aliquots of the appropriately diluted cell suspensions were slowly applied to the wells or coverslips as repeated drops, which

were positioned as to ensure that the cells were distributed evenly over the entire surface of the coverslip or well.

5.3.3. Immunohistochemical Characterisation of the PC12 Cell Line Used

Immunohistochemistry experiments were carried out to confirm that the PC12 cells retained a catecholaminergic phenotype by evaluating if the cells expressed TH. Additionally, the cells were also characterised to determine if the FGFR1, 3, and 4 were localised in the PC12 cells.

PC12 cells were plated onto poly-D-lysine coated glass coverslips at a density of 50000 cells/coverslip, grown in DMEM FBS+ media until the coverslips were around ~80-100% confluent, and at this point the cells were fixed by immersing them in a 4% PFA solution for 10min. The fixed PC12 cells were then immunohistochemically stained for TH, and FGFR1, 3, and 4 with the HRP/DAB/ABC method using nearly exactly the same protocol as was used in ***2.3.3.2***. The only difference is that in this experiment the visualisation protocol was carried out on the fixed PC12 cultures rather than brain sections. To detect TH, and the FGFR1, 3, and 4, PC12 cell cultures were incubated with rabbit anti-TH (Chemicon, AB152, 1/1000), anti-FGFR1 (Sigma, F5421, 1/50), anti-FGFR3 (Santa Cruz Biotechnology, sc-9006), and anti-FGFR4 (Santa Cruz Biotechnology, sc-123, 1/50) primary antibody overnight at RT, respectively.

5.3.4. Cell Viability Studies

Four different cell viability studies were carried out in the PC12 cells with FGF20. In an initial cell viability study it was evaluated whether FGF20 is able to protect PC12 cells against 6OHDA toxicity. In a second and third subsequent study, cell viability experiments were carried out with the selective FGFR inhibitor, PD173074 and the selective MEK1/2 inhibitor, SL327 to determine if FGF20's neuroprotective effects against 6OHDA is mediated by the FGFRs and the ERK1/2 MAPK pathway, respectively. In the fourth study, experiments were carried to evaluate whether the HSPG, agrin is able to modulate the neuroprotective effects mediated by both a sub and supra-maximal concentration of FGF20. In the neuroprotection cell viability study, a 10ng/ml and a 200ng/ml concentration was identified as representing sub-maximal and supra-maximal FGF20 concentrations, respectively, in relation to FGF20's ability to protect PC12 cells against 6OHDA toxicity.

In all of the cell viability studies, PC12 cells were plated at a density of 50000 cells/well directly into 24 well NunC tissue culture plates. The plated cells were then placed in a cell incubator and left to grow for ~24h, at which point the cultures normally reached ~80-100% confluence. In the initial FGF20 neuroprotection studies, cells were then treated either with FGF20's vehicle (1ng/ml rat serum albumin dissolved in FBS-DMEM media), or with a range of concentrations of FGF20 (10, 100, or 500ng/ml).

In PD173074 experiments, cultures were treated for 24h either with FGF20 alone (200ng/ml), or with a FGF20 treatment (200ng/ml) added in combination with a range of concentrations of PD173074 (10, 100, or 1000nM, dissolved in FBS- media containing 0.02% DMSO). A 100nM concentration of PD173074 has in a previous study been demonstrated to maximally inhibit the pro-survival effects mediated by FGF2 on cerebellar granule neurones, *in vitro* (Skaper *et al.*, 2000). The concentrations of PD173074 employed in this study were, thus, selected as to include both sub and supra-maximal concentrations.

In the SL327 experiments, cultures were treated for 24h either with FGF20 alone (200ng/ml), or with a FGF20 treatment (200ng/ml) added in combination with a range of concentrations of SL327 (10, 50, or 100µM, dissolved in FBS- media containing 0.2% DMSO). The concentration range used in this study was selected based on previous studies using between 10 to 50µM SL327 to inhibit MEK1/2 signalling in various tissue culture preparations (Caughlan *et al.*, 2004; Chen-Roetling *et al.*, 2009; Lee *et al.*, 2010).

In the experiment with agrin, cultures were treated for 24h with one of six different treatments, agrin's vehicle + FGF20's vehicle, 500ng/ml agrin + FGF20's vehicle, agrin's vehicle + 10ng/ml FGF20 (submaximal conc.), 500ng/ml agrin + 10ng/ml FGF20, agrin's vehicle + 200ng/ml FGF20 (supramaximal conc.), 500ng/ml agrin + 200ng/ml FGF20. All of the treatments were delivered to each well as 500µl volumes. In a previous study, a 200ng/ml concentration of agrin was shown to potentiate ERK1/2 activation in PC12 cells (Kim *et al.*, 2003), and the 500ng/ml concentration of agrin was, thus, selected so as to ensure a supra-maximally effective concentration was used.

Thereafter, in all of the above cases, cells were exposed to 6OHDA (either 30, 40, or 50µM, depending on the sensitivity of the cultures, see next paragraph for details) for 6h. Final 6OHDA concentrations were applied to the cultures by adding 50µl of a 10x more concentrated 6OHDA stock solution directly to 450µl of DMEM FBS- media

previously added to each well. All the stock concentrations of 6OHDA were dissolved in a 0.2% ascorbate solution (dissolved in PBS, pH7.6) to limit the inactivation of 6OHDA by auto-oxidation. Immediately after this, the 6OHDA treatment solutions were removed, and cell viability measured using the colourimetric MTS assay (***see section 5.3.5 below***).

As with the VM cultures, different PC12 culture preparations were found also to have varying sensitivities to 6OHDA toxicity. After carrying out a number of repeat experiments, it was determined that depending on the sensitivity of the culture, a dose of between 30-50µM 6OHDA induced an ~50-80% reduction in cell viability relative to control. To accommodate for this variability, all FGF20 neuroprotection experiments were carried out in parallel in cells treated with either a 30, 40 or 50µM concentration of 6OHDA. Results from only the 6OHDA concentration groups that caused ~50-80% of cell death were then selected for inclusion in analyses.

5.3.5. Measurement of Cell Viability using the MTS Assay

In the MTS assay, the overall metabolic activity that is present in a cell culture is quantified. In living cell cultures, the yellow coloured water soluble tetrazolium compound, 3-(4,5-dimethylthiazol-2-yl)-5-(3-carboxymethoxyphenyl)-2-(4 sulfophenyl)-2H-tetrazolium (MTS) diffuses freely into the cytosol of living cells. Once inside, MTS is converted into a purple formazan product through the action of cytosolic dehydrogenase enzymes in the presence of phenazine methosulfate (PMS). As formazan absorbs light at 490-500nm, the degree of formazan formation in a specific cell culture can, thus, be quantified spectrophotometrically by measuring the degree of light that is absorbed at 490nm by the cell culture solution. And, in the MTS assay, this measure of metabolic activity is used as an indirect quantitative measure of cell viability, as the amount of formazan product that is produced has been shown to be directly proportional to the number of living cells that are present in a cell culture.

A working MTS solution (330µg/ml MTS and 20µM PMS dissolved in serum free DMEM media) was prepared using MTS/PMS stock solutions provided in a CellTiter Aqueous non-Radioactive Cell Proliferation Assay kit (Promega). 200µl of this MTS working solution was added to each cell culture well. Cells were then left to incubate for 1h in the MTS solution while kept at 37°C in the cell culture incubator. Immediately thereafter, the cell cultures were analysed using a Flexstation (Molecular Devices) to quantify the degree of MTS to formazan conversion that occurred in each of

the different wells by measuring absorbance at 490nm. The degree of cell viability that was detected in each of the different treatment groups was expressed as a percentage of the cell viability that was present in the control group. These % control cell viability measurements were calculated by dividing the absolute 490nm absorbance value generated for each group by that of the control group, and by multiplying the resulting value by 100. For each treatment group, mean (±sem) % control cell viability values were derived from results from 3 independent repeat experiments, and in each repeat experiment, each treatment group comprised of 4 coverslips. In the initial FGF20 neuroprotection experiment, cell viability results were analysed using one-way ANOVAs and Dunnett's post hoc tests. Results were analysed to determine if cell viability measurements in each of the FGF20 treatment groups were significantly different compared to the vehicle + 6OHDA group.

In the experiments with PD173074 and SL327, cell viability results were analysed with one-way ANOVA's, and Bonferroni post-hoc tests. Results were analysed to determine whether cell viability measurements in each of the treatment groups were significantly different compared to the vehicle + 6OHDA group, and also whether cell viability measurements in any of the FGF20 + PD173074/SL327 groups were significantly different compared to the FGF20 + 6OHDA group. In the cell viability studies with agrin, results were analysed with two-way ANOVAs and Bonferroni post-hoc tests. Results were analysed to determine if cell viability measurements in each of the treatment groups were significantly different compared to the vehicle + 6OHDA group. Additionally, it was also evaluated if cell viability in the sub-maximal (10ng/ml) and supra-maximal (200ng/ml) agrin negative FGF20 treatment groups were significantly different compared to the respective agrin positive FGF20 treatment groups.

5.3.6. ERK1/2 Phosphorylation Experiments

5.3.6.1. Application of Treatments to PC12 Cells

Four different ERK1/2 phosphorylation experiments were carried out in the PC12 cells with FGF20. In an initial experiment, it was evaluated whether FGF20 and FGF2 were able to stimulate ERK1/2 activation in the PC12 cells to determine if the PC12 cells contain a functioning FGF signalling system. In a second and third subsequent study, it was evaluated whether the selective FGFR inhibitor, PD173074 and/or the selective

MEK1/2 inhibitor, SL327 were able to inhibit FGF20 stimulated ERK1/2 phosphorylation in the PC12 cells. In the fourth study, experiments were carried to evaluate whether the HSPG, agrin is able to modulate the degree of ERK1/2 activation stimulated by both a sub and supra-maximal concentration of FGF20. In preliminary experiments, a 10ng/ml and a 200ng/ml concentration was identified as representing sub-maximal and supra-maximal FGF20 concentrations, respectively, in relation to FGF20's ability to stimulate ERK1/2 activation in PC12 cells. In all of these experiments, PC12 cells were grown in 75cm^2 tissue culture flasks in FBS+ DMEM media until they were ~80-100% confluent. After overnight serum withdrawal, the FBS-DMEM media was removed from the flasks, and test treatments applied to the cells. In all cases, test treatments were dissolved in serum free DMEM media, and delivered as 5ml volumes. Initial ERK1/2 phosphorylation experiments were carried out to determine if the PC12 cells contained functional FGFRs coupled to the ERK1/2 MAPK signalling pathway by evaluating if FGF2 and FGF20 were able to stimulate ERK1/2 activation in the PC12 cells. In these experiments, serum starved PC12 cells were exposed to either a vehicle solution (1ng/ml rat serum albumin dissolved in FBS-DMEM media), 200ng/ml FGF20, 200ng/ml FGF2, or 100ng/ml nerve growth factor (NGF). NGF was used as a positive control in these experiments, as PC12 are widely known to be responsive to NGF application (Sabban, 1997; Spear *et al.*, 1997; Wert & Palfrey, 2000b; Shimoke & Chiba, 2001; Kavanagh *et al.*, 2006).

In experiments carried out to determine if PD173074 blocks FGF20 stimulated ERK1/2 activation, cells were pre-treated for 1h with either PD173074's vehicle (0.02% DMSO dissolved in serum free media), or with one of two concentrations of PD173074 (50nM or 1000nM). A 50nM concentration of PD173074 has in previous studies been shown to mediate a maximal or complete inhibitory effect on FGF2 stimulated ERK1/2 activation, *in vitro* (Skaper et al., 2000), and the 1000nM concentration, thus, represents a supra-maximal concentration. Thereafter, pre-treatment solutions were removed, and the cells that were pre-treated with PD173074's vehicle, 50nM PD173074, and 1000nM PD173074 were then exposed for 5min to 200ng/ml FGF20 alone, 200ng/ml FGF20 + 50nM PD173074, and 200ng/ml FGF20 + 1000nM PD173074, respectively.

In experiments carried out to determine if SL327 blocks FGF20 stimulated ERK1/2 activation, cells were pre-treated for 1h with either SL327's vehicle (0.2% DMSO dissolved in serum free media), or with one of two concentrations of SL327 (10µM or 100µM). Thereafter, pre-treatment solutions were removed, and the cells pre-

treated with SL327's vehicle, 10µM SL327, and 100µM SL327 were then exposed for 5min to 200ng/ml FGF20 alone, 200ng/ml FGF20 + 10µM SL327, and 200ng/ml FGF20 + 100µM SL327, respectively.

In the experiments carried out to determine if agrin modulated FGF20 simulated ERK1/2 activation, cultures were treated for 5min with one of six different treatments, agrin's vehicle + FGF20's vehicle (unstimulated control), 500ng/ml agrin + FGF20's vehicle, agrin's vehicle + 10ng/ml FGF20 (submaximal conc.), 500ng/ml agrin + 10ng/ml FGF20, agrin's vehicle + 200ng/ml FGF20 (supramaximal conc.), or 500ng/ml agrin + 200ng/ml FGF20. All of the treatments were delivered to each well as 500µl volumes.

5.3.6.2. Preparation of Cell Lysates from the Stimulated PC12 Cells

In all cases, immediately after the application of the last test treatment, the treatment solutions were removed and cell lysates prepared from the stimulated cells using exactly the same protocol as detailed in ***section 4.3.3.4***.

5.3.6.3. Quantification of ERK1/2 phosphorylation using Western Blot Analyses

The level of ERK1/2 activation stimulated by each of the different treatment combinations was then quantified by Western blot analyses using exactly the same protocol as detailed in ***section 4.3.3.5***.

5.3.7. Drugs and Chemicals

SL327 was obtained from Tocris Bioscience Ltd (UK, Bristol), and recombinant human FGF2 (FGF basic), recombinant rat agrin, and recombinant rat β-NGF were purchased from R&D Systems (US, MN). All other drugs and chemicals were obtained from the same suppliers detailed in ***section 3.3.5 and 4.3.5***, or from Sigma Aldrich Ltd. (UK, Dorset).

5.4. Results

5.4.1. Immunohistochemical Characterisation of the PC12 cell line

Immunohistochemistry experiments were carried out to confirm that the PC12 cells expressed TH, and to determine whether FGF20's receptors, the FGFRs are localised in the cells. The cells were shown to possess a catecholaminergic phenotype, as they were positive for TH (***Fig 5.2***), and the cells were also judged to have a characteristic polygonal morphology representative of PC12 cells. Additionally, FGFR1 and 3 were found to be present in the cells (***Fig 5.2***), but not FGFR4 (results not shown). For both FGFR1 and FGFR3, a cytoplasmic staining pattern was observed in some cells, while in other cells, the receptors were localised to both the cytoplasm and also to the nucleus.

To determine whether the FGFRs localised in the PC12 cells were functional, it was evaluated whether the two FGFR ligands, FGF20 and FGF2 are able to stimulate ERK1/2 phosphorylation in the cells. The FGFR's present in the PC12 cells were found to be functional as both FGF20 and FGF2 successfully induced ERK1/2 phosphorylation in the cells (***Fig 5.3***). In the un-stimulated control group, normalised phospho-ERK1/2 band densities were around ~0.05 arbitrary units. Both the FGF20 and the FGF2 treatment stimulated ~3 fold increase in ERK1/2 activation compared to control, as phospho-ERK1/2 band densities were ~0.16-0.19 in the later 2 groups. NGF, however, had an immensely greater capacity to stimulate ERK1/2 activation. A supramaximal concentration of NGF induced ~5 fold greater degree of ERK1/2 phosphorylation relative that stimulated by a supra-maximal concentration of the FGF ligands (***Fig 5.3***).

Figure 5.2. The PC12 Cell Line Used in Experiments with FGF20 Expressed TH, and FGFR1 and 3

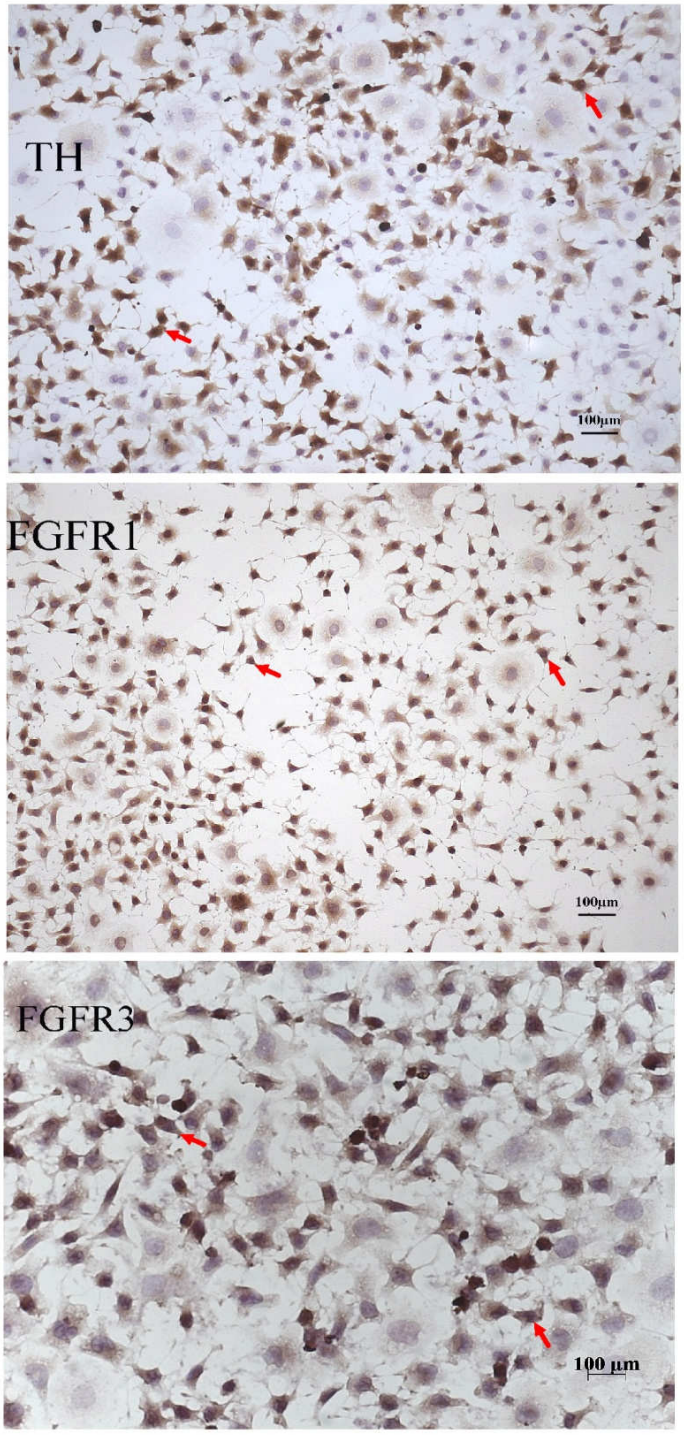

Figure 5.2. The PC12 cell line used in cell viability experiments with FGF20 expressed tyrosine hydroxylase (TH, a marker of dopaminergic neurones), and FGFR1 and 3. PC12 cells were fixed with paraformaldehyde and immunohistochemically stained for the aforementioned antigens. Red arrows: Brown DAB stained positive cells. Blue: Haematoxylin stained nuclei.

Figure 5.3. FGF20 Stimulated ERK1/2 Activation in the PC12 Cell Line used in Cell Viability Experiments

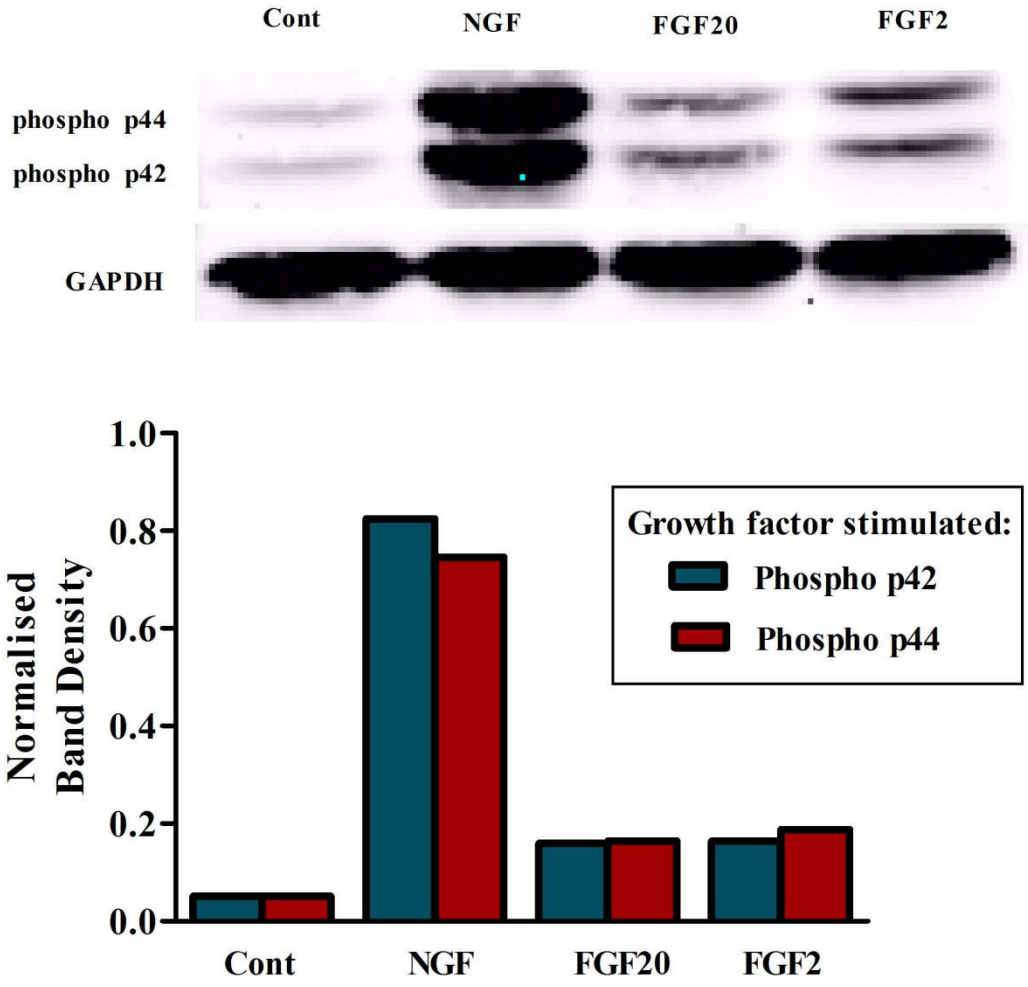

Figure 5.3. Activation of both the NGF and FGF signalling systems in PC12 cells stimulated ERK1/2 (p42/p44) activation. Cells were exposed to a supra-maximal dose of either NGF (200ng/ml), FGF20 (200ng/ml), or FGF2 (200ng/ml) for 5min, and the cells immediately lysed thereafter. ERK1/2 phosphorylation was measured using Western blot analysis. All phosho-ERK1/2 band densities were normalised by adjusting them to corresponding GAPDH loading control bands.

5.4.2. FGF20 Protects PC12 cells against 6OHDA Toxicity

In the initial neuroprotection cell viability study, FGF20 concentration-dependently protected PC12 cells from 6OHDA toxicity (***Fig 5.4***). In the FGF20 vehicle + 6OHDA group, cell viability was reduced by ~50% compared to control (FGF20 vehicle + 6OHDA vehicle group). Cell viability (% control) was significantly higher in all of the FGF20 + 6OHDA treatment groups vs. the FGF20 vehicle + 6OHDA group, with the 10, 100, and 500ng/ml concentrations preserving cell viability at ~17% ($p<0.01$), ~28% ($p<0.01$), and ~26% ($p<0.01$) higher levels. The positive control, NGF preserved cell viability at substantially higher levels compared to the two higher doses of FGF20, as cell viability was preserved at ~97% in this treatment group (***Fig 5.4***).

Figure 5.4. FGF20 Protected PC12 Cells against 6OHDA Toxicity

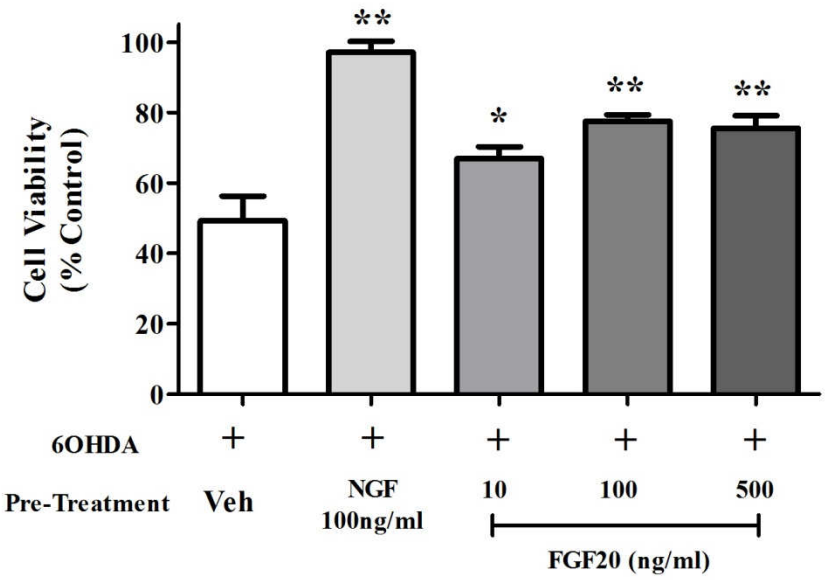

Figure 5.4. FGF20 concentration-dependently protected PC12 cells against 6OHDA toxicity. Cultures were treated with FGF20 for 24h, exposed to 6-OHDA for 6h, and their viability measured immediately thereafter using the MTS assay. Cell viability is expressed as a percentage of the absorbance that was observed in each group at 490nm relative to vehicle control. NGF served as a positive control. Data points represent mean±sem calculated from data generated in 3 independent repeat experiments. *$p<0.05$ and **$p<0.01$ compared to the FGF20 vehicle + 6OHDA group.

5.4.3. FGF20's Protective Effects are FGFR-Mediated

The selective FGFR inhibitor, PD173074 was used to investigate if FGF20's protective effects against 6ODHA toxicity were FGFR-mediated in PC12 cells. In ERK1/2 phosphorylation assays, both a 50nM and a 1000nM concentration of PD173074 completely blocked FGF20 stimulated ERK1/2 phosphorylation in the PC12 cells (***Fig 5.5.A***). In the un-stimulated control group, normalised phospho-ERK1/2 band densities were around ~0.17 arbitrary units. The 200ng/ml FGF20 treatment stimulated ~2 fold increase in ERK1/2 activation compared to control, as phospho-ERK1/2 band densities were ~0.3-0.4 in this group. Both of the concentrations of PD173074 completely blocked this FGF20 stimulated increase in ERK1/2 activation, as phospho-ERK1/2 band densities in the PD173074 + FGF20 groups were ~0.12-0.17, levels equivalent or slightly below that observed in the control group.

In cell viability experiments, PD173074 concentration-dependently inhibited FGF20's ability to protect PC12 cells against 6OHDA toxicity (***Fig 5.5.B***). In the FGF20 vehicle + 6OHDA group, cell viability was 36% (relative to control). FGF20 treatment preserved cell viability at significantly higher levels (~22% higher) vs. the FGF20 vehicle + 6OHDA group ($p<0.01$). PD173074 concentration–dependently inhibited FGF20's protective effects, with cell viability in the 0.1, 0.5, and 1µM PD173074 groups being ~12%, ~26%, and ~32% lower compared to the FGF20 + 6OHDA group, respectively. All of the PD173074 concentrations reduced cell viability levels to levels that were not significantly different to the FGF20 vehicle + 6OHDA group, and the cell viability levels in the 0.5, and 1µM PD173074 groups were also significantly lower compared to the FGF20 + 6OHDA group ($p<0.01$).

Figure 5.5. PD173074 Inhibited FGF20's Neuroprotective Effects against 6OHDA in PC12 Cells

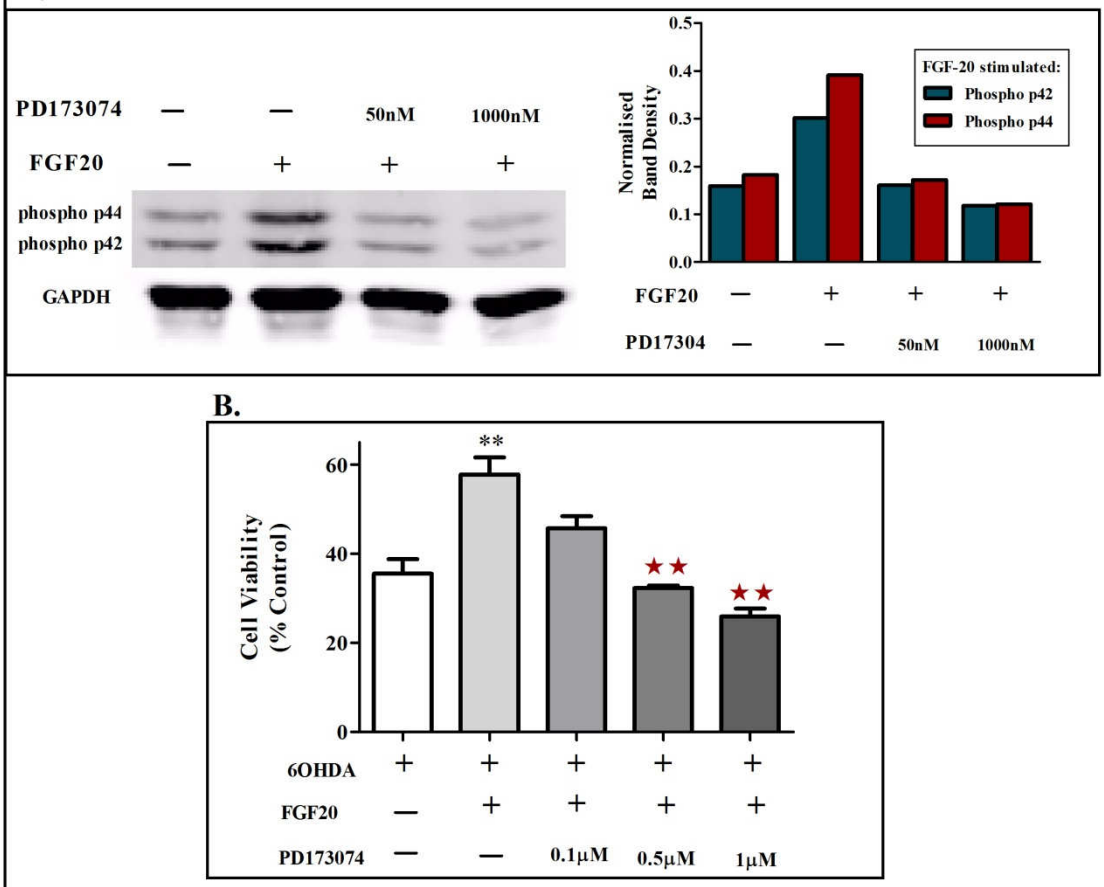

Figure 5.5. **A.** The FGFR inhibitor, PD173074 inhibited FGF20-induced activation of extracellular regulated kinase-1/2 (ERK1/2, p42/p44) in PC12 cells. Cells were exposed to FGF20 (200ng/ml) alone, or to FGF20 + PD173074 for 5min, and the cells immediately lysed thereafter. ERK1/2 phosphorylation was measured using Western blot analysis. All phosho-ERK1/2 band densities were normalised by adjusting them to corresponding GAPDH loading control bands. **B**. PD173074 concentration-dependently inhibited FGF20's protective effects against 6OHDA toxicity in PC12 cells. Cultures were treated for 24h with FGF20 (200ng/ml), or with FGF20 + PD173074, exposed to 6OHDA for 6h, and their viability measured immediately thereafter using the MTS assay. Cell viability is expressed as a percentage of the absorbance that was observed in each group at 490nm relative to vehicle control. Data points represent mean±sem calculated from data generated in 3 independent repeat experiments. **p<0.01 compared to the FGF-20 vehicle + 6OHDA group. ★★p<0.01 compared to the FGF-20 + 6OHDA group.

5.4.4. FGF20's Protective Effects against 6OHDA Toxicity are Mediated by the ERK1/2 MAPK Signalling Pathway

The MEK1/2 inhibitor, SL327 was used to investigate if FGF20's protective effects are mediated by the ERK1/2 MAPK signalling pathway at an intracellular level in PC12 cells. In ERK1/2 phosphorylation assays, both a 10µM and a 100µM concentration of SL327 completely blocked FGF20 stimulated ERK1/2 phosphorylation (***Fig 5.6.A***). In the un-stimulated control group, normalised phospho-ERK1/2 band densities were around ~0.12-0.22 arbitrary units. The 200ng/ml FGF20 treatment stimulated ~0.7-4 fold increase in ERK1/2 activation compared to control, as phospho-ERK1/2 band densities were ~0.31-0.45 in this group. Both of the concentrations of SL327 completely blocked this FGF20 stimulated increase in ERK1/2 activation, as phospho-ERK1/2 band densities in the SL327 + FGF20 groups were ~0.02-0.05, levels slightly below that observed in the control group.

In cell viability experiments, SL327 concentration-dependently inhibited FGF20's ability to protect PC12 cells against 6OHDA toxicity (***Fig 5.6.B***). In the FGF20 vehicle + 6OHDA group, cell viability was ~21% (relative to control). FGF20 treatment preserved cell viability at significantly higher levels (~14% higher) vs. the vehicle + 6OHDA group ($p<0.05$). PD173074 concentration–dependently inhibited FGF20's protective effects, with cell viability in the 0.1µM, 0.5µM, and 1µM SL327 groups being ~8%, ~11%, and ~17% lower compared to the FGF20 + 6OHDA group, respectively. Both the 50µM and 100µM SL327 concentrations reduced cell viability to levels not significantly different to the FGF20 vehicle + 6OHDA group, and the cell viability levels in all three of the SL327 groups were also significantly lower compared to the FGF20 + 6OHDA group ($p<0.01$).

Figure 5.6. SL327 Inhibited FGF20's Neuroprotective Effects against 6OHDA Toxicity in PC12 Cells

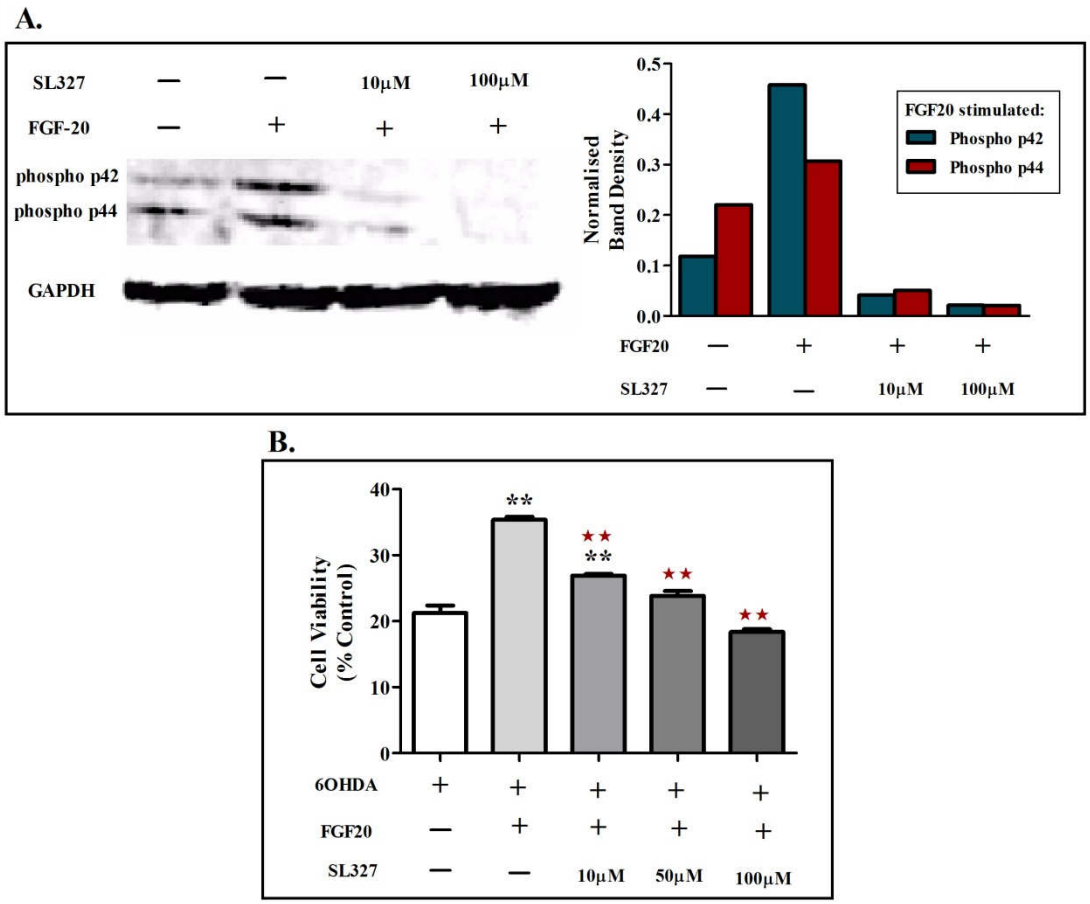

Figure 5.6. **A.** The MEK1/2 inhibitor, SL327 inhibited FGF20-induced activation of extracellular regulated kinase-1/2 (ERK1/2, p42/p44) in PC12 cells. Cells were exposed to FGF20 (200ng/ml) alone, or to FGF20 + SL327 for 5min, and the cells immediately lysed thereafter. ERK1/2 phosphorylation was measured using Western blot analysis. All phosho-ERK1/2 band densities were normalised by adjusting them to corresponding GAPDH loading control bands. **B**. SL327 concentration-dependently inhibited FGF20's protective effects against 6OHDA toxicity in PC12 cells. Cultures were treated for 24h with FGF20 (200ng/ml), or with FGF20 + SL327, exposed to 6OHDA for 6h, and their viability measured immediately thereafter using the MTS assay. Cell viability is expressed as a percentage of the absorbance that was observed in each group at 490nm relative to vehicle control. Data points represent mean±sem calculated from data generated in 3 independent repeat experiments. **p<0.01 compared to the FGF-20 vehicle + 6OHDA group. ★★p<0.01 compared to the FGF-20 + 6OHDA group.

5.4.5. The HSPG, Agrin Potentiates FGF20 Stimulated ERK1/2 activation, but Fails to Potentiate FGF20's Neuroprotective Effects against 6OHDA Toxicity

Agrin was investigated in ERK1/2 phosphorylation experiments for its ability to modulate FGF20's ability to stimulate ERK1/2 activation, and in cell viability experiments, agrin was also evaluated for its ability to modulate the ability of FGF20 to protect PC12 cells against 6OHDA toxicity.

In ERK1/2 phosphorylation experiments (***Fig 5.7***), no baseline ERK1/2 activation was detected in the un-stimulated control group, as normalised phospho-ERK1/2 band densities were around ~0.02-0.05 arbitrary units in this group. When agrin was applied alone, it failed to stimulate ERK1/2 phosphorylation, as phospho-ERK1/2 band densities of ~0.02-0.05 were detected in this group, densities similar to that observed in the control group. The sub-maximal 10ng/ml concentration of FGF20 also failed to stimulate any ERK1/2 activation when added alone, as phospho-ERK1/2 band densities of ~0.01 were detected in this group. The supra-maximal 200ng/ml concentration of FGF20, on the other hand, stimulated ERK1/2 activation when applied by itself, as phospho-ERK1/2 band densities of ~0.11-0.28 were detected in this group, levels ~5.5 fold higher than in the control cells. When the 10ng/ml FGF20 concentration was applied in combination with agrin, it stimulated ERK1/2 phosphorylation at levels at least equivalent to that stimulated by the supra-maximal 200ng/ml concentration of FGF20 when applied alone, as phospho-ERK1/2 band densities in this group were ~0.13-0.29. When the 200ng/ml concentration of FGF20 was applied in combination with agrin, an equivalent degree of ERK1/2 activation was stimulated compared to when it was applied alone. Agrin, thus, potentiated the degree of ERK1/2 activation stimulated by the sub-maximal concentration of FGF20, and it failed to modify the degree of ERK1/2 activation stimulated by the supra-maximal concentration of FGF20.

In cell viability studies, agrin failed to significantly potentiate the protective effects mediated by FGF20 in PC12 cells (***Fig 5.8***). In the vehicle + 6OHDA group, cell viability was ~56% (relative to control). The sub-maximal 10ng/ml FGF20 concentration when applied alone, failed to protect the PC12 cells against 6OHDA, as cell viability was not significantly different in this group compared to the vehicle + 6OHDA group. Agrin failed to alter the protective effect mediated by the 10ng/ml FGF20 conc., as cell viability in the agrin + 10ng/ml FGF20 group was not significantly different to that in either the vehicle + 6OHDA, or the agrin vehicle + 10/ng/ml FGF20 groups. The supra-maximal 200ng/ml FGF20 conc., on the other hand, significantly

protected the PC12 cells against 6OHDA toxicity, as cell viability was preserved at ~79% in this group, at levels significantly higher than compared to the vehicle + 6OHDA group ($p<0.01$). Interestingly, when the 200ng/ml FGF20 concentration was co-applied with agrin, cell viability actually decreased by ~6% compared to when the 200ng/ml concentration was added alone, lowering cell viability to levels that were no longer significantly higher compared to the vehicle treated 6OHDA group. The neuroprotective effect mediated by the supra-maximal FGF20 concentration, thus, appeared to have been inhibited by agrin rather than being potentiated.

Figure 5.7. Agrin Potentiated FGF20-induced ERK1/2 Activation in PC12 Cells

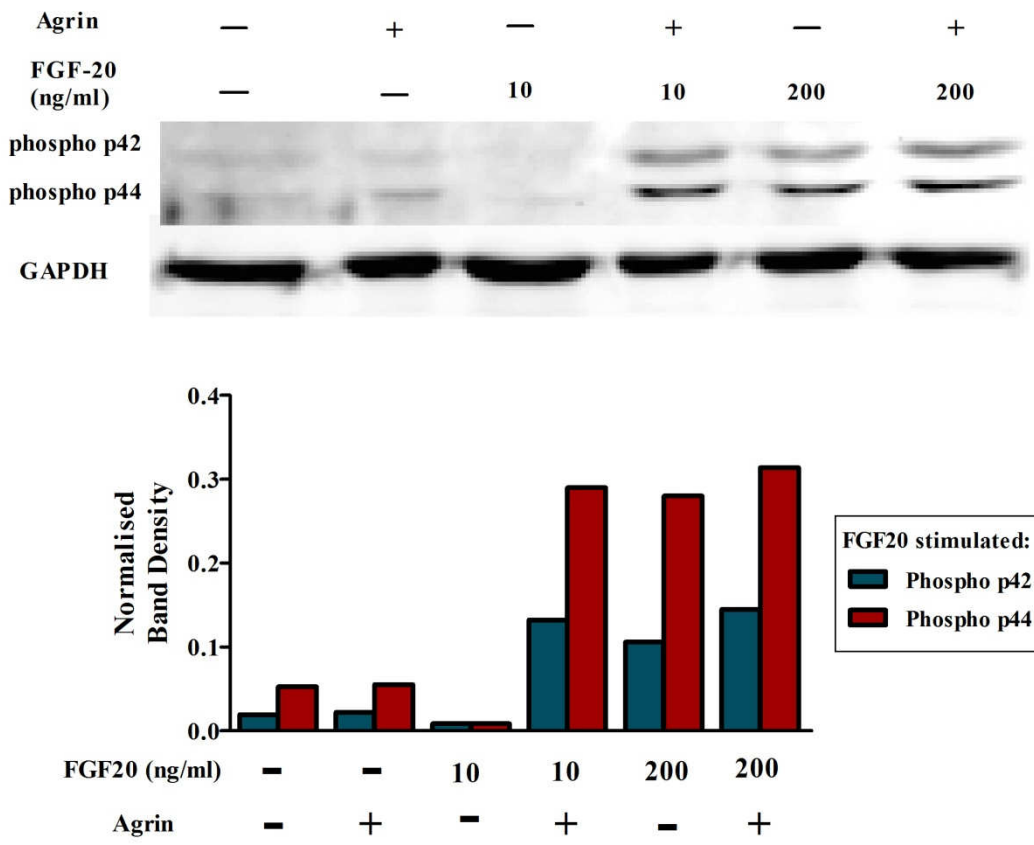

Figure 5.7. Agrin potentiated extracellular regulated kinase-1/2 (ERK1/2, p42/p44) activation stimulated by a sub-maximal concentration of FGF20. Cells were exposed to either FGF20 alone, or to FGF20 + Agrin (500ng/ml) for 5min, and the cells immediately lysed thereafter. ERK1/2 phosphorylation was measured using Western blot analyses. All phosho-ERK1/2 band densities were normalised by adjusting them to corresponding GAPDH loading control bands.

Figure 5.8. Agrin Failed to Potentiate FGF20's Neuroprotective Effects against 6OHDA Toxicity in PC12 Cells

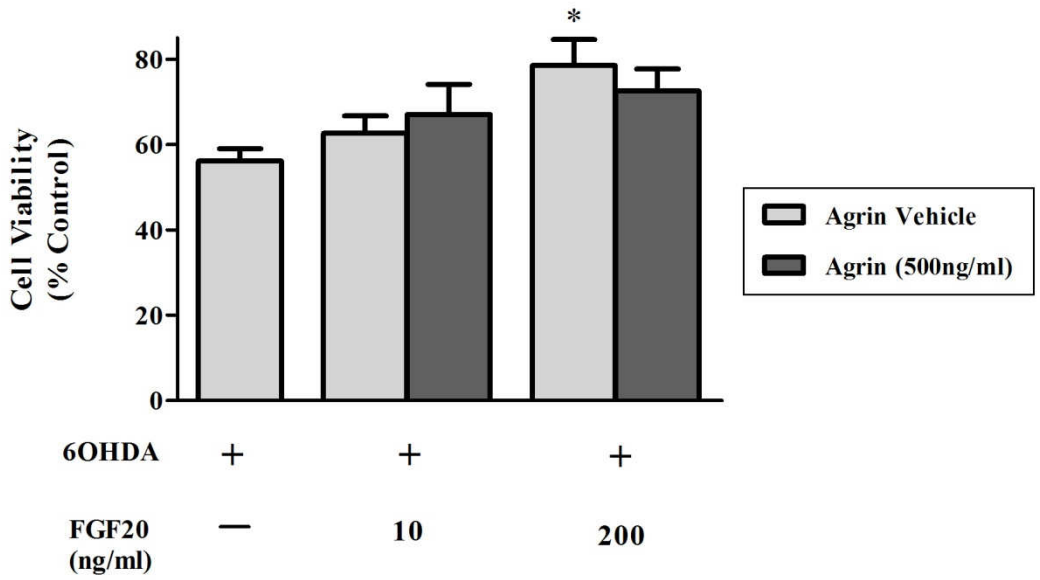

Figure 5.8. Agrin had no effect on the neuroprotective effects mediated by a sub-maximal FGF20 concentration (10ng/ml), and it appeared to ihnibit the protective effects mediated by a supra-maximal FGF20 concentration (200ng/ml). Cultures were treated for 24h with FGF20 alone, or FGF20 + Agrin (500ng/ml), exposed to 6-OHDA for 6h, and their viability measured immediately thereafter using the MTS assay. Cell viability is expressed as a percentage of the absorbance that was observed in each group at 490nm relative to vehicle control. Data points represent mean±sem calculated from data generated in 3 independent repeat experiments. *$p<0.05$ compared to the FGF-20 vehicle treated 6OHDA+ group.

5.5. Discussion

5.5.1. A Functional FGF Signalling System is Present in the PC12 Cell Line

In previous studies carried out as part of Chapter 4, FGF20 was shown to protect dopamine neurones against 6OHDA-induced cell death, *in vitro*, in VM embryonic cultures and also, *in vivo*, in the 6OHDA rat model of PD. In the current Chapter, a PC12 cell culture system was used to study the signalling mechanisms through which FGF20 mediates it neuroprotective effects against 6OHDA toxicity. The PC12 cell culture system was selected as an appropriate model to carry out these experiments not only because PC12 cells have a dopaminergic phenotype, but also because PC12 cells are known to possess a functional FGFR signalling system. PC12 cells have previously been shown to contain mRNA for FGFR1, 3, and 4, and the FGFs stimulate a number of biological responses in PC12 cells, including differentiation and cell survival (***detailed in section 5.1.8***). However, it is widely known that there is considerable variation between the phenotype of different PC12 cell sub-clones, and some sub-clones of PC12 cells have been found to be un-responsive to FGF (Altin *et al.*, 1991; Lin *et al.*, 1996). For this reason, several validation experiments were carried out to ensure that the clone of PC12 cells used in this study does, indeed, contain a functional FGF system. Using immunohistochemistry, it was evaluated whether the FGFR1, 3, and 4 proteins were present in the PC12 cells, and FGFR1 and 3 but not FGFR4 were found to be localised in the PC12 cell line. It was not examined if FGFR2 is present, but this receptor is unlikely to be present, as two previous studies have reported FGFR2 mRNA not to be expressed in PC12 cells (Foehr *et al.*, 1998; Muller-Ostermeyer *et al.*, 2001). Interestingly, for both FGFR1 and FGFR3, a cytoplasmic staining pattern was observed in some cells, while in other cells, the receptors were localised to both the cytoplasm and also to the nucleus. The FGFRs are RTKs, and they are, therefore, traditionally considered to exist and function as classical plasma membrane receptors that signal through various second messenger systems. Recent findings have, however, conclusively demonstrated that a number of plasma membrane receptors also signal through an unorthodox nuclear signalling pathway that involves the translocation of the receptors from the plasma membrane to the nucleus, and the FGFRs are a prototypical example of such receptors (Bryant & Stow, 2005). Activation of membrane bound FGFR1 by FGF2, for example, leads to the nuclear translocation of some of the FGFR1-FGF2 complexes (Bryant & Stow, 2005), and this nuclear translocation has been shown

to be essential in allowing FGFR1's full mitogenic effects to be expressed (Bossard *et al.*, 2003). This concomitant nuclear and cytoplasmic localisation of the FGFR1 and FGFR3, thus, indicates that these receptors might signal through such a nuclear signalling pathway in the PC12 cells. Results showing FGFR4 not to be present in the PC12 cell line conflicts with previous studies which showed mRNA for FGFR1, 3, and 4 to be present in PC12 cells (Foehr *et al.*, 1998; Muller-Ostermeyer *et al.*, 2001). As mentioned before, the phenotype of different PC12 cell sub-clones are known to vary considerably, and it is possible that the specific sub-clone used in this study had ceased to express FGFR4. Furthermore, the previous studies have only demonstrated FGFR4 mRNA to be present in the PC12 cells, and results from this study are the first to characterise the localisation of the FGFR proteins in PC12 cells. Alternatively, this discrepancy could, thus, be due to FGFR4 mRNA being expressed but not translated in the PC12 cells.

After ascertaining that the PC12 cell line used in this study did, indeed, express the FGFR1 and 3 proteins, experiments were subsequently carried out to confirm that the receptors are not only present but also functional and coupled to downstream intracellular signalling pathways. The FGF prototype, FGF2 has previously been shown to stimulate ERK1/2 phosphorylation in PC12 cells (Foehr *et al.*, 1998; Kim *et al.*, 2003). The functionality of the FGF system was therefore tested by evaluating whether not only FGF20 but also FGF2 is able to stimulate ERK1/2 phosphorylation in the PC12 cells. Additionally, NGF was also used in these experiments as an additional positive control, as PC12 cells are widely known to be responsive to NGF (Sabban, 1997; Spear *et al.*, 1997; Wert & Palfrey, 2000b; Shimoke & Chiba, 2001; Kavanagh *et al.*, 2006). Results from these ERK1/2 phosphorylation studies confirmed that the FGFRs in the PC12 cells were, indeed, functional, as both FGF2 and FGF20 stimulated an increase in ERK1/2 phosphorylation in the cells. Interestingly, a supra-maximal concentration of NGF was found to have a substantially greater potency at stimulating ERK1/2 activation compared to a supra-maximal dose of FGF2 and FGF20. As previous studies have reported FGF2 to produce a similar degree of ERK1/2 activation in PC12 cells as seen in this study (Foehr *et al.*, 1998; Muller-Ostermeyer *et al.*, 2001), it appears that, at least in PC12 cells, the FGF system is more weakly linked to the ERK1/2 MAPK pathway compared to the NGF system.

5.5.2. FGF20 Protects PC12 Cells against 6OHDA Toxicity

After confirming that the PC12 cells possessed functional FGFRs, a number of subsequent cell survival experiments were then carried out, firstly to demonstrate that FGF20 is, indeed, able to protect PC12 cells against 6OHDA toxicity, and secondly to try and identify the signalling mechanisms mediating FGF20's protective effects. In the initial neuroprotection studies in which FGF20 was evaluated for its ability to protect PC12 cells against 6OHDA, FGF20 was found to concentration-dependently protect the PC12 cells against 6OHDA toxicity. A 10ng/ml concentration of FGF20 mediated a significant but sub-maximal protective effect against 6OHDA, while a maximal protective effect was produced by a 100ng/ml concentration of FGF20. Based on these results, a 200ng/ml supra-maximal concentration of FGF20 was used in all subsequent cell viability studies carried out to identify the signalling mechanisms mediating FGF20's protective effects against 6OHDA. Moreover, in these initial neuroprotection experiments, a supra-maximal concentration of FGF20 was found to preserve PC12 cell viability at around ~20% higher levels compared the 6OHDA control group. Interestingly, the NGF positive control treatment had a much more potent neuroprotective effect, as NGF preserved cell viability at control levels, at levels around 30% higher compared to the maximal effect achieved by FGF20. In later experiments, FGF20's protective effects against 6OHDA toxicity was shown to be mediated by the ERK1/2 MAPK signalling pathway, and this difference in neuroprotective potency could, thus, be down to the fact that NGF has a substantially greater potency at stimulating ERK1/2 activation, as demonstrated by results from the phosphorylation experiments.

5.5.3. FGF20's Neuroprotective Effects in PC12 Cells against 6OHDA is Mediated through the FGFRs at the Receptor Level

FGF20 appears to be a relatively non-selective agonist at its cognate receptors, the FGFRs, as FGF20 is able to stimulate mitogenesis through most of the FGFR subtypes (Zhang *et al.*, 2006). There have, however, been no specific investigations, thus far, investigating whether FGF20 is capable of stimulating any biological effects by non-selectively activating receptors other than the FGFRs. As most receptor agonists stimulate effects by non-selectively activating receptors that are not designated as their cognate receptor class, it is possible that FGF20's protective effects might in full or in

part result from it non-selectively activating receptors other than the FGFRs. Thus, to confirm that FGF20's neuroprotective effects are, indeed, mediated by the FGFRs, it was evaluated whether FGF20's protective effects could be inhibited by the selective FGFR antagonist, PD173074. In these experiments, PD173074 concentration-dependently inhibited FGF20's neuroprotective effects against 6OHDA, with a 100nM concentration of PD173074 preventing a supra-maximal concentration of FGF20 from having a significant protective effect. These results indicate that FGF20's protective effects are, indeed, being wholly mediated through an FGFR-dependent mechanism. However, although PD173074 is a relatively selective inhibitor at the FGFRs, it is also known to have antagonistic effects at the vascular epithelial growth factor receptor 2 (VEGFR2) at concentrations of ~100nM. PC12 cells express the VEGFR2, and activation of this receptor has been shown to stimulate anti-apoptotic effects in PC12 cells (Berger *et al.*, 2006). The possibility that FGF20's neuroprotective effects could be partially mediated through the VEGFR2 can, therefore, not be ruled out.

Moreover, as PD173074 is a non-selective inhibitor of the FGFRs, it cannot be directly concluded from these results which specific FGFR subtype FGF20 is mediating its neuroprotective effects through. However, based on the immunohistochemical results showing the PC12 cell line to only express FGFR1 and 3, and also on previous findings showing FGFR2 mRNA not to be present in PC12 cells, it can be deduced that FGF20's protective effects are most likely mediated through the FGFR1 and/or FGFR3 in the PC12 cells used in this study. To determine the extent to which FGF20 mediates its protective effects through activation of each the two FGFR receptor subtypes, further experiments with inhibitors selective for the FGFR1 and FGFR3 would be needed. This is, however, currently not possible, due to inhibitors selective for the latter receptors currently not being commercially available.

5.5.4. FGF20's Neuroprotective Effects in PC12 Cells against 6OHDA is Mediated through the ERK1/2 MAPK Pathway at the Intracellular Level

After showing FGF20's effects to be mediated by the FGFRs at the receptor level, experiments were carried out to investigate the signalling pathways mediating FGF20's protective effects at an intracellular level. Activation of the FGFRs in PC12 cells have been shown to lead to the recruitment and activation of many of the classical RTK linked intracellular signalling pathways, including the PI3K, PKC, and various MAPK pathways (***detailed in section 5.1.8***). Of all these intracellular signalling pathways

recruited by FGFR activation, only the ERK1/2 MAPK and the PI3K pathways have, however, been implicated in mediating the pro-survival effects stimulated by FGFR activation in PC12 cells. As the ERK1/2 MAPK signalling pathway has most widely been reported to mediate the protective and/or pro-survival effects stimulated by FGFR activation, not only in PC12 cells, but also in many other tissues and animal models, experiments were carried out to investigate whether this pathway was mediating FGF20's protective effects in the PC12 cells. To do this, it was evaluated if the selective MEK1/2 inhibitor, SL327 is able to inhibit FGF20's neuroprotective effects against 6OHDA toxicity in the PC12 cells. In these experiments, SL327 concentration-dependently inhibited FGF20's protective effects, with a 10µM concentration of SL327 significantly inhibiting FGF20's protective effects, and a 50µM concentration completely abolishing FGF20's neuroprotective effects. The concentrations of SL327 used in these experiments are consistent with that commonly used in the literature to selectively inhibit MEK1/2 (Caughlan *et al.*, 2004; Chen-Roetling *et al.*, 2009; Lee *et al.*, 2010). These results, thus, show that FGF20's neuroprotective effects in PC12 cells are mediated through the ERK1/2 MAPK pathway.

The results showing FGF20 to protect against 6OHDA toxicity in PC12 cells are consistent with results from the Murase & McKay, 2006 study and from the VM neuroprotection experiments carried out in this thesis in Chapter 4 which showed FGF20 to protect dopamine neurones in VM embryonic cultures against 6ODHA toxicity. The magnitude of the maximal protective effect mediated by FGF20, however, differed substantially between the two culture systems. In the VM cultures, FGF20 - both in the VM study carried out in Chapter 4 and in the Murase & McKay, 2006 study – preserved TH+ cell numbers at control levels, whereas in the PC12 cells, FGF20 only preserved cell viability at around 70% compared to control, and at ~20% higher levels compared to the 6ODHA group. FGF20's more pronounced neuroprotective potency in the VM culture system compared to the PC12 cells could be due to a number of reasons. One explanation for the difference could be that the FGFRs in the PC12 cells are less responsive than those present in the VM cultures. This is, however, unlikely to be the case, as the degree of ERK1/2 phosphorylation stimulated by FGF20 in VM cultures in the Murase & McKay, 2006 study appears to be equivalent to that observed in the PC12 cells in this study. Another explanation might be that FGF20 stimulates the recruitment of a more limited number of pro-survival pathways in the PC12 cells compared to the VM cultures. Support for this possibility is provided by the fact that FGF20's protective

effects on VM dopamine neurones were shown to be mediated through both the ERK1/2 and the PI3K pathways (Murase & McKay, 2006), whereas in this study it appeared that FGF20's protective effects were wholly mediated by the ERK1/2 signalling pathway. However, results from this study do not rule out the possibility that other signalling pathways are also involved in mediating the protective effects of FGF20 against 6OHDA in the PC12 cells, as the role of other signalling pathways were not specifically investigated in this study. The latter explanation for the discrepancy in FGF20's neuroprotective potency in the two culture systems could, therefore, only be considered plausible if results from further studies specifically demonstrate the PI3K or other pathways not to be involved in mediating FGF20's protective effects in PC12 cells. In Chapter 2, FGFR1, 3, and 4 were shown to be abundantly localised in astrocytes within VM cultures, and the neuroprotective effects mediated by the FGFs have been demonstrated to be at least partially mediated by an astrocyte-dependent indirect mechanism (***detailed in section 4.1.4***). Therefore, if this is also the case with FGF20, the less potent neuroprotective effects observed in the PC12 cells could be due to the absence of astrocytes within the PC12 cells.

The primary toxic events induced by 6OHDA in cells include increased ROS production, inactivation of endogenous anti-oxidant mechanisms, and inhibition of mitochondrial respiratory chain enzymes (***detailed in section 3.1.1.4.3***). These 6OHDA-induced toxic events then in turn stimulate increased activity of pro-apoptotic signals and/or decreased activity of anti-apoptotic signals in the cells. The overall pro-apoptotic signalling environment in the cell then leads to the activation of caspase enzymes, which act to induce cell death through the controlled breakdown of the cell contents. It is, thus, possible for a neuroprotective treatment to protect against 6OHDA-induced cell death by inhibiting the primary toxic events induced by 6OHDA and/or by counteracting the pro-apoptotic signalling events that are triggered by the primary 6OHDA-induced toxic events. In the first instance, a neuroprotective treatment can, for example, stimulate an upregulation of endogenous anti-oxidant systems within the cells, which then acts to reduce the toxic levels of ROS induced by 6OHDA to non-toxic levels, and by doing so it could prevent the ROS initiated activation pro-apoptotic signalling pathways. In the second instance, a neuroprotective treatment can, for example, prevent 6ODHA-induced apoptosis by upregulating anti-apoptotic signalling pathways and/or by downregulating pro-apoptotic pathways. Alternatively, a treatment could potentially also act further downstream of the apoptotic cascades, by inhibiting

the activation of caspase enzymes. As neuroprotective treatments, especially in the case of growth factors, are known to activate a number of different intracellular signalling pathways, it is likely that their neuroprotective effects are mediated through a number of different anti-apoptotic effector mechanisms. Recent results, however, indicate that ERK1/2-stimulated anti-apoptotic effects are not mediated by effector mechanisms that attenuate any of the primary toxic effects of 6OHDA, but rather through modulation of apoptotic signalling pathways downstream of the toxic events. No effector mechanisms targeting any of the primary 6OHDA-induced toxic events have, thus far, been identified to mediate the anti-apoptotic effects of ERK1/2 activation. There are, however, numerous reports, on the other hand, that have implicated a number of different effector mechanisms targeting apoptotic signalling pathways to be responsible for mediating the anti-apoptotic effects mediated by ERK1/2 activation (Lu & Xu, 2006). The specific anti-apoptotic mechanism through which ERK1/2 mediates its pro-survival effects, however, appears to be dependent on the specific experimental context. Some of the specific apoptotic mechanisms through which ERK1/2 brings about its pro-survival effects have been shown to include inactivation of the pro-apoptotic bcl2 family members, BAD and BIM, stimulation of the activity of the anti-apoptotic Bcl-2 family member, Mc-1, inhibition of caspase activation, stimulation of the activity of the caspase inhibitor, C-flip, and upregulation and downregulation of the anti-apoptotic transcription factor, cAMP response element binding (CREB), and the pro-apoptotic transcription factor, STAT3/5, respectively (Lu & Xu, 2006). Furthermore, FGF20 has been shown to stimulate an upregulation of the anti-apoptotic protein BAD, and downregulation of the pro-apoptotic Bax protein in VM dopamine neurone cultures (Murase & McKay, 2006). Based on these findings, it is, thus, likely that the ERK1/2-dependent neuroprotective effects stimulated by FGF20 in the PC12 cells are also ultimately brought about by effector mechanisms modulating apoptotic signals as to favour cell survival.

As the specific signalling pathways mediating the neuroprotective effects stimulated by FGFR activation could potentially become therapeutic targets for PD, further research is needed to identify the specific signalling pathways mediating the neuroprotective effects stimulated by the FGFs and other neurotrophins. In particular, there is a need for more research aimed at identifying the signalling pathways mediating the neuroprotective effects of the FGFs on dopamine neurones at the *in vivo* level, as most of the literature in this area is currently based on only *in vitro* findings. Moreover,

it is possible that superior neuroprotective effects might be achieved if two or more neurotrophins from different growth factor families are co-administered. And it is likely that such a neurotrophin combination therapy would have the greatest likelihood of having superior therapeutic effects if the different neurotrophins used all bring about their neuroprotective effects through differing intracellular mechanisms. The availability of extensive knowledge about the specific mechanisms mediating the neuroprotective effects of different neurotrophins would, thus, also allow for the selection of the most appropriate neurotrophin combinations to evaluate in neuroprotection studies.

5.5.5. The HSPG, Agrin potentiates FGF20 Stimulated ERK1/2 Activation, but it Fails to Potentiate FGF20's Neuroprotective Effects against 6OHDA in PC12 Cells

The HSPGs are known to play an important role in modulating FGFR signalling. The HSPG, agrin has previously been demonstrated to potentiate FGF2 stimulated ERK1/2 activation and neurite outgrowth in PC12 cells (Kim *et al.*, 2003). In the current study it was investigated whether agrin is also able to potentiate FGF20 stimulated ERK1/2 activation in PC12 cells. Additionally, experiments were also carried out to evaluate if agrin is able to potentiate FGF20's neuroprotective effects in the PC12 cells. Results from these experiments showed that agrin modulated FGF20's ability to stimulate ERK1/2 activation in PC12 cells in an equivalent manner to that reported for FGF2 (Kim *et al.*, 2003). In this study, agrin did not stimulate any ERK1/2 activation when applied alone, but when concurrently applied with FGF20, it potentiated the magnitude of ERK1/2 activation stimulated by a sub-maximal but not a supra-maximal concentration of FGF20. Interestingly, agrin, however, failed to potentiate the neuroprotective effects mediated by both a sub and supra-maximal concentration of FGF20 in cell viability experiments. In ERK1/2 phosphorylation experiments, a 10ng/ml sub-maximal concentration of FGF20 failed to stimulate an increase in ERK1/2 phosphorylation when applied alone. But when agrin was co-applied with the 10ng/ml concentration of FGF20, agrin potentiated the FGF20 stimulated ERK1/2 activation to levels equivalent to that observed with a supra-maximal FGF20 concentration. This potentiated FGF20 stimulated ERK1/2 activation, however, did not result in the sub-maximal concentration of FGF20 producing a significantly greater degree of neuroprotection. This is surprising, as FGF20's protective effects were completely inhibited when ERK1/2 signalling was blocked with SL327. One would, thus, have

expected the potentiated ERK1/2 activation to have resulted in the 10ng/ml FGF20 concentration producing a significant protective effect when it was co-applied with agrin. A possible explanation for this could be that agrin mediates some additional pharmacological effects on the PC12 cells which act to inhibit FGF20's neuroprotective effects, with these inhibitory effects being pronounced enough to counteract the increased protective effects which might result from its potentiating effects on FGF20 stimulated ERK1/2 activation. Indeed, the results showing agrin to actually inhibit the neuroprotective effects mediated by the supra-maximal concentration of FGF20, provides strong evidence that this is indeed the case. Additionally, further support for this possibility is provided by results from two studies which showed heparin to inhibit the biological effects stimulated by FGF2. In one study, heparin inhibited FGF2's ability to protect endothelial cells against hyperglycaemia-induced cell death (Han *et al.*, 2005), while in another study heparin partially inhibited the neurotrophic effects mediated by a low concentration of FGF2 in PC12 cells (Neufeld *et al.*, 1987).

These results, however, do not rule out the possibility that FGF20's protective effects could be potentiated by a different type of HSPG molecule. The modulating effects that HSPGs have on FGF signalling have been shown to be fairly complex. The heparin sulphate side chains of HSPGs consist of linear polysaccharide chains composed of repeating sulphated disaccharide units (Yanagishita & Hascall, 1992). The existence of several different disaccharide building blocks, with varying spatial sulphation patterns, gives rise to a large number of heparin sulphate polymer subtypes, and HSPG's with different sulphation patterns have been shown to mediate different biological effects (***detailed in section 5.1.6***). It is, thus, possible that the specific sulphation pattern and/or chemical composition of agrin results in it being able to potentiate FGF20 stimulated ERK1/2 activation, but not FGF20's neuroprotective effects against 6OHDA toxicity. A different HSPG with an alternative sulphation pattern and/or chemical structure might, thus, potentially be able to potentiate FGF20's neuroprotective effects. Further studies are, therefore, needed to more thoroughly investigate the potential that HSPGs and HSPG-like molecules might have in potentiating the neuroprotective effects of FGF20. In Chapter 4, FGF20 was shown to protect nigrostriatal dopamine neurones in the 6OHDA rat model of PD. The magnitude of the neuroprotective effect mediated by FGF20 in this study was, however, only moderate. In the study, 6ODHA induced a reduction in striatal TH levels and nigral TH+ cell counts of ~54% and ~71%, respectively, in the vehicle treated rats, and the

highest and most effective dose of FGF20 tested preserved striatal TH levels and nigral TH+ cell counts at ~20% higher levels compared to the vehicle treated 6OHDA lesioned rats. The discovery of a specific HSPG with the ability to potentiate FGF20's neuroprotective effects on dopamine neurones, would, thus, further increase FGF20's therapeutic potential as a neuroprotective treatment in PD. Heparin is a highly sulphated glycosaminoglycan, and despite this molecule lacking the proteoglycan core that is present in HSPGs, it has been demonstrated to increase FGF2's stability in solution (Caldwell *et al.,* 2004), and also to potentiate a number of different biological effects stimulated by the FGFs, including neurite outgrowth and mitogenesis (Damon *et al.*, 1988; Caldwell & Svendsen, 1998). Importantly, heparin has specifically been shown to potentiate the pro-survival effects mediated by FGF2 in a number of different contexts (Unsicker *et al.*, 1987; Sensenbrenner, 1993; Renaud *et al.*, 1996; Bouleau *et al.*, 2007). It would, thus, be worthwhile investigating whether heparin might be able to potentiate FGF20's protective effects.

5.5.6. Conclusion

In chapter 4, FGF20 was shown to protect dopamine neurones against 6OHDA toxicity both, *in vitro*, in VM embryonic cultures, and also, *in vivo*, in the 6OHDA rat model of PD. In the current Chapter, cell viability studies were carried out in PC12 cells to try and identify the signalling pathways mediating FGF20's neuroprotective effects against 6ODHA toxicity. Results from this study show for the first time that FGF20 is also able to protect PC12 cells against 6ODHA toxicity. Furthermore, FGF20's neuroprotective effects against 6OHDA toxicity was found to be mediated by the FGFRs at the receptor level, and by the ERK1/2 MAPK pathway at the intracellular level in the PC12 cells. HSPGs play an important role in modulating the signalling and biological effects stimulated by the FGFs. In the current study it was evaluated whether the HSPG, agrin is able to modulate FGF20's ability to stimulate ERK1/2 phosphorylation in PC12 cells and/or its ability to protect PC12 cells against 6OHDA toxicity. In these studies, agrin was found to potentiate FGF20 stimulated ERK1/2 activation, but it failed to potentiate FGF20's neuroprotective effects against 6OHDA in the PC12 cells.

6. General Conclusion

There is currently an urgent clinical need for more effective treatments for the motor symptoms in PD. Since all of the currently available treatments for PD fail to slow down the ongoing nigrostriatal degeneration that occurs in PD, there is in particular a need for new neuroprotective treatments that are able to slow or halt disease progression by preventing the remaining functional nigrostriatal dopaminergic neurones in the PD brain from degenerating. Recent findings have demonstrated FGF20 to have neuroprotective effects on dopaminergic neurones, *in vitro*. These findings can be taken to suggest that FGF20 might have neuroprotective potential in PD, and the studies undertaken in this thesis aimed to further investigate FGF20's neuroprotective potential. Two of the primary aims of this thesis were, firstly, to confirm FGF20's previously reported *in vitro* neuroprotective effects, by testing if FGF20 was able to protect VM embryonic dopamine neurones against 6OHDA, and, secondly, to evaluate for the first time whether FGF20's neuroprotective effects on dopamine neurones are also present *in vivo*, in the partially lesioned 6OHDA rat model of PD.

Prior to carrying out the planned *in vitro* and *in vivo* neuroprotection studies with FGF20, it was important to ensure that FGF20's receptors, the FGFRs were, indeed, present in both of the abovementioned model systems. Therefore, in Chapter 2, using immunohistochemistry, the colocalisation profiles of FGF20, and the FGFR1, 3, and 4 were characterised in detail in both VM cultures, and in the nigrostriatal tract of rats. Results from these studies demonstrated the FGFR1, 3, and 4 to be present abundantly within VM cultures and also throughout the nigrostriatal tract of the rat brain. In a previous study, FGFR2 has also been shown to be present in the SN and striatum, although it was found to be exclusively localised to astrocytes (Chadashvili & Peterson, 2006). The widespread presence of all 4 of the FGFRs within the nigrostriatal tract, and more particularly, the localisation of FGFR1, 3, and 4 to nigrostriatal dopamine neurones, provided a sound anatomical rationale for investigating the neuroprotective potential that pharmacological activation of the FGF system might have in PD. Furthermore, if the FGFs are protecting dopamine neurones by directly activating FGFRs on nigrostriatal dopamine neurones, the immunohistochemistry results indicated that targeting the FGF system at the level of the substantia nigra, rather than the striatum, is likely to have the greatest neuroprotective potential. This is as, at the nigral level, FGFR1, 3, and 4 were found to be present in TH+ nigrostriatal

dopamine neurones within the SNc. In the striatum, on the other hand, only FGFR1 co-localised with striatal dopamine neurone terminals, and of all the TH+ striatal nerve terminals, only a subset appeared to be positive for FGFR1.

In Chapter 3 of this thesis, experiments were carried out with the aim of establishing an appropriate partially lesioned 6OHDA rat model of PD, in which FGF20 could be evaluated for its neuroprotective effects on dopamine neurones, *in vivo*. To accomplish this objective, 6OHDA dose-response experiments were carried out to identify an intra-nigrally delivered dose of 6OHDA that induces an ~60-80% partial nigrostriatal lesion. Full nigrostriatal 6OHDA lesions induce robust motor impairments in rats which can be easily measured by numerous behavioural tests of motor function. Partial 6OHDA-induced nigrostriatal lesions, on the other hand, produce more subtle motor deficits which can only be detected by a number of the more sensitive motor tests. Therefore, two drug-induced motor tests (apomorphine and amphetamine induced rotations) and two spontaneous motor tests (adjusted stepping test and cylinder test) were evaluated in the dose response experiments to identify tests that are capable of detecting motor deficits induced by a partial 6OHDA lesion. In these studies, a 6OHDA lesioning procedure that induces a negligible degree of non-specific nigrostriatal degeneration by itself was successfully developed. The use of an injection needle with the smallest possible gauge and also a physiological vehicle solution, in the lesioning procedure, was demonstrated to be essential in minimising non-specific nigrostriatal degeneration. Importantly, in the 6OHDA dose-response studies, a 4µg 6OHDA dose was identified as producing an appropriate partial nigrostriatal dopaminergic lesion, while both a 6µg and an 8µg dose was found to induce an undesirable near complete lesion. Based on these results it was decided that, the ability of FGF20 to protect against a partial nigrostriatal lesion would be evaluated in rats that have received a 4µg intra-nigrally delivered dose of 6OHDA. Furthermore, the cylinder test and the amphetamine-induced rotational test were identified as being the only tests with the appropriate degree of sensitivity to allow them to be used to assess if FGF20 improves the motor deficits induced by the partial nigrostriatal lesion. To successfully evaluate FGF20's neuroprotective efficacy, *in vivo*, it was also essential that a biologically active dose of the growth factor was tested. By using phosho-ERK1/2 as a marker of FGF20 mediated FGFR1 activation, an attempt was made in Chapter 3 to identify a biologically active intra-nigrally delivered dose of FGF20, but, unfortunately, this study failed to successfully identify a biologically active dose. Therefore, it was

decided that a range of FGF20 doses based on findings from pilot studies previously conducted in this lab would be used in the *in vivo* neuroprotection study.

In Chapter 4, studies were carried out to evaluate if FGF20 is able to protect dopamine neurones both *in vitro* and *in vivo*. FGF20 has previously been shown to protect dopamine neurones, *in vitro*, against a number of different insults, and the first objective of this Chapter was to confirm these findings by evaluating whether FGF20 was able to protect VM dopamine neurones against 6OHDA toxicity. A VM embryonic dopamine neurone culture system was established, and neuroprotection experiments carried out with FGF20 in the VM cultures, and results from these experiments demonstrated FGF20 to protect VM dopaminergic neurones against 6OHDA toxicity, confirming the previously published findings. Thus far, there are no published studies that have investigated whether FGF20's neuroprotective effects on dopamine neurones are also present, *in vivo*, in animal models of PD. Therefore, experiments were subsequently carried out to evaluate whether FGF20 has neuroprotective effects on dopamine neurones in the partial 6OHDA rat model of PD established within Chapter 3. In this study, FGF20 was continuously and chronically delivered to the SN of the 6OHDA lesioned rats with the use of osmotic mini-pumps that were connected to chronically implanted supra-nigral cannulae. Results from the neuroprotection study shows for the first time that FGF20 is also able to protect dopamine neurones in the partially lesioned 6OHDA rat model of PD. Importantly, FGF20 not only protected nigrostriatal dopaminergic neurones against 6OHDA-induced degeneration, but it also preserved motor function to some degree in the 6OHDA lesioned rats. The FGF system plays an important physiological role in both the developing and the intact adult nigrostriatal dopaminergic system, and evidence from a number of studies has indicated that one of the main roles of the endogenous FGF system in the nigrostriatal tract is to stimulate and maintain the survival of dopamine neurones. In a separate *in vivo* study carried out in Chapter 4, it was evaluated if the endogenous FGF system does, indeed, play a role in protecting nigrostriatal dopamine neurones by evaluating whether chronic pharmacological inhibition of FGFR signaling potentiates 6OHDA-induced nigrostriatal dopamine neurone degeneration in the rat. Results from this study suggest that the endogenous FGF system might, indeed, play a protective role in the nigrostriatal tract, although further studies are needed to provide more conclusive evidence for this.

After demonstrating FGF20 to protect dopamine neurones against 6OHDA toxicity both, *in vitro* and *in vivo*, further *in vitro* experiments with FGF20 were carried

out in Chapter 5, this time in PC12 cells, to investigate the signalling mechanisms mediating FGF20's neuroprotective effects against 6OHDA toxicity. More specifically, experiments were carried out to determine if FGF20's neuroprotective effects are, indeed, mediated by the FGFRs, and at the intracellular level, it was evaluated if FGF20's neuroprotective effects are mediated by the ERK1/2 MAPK pathway. Results from these experiments reveal, for the first time, that FGF20 is able to protect PC12 cells against 6ODHA toxicity. Furthermore, with the use of selective inhibitors, FGF20's neuroprotective effects against 6OHDA toxicity were found to be mediated by the FGFRs at the receptor level, and by the ERK1/2 MAPK pathway at the intracellular level in the PC12 cells. The HSPGs play an important role in modulating FGF signaling, and the HSPG, agrin, when co-applied with FGF2, potentiates both FGF2-stimulated ERK1/2 activation and neurite outgrowth in PC12 cells. In additional studies, experiments were carried out not only to evaluate whether agrin is able to potentiate FGF20 induced ERK1/2 activation, but also whether agrin is able modulate FGF20's neuroprotective effects against 6OHDA toxicity in PC12 cells. In this study, agrin was found to potentiate FGF20 stimulated ERK1/2 activation, but it failed to potentiate FGF20's neuroprotective effects against 6OHDA in the PC12 cells.

Taken together, the findings presented in this thesis provide further support for the neuroprotective potential of FGF20 in PD. Together with findings from others showing several members of the FGF family to have neuroprotective effects on dopamine neurones in pre-clinical models of PD, these results also, more generally, provide further support for the FGFRs in the nigrostriatal tract being a promising neuroprotective therapeutic target in PD. Due to the technical difficulties in delivering growth factors to the brains of PD patients, the most effective way of utilising the FGF system to treat PD would, however, be to develop small molecule agonists targeting the FGFRs. For this reason, further research is needed to identify the specific FGFR subtype(s) that are responsible for mediating the neuroprotective effects of the FGFs, so that small molecule systemically active agonists selective for these receptors could be developed and assessed for their neuroprotective efficacy in future studies

7. References

Agarwala S & Kalil RE. (1998). Long-term protection of axotomized neurons in the dorsal lateral geniculate nucleus in the rat following a single administration of basic fibroblast growth factor or ciliary neurotrophic factor. *The Journal of comparative neurology* **392,** 264-272.

Agid Y, Cervera P, Hirsch E, Javoy-Agid F, Lehericy S, Raisman R & Ruberg M. (1989). Biochemistry of Parkinson's disease 28 years later: a critical review. *Movement disorders : official journal of the Movement Disorder Society* **4 Suppl 1,** S126-144.

Alexi T, Borlongan CV, Faull RL, Williams CE, Clark RG, Gluckman PD & Hughes PE. (2000). Neuroprotective strategies for basal ganglia degeneration: Parkinson's and Huntington's diseases. *Progress in neurobiology* **60,** 409-470.

Altin JG, Kujubu DA, Raffioni S, Eveleth DD, Herschman HR & Bradshaw RA. (1991). Differential induction of primary-response (TIS) genes in PC12 pheochromocytoma cells and the unresponsive variant PC12nnr5. *The Journal of biological chemistry* **266,** 5401-5406.

Alves G, Forsaa EB, Pedersen KF, Dreetz Gjerstad M & Larsen JP. (2008). Epidemiology of Parkinson's disease. *J Neurol* **255 Suppl 5,** 18-32.

Ascherio A, Chen H, Weisskopf MG, O'Reilly E, McCullough ML, Calle EE, Schwarzschild MA & Thun MJ. (2006). Pesticide exposure and risk for Parkinson's disease. *Ann Neurol* **60,** 197-203.

Bailly K, Soulet F, Leroy D, Amalric F & Bouche G. (2000). Uncoupling of cell proliferation and differentiation activities of basic fibroblast growth factor. *Faseb J* **14,** 333-344.

Baird A & Ling N. (1987). Fibroblast growth factors are present in the extracellular matrix produced by endothelial cells in vitro: implications for a role of heparinase-like enzymes in the neovascular response. *Biochemical and biophysical research communications* **142,** 428-435.

Banati RB, Gehrmann J, Schubert P & Kreutzberg GW. (1993). Cytotoxicity of microglia. *Glia* **7,** 111-118.

Bao YL, Tsuchida K, Liu B, Kurisaki A, Matsuzaki T & Sugino H. (2005). Synergistic activity of activin A and basic fibroblast growth factor on tyrosine hydroxylase

expression through Smad3 and ERK1/ERK2 MAPK signaling pathways. *J Endocrinol* **184,** 493-504.

Beal MF. (2001). Experimental models of Parkinson's disease. *Nat Rev Neurosci* **2,** 325-334.

Bean AJ, Elde R, Cao YH, Oellig C, Tamminga C, Goldstein M, Pettersson RF & Hokfelt T. (1991). Expression of acidic and basic fibroblast growth factors in the substantia nigra of rat, monkey, and human. *Proceedings of the National Academy of Sciences of the United States of America* **88,** 10237-10241.

Bean AJ, Oellig C, Pettersson RF & Hokfelt T. (1992). Differential expression of acidic and basic FGF in the rat substantia nigra during development. *Neuroreport* **3,** 993-996.

Bekris LM, Mata IF & Zabetian CP. (2010). The genetics of Parkinson disease. *J Geriatr Psychiatry Neurol* **23,** 228-242.

Belluardo N, Wu G, Mudo G, Hansson AC, Pettersson R & Fuxe K. (1997). Comparative localization of fibroblast growth factor receptor-1, -2, and -3 mRNAs in the rat brain: in situ hybridization analysis. *J Comp Neurol* **379,** 226-246.

Bennett MC. (2005). The role of alpha-synuclein in neurodegenerative diseases. *Pharmacol Ther* **105,** 311-331.

Berger I, Stahl S, Rychkova N & Felbor U. (2006). VEGF receptors on PC12 cells mediate transient activation of ERK1/2 and Akt: comparison of nerve growth factor and vascular endothelial growth factor. *J Negat Results Biomed* **5,** 8.

Bernstein HG, Keilhoff G, Bukowska A, Ziegeler A, Funke S, Dobrowolny H, Kanakis D, Bogerts B & Lendeckel U. (2004). ADAM (a disintegrin and metalloprotease) 12 is expressed in rat and human brain and localized to oligodendrocytes. *Journal of neuroscience research* **75,** 353-360.

Betarbet R, Sherer TB & Greenamyre JT. (2002). Animal models of Parkinson's disease. *BioEssays : news and reviews in molecular, cellular and developmental biology* **24,** 308-318.

Betarbet R, Sherer TB, MacKenzie G, Garcia-Osuna M, Panov AV & Greenamyre JT. (2000). Chronic systemic pesticide exposure reproduces features of Parkinson's disease. *Nature neuroscience* **3,** 1301-1306.

Bezard E, Gross CE & Brotchie JM. (2003). Presymptomatic compensation in Parkinson's disease is not dopamine-mediated. *Trends in neurosciences* **26,** 215-221.

Biskup S & West AB. (2009). Zeroing in on LRRK2-linked pathogenic mechanisms in Parkinson's disease. *Biochimica et biophysica acta* **1792,** 625-633.

Blanco RE, Lopez-Roca A, Soto J & Blagburn JM. (2000). Basic fibroblast growth factor applied to the optic nerve after injury increases long-term cell survival in the frog retina. *The Journal of comparative neurology* **423,** 646-658.

Blandini F, Nappi G, Tassorelli C & Martignoni E. (2000). Functional changes of the basal ganglia circuitry in Parkinson's disease. *Progress in neurobiology* **62,** 63-88.

Blum D, Torch S, Lambeng N, Nissou M, Benabid AL, Sadoul R & Verna JM. (2001). Molecular pathways involved in the neurotoxicity of 6-OHDA, dopamine and MPTP: contribution to the apoptotic theory in Parkinson's disease. *Progress in neurobiology* **65,** 135-172.

Bohnen NI & Albin RL. (2011). The cholinergic system and Parkinson disease. *Behav Brain Res* **221,** 564-573.

Boniece IR & Wagner JA. (1993). Growth factors protect PC12 cells against ischemia by a mechanism that is independent of PKA, PKC, and protein synthesis. *The Journal of neuroscience : the official journal of the Society for Neuroscience* **13,** 4220-4228.

Bossard C, Laurell H, Van den Berghe L, Meunier S, Zanibellato C & Prats H. (2003). Translokin is an intracellular mediator of FGF-2 trafficking. *Nat Cell Biol* **5,** 433-439.

Bouleau S, Parvu-Ferecatu I, Rodriguez-Enfedaque A, Rincheval V, Grimal H, Mignotte B, Vayssiere JL & Renaud F. (2007). Fibroblast Growth Factor 1 inhibits p53-dependent apoptosis in PC12 cells. *Apoptosis* **12,** 1377-1387.

Bouvier MM & Mytilineou C. (1995a). Basic fibroblast growth factor increases division and delays differentiation of dopamine precursors in vitro. *The Journal of neuroscience : the official journal of the Society for Neuroscience* **15,** 7141-7149.

Bouvier MM & Mytilineou C. (1995b). Basic fibroblast growth factor increases division and delays differentiation of dopamine precursors in vitro. *J Neurosci* **15,** 7141-7149.

Bowenkamp KE, David D, Lapchak PL, Henry MA, Granholm AC, Hoffer BJ & Mahalik TJ. (1996). 6-hydroxydopamine induces the loss of the dopaminergic phenotype in substantia nigra neurons of the rat. A possible mechanism for restoration of the nigrostriatal circuit mediated by glial cell line-derived neurotrophic factor. *Experimental brain research Experimentelle Hirnforschung* **111,** 1-7.

Bowenkamp KE, Hoffman AF, Gerhardt GA, Henry MA, Biddle PT, Hoffer BJ & Granholm AC. (1995). Glial cell line-derived neurotrophic factor supports survival of injured midbrain dopaminergic neurons. *The Journal of comparative neurology* **355,** 479-489.

Brederlau A, Correia AS, Anisimov SV, Elmi M, Paul G, Roybon L, Morizane A, Bergquist F, Riebe I, Nannmark U, Carta M, Hanse E, Takahashi J, Sasai Y, Funa K, Brundin P, Eriksson PS & Li JY. (2006). Transplantation of human embryonic stem cell-derived cells to a rat model of Parkinson's disease: effect of in vitro differentiation on graft survival and teratoma formation. *Stem Cells* **24,** 1433-1440.

Bryant DM & Stow JL. (2005). Nuclear translocation of cell-surface receptors: lessons from fibroblast growth factor. *Traffic* **6,** 947-954.

Butt AM & Berry M. (2000). Oligodendrocytes and the control of myelination in vivo: new insights from the rat anterior medullary velum. *Journal of neuroscience research* **59,** 477-488.

Butt AM & Dinsdale J. (2005a). Fibroblast growth factor 2 induces loss of adult oligodendrocytes and myelin in vivo. *Exp Neurol* **192,** 125-133.

Butt AM & Dinsdale J. (2005b). Fibroblast growth factor 2 mediated disruption of myelin-forming oligodendrocytes in vivo is associated with increased tau immunoreactivity. *Neuroscience letters* **375,** 28-32.

Caldwell MA, Garcion E, terBorg MG, He X & Svendsen CN. (2004). Heparin stabilizes FGF-2 and modulates striatal precursor cell behavior in response to EGF. *Exp Neurol* **188,** 408-420.

Caldwell MA & Svendsen CN. (1998). Heparin, but not other proteoglycans potentiates the mitogenic effects of FGF-2 on mesencephalic precursor cells. *Exp Neurol* **152,** 1-10.

Cammer W, Downing M, Clarke W & Schenkman JB. (1991). Immunocytochemical staining of the RLM6 form of cytochrome P-450 in oligodendrocytes and myelin of rat brain. *J Histochem Cytochem* **39,** 1089-1094.

Casper D & Blum M. (1995). Epidermal growth factor and basic fibroblast growth factor protect dopaminergic neurons from glutamate toxicity in culture. *J Neurochem* **65,** 1016-1026.

Caughlan A, Newhouse K, Namgung U & Xia Z. (2004). Chlorpyrifos induces apoptosis in rat cortical neurons that is regulated by a balance between p38 and ERK/JNK MAP kinases. *Toxicological sciences : an official journal of the Society of Toxicology* **78,** 125-134.

Chadashvili T & Peterson DA. (2006). Cytoarchitecture of fibroblast growth factor receptor 2 (FGFR-2) immunoreactivity in astrocytes of neurogenic and non-neurogenic regions of the young adult and aged rat brain. *The Journal of comparative neurology* **498,** 1-15.

Chadi G, Cao Y, Pettersson RF & Fuxe K. (1994). Temporal and spatial increase of astroglial basic fibroblast growth factor synthesis after 6-hydroxydopamine-induced degeneration of the nigrostriatal dopamine neurons. *Neuroscience* **61,** 891-910.

Chadi G & Gomide VC. (2004). FGF-2 and S100beta immunoreactivities increase in reactive astrocytes, but not in microglia, in ascending dopamine pathways following a striatal 6-OHDA-induced partial lesion of the nigrostriatal system. *Cell Biol Int* **28,** 849-861.

Chadi G, Moller A, Rosen L, Janson AM, Agnati LA, Goldstein M, Ogren SO, Pettersson RF & Fuxe K. (1993). Protective actions of human recombinant basic fibroblast growth factor on MPTP-lesioned nigrostriatal dopamine neurons after intraventricular infusion. *Exp Brain Res* **97,** 145-158.

Chadi G, Silva C, Maximino JR, Fuxe K & da Silva GO. (2008). Adrenalectomy counteracts the local modulation of astroglial fibroblast growth factor system without interfering with the pattern of 6-OHDA-induced dopamine degeneration in regions of the ventral midbrain. *Brain research* **1190,** 23-38.

Chen-Roetling J, Li Z, Chen M, Awe OO & Regan RF. (2009). Heme oxygenase activity and hemoglobin neurotoxicity are attenuated by inhibitors of the MEK/ERK pathway. *Neuropharmacology* **56,** 922-928.

Chen Y, Li X, Eswarakumar VP, Seger R & Lonai P. (2000). Fibroblast growth factor (FGF) signaling through PI 3-kinase and Akt/PKB is required for embryoid body differentiation. *Oncogene* **19,** 3750-3756.

Chiba S, Lee YM, Zhou W & Freed CR. (2008). Noggin enhances dopamine neuron production from human embryonic stem cells and improves behavioral outcome after transplantation into Parkinsonian rats. *Stem Cells* **26,** 2810-2820.

Cho MS, Lee YE, Kim JY, Chung S, Cho YH, Kim DS, Kang SM, Lee H, Kim MH, Kim JH, Leem JW, Oh SK, Choi YM, Hwang DY, Chang JW & Kim DW. (2008). Highly efficient and large-scale generation of functional dopamine neurons from human embryonic stem cells. *Proceedings of the National Academy of Sciences of the United States of America* **105,** 3392-3397.

Chung KK, Dawson VL & Dawson TM. (2001). The role of the ubiquitin-proteasomal pathway in Parkinson's disease and other neurodegenerative disorders. *Trends Neurosci* **24,** S7-14.

Chung S, Hedlund E, Hwang M, Kim DW, Shin BS, Hwang DY, Jung Kang U, Isacson O & Kim KS. (2005). The homeodomain transcription factor Pitx3 facilitates differentiation of mouse embryonic stem cells into AHD2-expressing dopaminergic neurons. *Molecular and cellular neurosciences* **28,** 241-252.

Chung S, Shin BS, Hedlund E, Pruszak J, Ferree A, Kang UJ, Isacson O & Kim KS. (2006). Genetic selection of sox1GFP-expressing neural precursors removes residual tumorigenic pluripotent stem cells and attenuates tumor formation after transplantation. *Journal of neurochemistry* **97,** 1467-1480.

Clarimon J, Xiromerisiou G, Eerola J, Gourbali V, Hellstrom O, Dardiotis E, Peuralinna T, Papadimitriou A, Hadjigeorgiou GM, Tienari PJ & Singleton AB. (2005). Lack of evidence for a genetic association between FGF20 and Parkinson's disease in Finnish and Greek patients. *BMC Neurol* **5,** 11.

Clarke WE, Berry M, Smith C, Kent A & Logan A. (2001). Coordination of fibroblast growth factor receptor 1 (FGFR1) and fibroblast growth factor-2 (FGF-2) trafficking to nuclei of reactive astrocytes around cerebral lesions in adult rats. *Molecular and cellular neurosciences* **17,** 17-30.

Claus P, Werner S, Timmer M & Grothe C. (2004). Expression of the fibroblast growth factor-2 isoforms and the FGF receptor 1-4 transcripts in the rat model system of Parkinson's disease. *Neurosci Lett* **360,** 117-120.

Clyman RI, Peters KG, Chen YQ, Escobedo J, Williams LT, Ives HE & Wilson E. (1994). Phospholipase C gamma activation, phosphotidylinositol hydrolysis, and

calcium mobilization are not required for FGF receptor-mediated chemotaxis. *Cell Adhes Commun* **1,** 333-342.

Collins MA & Neafsey EJ. (2002). Potential neurotoxic "agents provocateurs" in Parkinson's disease. *Neurotoxicology and Teratology* **24,** 571-577.

Cordato DJ & Chan DK. (2004). Genetics and Parkinson's disease. *J Clin Neurosci* **11,** 119-123.

Correia AS, Anisimov SV, Li JY & Brundin P. (2005). Stem cell-based therapy for Parkinson's disease. *Ann Med* **37,** 487-498.

Correia AS, Anisimov SV, Roybon L, Li JY & Brundin P. (2007). Fibroblast growth factor-20 increases the yield of midbrain dopaminergic neurons derived from human embryonic stem cells. *Front Neuroanat* **1,** 4.

Corso TD, Torres G, Goulah C, Roy I, Gambino AS, Nayda J, Buckley T, Stachowiak EK, Bergey EJ, Pudavar H, Dutta P, Bloom DC, Bowers WJ & Stachowiak MK. (2005). Transfection of tyrosine kinase deleted FGF receptor-1 into rat brain substantia nigra reduces the number of tyrosine hydroxylase expressing neurons and decreases concentration levels of striatal dopamine. *Brain research Molecular brain research* **139,** 361-366.

Cross MJ, Hodgkin MN, Roberts S, Landgren E, Wakelam MJ & Claesson-Welsh L. (2000). Tyrosine 766 in the fibroblast growth factor receptor-1 is required for FGF-stimulation of phospholipase C, phospholipase D, phospholipase A(2), phosphoinositide 3-kinase and cytoskeletal reorganisation in porcine aortic endothelial cells. *J Cell Sci* **113 (Pt 4),** 643-651.

Cross MJ, Lu L, Magnusson P, Nyqvist D, Holmqvist K, Welsh M & Claesson-Welsh L. (2002). The Shb adaptor protein binds to tyrosine 766 in the FGFR-1 and regulates the Ras/MEK/MAPK pathway via FRS2 phosphorylation in endothelial cells. *Mol Biol Cell* **13,** 2881-2893.

Cucchiarini M, Madry H, Ma C, Thurn T, Zurakowski D, Menger MD, Kohn D, Trippel SB & Terwilliger EF. (2005). Improved tissue repair in articular cartilage defects in vivo by rAAV-mediated overexpression of human fibroblast growth factor 2. *Mol Ther* **12,** 229-238.

Cuevas P, Carceller F & Gimenez-Gallego G. (1995). Acidic fibroblast growth factor prevents post-axotomy neuronal death of the newborn rat facial nerve. *Neuroscience letters* **197,** 183-186.

Damon DH, D'Amore PA & Wagner JA. (1988). Sulfated glycosaminoglycans modify growth factor-induced neurite outgrowth in PC12 cells. *Journal of cellular physiology* **135,** 293-300.

Dauer W & Przedborski S. (2003). Parkinson's disease: mechanisms and models. *Neuron* **39,** 889-909.

Dawbarn D & Allen SJ. (2003). Neurotrophins and neurodegeneration. *Neuropathol Appl Neurobiol* **29,** 211-230.

Dawson TM, Ko HS & Dawson VL. (2010). Genetic animal models of Parkinson's disease. *Neuron* **66,** 646-661.

de Mena L, Cardo LF, Coto E, Miar A, Diaz M, Corao AI, Alonso B, Ribacoba R, Salvador C, Menendez M, Moris G & Alvarez V. (2010). FGF20 rs12720208 SNP and microRNA-433 variation: no association with Parkinson's disease in Spanish patients. *Neuroscience letters* **479,** 22-25.

Detillieux KA, Cattini PA & Kardami E. (2004). Beyond angiogenesis: the cardioprotective potential of fibroblast growth factor-2. *Can J Physiol Pharmacol* **82,** 1044-1052.

Deumens R, Blokland A & Prickaerts J. (2002). Modeling Parkinson's disease in rats: an evaluation of 6-OHDA lesions of the nigrostriatal pathway. *Exp Neurol* **175,** 303-317.

Dexter DT, Wells FR, Lees AJ, Agid F, Agid Y, Jenner P & Marsden CD. (1989). Increased nigral iron content and alterations in other metal ions occurring in brain in Parkinson's disease. *J Neurochem* **52,** 1830-1836.

Dodson MW & Guo M. (2007). Pink1, Parkin, DJ-1 and mitochondrial dysfunction in Parkinson's disease. *Curr Opin Neurobiol* **17,** 331-337.

Dono R. (2003). Fibroblast growth factors as regulators of central nervous system development and function. *Am J Physiol Regul Integr Comp Physiol* **284,** R867-881.

Drucker-Colin R & Verdugo-Diaz L. (2004). Cell transplantation for Parkinson's disease: present status. *Cell Mol Neurobiol* **24,** 301-316.

Duty S & Jenner P. (2011). Animal models of Parkinson's disease: a source of novel treatments and clues to the cause of the disease. *Br J Pharmacol* **164,** 1357-1391.

Eckenstein FP. (1994). Fibroblast growth factors in the nervous system. *J Neurobiol* **25,** 1467-1480.

Ekstrand MI & Galter D. (2009). The MitoPark Mouse - an animal model of Parkinson's disease with impaired respiratory chain function in dopamine neurons. *Parkinsonism & related disorders* **15 Suppl 3,** S185-188.

Ekstrand MI, Terzioglu M, Galter D, Zhu S, Hofstetter C, Lindqvist E, Thams S, Bergstrand A, Hansson FS, Trifunovic A, Hoffer B, Cullheim S, Mohammed AH, Olson L & Larsson NG. (2007). Progressive parkinsonism in mice with respiratory-chain-deficient dopamine neurons. *Proc Natl Acad Sci U S A* **104,** 1325-1330.

Ellsworth JL, Garcia R, Yu J & Kindy MS. (2004). Time window of fibroblast growth factor-18-mediated neuroprotection after occlusion of the middle cerebral artery in rats. *J Cereb Blood Flow Metab* **24,** 114-123.

Emborg ME. (2004). Evaluation of animal models of Parkinson's disease for neuroprotective strategies. *J Neurosci Methods* **139,** 121-143.

Esch F, Baird A, Ling N, Ueno N, Hill F, Denoroy L, Klepper R, Gospodarowicz D, Bohlen P & Guillemin R. (1985). Primary structure of bovine pituitary basic fibroblast growth factor (FGF) and comparison with the amino-terminal sequence of bovine brain acidic FGF. *Proc Natl Acad Sci U S A* **82,** 6507-6511.

Eswarakumar VP, Lax I & Schlessinger J. (2005). Cellular signaling by fibroblast growth factor receptors. *Cytokine & growth factor reviews* **16,** 139-149.

Ezzat S, Zheng L, Yu S & Asa SL. (2001). A soluble dominant negative fibroblast growth factor receptor 4 isoform in human MCF-7 breast cancer cells. *Biochemical and biophysical research communications* **287,** 60-65.

Faham S, Linhardt RJ & Rees DC. (1998). Diversity does make a difference: fibroblast growth factor-heparin interactions. *Curr Opin Struct Biol* **8,** 578-586.

Fan H, Vitharana SN, Chen T, O'Keefe D & Middaugh CR. (2007). Effects of pH and polyanions on the thermal stability of fibroblast growth factor 20. *Mol Pharm* **4,** 232-240.

Fannon M & Nugent MA. (1996). Basic fibroblast growth factor binds its receptors, is internalized, and stimulates DNA synthesis in Balb/c3T3 cells in the absence of heparan sulfate. *J Biol Chem* **271,** 17949-17956.

Ferrer I. (2011). Neuropathology and neurochemistry of nonmotor symptoms in Parkinson's disease. *Parkinsons Dis* **2011,** 708404.

Ferrer I & Marti E. (1998). Distribution of fibroblast growth factor receptor-1 (FGFR-1) and FGFR-3 in the hippocampus of patients with Alzheimer's disease. *Neuroscience letters* **240,** 139-142.

Flaumenhaft R, Moscatelli D, Saksela O & Rifkin DB. (1989). Role of extracellular matrix in the action of basic fibroblast growth factor: matrix as a source of growth factor for long-term stimulation of plasminogen activator production and DNA synthesis. *J Cell Physiol* **140,** 75-81.

Floor E & Wetzel MG. (1998). Increased protein oxidation in human substantia nigra pars compacta in comparison with basal ganglia and prefrontal cortex measured with an improved dinitrophenylhydrazine assay. *J Neurochem* **70,** 268-275.

Flores JA, Galan-Rodriguez B, Rojo AI, Ramiro-Fuentes S, Cuadrado A & Fernandez-Espejo E. (2010). Fibroblast growth factor-1 within the ventral tegmental area participates in motor sensitizing effects of morphine. *Neuroscience* **165,** 198-211.

Foehr ED, Raffioni S, Fuji R & Bradshaw RA. (1998). FGF signal transduction in PC12 cells: comparison of the responses induced by endogenous and chimeric receptors. *Immunol Cell Biol* **76,** 406-413.

Folkman J, Klagsbrun M, Sasse J, Wadzinski M, Ingber D & Vlodavsky I. (1988). A heparin-binding angiogenic protein--basic fibroblast growth factor--is stored within basement membrane. *Am J Pathol* **130,** 393-400.

Fontan A, Rojo A, Sanchez Pernaute R, Hernandez I, Lopez I, Castilla C, Sanchez Albisua J, Perez Higueras A, Al-Rashid I, Rabano A, Gonzalo I, Angeles Mena M, Cools A, Eshuis S, Maguire P, Pruim J, Leenders K & Garcia de Yebenes J. (2002). Effects of fibroblast growth factor and glial-derived neurotrophic factor on akinesia, F-DOPA uptake and dopamine cells in parkinsonian primates. *Parkinsonism Relat Disord* **8,** 311-323.

Ford-Perriss M, Abud H & Murphy M. (2001). Fibroblast growth factors in the developing central nervous system. *Clin Exp Pharmacol Physiol* **28,** 493-503.

Fornai F, Lenzi P, Gesi M, Ferrucci M, Lazzeri G, Busceti CL, Ruffoli R, Soldani P, Ruggieri S, Alessandri MG & Paparelli A. (2003). Fine structure and biochemical mechanisms underlying nigrostriatal inclusions and cell death after

proteasome inhibition. *The Journal of neuroscience : the official journal of the Society for Neuroscience* **23,** 8955-8966.

Forough R, Weylie B, Patel C, Ambrus S, Singh US & Zhu J. (2005). Role of AKT/PKB signaling in fibroblast growth factor-1 (FGF-1)-induced angiogenesis in the chicken chorioallantoic membrane (CAM). *J Cell Biochem* **94,** 109-116.

Fox CM, Gash DM, Smoot MK & Cass WA. (2001). Neuroprotective effects of GDNF against 6-OHDA in young and aged rats. *Brain research* **896,** 56-63.

Fox SH, Brotchie JM & Lang AE. (2008). Non-dopaminergic treatments in development for Parkinson's disease. *Lancet Neurol* **7,** 927-938.

Friling S, Andersson E, Thompson LH, Jonsson ME, Hebsgaard JB, Nanou E, Alekseenko Z, Marklund U, Kjellander S, Volakakis N, Hovatta O, El Manira A, Bjorklund A, Perlmann T & Ericson J. (2009). Efficient production of mesencephalic dopamine neurons by Lmx1a expression in embryonic stem cells. *Proceedings of the National Academy of Sciences of the United States of America* **106,** 7613-7618.

Gall CM, Gold SJ, Isackson PJ & Seroogy KB. (1992). Brain-derived neurotrophic factor and neurotrophin-3 mRNAs are expressed in ventral midbrain regions containing dopaminergic neurons. *Molecular and cellular neurosciences* **3,** 56-63.

Gao HM, Liu B, Zhang W & Hong JS. (2003). Novel anti-inflammatory therapy for Parkinson's disease. *Trends in pharmacological sciences* **24,** 395-401.

Gao X, Scott WK, Wang G, Mayhew G, Li YJ, Vance JM & Martin ER. (2008). Gene-gene interaction between FGF20 and MAOB in Parkinson disease. *Ann Hum Genet* **72,** 157-162.

Gardner AM & Johnson GL. (1996). Fibroblast growth factor-2 suppression of tumor necrosis factor alpha-mediated apoptosis requires Ras and the activation of mitogen-activated protein kinase. *J Biol Chem* **271,** 14560-14566.

Gash DM, Zhang Z, Cass WA, Ovadia A, Simmerman L, Martin D, Russell D, Collins F, Hoffer BJ & Gerhardt GA. (1995). Morphological and functional effects of intranigrally administered GDNF in normal rhesus monkeys. *The Journal of comparative neurology* **363,** 345-358.

Gash DM, Zhang Z, Ovadia A, Cass WA, Yi A, Simmerman L, Russell D, Martin D, Lapchak PA, Collins F, Hoffer BJ & Gerhardt GA. (1996). Functional recovery in parkinsonian monkeys treated with GDNF. *Nature* **380,** 252-255.

Gaul G & Lubbert H. (1992). Cortical astrocytes activated by basic fibroblast growth factor secrete molecules that stimulate differentiation of mesencephalic dopaminergic neurons. *Proc Biol Sci* **249,** 57-63.

Gelinas S & Martinoli MG. (2002). Neuroprotective effect of estradiol and phytoestrogens on MPP+-induced cytotoxicity in neuronal PC12 cells. *Journal of neuroscience research* **70,** 90-96.

German DC, Manaye KF, Sonsalla PK & Brooks BA. (1992). Midbrain dopaminergic cell loss in Parkinson's disease and MPTP-induced parkinsonism: sparing of calbindin-D28k-containing cells. *Annals of the New York Academy of Sciences* **648,** 42-62.

Gibb WR. (1992). Melanin, tyrosine hydroxylase, calbindin and substance P in the human midbrain and substantia nigra in relation to nigrostriatal projections and differential neuronal susceptibility in Parkinson's disease. *Brain research* **581,** 283-291.

Gill SS, Patel NK, Hotton GR, O'Sullivan K, McCarter R, Bunnage M, Brooks DJ, Svendsen CN & Heywood P. (2003). Direct brain infusion of glial cell line-derived neurotrophic factor in Parkinson disease. *Nature medicine* **9,** 589-595.

Giuditta A, Chun JT, Eyman M, Cefaliello C, Bruno AP & Crispino M. (2008). Local gene expression in axons and nerve endings: the glia-neuron unit. *Physiol Rev* **88,** 515-555.

Glinka Y, Tipton KF & Youdim MB. (1996). Nature of inhibition of mitochondrial respiratory complex I by 6-Hydroxydopamine. *Journal of neurochemistry* **66,** 2004-2010.

Glinka YY & Youdim MB. (1995). Inhibition of mitochondrial complexes I and IV by 6-hydroxydopamine. *Eur J Pharmacol* **292,** 329-332.

Goddard DR, Berry M & Butt AM. (1999). In vivo actions of fibroblast growth factor-2 and insulin-like growth factor-I on oligodendrocyte development and myelination in the central nervous system. *Journal of neuroscience research* **57,** 74-85.

Goddard DR, Berry M, Kirvell SL & Butt AM. (2001). Fibroblast growth factor-2 inhibits myelin production by oligodendrocytes in vivo. *Molecular and cellular neurosciences* **18,** 557-569.

Goldfarb M, Bates B, Drucker B, Hardin J & Haub O. (1991). Expression and possible functions of the FGF-5 gene. *Annals of the New York Academy of Sciences* **638,** 38-52.

Gonzalez AM, Berry M, Maher PA, Logan A & Baird A. (1995). A comprehensive analysis of the distribution of FGF-2 and FGFR1 in the rat brain. *Brain research* **701,** 201-226.

Gorell JM, Rybicki BA, Cole Johnson C & Peterson EL. (1999). Occupational metal exposures and the risk of Parkinson's disease. *Neuroepidemiology* **18,** 303-308.

Gospodarowicz D & Cheng J. (1986). Heparin protects basic and acidic FGF from inactivation. *J Cell Physiol* **128,** 475-484.

Gospodarowicz D, Neufeld G & Schweigerer L. (1986). Fibroblast growth factor. *Mol Cell Endocrinol* **46,** 187-204.

Gowda DC, Goossen B, Margolis RK & Margolis RU. (1989). Chondroitin sulfate and heparan sulfate proteoglycans of PC12 pheochromocytoma cells. *The Journal of biological chemistry* **264,** 11436-11443.

Greene LA & Tischler AS. (1976). Establishment of a noradrenergic clonal line of rat adrenal pheochromocytoma cells which respond to nerve growth factor. *Proceedings of the National Academy of Sciences of the United States of America* **73,** 2424-2428.

Grondin R, Zhang Z, Yi A, Cass WA, Maswood N, Andersen AH, Elsberry DD, Klein MC, Gerhardt GA & Gash DM. (2002). Chronic, controlled GDNF infusion promotes structural and functional recovery in advanced parkinsonian monkeys. *Brain* **125,** 2191-2201.

Grothe C, Schulze A, Semkova I, Muller-Ostermeyer F, Rege A & Wewetzer K. (2000). The high molecular weight fibroblast growth factor-2 isoforms (21,000 mol. wt and 23,000 mol. wt) mediate neurotrophic activity on rat embryonic mesencephalic dopaminergic neurons in vitro. *Neuroscience* **100,** 73-86.

Grothe C, Timmer M, Scholz T, Winkler C, Nikkhah G, Claus P, Itoh N & Arenas E. (2004). Fibroblast growth factor-20 promotes the differentiation of Nurr1-overexpressing neural stem cells into tyrosine hydroxylase-positive neurons. *Neurobiology of disease* **17,** 163-170.

Grothe C & Wewetzer K. (1996). Fibroblast growth factor and its implications for developing and regenerating neurons. *Int J Dev Biol* **40,** 403-410.

Gu Q, Wang D, Wang X, Peng R, Liu J, Jiang T, Wang Z, Wang S & Deng H. (2004). Basic fibroblast growth factor inhibits radiation-induced apoptosis of HUVECs. I. The PI3K/AKT pathway and induction of phosphorylation of BAD. *Radiat Res* **161,** 692-702.

Guan J, Krishnamurthi R, Waldvogel HJ, Faull RL, Clark R & Gluckman P. (2000). N-terminal tripeptide of IGF-1 (GPE) prevents the loss of TH positive neurons after 6-OHDA induced nigral lesion in rats. *Brain research* **859,** 286-292.

Hadari YR, Kouhara H, Lax I & Schlessinger J. (1998). Binding of Shp2 tyrosine phosphatase to FRS2 is essential for fibroblast growth factor-induced PC12 cell differentiation. *Mol Cell Biol* **18,** 3966-3973.

Hajihosseini MK, De Langhe S, Lana-Elola E, Morrison H, Sparshott N, Kelly R, Sharpe J, Rice D & Bellusci S. (2008). Localization and fate of Fgf10-expressing cells in the adult mouse brain implicate Fgf10 in control of neurogenesis. *Molecular and cellular neurosciences* **37,** 857-868.

Hald A & Lotharius J. (2005). Oxidative stress and inflammation in Parkinson's disease: is there a causal link? *Exp Neurol* **193,** 279-290.

Halliwell B. (2006). Oxidative stress and neurodegeneration: where are we now? *J Neurochem* **97,** 1634-1658.

Han J, Mandal AK & Hiebert LM. (2005). Endothelial cell injury by high glucose and heparanase is prevented by insulin, heparin and basic fibroblast growth factor. *Cardiovasc Diabetol* **4,** 12.

Harvey BK, Wang Y & Hoffer BJ. (2008). Transgenic rodent models of Parkinson's disease. *Acta Neurochir Suppl* **101,** 89-92.

Hauser RA. (2010). Early pharmacologic treatment in Parkinson's disease. *Am J Manag Care* **16 Suppl Implications,** S100-107.

Hedlund E, Pruszak J, Lardaro T, Ludwig W, Vinuela A, Kim KS & Isacson O. (2008). Embryonic stem cell-derived Pitx3-enhanced green fluorescent protein midbrain dopamine neurons survive enrichment by fluorescence-activated cell sorting and function in an animal model of Parkinson's disease. *Stem Cells* **26,** 1526-1536.

Hegde AN & Upadhya SC. (2007). The ubiquitin-proteasome pathway in health and disease of the nervous system. *Trends Neurosci* **30,** 587-595.

Heinzle C, Sutterluty H, Grusch M, Grasl-Kraupp B, Berger W & Marian B. (2011). Targeting fibroblast-growth-factor-receptor-dependent signaling for cancer therapy. *Expert Opin Ther Targets* **15,** 829-846.

Hirsch EC & Hunot S. (2009). Neuroinflammation in Parkinson's disease: a target for neuroprotection? *Lancet Neurol* **8,** 382-397.

Honda T, Wada E, Battey JF & Wank SA. (1993). Differential Gene Expression of CCK(A) and CCK(B) Receptors in the Rat Brain. *Molecular and cellular neurosciences* **4,** 143-154.

Hou JG, Cohen G & Mytilineou C. (1997). Basic fibroblast growth factor stimulation of glial cells protects dopamine neurons from 6-hydroxydopamine toxicity: involvement of the glutathione system. *J Neurochem* **69,** 76-83.

Howells DW, Porritt MJ, Wong JY, Batchelor PE, Kalnins R, Hughes AJ & Donnan GA. (2000). Reduced BDNF mRNA expression in the Parkinson's disease substantia nigra. *Exp Neurol* **166,** 127-135.

Hsuan SL, Klintworth HM & Xia Z. (2006). Basic fibroblast growth factor protects against rotenone-induced dopaminergic cell death through activation of extracellular signal-regulated kinases 1/2 and phosphatidylinositol-3 kinase pathways. *J Neurosci* **26,** 4481-4491.

Huang JY, Hong YT & Chuang JI. (2009). Fibroblast growth factor 9 prevents MPP+-induced death of dopaminergic neurons and is involved in melatonin neuroprotection in vivo and in vitro. *Journal of neurochemistry* **109,** 1400-1412.

Humpel C, Chadi G, Lippoldt A, Ganten D, Fuxe K & Olson L. (1994). Increase of basic fibroblast growth factor (bFGF, FGF-2) messenger RNA and protein following implantation of a microdialysis probe into rat hippocampus. *Experimental brain research Experimentelle Hirnforschung* **98,** 229-237.

Hunot S, Dugas N, Faucheux B, Hartmann A, Tardieu M, Debre P, Agid Y, Dugas B & Hirsch EC. (1999). FcepsilonRII/CD23 is expressed in Parkinson's disease and induces, in vitro, production of nitric oxide and tumor necrosis factor-alpha in glial cells. *The Journal of neuroscience : the official journal of the Society for Neuroscience* **19,** 3440-3447.

Hyman C, Juhasz M, Jackson C, Wright P, Ip NY & Lindsay RM. (1994). Overlapping and distinct actions of the neurotrophins BDNF, NT-3, and NT-4/5 on cultured dopaminergic and GABAergic neurons of the ventral mesencephalon. *The Journal of neuroscience : the official journal of the Society for Neuroscience* **14,** 335-347.

Inazu M, Takeda H, Ikoshi H, Uchida Y, Kubota N, Kiuchi Y, Oguchi K & Matsumiya T. (1999). Regulation of dopamine uptake by basic fibroblast growth factor and epidermal growth factor in cultured rat astrocytes. *Neurosci Res* **34,** 235-244.

Jacques TS, Skepper JN & Navaratnam V. (1999). Fibroblast growth factor-1 improves the survival and regeneration of rat vagal preganglionic neurones following axon injury. *Neuroscience letters* **276,** 197-200.

Jeffers M, Shimkets R, Prayaga S, Boldog F, Yang M, Burgess C, Fernandes E, Rittman B, Shimkets J, LaRochelle WJ & Lichenstein HS. (2001). Identification of a novel human fibroblast growth factor and characterization of its role in oncogenesis. *Cancer Res* **61,** 3131-3138.

Jenner P. (2008). Functional models of Parkinson's disease: a valuable tool in the development of novel therapies. *Annals of neurology* **64 Suppl 2,** S16-29.

Jeon BS, Jackson-Lewis V & Burke RE. (1995). 6-Hydroxydopamine lesion of the rat substantia nigra: time course and morphology of cell death. *Neurodegeneration* **4,** 131-137.

Jeon CY, Kim HJ, Morii H, Mori N, Settleman J, Lee JY, Kim J, Kim SC & Park JB. (2010). Neurite outgrowth from PC12 cells by basic fibroblast growth factor (bFGF) is mediated by RhoA inactivation through p190RhoGAP and ARAP3. *Journal of cellular physiology* **224,** 786-794.

Jin BK & Iacovitti L. (1995). Dopamine differentiation factors produce partial motor recovery in 6-hydroxydopamine lesioned rats. *Neurobiology of disease* **2,** 1-12.

Johnson DE, Lee PL, Lu J & Williams LT. (1990). Diverse forms of a receptor for acidic and basic fibroblast growth factors. *Mol Cell Biol* **10,** 4728-4736.

Johnson DE, Lu J, Chen H, Werner S & Williams LT. (1991). The human fibroblast growth factor receptor genes: a common structural arrangement underlies the mechanisms for generating receptor forms that differ in their third immunoglobulin domain. *Mol Cell Biol* **11,** 4627-4634.

Johnston CL, Cox HC, Gomm JJ & Coombes RC. (1995). Fibroblast growth factor receptors (FGFRs) localize in different cellular compartments. A splice variant of FGFR-3 localizes to the nucleus. *The Journal of biological chemistry* **270,** 30643-30650.

Jungnickel J, Haase K, Konitzer J, Timmer M & Grothe C. (2006). Faster nerve regeneration after sciatic nerve injury in mice over-expressing basic fibroblast growth factor. *Journal of neurobiology* **66,** 940-948.

Kadota T, Yamaai T, Saito Y, Akita Y, Kawashima S, Moroi K, Inagaki N & Kadota K. (1996). Expression of dopamine transporter at the tips of growing neurites of PC12 cells. *J Histochem Cytochem* **44,** 989-996.

Kanda S, Miyata Y, Kanetake H & Smithgall TE. (2006). Fibroblast growth factor-2 induces the activation of Src through Fes, which regulates focal adhesion disassembly. *Exp Cell Res* **312,** 3015-3022.

Karlsson T, Kullander K & Welsh M. (1998). The Src homology 2 domain protein Shb transmits basic fibroblast growth factor- and nerve growth factor-dependent differentiation signals in PC12 cells. *Cell Growth Differ* **9,** 757-766.

Karsan A, Yee E, Poirier GG, Zhou P, Craig R & Harlan JM. (1997). Fibroblast growth factor-2 inhibits endothelial cell apoptosis by Bcl-2-dependent and independent mechanisms. *The American journal of pathology* **151,** 1775-1784.

Kavanagh ET, Loughlin JP, Herbert KR, Dockery P, Samali A, Doyle KM & Gorman AM. (2006). Functionality of NGF-protected PC12 cells following exposure to 6-hydroxydopamine. *Biochemical and biophysical research communications* **351,** 890-895.

Kawamata T, Yamaguchi T, Shin-ya K & Hori T. (2001). Time courses of increased expression of signaling transduction molecules induced by basic fibroblast growth factor in PC12 cells. *Neurol Res* **23,** 327-330.

Kawamata T, Yamaguchi T, Shin-ya K & Hori T. (2003). Divergence in signaling pathways involved in promotion of cell viability mediated by bFGF, NGF, and EGF in PC12 cells. *Neurochem Res* **28,** 1221-1225.

Kawasaki H, Mizuseki K, Nishikawa S, Kaneko S, Kuwana Y, Nakanishi S, Nishikawa SI & Sasai Y. (2000). Induction of midbrain dopaminergic neurons from ES cells by stromal cell-derived inducing activity. *Neuron* **28,** 31-40.

Keane PC, Kurzawa M, Blain PG & Morris CM. (2011). Mitochondrial dysfunction in Parkinson's disease. *Parkinsons Dis* **2011,** 716871.

Kearns CM & Gash DM. (1995). GDNF protects nigral dopamine neurons against 6-hydroxydopamine in vivo. *Brain research* **672,** 104-111.

Keegan K, Meyer S & Hayman MJ. (1991). Structural and biosynthetic characterization of the fibroblast growth factor receptor 3 (FGFR-3) protein. *Oncogene* **6,** 2229-2236.

Khalil N, Xu YD, O'Connor R & Duronio V. (2005). Proliferation of pulmonary interstitial fibroblasts is mediated by transforming growth factor-beta1-induced release of extracellular fibroblast growth factor-2 and phosphorylation of p38 MAPK and JNK. *J Biol Chem* **280,** 43000-43009.

Kim JH, Auerbach JM, Rodriguez-Gomez JA, Velasco I, Gavin D, Lumelsky N, Lee SH, Nguyen J, Sanchez-Pernaute R, Bankiewicz K & McKay R. (2002). Dopamine neurons derived from embryonic stem cells function in an animal model of Parkinson's disease. *Nature* **418,** 50-56.

Kim MJ, Cotman SL, Halfter W & Cole GJ. (2003). The heparan sulfate proteoglycan agrin modulates neurite outgrowth mediated by FGF-2. *Journal of neurobiology* **55,** 261-277.

Kirik D, Georgievska B & Bjorklund A. (2004). Localized striatal delivery of GDNF as a treatment for Parkinson disease. *Nature neuroscience* **7,** 105-110.

Kirikoshi H, Sagara N, Saitoh T, Tanaka K, Sekihara H, Shiokawa K & Katoh M. (2000). Molecular cloning and characterization of human FGF-20 on chromosome 8p21.3-p22. *Biochemical and biophysical research communications* **274,** 337-343.

Klint P, Kanda S & Claesson-Welsh L. (1995). Shc and a novel 89-kDa component couple to the Grb2-Sos complex in fibroblast growth factor-2-stimulated cells. *J Biol Chem* **270,** 23337-23344.

Klint P, Kanda S, Kloog Y & Claesson-Welsh L. (1999). Contribution of Src and Ras pathways in FGF-2 induced endothelial cell differentiation. *Oncogene* **18,** 3354-3364.

Kojima A & Tator CH. (2002). Intrathecal administration of epidermal growth factor and fibroblast growth factor 2 promotes ependymal proliferation and functional recovery after spinal cord injury in adult rats. *Journal of neurotrauma* **19,** 223-238.

Kouhara H, Hadari YR, Spivak-Kroizman T, Schilling J, Bar-Sagi D, Lax I & Schlessinger J. (1997). A lipid-anchored Grb2-binding protein that links FGF-receptor activation to the Ras/MAPK signaling pathway. *Cell* **89,** 693-702.

Kremer NE, D'Arcangelo G, Thomas SM, DeMarco M, Brugge JS & Halegoua S. (1991). Signal transduction by nerve growth factor and fibroblast growth factor in PC12 cells requires a sequence of src and ras actions. *The Journal of cell biology* **115,** 809-819.

Kreutzberg GW. (1996). Microglia: a sensor for pathological events in the CNS. *Trends in neurosciences* **19,** 312-318.

Krieglstein K. (2004). Factors promoting survival of mesencephalic dopaminergic neurons. *Cell and tissue research* **318,** 73-80.

Krieglstein K, Reuss B, Maysinger D & Unsicker K. (1998). Short communication: transforming growth factor-beta mediates the neurotrophic effect of fibroblast growth factor-2 on midbrain dopaminergic neurons. *The European journal of neuroscience* **10,** 2746-2750.

Kriks S, Shim JW, Piao J, Ganat YM, Wakeman DR, Xie Z, Carrillo-Reid L, Auyeung G, Antonacci C, Buch A, Yang L, Beal MF, Surmeier DJ, Kordower JH, Tabar V & Studer L. (2011). Dopamine neurons derived from human ES cells efficiently engraft in animal models of Parkinson's disease. *Nature* **480,** 547-551.

Kuhn HG, Winkler J, Kempermann G, Thal LJ & Gage FH. (1997). Epidermal growth factor and fibroblast growth factor-2 have different effects on neural progenitors in the adult rat brain. *J Neurosci* **17,** 5820-5829.

Kuo WL, Chung KC & Rosner MR. (1997). Differentiation of central nervous system neuronal cells by fibroblast-derived growth factor requires at least two signaling pathways: roles for Ras and Src. *Mol Cell Biol* **17,** 4633-4643.

Kuslak SL & Marker PC. (2007). Fibroblast growth factor receptor signaling through MEK-ERK is required for prostate bud induction. *Differentiation* **75,** 638-651.

Kuzis K, Reed S, Cherry NJ, Woodward WR & Eckenstein FP. (1995). Developmental time course of acidic and basic fibroblast growth factors' expression in distinct cellular populations of the rat central nervous system. *The Journal of comparative neurology* **358,** 142-153.

Kwiatkowski BA, Kirillova I, Richard RE, Israeli D & Yablonka-Reuveni Z. (2008). FGFR4 and its novel splice form in myogenic cells: Interplay of glycosylation and tyrosine phosphorylation. *Journal of cellular physiology* **215,** 803-817.

Lai BC, Marion SA, Teschke K & Tsui JK. (2002). Occupational and environmental risk factors for Parkinson's disease. *Parkinsonism & related disorders* **8,** 297-309.

Laird JM, Mason GS, Thomas KA, Hargreaves RJ & Hill RG. (1995). Acidic fibroblast growth factor stimulates motor and sensory axon regeneration after sciatic nerve crush in the rat. *Neuroscience* **65,** 209-216.

Larsson H, Klint P, Landgren E & Claesson-Welsh L. (1999). Fibroblast growth factor receptor-1-mediated endothelial cell proliferation is dependent on the Src homology (SH) 2/SH3 domain-containing adaptor protein Crk. *J Biol Chem* **274,** 25726-25734.

Lax I, Wong A, Lamothe B, Lee A, Frost A, Hawes J & Schlessinger J. (2002). The docking protein FRS2alpha controls a MAP kinase-mediated negative feedback mechanism for signaling by FGF receptors. *Mol Cell* **10,** 709-719.

Lee CS, Park SY, Ko HH, Song JH, Shin YK & Han ES. (2005). Inhibition of MPP+-induced mitochondrial damage and cell death by trifluoperazine and W-7 in PC12 cells. *Neurochemistry international* **46,** 169-178.

Lee CS, Sauer H & Bjorklund A. (1996). Dopaminergic neuronal degeneration and motor impairments following axon terminal lesion by instrastriatal 6-hydroxydopamine in the rat. *Neuroscience* **72,** 641-653.

Lee EO, Park HJ, Kang JL, Kim HS & Chong YH. (2010). Resveratrol reduces glutamate-mediated monocyte chemotactic protein-1 expression via inhibition of extracellular signal-regulated kinase 1/2 pathway in rat hippocampal slice cultures. *Journal of neurochemistry* **112,** 1477-1487.

Lemaitre H, Mattay VS, Sambataro F, Verchinski B, Straub RE, Callicott JH, Kittappa R, Hyde TM, Lipska BK, Kleinman JE, McKay R & Weinberger DR. (2010). Genetic variation in FGF20 modulates hippocampal biology. *The Journal of neuroscience : the official journal of the Society for Neuroscience* **30,** 5992-5997.

Lenhard T, Schober A, Suter-Crazzolara C & Unsicker K. (2002). Fibroblast growth factor-2 requires glial-cell-line-derived neurotrophic factor for exerting its neuroprotective actions on glutamate-lesioned hippocampal neurons. *Molecular and cellular neurosciences* **20,** 181-197.

Li A, Guo H, Luo X, Sheng J, Yang S, Yin Y, Zhou J & Zhou J. (2006). Apomorphine-induced activation of dopamine receptors modulates FGF-2 expression in

astrocytic cultures and promotes survival of dopaminergic neurons. *Faseb J* **20,** 1263-1265.

Li Q & Stephenson D. (2002). Postischemic administration of basic fibroblast growth factor improves sensorimotor function and reduces infarct size following permanent focal cerebral ischemia in the rat. *Exp Neurol* **177,** 531-537.

Li Z, Hu Y, Zhu Q & Zhu J. (2008). Neurotrophin-3 reduces apoptosis induced by 6-OHDA in PC12 cells through Akt signaling pathway. *Int J Dev Neurosci* **26,** 635-640.

Lin HY, Xu J, Ischenko I, Ornitz DM, Halegoua S & Hayman MJ. (1998). Identification of the cytoplasmic regions of fibroblast growth factor (FGF) receptor 1 which play important roles in induction of neurite outgrowth in PC12 cells by FGF-1. *Molecular and cellular biology* **18,** 3762-3770.

Lin HY, Xu J, Ornitz DM, Halegoua S & Hayman MJ. (1996). The fibroblast growth factor receptor-1 is necessary for the induction of neurite outgrowth in PC12 cells by aFGF. *The Journal of neuroscience : the official journal of the Society for Neuroscience* **16,** 4579-4587.

Liu B. (2006). Modulation of microglial pro-inflammatory and neurotoxic activity for the treatment of Parkinson's disease. *Aaps J* **8,** E606-621.

Liu Y, Schweitzer ES, Nirenberg MJ, Pickel VM, Evans CJ & Edwards RH. (1994). Preferential localization of a vesicular monoamine transporter to dense core vesicles in PC12 cells. *The Journal of cell biology* **127,** 1419-1433.

Lonardo E, Parish CL, Ponticelli S, Marasco D, Ribeiro D, Ruvo M, De Falco S, Arenas E & Minchiotti G. (2010). A small synthetic cripto blocking Peptide improves neural induction, dopaminergic differentiation, and functional integration of mouse embryonic stem cells in a rat model of Parkinson's disease. *Stem Cells* **28,** 1326-1337.

Long-Smith CM, Sullivan AM & Nolan YM. (2009). The influence of microglia on the pathogenesis of Parkinson's disease. *Progress in neurobiology* **89,** 277-287.

Lu Z & Xu S. (2006). ERK1/2 MAP kinases in cell survival and apoptosis. *IUBMB Life* **58,** 621-631.

Lundin L, Larsson H, Kreuger J, Kanda S, Lindahl U, Salmivirta M & Claesson-Welsh L. (2000). Selectively desulfated heparin inhibits fibroblast growth factor-induced mitogenicity and angiogenesis. *J Biol Chem* **275,** 24653-24660.

Lundin L, Ronnstrand L, Cross M, Hellberg C, Lindahl U & Claesson-Welsh L. (2003). Differential tyrosine phosphorylation of fibroblast growth factor (FGF) receptor-1 and receptor proximal signal transduction in response to FGF-2 and heparin. *Exp Cell Res* **287,** 190-198.

Luo J, West JR & Pantazis NJ. (1997). Nerve growth factor and basic fibroblast growth factor protect rat cerebellar granule cells in culture against ethanol-induced cell death. *Alcohol Clin Exp Res* **21,** 1108-1120.

Maity H, Karkaria C & Davagnino J. (2009). Effects of pH and arginine on the solubility and stability of a therapeutic protein (Fibroblast Growth Factor 20): relationship between solubility and stability. *Curr Pharm Biotechnol* **10,** 609-625.

Mark RJ, Fuson KS, Keane-Lazar K & May PC. (1999). Fibroblast growth factor-8 protects cultured rat hippocampal neurons from oxidative insult. *Brain research* **830,** 88-93.

Matsubara K, Kobayashi S, Kobayashi Y, Yamashita K, Koide H, Hatta M, Iwamoto K, Tanaka O & Kimura K. (1995). beta-Carbolinium cations, endogenous MPP+ analogs, in the lumbar cerebrospinal fluid of patients with Parkinson's disease. *Neurology* **45,** 2240-2245.

Mayer E, Dunnett SB, Pellitteri R & Fawcett JW. (1993a). Basic fibroblast growth factor promotes the survival of embryonic ventral mesencephalic dopaminergic neurons--I. Effects in vitro. *Neuroscience* **56,** 379-388.

Mayer E, Fawcett JW & Dunnett SB. (1993b). Basic fibroblast growth factor promotes the survival of embryonic ventral mesencephalic dopaminergic neurons--II. Effects on nigral transplants in vivo. *Neuroscience* **56,** 389-398.

McCormack AL, Thiruchelvam M, Manning-Bog AB, Thiffault C, Langston JW, Cory-Slechta DA & Di Monte DA. (2002). Environmental risk factors and Parkinson's disease: selective degeneration of nigral dopaminergic neurons caused by the herbicide paraquat. *Neurobiology of disease* **10,** 119-127.

McNaught KS, Belizaire R, Isacson O, Jenner P & Olanow CW. (2003). Altered proteasomal function in sporadic Parkinson's disease. *Exp Neurol* **179,** 38-46.

McNaught KS, Bjorklund LM, Belizaire R, Isacson O, Jenner P & Olanow CW. (2002). Proteasome inhibition causes nigral degeneration with inclusion bodies in rats. *Neuroreport* **13,** 1437-1441.

McNaught KS, Perl DP, Brownell AL & Olanow CW. (2004). Systemic exposure to proteasome inhibitors causes a progressive model of Parkinson's disease. *Ann Neurol* **56,** 149-162.

Meng H, Li C, Feng L, Cheng B, Wu F, Wang X, Li Z & Liu S. (2007). Effects of Ginkgolide B on 6-OHDA-induced apoptosis and calcium over load in cultured PC12. *Int J Dev Neurosci* **25,** 509-514.

Mercuri NB & Bernardi G. (2005). The 'magic' of L-dopa: why is it the gold standard Parkinson's disease therapy? *Trends in pharmacological sciences* **26,** 341-344.

Mirza B, Hadberg H, Thomsen P & Moos T. (2000). The absence of reactive astrocytosis is indicative of a unique inflammatory process in Parkinson's disease. *Neuroscience* **95,** 425-432.

Miyake A & Itoh N. (1996). Rat fibroblast growth factor receptor-4 mRNA in the brain is preferentially expressed in cholinergic neurons in the medial habenular nucleus. *Neurosci Lett* **203,** 101-104.

Mizuno Y, Hattori N, Mori H, Suzuki T & Tanaka K. (2001). Parkin and Parkinson's disease. *Curr Opin Neurol* **14,** 477-482.

Mizuno Y, Ohta S, Tanaka M, Takamiya S, Suzuki K, Sato T, Oya H, Ozawa T & Kagawa Y. (1989). Deficiencies in complex I subunits of the respiratory chain in Parkinson's disease. *Biochemical and biophysical research communications* **163,** 1450-1455.

Mizuta I, Satake W, Nakabayashi Y, Ito C, Suzuki S, Momose Y, Nagai Y, Oka A, Inoko H, Fukae J, Saito Y, Sawabe M, Murayama S, Yamamoto M, Hattori N, Murata M & Toda T. (2006). Multiple candidate gene analysis identifies alpha-synuclein as a susceptibility gene for sporadic Parkinson's disease. *Hum Mol Genet* **15,** 1151-1158.

Mizuta I, Tsunoda T, Satake W, Nakabayashi Y, Watanabe M, Takeda A, Hasegawa K, Nakashima K, Yamamoto M, Hattori N, Murata M & Toda T. (2008). Calbindin 1, fibroblast growth factor 20, and alpha-synuclein in sporadic Parkinson's disease. *Hum Genet* **124,** 89-94.

Mnich K, Finn DP, Dowd E & Gorman AM. (2010). Inhibition by anandamide of 6-hydroxydopamine-induced cell death in PC12 cells. *Int J Cell Biol* **2010,** 818497.

Mohammadi M, Dikic I, Sorokin A, Burgess WH, Jaye M & Schlessinger J. (1996). Identification of six novel autophosphorylation sites on fibroblast growth factor

receptor 1 and elucidation of their importance in receptor activation and signal transduction. *Mol Cell Biol* **16,** 977-989.

Mohammadi M, Dionne CA, Li W, Li N, Spivak T, Honegger AM, Jaye M & Schlessinger J. (1992). Point mutation in FGF receptor eliminates phosphatidylinositol hydrolysis without affecting mitogenesis. *Nature* **358,** 681-684.

Mohammadi M, Froum S, Hamby JM, Schroeder MC, Panek RL, Lu GH, Eliseenkova AV, Green D, Schlessinger J & Hubbard SR. (1998). Crystal structure of an angiogenesis inhibitor bound to the FGF receptor tyrosine kinase domain. *The EMBO journal* **17,** 5896-5904.

Mohammadi M, Honegger AM, Rotin D, Fischer R, Bellot F, Li W, Dionne CA, Jaye M, Rubinstein M & Schlessinger J. (1991). A tyrosine-phosphorylated carboxy-terminal peptide of the fibroblast growth factor receptor (Flg) is a binding site for the SH2 domain of phospholipase C-gamma 1. *Mol Cell Biol* **11,** 5068-5078.

Monfils MH, Driscoll I, Melvin NR & Kolb B. (2006). Differential expression of basic fibroblast growth factor-2 in the developing rat brain. *Neuroscience* **141,** 213-221.

Monte DAD. (2001). The role of environmental agents in Parkinson's disease. *clinic neurosci res***,** 419-426.

Moscatelli D. (1987). High and low affinity binding sites for basic fibroblast growth factor on cultured cells: absence of a role for low affinity binding in the stimulation of plasminogen activator production by bovine capillary endothelial cells. *J Cell Physiol* **131,** 123-130.

Muller-Ostermeyer F, Claus P & Grothe C. (2001). Distinctive effects of rat fibroblast growth factor-2 isoforms on PC12 and Schwann cells. *Growth Factors* **19,** 175-191.

Murase S & McKay RD. (2006). A specific survival response in dopamine neurons at most risk in Parkinson's disease. *J Neurosci* **26,** 9750-9760.

Muthane UB, Swamy HS, Satishchandra P, Subhash MN, Rao S & Subbakrishna D. (1994). Early onset Parkinson's disease: are juvenile- and young-onset different? *Mov Disord* **9,** 539-544.

Nakamura T, Mochizuki Y, Kanetake H & Kanda S. (2001). Signals via FGF receptor 2 regulate migration of endothelial cells. *Biochemical and biophysical research communications* **289,** 801-806.

Nakatake Y, Hoshikawa M, Asaki T, Kassai Y & Itoh N. (2001). Identification of a novel fibroblast growth factor, FGF-22, preferentially expressed in the inner root sheath of the hair follicle. *Biochimica et biophysica acta* **1517,** 460-463.

Nalls MA, Plagnol V, Hernandez DG, Sharma M, Sheerin UM, Saad M, Simon-Sanchez J, Schulte C, Lesage S, Sveinbjornsdottir S, Stefansson K, Martinez M, Hardy J, Heutink P, Brice A, Gasser T, Singleton AB & Wood NW. (2011). Imputation of sequence variants for identification of genetic risks for Parkinson's disease: a meta-analysis of genome-wide association studies. *Lancet* **377,** 641-649.

Neufeld G, Gospodarowicz D, Dodge L & Fujii DK. (1987). Heparin modulation of the neurotropic effects of acidic and basic fibroblast growth factors and nerve growth factor on PC12 cells. *Journal of cellular physiology* **131,** 131-140.

Niu C, Mei J, Pan Q & Fu X. (2009). Nigral degeneration with inclusion body formation and behavioral changes in rats after proteasomal inhibition. *Stereotact Funct Neurosurg* **87,** 69-81.

O'Keeffe FE, Scott SA, Tyers P, O'Keeffe GW, Dalley JW, Zufferey R & Caldwell MA. (2008). Induction of A9 dopaminergic neurons from neural stem cells improves motor function in an animal model of Parkinson's disease. *Brain : a journal of neurology* **131,** 630-641.

Obara K, Ishihara M, Fujita M, Kanatani Y, Hattori H, Matsui T, Takase B, Ozeki Y, Nakamura S, Ishizuka T, Tominaga S, Hiroi S, Kawai T & Maehara T. (2005). Acceleration of wound healing in healing-impaired db/db mice with a photocrosslinkable chitosan hydrogel containing fibroblast growth factor-2. *Wound Repair Regen* **13,** 390-397.

Ohmachi S, Mikami T, Konishi M, Miyake A & Itoh N. (2003). Preferential neurotrophic activity of fibroblast growth factor-20 for dopaminergic neurons through fibroblast growth factor receptor-1c. *Journal of neuroscience research* **72,** 436-443.

Ohmachi S, Watanabe Y, Mikami T, Kusu N, Ibi T, Akaike A & Itoh N. (2000). FGF-20, a novel neurotrophic factor, preferentially expressed in the substantia nigra pars compacta of rat brain. *Biochemical and biophysical research communications* **277,** 355-360.

Ohta M, Suzuki Y, Chou H, Ishikawa N, Suzuki S, Tanihara M, Mizushima Y, Dezawa M & Ide C. (2004). Novel heparin/alginate gel combined with basic fibroblast growth factor promotes nerve regeneration in rat sciatic nerve. *J Biomed Mater Res A* **71,** 661-668.

Ohta Y, Nagai M, Nagata T, Murakami T, Nagano I, Narai H, Kurata T, Shiote M, Shoji M & Abe K. (2006). Intrathecal injection of epidermal growth factor and fibroblast growth factor 2 promotes proliferation of neural precursor cells in the spinal cords of mice with mutant human SOD1 gene. *Journal of neuroscience research* **84,** 980-992.

Olanow CW & McNaught KS. (2006). Ubiquitin-proteasome system and Parkinson's disease. *Mov Disord* **21,** 1806-1823.

Olanow CW, Obeso JA & Stocchi F. (2006). Continuous dopamine-receptor treatment of Parkinson's disease: scientific rationale and clinical implications. *Lancet Neurol* **5,** 677-687.

Ong SH, Guy GR, Hadari YR, Laks S, Gotoh N, Schlessinger J & Lax I. (2000). FRS2 proteins recruit intracellular signaling pathways by binding to diverse targets on fibroblast growth factor and nerve growth factor receptors. *Mol Cell Biol* **20,** 979-989.

Ong SH, Hadari YR, Gotoh N, Guy GR, Schlessinger J & Lax I. (2001). Stimulation of phosphatidylinositol 3-kinase by fibroblast growth factor receptors is mediated by coordinated recruitment of multiple docking proteins. *Proc Natl Acad Sci U S A* **98,** 6074-6079.

Ornitz DM, Xu J, Colvin JS, McEwen DG, MacArthur CA, Coulier F, Gao G & Goldfarb M. (1996). Receptor specificity of the fibroblast growth factor family. *The Journal of biological chemistry* **271,** 15292-15297.

Otto D & Unsicker K. (1993). FGF-2-mediated protection of cultured mesencephalic dopaminergic neurons against MPTP and MPP+: specificity and impact of culture conditions, non-dopaminergic neurons, and astroglial cells. *Journal of neuroscience research* **34,** 382-393.

Ouchi Y, Yoshikawa E, Sekine Y, Futatsubashi M, Kanno T, Ogusu T & Torizuka T. (2005). Microglial activation and dopamine terminal loss in early Parkinson's disease. *Annals of neurology* **57,** 168-175.

Parish CL, Castelo-Branco G, Rawal N, Tonnesen J, Sorensen AT, Salto C, Kokaia M, Lindvall O & Arenas E. (2008). Wnt5a-treated midbrain neural stem cells improve dopamine cell replacement therapy in parkinsonian mice. *The Journal of clinical investigation* **118,** 149-160.

Park TH & Mytilineou C. (1992). Protection from 1-methyl-4-phenylpyridinium (MPP+) toxicity and stimulation of regrowth of MPP(+)-damaged dopaminergic

fibers by treatment of mesencephalic cultures with EGF and basic FGF. *Brain research* **599,** 83-97.

Partanen J, Makela TP, Eerola E, Korhonen J, Hirvonen H, Claesson-Welsh L & Alitalo K. (1991). FGFR-4, a novel acidic fibroblast growth factor receptor with a distinct expression pattern. *The EMBO journal* **10,** 1347-1354.

Pascal LE, True LD, Campbell DS, Deutsch EW, Risk M, Coleman IM, Eichner LJ, Nelson PS & Liu AY. (2008). Correlation of mRNA and protein levels: cell type-specific gene expression of cluster designation antigens in the prostate. *BMC Genomics* **9,** 246.

Pascual A, Hidalgo-Figueroa M, Piruat JI, Pintado CO, Gomez-Diaz R & Lopez-Barneo J. (2008). Absolute requirement of GDNF for adult catecholaminergic neuron survival. *Nature neuroscience* **11,** 755-761.

Paxinos G & Watson C. (1993). *The Rat Brain in Stereotaxic Coordinates*. Academic Press, London.

Pearce RK, Owen A, Daniel S, Jenner P & Marsden CD. (1997). Alterations in the distribution of glutathione in the substantia nigra in Parkinson's disease. *J Neural Transm* **104,** 661-677.

Pellegrini L. (2001). Role of heparan sulfate in fibroblast growth factor signalling: a structural view. *Curr Opin Struct Biol* **11,** 629-634.

Peterson AL & Nutt JG. (2008). Treatment of Parkinson's disease with trophic factors. *Neurotherapeutics* **5,** 270-280.

Porritt MJ, Batchelor PE & Howells DW. (2005). Inhibiting BDNF expression by antisense oligonucleotide infusion causes loss of nigral dopaminergic neurons. *Exp Neurol* **192,** 226-234.

Powell PP, Finklestein SP, Dionne CA, Jaye M & Klagsbrun M. (1991). Temporal, differential and regional expression of mRNA for basic fibroblast growth factor in the developing and adult rat brain. *Brain research Molecular brain research* **11,** 71-77.

Prats H, Kaghad M, Prats AC, Klagsbrun M, Lelias JM, Liauzun P, Chalon P, Tauber JP, Amalric F, Smith JA & et al. (1989). High molecular mass forms of basic fibroblast growth factor are initiated by alternative CUG codons. *Proc Natl Acad Sci U S A* **86,** 1836-1840.

Raffioni S, Thomas D, Foehr ED, Thompson LM & Bradshaw RA. (1999). Comparison of the intracellular signaling responses by three chimeric fibroblast growth factor receptors in PC12 cells. *Proceedings of the National Academy of Sciences of the United States of America* **96,** 7178-7183.

Rapraeger AC, Krufka A & Olwin BB. (1991). Requirement of heparan sulfate for bFGF-mediated fibroblast growth and myoblast differentiation. *Science* **252,** 1705-1708.

Rascol O & Perez-Lloret S. (2009). Rotigotine transdermal delivery for the treatment of Parkinson's disease. *Expert Opin Pharmacother* **10,** 677-691.

Renaud F, Desset S, Oliver L, Gimenez-Gallego G, Van Obberghen E, Courtois Y & Laurent M. (1996). The neurotrophic activity of fibroblast growth factor 1 (FGF1) depends on endogenous FGF1 expression and is independent of the mitogen-activated protein kinase cascade pathway. *The Journal of biological chemistry* **271,** 2801-2811.

Reuss B & von Bohlen und Halbach O. (2003). Fibroblast growth factors and their receptors in the central nervous system. *Cell Tissue Res* **313,** 139-157.

Rezak M. (2007). Current pharmacotherapeutic treatment options in Parkinson's disease. *Dis Mon* **53,** 214-222.

Richardson JR, Caudle WM, Guillot TS, Watson JL, Nakamaru-Ogiso E, Seo BB, Sherer TB, Greenamyre JT, Yagi T, Matsuno-Yagi A & Miller GW. (2007). Obligatory role for complex I inhibition in the dopaminergic neurotoxicity of 1-methyl-4-phenyl-1,2,3,6-tetrahydropyridine (MPTP). *Toxicol Sci* **95,** 196-204.

Rifkin DB & Moscatelli D. (1989). Recent developments in the cell biology of basic fibroblast growth factor. *J Cell Biol* **109,** 1-6.

Roceri M, Molteni R, Fumagalli F, Racagni G, Gennarelli M, Corsini G, Maggio R & Riva M. (2001). Stimulatory role of dopamine on fibroblast growth factor-2 expression in rat striatum. *J Neurochem* **76,** 990-997.

Rodriguez-Enfedaque A, Bouleau S, Laurent M, Courtois Y, Mignotte B, Vayssiere JL & Renaud F. (2009). FGF1 nuclear translocation is required for both its neurotrophic activity and its p53-dependent apoptosis protection. *Biochimica et biophysica acta* **1793,** 1719-1727.

Rodriguez-Gomez JA, Lu JQ, Velasco I, Rivera S, Zoghbi SS, Liow JS, Musachio JL, Chin FT, Toyama H, Seidel J, Green MV, Thanos PK, Ichise M, Pike VW, Innis RB & McKay RD. (2007). Persistent dopamine functions of neurons derived

from embryonic stem cells in a rodent model of Parkinson disease. *Stem Cells* **25,** 918-928.

Roghani M, Mansukhani A, Dell'Era P, Bellosta P, Basilico C, Rifkin DB & Moscatelli D. (1994). Heparin increases the affinity of basic fibroblast growth factor for its receptor but is not required for binding. *J Biol Chem* **269,** 3976-3984.

Root LL & Shipley GD. (2000). Normal human fibroblasts produce membrane-bound and soluble isoforms of FGFR-1. *Mol Cell Biol Res Commun* **3,** 87-97.

Roussa E, Farkas LM & Krieglstein K. (2004). TGF-beta promotes survival on mesencephalic dopaminergic neurons in cooperation with Shh and FGF-8. *Neurobiology of disease* **16,** 300-310.

Roy NS, Cleren C, Singh SK, Yang L, Beal MF & Goldman SA. (2006). Functional engraftment of human ES cell-derived dopaminergic neurons enriched by coculture with telomerase-immortalized midbrain astrocytes. *Nature medicine* **12,** 1259-1268.

Rudland PS, Seifert W & Gospodarowicz D. (1974). Growth control in cultured mouse fibroblasts: induction of the pleiotypic and mitogenic responses by a purified growth factor. *Proc Natl Acad Sci U S A* **71,** 2600-2604.

Saad M, Lesage S, Saint-Pierre A, Corvol JC, Zelenika D, Lambert JC, Vidailhet M, Mellick GD, Lohmann E, Durif F, Pollak P, Damier P, Tison F, Silburn PA, Tzourio C, Forlani S, Loriot MA, Giroud M, Helmer C, Portet F, Amouyel P, Lathrop M, Elbaz A, Durr A, Martinez M & Brice A. (2011). Genome-wide association study confirms BST1 and suggests a locus on 12q24 as the risk loci for Parkinson's disease in the European population. *Hum Mol Genet* **20,** 615-627.

Sabban EL. (1997). Control of tyrosine hydroxylase gene expression in chromaffin and PC12 cells. *Semin Cell Dev Biol* **8,** 101-111.

Samii A, Nutt JG & Ransom BR. (2004). Parkinson's disease. *Lancet* **363,** 1783-1793.

Sanchez-Pernaute R, Lee H, Patterson M, Reske-Nielsen C, Yoshizaki T, Sonntag KC, Studer L & Isacson O. (2008). Parthenogenetic dopamine neurons from primate embryonic stem cells restore function in experimental Parkinson's disease. *Brain : a journal of neurology* **131,** 2127-2139.

Sanchez-Pernaute R, Studer L, Bankiewicz KS, Major EO & McKay RD. (2001). In vitro generation and transplantation of precursor-derived human dopamine neurons. *Journal of neuroscience research* **65,** 284-288.

Sanchez-Ramos JR, Hefti F & Weiner WJ. (1987). Paraquat and Parkinson's disease. *Neurology* **37,** 728.

Sapieha PS, Peltier M, Rendahl KG, Manning WC & Di Polo A. (2003). Fibroblast growth factor-2 gene delivery stimulates axon growth by adult retinal ganglion cells after acute optic nerve injury. *Molecular and cellular neurosciences* **24,** 656-672.

Satake W, Mizuta I, Suzuki S, Nakabayashi Y, Ito C, Watanabe M, Takeda A, Hasegawa K, Sakoda S, Yamamoto M, Hattori N, Murata M & Toda T. (2007). Fibroblast growth factor 20 gene and Parkinson's disease in the Japanese population. *Neuroreport* **18,** 937-940.

Schallert T & Tillerson JL. (2000).*). Intervention strategies for degeneration of dopamine neurons in parkinsonism: Optimizing behavioral assessment of outcome. In Central Nervous System Diseases: Innovative models of CNS diseases from molecule to therapy.* Humana Press, Totowa, N.J.

Schapira AH. (2007). Future directions in the treatment of Parkinson's disease. *Movement disorders : official journal of the Movement Disorder Society* **22 Suppl 17,** S385-391.

Schapira AH. (2009). Neurobiology and treatment of Parkinson's disease. *Trends in pharmacological sciences* **30,** 41-47.

Schapira AH, Bezard E, Brotchie J, Calon F, Collingridge GL, Ferger B, Hengerer B, Hirsch E, Jenner P, Le Novere N, Obeso JA, Schwarzschild MA, Spampinato U & Davidai G. (2006). Novel pharmacological targets for the treatment of Parkinson's disease. *Nat Rev Drug Discov* **5,** 845-854.

Schapira AH, Cooper JM, Dexter D, Jenner P, Clark JB & Marsden CD. (1989). Mitochondrial complex I deficiency in Parkinson's disease. *Lancet* **1,** 1269.

Schlessinger J. (2000). Cell signaling by receptor tyrosine kinases. *Cell* **103,** 211-225.

Schober A. (2004). Classic toxin-induced animal models of Parkinson's disease: 6-OHDA and MPTP. *Cell Tissue Res* **318,** 215-224.

Schulz JB & Falkenburger BH. (2004). Neuronal pathology in Parkinson's disease. *Cell Tissue Res* **318,** 135-147.

Schwarting RK & Huston JP. (1996a). The unilateral 6-hydroxydopamine lesion model in behavioral brain research. Analysis of functional deficits, recovery and treatments. *Progress in neurobiology* **50,** 275-331.

Schwarting RK & Huston JP. (1996b). Unilateral 6-hydroxydopamine lesions of meso-striatal dopamine neurons and their physiological sequelae. *Progress in neurobiology* **49,** 215-266.

Sensenbrenner M. (1993). The neurotrophic activity of fibroblast growth factors. *Progress in neurobiology* **41,** 683-704.

Setsuie R & Wada K. (2007). The functions of UCH-L1 and its relation to neurodegenerative diseases. *Neurochemistry international* **51,** 105-111.

Shakkottai VG, Xiao M, Xu L, Wong M, Nerbonne JM, Ornitz DM & Yamada KA. (2009). FGF14 regulates the intrinsic excitability of cerebellar Purkinje neurons. *Neurobiology of disease* **33,** 81-88.

Sherer TB, Betarbet R & Greenamyre JT. (2002). Environment, mitochondria, and Parkinson's disease. *Neuroscientist* **8,** 192-197.

Shi B, Huang W & Cheng J. (2007). Determination of neurotransmitters in PC 12 cells by microchip electrophoresis with fluorescence detection. *Electrophoresis* **28,** 1595-1600.

Shim JW, Park CH, Bae YC, Bae JY, Chung S, Chang MY, Koh HC, Lee HS, Hwang SJ, Lee KH, Lee YS, Choi CY & Lee SH. (2007). Generation of functional dopamine neurons from neural precursor cells isolated from the subventricular zone and white matter of the adult rat brain using Nurr1 overexpression. *Stem Cells* **25,** 1252-1262.

Shimada H, Yoshimura N, Tsuji A & Kunisada T. (2009). Differentiation of dopaminergic neurons from human embryonic stem cells: modulation of differentiation by FGF-20. *J Biosci Bioeng* **107,** 447-454.

Shimoke K & Chiba H. (2001). Nerve growth factor prevents 1-methyl-4-phenyl-1,2,3,6-tetrahydropyridine-induced cell death via the Akt pathway by suppressing caspase-3-like activity using PC12 cells: relevance to therapeutical application for Parkinson's disease. *Journal of neuroscience research* **63,** 402-409.

Shono T, Kanetake H & Kanda S. (2001). The role of mitogen-activated protein kinase activation within focal adhesions in chemotaxis toward FGF-2 by murine brain capillary endothelial cells. *Exp Cell Res* **264,** 275-283.

Shults CW, Ray J, Tsuboi K & Gage FH. (2000). Fibroblast growth factor-2-producing fibroblasts protect the nigrostriatal dopaminergic system from 6-hydroxydopamine. *Brain research* **883,** 192-204.

Sigmund O, Naor Z, Anderson DJ & Stein R. (1990). Effect of nerve growth factor and fibroblast growth factor on SCG10 and c-fos expression and neurite outgrowth in protein kinase C-depleted PC12 cells. *The Journal of biological chemistry* **265,** 2257-2261.

Silani V, Mariani D, Donato FM, Ghezzi C, Mazzucchelli F, Buscaglia M, Pardi G & Scarlato G. (1994). Development of dopaminergic neurons in the human mesencephalon and in vitro effects of basic fibroblast growth factor treatment. *Exp Neurol* **128,** 59-76.

Simola N, Morelli M & Carta AR. (2007). The 6-hydroxydopamine model of Parkinson's disease. *Neurotox Res* **11,** 151-167.

Simuni T & Sethi K. (2008). Nonmotor manifestations of Parkinson's disease. *Annals of neurology* **64 Suppl 2,** S65-80.

Singh N, Pillay V & Choonara YE. (2007). Advances in the treatment of Parkinson's disease. *Progress in neurobiology* **81,** 29-44.

SiuYi Leung D, Unsicker K & Reuss B. (2001). Gap junctions modulate survival-promoting effects of fibroblast growth factor-2 on cultured midbrain dopaminergic neurons. *Mol Cell Neurosci* **18,** 44-55.

Skaper SD, Kee WJ, Facci L, Macdonald G, Doherty P & Walsh FS. (2000). The FGFR1 inhibitor PD 173074 selectively and potently antagonizes FGF-2 neurotrophic and neurotropic effects. *Journal of neurochemistry* **75,** 1520-1527.

Snyder BJ & Olanow CW. (2005). Stem cell treatment for Parkinson's disease: an update for 2005. *Curr Opin Neurol* **18,** 376-385.

Sofic E, Lange KW, Jellinger K & Riederer P. (1992). Reduced and oxidized glutathione in the substantia nigra of patients with Parkinson's disease. *Neurosci Lett* **142,** 128-130.

Sonntag KC, Pruszak J, Yoshizaki T, van Arensbergen J, Sanchez-Pernaute R & Isacson O. (2007). Enhanced yield of neuroepithelial precursors and midbrain-like dopaminergic neurons from human embryonic stem cells using the bone morphogenic protein antagonist noggin. *Stem Cells* **25,** 411-418.

Soto-Otero R, Mendez-Alvarez E, Hermida-Ameijeiras A, Munoz-Patino AM & Labandeira-Garcia JL. (2000). Autoxidation and neurotoxicity of 6-hydroxydopamine in the presence of some antioxidants: potential implication in relation to the pathogenesis of Parkinson's disease. *Journal of neurochemistry* **74,** 1605-1612.

Soulet F, Bailly K, Roga S, Lavigne AC, Amalric F & Bouche G. (2005). Exogenously added fibroblast growth factor 2 (FGF-2) to NIH3T3 cells interacts with nuclear ribosomal S6 kinase 2 (RSK2) in a cell cycle-dependent manner. *J Biol Chem* **280,** 25604-25610.

Spear N, Estevez AG, Barbeito L, Beckman JS & Johnson GV. (1997). Nerve growth factor protects PC12 cells against peroxynitrite-induced apoptosis via a mechanism dependent on phosphatidylinositol 3-kinase. *Journal of neurochemistry* **69,** 53-59.

Spivak-Kroizman T, Lemmon MA, Dikic I, Ladbury JE, Pinchasi D, Huang J, Jaye M, Crumley G, Schlessinger J & Lax I. (1994a). Heparin-induced oligomerization of FGF molecules is responsible for FGF receptor dimerization, activation, and cell proliferation. *Cell* **79,** 1015-1024.

Spivak-Kroizman T, Mohammadi M, Hu P, Jaye M, Schlessinger J & Lax I. (1994b). Point mutation in the fibroblast growth factor receptor eliminates phosphatidylinositol hydrolysis without affecting neuronal differentiation of PC12 cells. *J Biol Chem* **269,** 14419-14423.

Srivastava N, Seth K, Srivastava N, Khanna VK & Agrawal AK. (2008). Functional restoration using basic fibroblast growth factor (bFGF) infusion in Kainic acid induced cognitive dysfunction in rat: neurobehavioural and neurochemical studies. *Neurochemical research* **33,** 1169-1177.

Steiger M. (2008). Constant dopaminergic stimulation by transdermal delivery of dopaminergic drugs: a new treatment paradigm in Parkinson's disease. *Eur J Neurol* **15,** 6-15.

Studer L, Tabar V & McKay RD. (1998). Transplantation of expanded mesencephalic precursors leads to recovery in parkinsonian rats. *Nature neuroscience* **1,** 290-295.

Su YR, Wang J, Wu JJ, Chen Y & Jiang YP. (2007). Overexpression of lentivirus-mediated glial cell line-derived neurotrophic factor in bone marrow stromal cells and its neuroprotection for the PC12 cells damaged by lactacystin. *Neurosci Bull* **23,** 67-74.

Sullivan AM, Opacka-Juffry J & Blunt SB. (1998). Long-term protection of the rat nigrostriatal dopaminergic system by glial cell line-derived neurotrophic factor against 6-hydroxydopamine in vivo. *The European journal of neuroscience* **10,** 57-63.

Sulzer D. (2007). Multiple hit hypotheses for dopamine neuron loss in Parkinson's disease. *Trends Neurosci* **30,** 244-250.

Takagi Y, Takahashi J, Saiki H, Morizane A, Hayashi T, Kishi Y, Fukuda H, Okamoto Y, Koyanagi M, Ideguchi M, Hayashi H, Imazato T, Kawasaki H, Suemori H, Omachi S, Iida H, Itoh N, Nakatsuji N, Sasai Y & Hashimoto N. (2005). Dopaminergic neurons generated from monkey embryonic stem cells function in a Parkinson primate model. *The Journal of clinical investigation* **115,** 102-109.

Takayama H, Ray J, Raymon HK, Baird A, Hogg J, Fisher LJ & Gage FH. (1995). Basic fibroblast growth factor increases dopaminergic graft survival and function in a rat model of Parkinson's disease. *Nature medicine* **1,** 53-58.

Tan EK & Skipper LM. (2007). Pathogenic mutations in Parkinson disease. *Hum Mutat* **28,** 641-653.

Tan SK, Hartung H, Sharp T & Temel Y. (2011). Serotonin-dependent depression in Parkinson's disease: a role for the subthalamic nucleus? *Neuropharmacology* **61,** 387-399.

Tanaka A, Kamiakito T, Hakamata Y, Fujii A, Kuriki K & Fukayama M. (2001). Extensive neuronal localization and neurotrophic function of fibroblast growth factor 8 in the nervous system. *Brain research* **912,** 105-115.

Tanner CM, Ottman R, Goldman SM, Ellenberg J, Chan P, Mayeux R & Langston JW. (1999). Parkinson disease in twins: an etiologic study. *JAMA* **281,** 341-346.

Taylor H & Minger SL. (2005). Regenerative medicine in Parkinson's disease: generation of mesencephalic dopaminergic cells from embryonic stem cells. *Curr Opin Biotechnol* **16,** 487-492.

Taylor TN, Greene JG & Miller GW. (2010). Behavioral phenotyping of mouse models of Parkinson's disease. *Behav Brain Res* **211,** 1-10.

Teismann P & Schulz JB. (2004). Cellular pathology of Parkinson's disease: astrocytes, microglia and inflammation. *Cell and tissue research* **318,** 149-161.

Terzioglu M & Galter D. (2008). Parkinson's disease: genetic versus toxin-induced rodent models. *Febs J* **275,** 1384-1391.

Thiruchelvam M, Richfield EK, Baggs RB, Tank AW & Cory-Slechta DA. (2000). The nigrostriatal dopaminergic system as a preferential target of repeated exposures to combined paraquat and maneb: implications for Parkinson's disease. *J Neurosci* **20,** 9207-9214.

Thisse B & Thisse C. (2005). Functions and regulations of fibroblast growth factor signaling during embryonic development. *Dev Biol* **287,** 390-402.

Thobois S, Delamarre-Damier F & Derkinderen P. (2005). Treatment of motor dysfunction in Parkinson's disease: an overview. *Clin Neurol Neurosurg* **107,** 269-281.

Todo T, Kondo T, Nakamura S, Kirino T, Kurokawa T & Ikeda K. (1998). Neuronal localization of fibroblast growth factor-9 immunoreactivity in human and rat brain. *Brain research* **783,** 179-187.

Tooyama I, McGeer EG, Kawamata T, Kimura H & McGeer PL. (1994). Retention of basic fibroblast growth factor immunoreactivity in dopaminergic neurons of the substantia nigra during normal aging in humans contrasts with loss in Parkinson's disease. *Brain research* **656,** 165-168.

Tretter YP, Hertel M, Munz B, ten Bruggencate G, Werner S & Alzheimer C. (2000). Induction of activin A is essential for the neuroprotective action of basic fibroblast growth factor in vivo. *Nature medicine* **6,** 812-815.

Unsicker K. (1994). Growth factors in Parkinson's disease. *Progress in growth factor research* **5,** 73-87.

Unsicker K, Reichert-Preibsch H, Schmidt R, Pettmann B, Labourdette G & Sensenbrenner M. (1987). Astroglial and fibroblast growth factors have neurotrophic functions for cultured peripheral and central nervous system neurons. *Proceedings of the National Academy of Sciences of the United States of America* **84,** 5459-5463.

van der Walt JM, Noureddine MA, Kittappa R, Hauser MA, Scott WK, McKay R, Zhang F, Stajich JM, Fujiwara K, Scott BL, Pericak-Vance MA, Vance JM & Martin ER. (2004). Fibroblast growth factor 20 polymorphisms and haplotypes strongly influence risk of Parkinson disease. *American journal of human genetics* **74,** 1121-1127.

van Heumen WR, Claxton C & Pickles JO. (1999). Fibroblast growth factor receptor-4 splice variants cause deletion of a critical tyrosine. *IUBMB Life* **48,** 73-78.

Vlodavsky I, Folkman J, Sullivan R, Fridman R, Ishai-Michaeli R, Sasse J & Klagsbrun M. (1987). Endothelial cell-derived basic fibroblast growth factor: synthesis and deposition into subendothelial extracellular matrix. *Proc Natl Acad Sci U S A* **84,** 2292-2296.

Wagle A & Singh JP. (2000). Fibroblast growth factor protects nitric oxide-induced apoptosis in neuronal SHSY-5Y cells. *J Pharmacol Exp Ther* **295,** 889-895.

Wakeman DR, Dodiya HB & Kordower JH. (2011). Cell transplantation and gene therapy in Parkinson's disease. *Mt Sinai J Med* **78,** 126-158.

Walker DG, Terai K, Matsuo A, Beach TG, McGeer EG & McGeer PL. (1998). Immunohistochemical analyses of fibroblast growth factor receptor-1 in the human substantia nigra. Comparison between normal and Parkinson's disease cases. *Brain research* **794,** 181-187.

Wanaka A, Johnson EM, Jr. & Milbrandt J. (1990). Localization of FGF receptor mRNA in the adult rat central nervous system by in situ hybridization. *Neuron* **5,** 267-281.

Wang G, van der Walt JM, Mayhew G, Li YJ, Zuchner S, Scott WK, Martin ER & Vance JM. (2008). Variation in the miRNA-433 binding site of FGF20 confers risk for Parkinson disease by overexpression of alpha-synuclein. *American journal of human genetics* **82,** 283-289.

Wang S, Cai Q, Hou J, Bei J, Zhang T, Yang J & Wan Y. (2003). Acceleration effect of basic fibroblast growth factor on the regeneration of peripheral nerve through a 15-mm gap. *J Biomed Mater Res A* **66,** 522-531.

Wernig M, Zhao JP, Pruszak J, Hedlund E, Fu D, Soldner F, Broccoli V, Constantine-Paton M, Isacson O & Jaenisch R. (2008). Neurons derived from reprogrammed fibroblasts functionally integrate into the fetal brain and improve symptoms of rats with Parkinson's disease. *Proceedings of the National Academy of Sciences of the United States of America* **105,** 5856-5861.

Wert MM & Palfrey HC. (2000a). Divergence in the anti-apoptotic signalling pathways used by nerve growth factor and basic fibroblast growth factor (bFGF) in PC12 cells: rescue by bFGF involves protein kinase C delta. *Biochem J* **352 Pt 1,** 175-182.

Wert MM & Palfrey HC. (2000b). Divergence in the anti-apoptotic signalling pathways used by nerve growth factor and basic fibroblast growth factor (bFGF) in PC12 cells: rescue by bFGF involves protein kinase C delta. *The Biochemical journal* **352 Pt 1,** 175-182.

Wider C, Dachsel JC, Soto AI, Heckman MG, Diehl NN, Yue M, Lincoln S, Aasly JO, Haugarvoll K, Trojanowski JQ, Papapetropoulos S, Mash D, Rajput A, Rajput AH, Gibson JM, Lynch T, Dickson DW, Uitti RJ, Wszolek ZK, Farrer MJ & Ross OA. (2009). FGF20 and Parkinson's disease: no evidence of association or pathogenicity via alpha-synuclein expression. *Movement disorders : official journal of the Movement Disorder Society* **24,** 455-459.

Wijeyekoon R & Barker RA. (2009). Cell replacement therapy for Parkinson's disease. *Biochimica et biophysica acta* **1792,** 688-702.

Wong A, Lamothe B, Lee A, Schlessinger J & Lax I. (2002). FRS2 alpha attenuates FGF receptor signaling by Grb2-mediated recruitment of the ubiquitin ligase Cbl. *Proc Natl Acad Sci U S A* **99,** 6684-6689.

Wu DC, Tieu K, Cohen O, Choi DK, Vila M, Jackson-Lewis V, Teismann P & Przedborski S. (2002). Glial cell response: A pathogenic factor in Parkinson's disease. *J Neurovirol* **8,** 551-558.

Wu HY, Dawson MR, Reynolds R & Hardy RJ. (2001). Expression of QKI proteins and MAP1B identifies actively myelinating oligodendrocytes in adult rat brain. *Molecular and cellular neurosciences* **17,** 292-302.

Yamamoto H, Ochiya T, Takahama Y, Ishii Y, Osumi N, Sakamoto H & Terada M. (2000). Detection of spatial localization of Hst-1/Fgf-4 gene expression in brain and testis from adult mice. *Oncogene* **19,** 3805-3810.

Yamashita T, Yoshioka M & Itoh N. (2000). Identification of a novel fibroblast growth factor, FGF-23, preferentially expressed in the ventrolateral thalamic nucleus of the brain. *Biochemical and biophysical research communications* **277,** 494-498.

Yanagishita M & Hascall VC. (1992). Cell surface heparan sulfate proteoglycans. *J Biol Chem* **267,** 9451-9454.

Yang H, Xia Y, Lu SQ, Soong TW & Feng ZW. (2008). Basic fibroblast growth factor-induced neuronal differentiation of mouse bone marrow stromal cells requires FGFR-1, MAPK/ERK, and transcription factor AP-1. *J Biol Chem* **283,** 5287-5295.

Yayon A, Klagsbrun M, Esko JD, Leder P & Ornitz DM. (1991). Cell surface, heparin-like molecules are required for binding of basic fibroblast growth factor to its high affinity receptor. *Cell* **64,** 841-848.

Yayon A, Zimmer Y, Shen GH, Avivi A, Yarden Y & Givol D. (1992). A confined variable region confers ligand specificity on fibroblast growth factor receptors: implications for the origin of the immunoglobulin fold. *Embo J* **11,** 1885-1890.

Yazaki N, Hosoi Y, Kawabata K, Miyake A, Minami M, Satoh M, Ohta M, Kawasaki T & Itoh N. (1994). Differential expression patterns of mRNAs for members of the fibroblast growth factor receptor family, FGFR-1-FGFR-4, in rat brain. *Journal of neuroscience research* **37,** 445-452.

Yoritaka A, Hattori N, Uchida K, Tanaka M, Stadtman ER & Mizuno Y. (1996). Immunohistochemical detection of 4-hydroxynonenal protein adducts in Parkinson disease. *Proc Natl Acad Sci U S A* **93,** 2696-2701.

Zecca L, Pietra R, Goj C, Mecacci C, Radice D & Sabbioni E. (1994). Iron and other metals in neuromelanin, substantia nigra, and putamen of human brain. *J Neurochem* **62,** 1097-1101.

Zhang J, Perry G, Smith MA, Robertson D, Olson SJ, Graham DG & Montine TJ. (1999). Parkinson's disease is associated with oxidative damage to cytoplasmic DNA and RNA in substantia nigra neurons. *Am J Pathol* **154,** 1423-1429.

Zhang X, Ibrahimi OA, Olsen SK, Umemori H, Mohammadi M & Ornitz DM. (2006). Receptor specificity of the fibroblast growth factor family. The complete mammalian FGF family. *The Journal of biological chemistry* **281,** 15694-15700.

Ziemssen T & Reichmann H. (2007). Non-motor dysfunction in Parkinson's disease. *Parkinsonism & related disorders* **13,** 323-332.